Using natural variation in *Nicotiana attenuata* to elucidate its defense response against herbivory

DISSERTATION

zur Erlangung des akademischen Grades eines
„doctor rerum naturalium"
(Dr. rer. nat.)

vorgelegt

dem Rat der Fakultät für Biowissenschaften
der Friedrich-Schiller-Universität Jena

von

Rishav Ray, M.Sc.
geboren am 29th Juni 1990 in Kolkata, India

Gutachter:

1. Prof. Dr. Günter Theißen
   Friedrich-Schiller-Universität, Jena

2. Prof. Dr. Ian T. Baldwin
   Max Planck Institute for Chemical Ecology, Jena

3. Prof. Dr. Gregg Howe
   Michigan State University, East Lansing

Tag der öffentlichen Verteidigung: Februar 15th, 2024

“The true laboratory is the mind,
where behind illusions we uncover the laws of truth”

– Sir Jagadish Chandra Bose

Contents

Introduction **1**
Plants: the cornerstone of Earth's lifeforms 1
Plant defense and jasmonate signaling 2
N. attenuata : an ecological model plant 4
Forward genetics: unveiling Nature's secrets 6
Harnessing the power of multi-omics for functional trait analysis 7
Overview of the dissertation 9
References 10

Using natural variation to achieve a whole-plant functional understanding of the responses mediated by jasmonate signaling **15**
Introduction 17
Natural variation in JA-mediated responses 18
Functional diversity of JA signaling in *N. attenuata* 20
Natural variation in JA signaling in *N. attenuata* populations 23
Capturing intra-species natural variation in JA signaling with a MAGIC population 24

A persistent major mutation in canonical jasmonate signaling is embedded in an herbivory-elicited gene network **29**
Results and Discussion 32
Conclusion 40
Materials and Methods 41
Supplementary Information 43

An unbiased approach elucidates variation in (S)-(+)-linalool, a context-specific mediator of a tri-trophic interaction in wild tobacco **83**
Results 86
Discussion 91
Conclusion 93
Materials and Methods 93
Supplementary Information 95

Discussion **125**
Ecology in the genomics era 125
The Selfish Gene model 128
Growth defense trade off 131
Conclusion and outlook 133
References 134

Summary **137**

Zusammenfassung **139**

Bibliography **141**

Erklärung **155**

Acknowledgments **157**

Appendix **159**

Introduction

Plants: the cornerstone of Earth's lifeforms

Plants, found across all the biospheres on Earth, have played a paramount role in shaping the natural history of our planet. Constituting nearly 80% of the Earth's biomass (Bar-On et al., 2018), they serve as the primary source of carbohydrates, synthesized through photosynthesis, thus providing the fundamental energy source for all heterotrophs (Field et al., 1998). In parallel, insects, dominating the animal kingdom's biomass, emerge as the most abundant herbivores in terms of sheer numbers (Bar-On et al., 2018), thereby exerting selective pressures that have driven the evolution of diverse plant defense strategies (Ehrlich and Raven, 1964). Consequently, the plant kingdom assumes a central position in Earth's ecological tapestry, intricately connecting nearly every species, either directly or indirectly, to its existence.

The exploration of plant-insect interactions dates back to the early 19th century when Anton Kerner von Marilaun conducted a meticulous six-year experiment in Vienna. In that study, he cultivated over 300 annual and perennial plant species in four distinct common garden experiments, each representing diverse climatic and geographical conditions. Kerner's findings revealed the pivotal role of biotic interactions in species distribution. He concluded that "adaptation" is not a direct consequence of external conditions, emphasizing that neither beneficial nor unfavorable conditions could induce heritable changes in the overall form or structure of plants, including the development of plant components (Von Marilaun, 1890). This was the first empirical example demonstrating environmental non-heritable changes in organisms, essentially phenotypic plasticity, which argued against the then prevalent hypothesis of "the heritability of acquired characters" by Jean Baptist Lamarck.

Following Kerner's pioneering work, subsequent research by Léo Errera emphasized the significance of plant chemicals in addition to mechanical defenses. Employing advanced histochemical techniques available at the time, Errera conducted a meticulous analysis to identify alkaloids within plants and precisely determined their distribution in different tissues, establishing a comprehensive understanding of the specific localization patterns of this compound class. Through careful examination of the spatial distribution, Errera concluded that these chemicals likely arise as a "by product" of the plant's developmental

processes while also serving as a robust defense mechanism against herbivores (Hartmann, 2008). Errera not only urged botanists to investigate plant defense mechanisms, but also encouraged zoologists to explore the counter adaptations, thereby laying the groundwork for studying the evolutionary arms race between plants and herbivores (Hartmann, 2008). Finally, Ernst Stahl's comprehensive ecological field observations and experiments in Jena with slugs and snails, provided invaluable insights into plant defenses (Stahl, 1888). Stahl came to the conclusion that the various plant defense mechanisms provide relative rather than absolute protection against different herbivores. He marveled at the diverse array of mechanically and chemically mediated defenses exhibited by plants, noting the distribution of these compounds within plant organs, their induced accumulation, and predicted that the overall quantitative design can only be comprehended by considering the impact of the surrounding animal interactions on them (Hartmann, 2008).

The concepts put forth by Errera, Stahl, and Kerner converged upon a shared evolutionary perspective. They recognized that compounds once regarded as mere "by-products" or considered "metabolically useless" or of "unknown functions," such as alkaloids and tannins, actually served as essential building blocks for the qualitative and quantitative optimization of plant chemical defenses, evolving in response to the selective pressure exerted by herbivores. This understanding harmonizes with Charles Darwin's theory of natural selection (Darwin, 1859). It is rather remarkable that these insights were largely overlooked for a span of 70 to 100 years. During the mid-20th century, entomologists renewed the recognition of secondary metabolites as the mediator of intricate interactions between plants and their environment, specifically highlighting the essential role of these metabolites in the host plant selection process of herbivorous insects. Gottfried Fraenkel's seminal paper notably emphasized the dual function of plant secondary metabolites in repelling or attracting herbivorous insects (Fraenkel, 1959). In the 1960s, the resurging field of chemical ecology gained momentum as the quantification and empirical observations firmly established the role of plant secondary metabolites in mediating the multifaceted interactions between plants and their surrounding environment (Rosenthal and Berenbaum, 2012). Thus, it took the active "interaction" of the entomologists with the ecologists to reinvigorate the field of chemical ecology and steer it forward in the genomics era.

Plant defense and jasmonate signaling

The transition of plants from their algal form residing in shallow freshwater habitats to colonizing terrestrial environments represents a significant and remarkable shift in their life history. This transition necessitated a series of adaptations, likely occurring gradually over time. Reconstructing the precise evolutionary processes and their sequence is challenging due to the limited availability of fossil records and the absence of extant species that serve as direct intermediates in this transition. Nevertheless, insights can be derived from the extant early-diverging land plants and closely related taxa to infer the evolutionary forces and their relative chronology. It can be argued that one such

adaptation involved the development of the ability to synthesize a diverse array of natural products, enabling plants to effectively overcome the numerous ecological challenges associated with their sessile lifestyle (Knudsen et al., 2018). These natural products play integral roles in plant growth, development, defense, and their overall Darwinian fitness, often being synthesized in response to environmental signals. Phytohormones emerge as crucial signaling regulators, governing plant responses to both biotic and abiotic stresses through these natural products (Blázquez et al., 2020). Among these phytohormones, jasmonate (JA) signaling assumes a pivotal role in coordinating a plant's natural product repertoire, enabling it to respond effectively to environmental stimuli, especially in relation to the sectors associated with herbivore and pathogen resistance (Wasternack and Hause, 2013; Howe et al., 2018; Wasternack and Feussner, 2018).

At the core of JA signaling pathway is the hormone jasmonic acid (JA), which is synthesized in response to various stimuli such as herbivory, pathogen attack, or mechanical stress (Wasternack and Feussner, 2018). Upon perception of the initial stress signal, JA is synthesized and conjugated to its bioactive form, jasmonoyl-L-isoleucine (JA-Ile) (Fonseca et al., 2009). JA-Ile is then recognized by the F-box protein COI1 (CORONITINE INSENSITIVE1) (Xie et al., 1998), which forms a receptor complex with the hyper-variable JAZ (JASMONATE ZIM DOMAIN) proteins as the target. In the absence of JA-Ile, JAZ proteins act as repressors by binding to transcription factors and preventing their activity. However, upon binding of JA-Ile to the COI1-JAZ complex, the JAZ proteins are degraded via the 26S proteasome pathway (Thines et al., 2007; Howe et al., 2018). The degradation of JAZ proteins releases the transcription factors, such as MYC2 (a basic helix-loop-helix transcription factor), allowing them to activate the expression of downstream genes involved in defense responses, secondary metabolite production, and other JA-responsive processes (Niu et al., 2011; Schweizer et al., 2013). These genes regulate the synthesis of various defense compounds in most higher plants, including proteinase inhibitors, volatile organic compounds (VOCs), and other secondary metabolites, which help them defend against herbivores, pathogens, and other stresses. The JA-Ile receptor complex is believed to be highly conserved among vascular land plants, which aligns with the observation that several biotrophic pathogens, including the well-studied model pathogen *Pseudomonas syringae*, produce coronatine, a structurally similar compound to JA-Ile that activates the COI1-JAZ receptor system, that serves as a crucial virulence factor by suppressing salicylic acid (SA) signaling responses (Katsir et al., 2008; Geng et al., 2014).

The molecular mechanisms of JA signaling and its associated metabolic and transcriptomic responses have been extensively studied in the *Nicotiana attenuata* – *Manduca sexta* model plant-herbivore system, which largely follows the canonical model. Typically, the JA signaling cascade in *N. attenuata* is triggered and strongly amplified when fatty acid amino acid elicitors in the oral secretions and regurgitants (OS) of Lepidopteran larvae are introduced into wounds during feeding (Halitschke et al., 2001; Roda et al., 2004; VanDoorn et al., 2010). The resulting metabolic and transcriptomic responses are mediated by JA-Ile (Kang et al., 2006) acting as a ligand for COI1 (Paschold et al., 2007,

2008) which forms a receptor complex with hyper-variable jasmonate ZIM-domain (JAZ) proteins (Oh et al., 2012; Li et al., 2016; Li et al., 2017; Bai et al., 2022). A wide array of induced specialized metabolites are then synthesized, that serve as both direct and indirect defense strategy against the herbivores. **Manuscript I** of this dissertation discusses in detail these strategies, delving into the various layers of its regulatory processes and their context-dependent responses.

N. attenuata : an ecological model plant

Fig. 1: The *N. attenuata* system in its native habitat in the Great Basin Desert of SW Utah. From top left to bottom: the wild fires that give germination cues to long lived seed-banks of this species, leading to large mono-cultures (D. Kessler and K. Gase). Middle, an *N. attenuata* plant in its native habitat (C. Diezel). Right, from top to bottom: a *M. sexta* moth feeding on *N. attenuata* flowers (D. Kessler), the predatory big-eyed bug Geocoris sp. feeding on a neonate *M. sexta* larvae (A. Kessler), an adult *M. sexta* caterpillar (R. Ray).

The annual plant, wild coyote tobacco: *N. attenuata*, is indigenous to the Great Basin Desert of North America. It exhibits a germination pattern driven by long-lived seedbanks in post-fire soils characteristic of high nitrogen content (Baldwin and Morse, 1994; Baldwin et al., 1994). This behavior often results in large scale germination event with near mono-cultures, which lead to high levels of competition for valuable resources among conspecifics. Previous research has identified key traits relevant to the interactions between *N. attenuata* and its associated community of pollinators and herbivores. JA signaling governs a substantial portion of the defense responses against both generalist and specialist herbivores, operating in both vegetative and reproductive tissues (Kessler et al., 2004; Li et al., 2017, 2018). JA signaling also influences floral scent emission and nectar production (Stitz et al., 2014), which serve to attract and reward the primary pollinator of

N. attenuata, the *M. sexta* moths, whose larvae also rely on this plant for nourishment.

Fascinatingly, this wild tobacco species has evolved both JA-mediated and JA-independent mechanisms that reconcile the dilemma between attracting pollinators and defending against herbivores, achieved through changes in flower phenology or attracting higher trophic predators that promote interactions with pollinators or predators, thus minimizing the chances of eggs developing into herbivores (Kessler and Baldwin, 2001; Kessler et al., 2010; Zhou et al., 2017; Cortés Llorca et al., 2020). Over the course of three decades, a combination of field observations and laboratory investigations, including the analysis of numerous transgenic lines with genes silenced in various key pathways and natural accessions, together with extensive transcriptomic and metabolomic data, has contributed to an enhanced understanding of how this plant navigates interactions with its adversaries, competitors, and pollinators.

VOCs emitted by plants has shown to play a crucial role in mediating ecological interactions, particularly herbivore host-plant choices as a function of VOC emission (Kessler and Baldwin, 2001; Carroll et al., 2006; Schuman et al., 2012). However, the precise impact of VOC-mediated interactions on ecological dynamics remains largely unexplored, and consequently, the extent to which these interactions exert selective pressure on host plants and its fitness outcome remains unknown (Kessler and Heil, 2011; Schuman, 2023). Measuring the impact of natural enemies as agents of natural selection on VOCs is challenging due to several interrelated factors: the presence of a herbivore species that consistently imposes negative fitness effects on the host plant; the attraction of natural enemies that exert significant negative effects on the herbivore population; and lastly the variation in natural enemy attraction in response to inducible VOC emission within a plant population (Kessler et al., 2023). Moreover, accurately quantifying VOCs in the natural environment is a challenging task from a practical point of view. For selective pressure to occur, the herbivore and predator populations must exhibit relative stability, which is not always the case in nature. Thus, a more nuanced assessment is required to evaluate Darwinian fitness in terms of information-mediated and/or resource-mediated defense mechanisms (Kessler and Heil, 2011), and the interaction should be evaluated under the broader ecological dynamics at play, for example in Schuman et al. (2012).

During the course of the *N. attenuata* research program, genome sequencing brought in a significant paradigm shift across the biological sciences, including the field of molecular ecology. The ability to decode an organism's complete genetic blueprint provided unprecedented insights into the intricate mechanisms underlying species' interactions with their environment. The *Arabidopsis* genome was sequenced back in 2000, a pioneering effort in plant genomics (Arabidopsis Genome Initiative, 2000), which also coincided with the release of the first draft of the human genome, marking the beginning of the "genomic era". The assembly of the *N. attenuata* genome was published 17 years later, benefiting from significant advancements in sequencing and assembly techniques along with a dramatic reduction in sequencing costs (Xu et al., 2017). The new genomic resource facilitated the rapid generation of *N. attenuata* transgenic lines which,

when released into the native habitat of the species, gave insights into the molecular basis of various ecological traits. While this "sledge hammer" reverse genetics approach provided within-plant mechanistic and functional understanding of *N. attenuata*, a population level understanding of this plant's interactions remained largely elusive. In **Manuscript I**, we argue why investigating within-population trait variance can lead to a more holistic functional understanding of the particular trait, with focus on JA-signaling in *N. attenuata*. And in **Manuscript II**, together with a contiguous reference *N. attenuata* reference genome, we show how a major mutation in the JA-signaling pathway can persist in natural population of the species, through a combination of spatio-temporally driven balancing selection, and a robust herbivory elicited gene regulatory network buffering the mutation.

Forward genetics: unveiling Nature's secrets

Population geneticists have long employed the genetic diversity observed in natural populations to investigate the underlying genetic basis of specific traits and also understand the evolutionary forces at play. In the case of *N. attenuata*, different accessions collected from regions covering the range distribution of the species, show considerable natural variation in OS-induced metabolic response profiles when grown under controlled glasshouse conditions (Li et al., 2015). This motivated the construction of a bi-parental mapping population, leveraging the allelic diversity of two natural accessions collected from Utah and Arizona (Glawe et al., 2003; Wu et al., 2008), resulting in an Advanced Intercross Recombinant Inbred Line (AI-RIL) population. This AI-RIL population has been instrumental in identifying the genetic factors associated with indirect defense mechanisms through VOCs (Zhou et al., 2017; He et al., 2019) (presented in **Manuscript III**) and exploring the interactions with arbuscular mycorrhizal fungi (Wang et al., 2018). Expanding upon the AI-RIL approach, a Multiparent Advanced Generation Inter Cross (MAGIC) population consisting of 26 parents was subsequently established together with a new contiguous *N. attenuata* genome, and its significance in elucidating the population-level fitness effects of natural variation in JA signaling is discussed in detail in **Manuscript II**.

Darwinian fitness, a concept introduced by Charles Darwin, refers to the measure of an organism's reproductive success and its ability to pass on its genetic material to subsequent generations, has been fundamental in understanding the evolutionary processes and diversification of species (Darwin, 1859). Darwin's theory of natural selection posits that individuals with advantageous traits that enhance their fitness are more likely to survive and reproduce, thereby increasing the frequency of those traits in the population over time. In early 20th century, Ronald Fisher proposed the geometric model of adaptation, reconciling Darwinian and Mendelian views on genetics, which laid the foundation of quantitative genetics and its use as a currency to study the process of evolution. His model predicted that most mutations are pleiotropic and that evolutionary adaptations, which drive populations to realize fitness optima, result from changes in many genes of small fitness effects, known as the infinitesimal model (Fisher, 1919; Barton et al., 2017).

However, with the advent of high-throughput genomic and transcriptomic data, counter evidence of single gene mutation with large fitness effect started pouring in (Linnen et al., 2013; Barrett et al., 2019; Berardi et al., 2021), and it became evident that the infinitesimal model alone could not fully explain genotype to phenotype connections and ultimately fitness outcomes. Recently, the "omnigene" model has been proposed which emphasizes the role of gene networks and their interactions in shaping phenotypic variation (Boyle et al., 2017; Liu et al., 2019). By considering the coordinated actions of multiple genes and their regulatory networks derived from large multi-omic studies, the omnigene model proposes a more comprehensive mechanistic model of the evolutionary forces driving trait variation and adaptation. These concepts are elaborated in **Manuscript II** to contextualize the natural variation uncovered in the core JA-signaling pathway of *N. attenuata*.

Harnessing the power of multi-omics for functional trait analysis

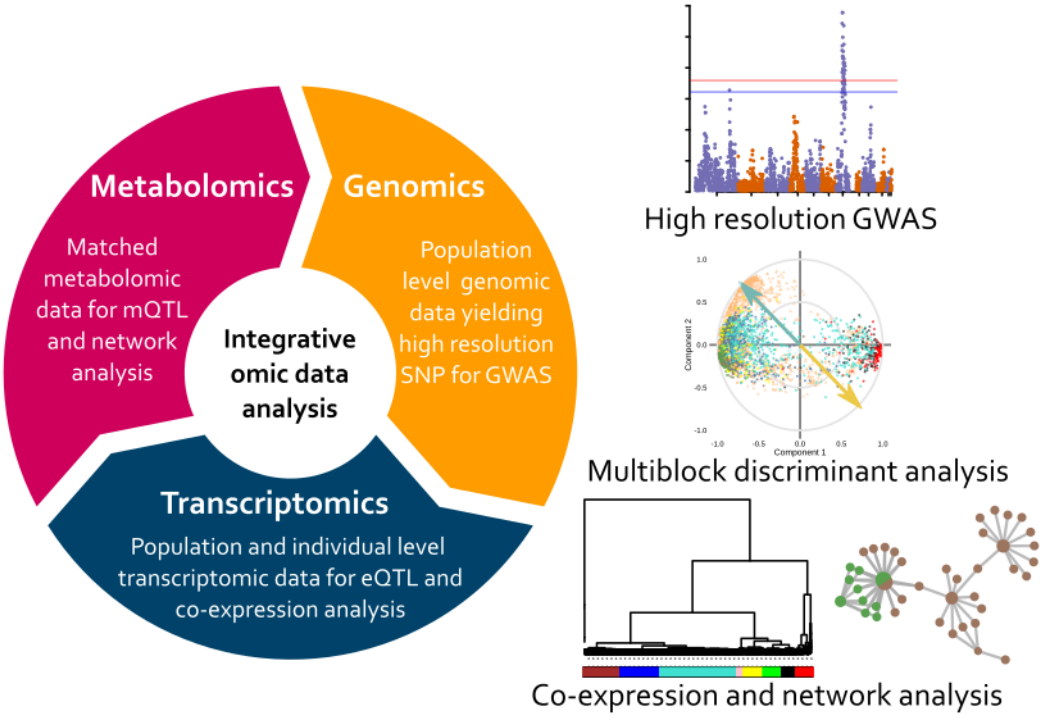

Fig. 2: A schematic diagram showing the broad analysis strategy of multi-omic data integration.

Integrative approaches that combine individual omics data, in a sequential or simultaneous manner, can be a powerful tool to understand the molecular basis of an adaptive trait. These approaches help in assessing the flow of information from one omics level to the other and thus help in bridging the gap from genotype to phenotype. Integrative analyses, by virtue of their ability to study the biological phenomenon holistically, have the ability to improve crop productivity, targeted pest control through genetic tools, disease resistance, and also facilitate broader molecular profiling of the system (Crossa et al., 2017; Scossa et al., 2021; Bai et al., 2022). Fig. 2 shows a broad schematic overview of the various multi-omic data

integration strategies that are typically employed.

The integration of genomics and phenomics data has proven to be a valuable approach in understanding the genetic basis of agronomic traits in crop species. This integration has been extensively employed through quantitative trait loci (QTL) mapping and genome-wide association studies (GWAS), leading to the identification of functional genes associated with traits of interest in rice, maize, cotton, etc. for domestication and improvement purposes (Wang et al., 2020; Zhao et al., 2022; Li et al., 2023). Building upon this foundation, the research focus in the last decade has shifted on gaining deeper insights into the specific genes and pathways that contribute to these traits. To achieve this, the integration of gene expression data with the genome and phenome layer is carried out through the use of expression QTL (eQTL) methods. More recently, transcriptome-wide association study (TWAS), has been developed to bridge the gap between genotype and phenotype. This method involves first identifying associations between a trait and gene expression, and then linking these associations back to the genome using eQTL or traditional GWAS approaches. This integrative approach has been applied successfully to dissect the genetic basis of leaf cuticular conductance in maize, which has important implications for improving crop productivity in drought-prone environments (Lin et al., 2022).

Recent advancements in untargeted mass spectrometry (MS)-based metabolomics have further expanded our knowledge of plant metabolites and their associations with complex traits. Integration of MS-based metabolomics data is facilitated by the establishment of metabolite-gene correlation networks, which can help identify candidate genes involved in specific metabolic pathways. This approach has been successfully applied to uncover key metabolic pathways related to cold tolerance in peanuts (Wang et al., 2021). In addition, the use of projection on latent variables (PLS-DA) approach, as employed in **Manuscript II**, offers another strategy for integrating multi-omics data. This approach entails the identification of underlying correlations across multiple datasets, facilitating the detection important features (genes and metabolites), together with outliers or batch effects in individual sets, thereby minimizing false positives. Consequently, it provides a robust selection of genes and metabolites for further downstream analyses (Meng et al., 2016). By simultaneously integrating multiple molecular-level omics data, we can develop a finer understanding of complex traits at an organismal level. However, it is important to exercise caution when handling such large data sets, and to minimize false-positive results, better filtering and refined *a priori* information must be provided for robust feature selection (Tini et al., 2019).

Thus, in the 21st century high-throughput "omics" era, with advanced computational algorithms and models, we can delve deeper into the mechanisms underlying biodiversity, adaptation, and species interactions. These molecular and computational tools enable the integration of vast amounts of data, facilitating the examination of genetic variation, gene expression patterns, and molecular interactions within ecosystems, providing unprecedented insights into the intricate workings of nature and finally validating the

foundational theories put forth centuries ago.

Overview of the dissertation

Manuscript I presents a framework to evaluate the natural variation within various *N. attenuata* accessions in the broader ecological context, specifically focusing on the JA-signaling pathway. We also review the literature pertaining to JA-signaling in *N. attenuata* and its various layers of defense response upon herbivory. The objective is to gain a holistic functional understanding at an organismal level, and to unravel the underlying ecological challenges that this natural variation helps address. It is to be noted that while utilizing molecular and bioinformatic tools to investigate these genetic variations can lead to valuable insights into novel biochemical components associated with the trait, the primary emphasis here is to comprehending the functional implications of the trait and its impact on ecological outcomes. Furthermore, it is crucial to assess how variations in the trait influence the plants' Darwinian fitness, thus highlighting the significance of studying the ecological consequences of natural variation.

Manuscript II investigates the intra-specific diversity in a 26-parent MAGIC population of *N. attenuata*, and uncovers a natural variation in the core JA signaling pathway linked to a mutation in the *NaJAR4* gene, which is involved in JA-Ile biosynthesis. From decades old seed collection of natural accessions, we show that this variation is persistent in the natural population, showing signatures of balancing selection through spatio-temporal variation. Through a series of experiments and analyses of natural accessions, we show that different variants of *NaJAR4* are associated with varying fitness outcomes in the absence of herbivores, as well as differences in foliar defenses. Furthermore, *NaJAR4* is part of a complex gene co-expression network that coordinates responses to OS-elicitation, which is validated by silencing hub genes in the network, and quantifying the resulting metabolic responses. The findings suggest that compensatory responses within gene networks can allow mutations with significant fitness consequences to persist in natural populations. These results provide insights into the role of natural variation and gene networks in shaping plant defense responses, and highlight the importance of considering the interplay between genetic variation and ecological factors in understanding the adaptation of plants' response to herbivory.

Manuscript III focuses on plant volatile organic compounds (VOCs) and their role in mediating ecological interactions. We investigate the genetic variation controlling VOCs in *N. attenuata*, which revealed that herbivory-induced emissions of leaf terpenoids vary greatly, while emissions of green leaf volatiles remain similar. From field experiments, we observe a significant correlation between the emission of linalool, a common VOC, and predation of the herbivore *M. sexta* by native predators. Through genetic mapping and genome mining, we identify a genetic variation in the enzyme *NaLIS*, that is responsible for the variation in linalool emissions among different natural accessions. By manipulating the linalool emission through heterologous gene expression, we show that the effect of linalool on *M. sexta* oviposition preference depends on the specific VOC chemistry (enantiomer

composition), plant genetic background, and environmental complexity. These results highlight the extensive variation in linalool emissions among geographically interspersed plants, and underscores the importance of considering genetic variation and environmental complexity in characterization of plant-insect interactions.

References

Arabidopsis Genome Initiative, 2000. Analysis of the genome sequence of the flowering plant *Arabidopsis thaliana*. *Nature* **408**, 796–815.

Bai, Y., Yang, C., Halitschke, R., Paetz, C., Kessler, D., Burkard, K., et al., 2022. Natural history–guided omics reveals plant defensive chemistry against leafhopper pests. *Science* **375**, eabm2948.

Baldwin, I.T., Morse, L., 1994. Up in smoke: II. Germination of *Nicotiana attenuata* in response to smoke-derived cues and nutrients in burned and unburned soils. *Journal of Chemical Ecology* **20**, 2373–2391.

Baldwin, I.T., Staszak-Kozinski, L., Davidson, R., 1994. Up in smoke: I. Smoke-derived germination cues for postfire annual, *Nicotiana attenuata* Torr. Ex. Watson. *Journal of Chemical Ecology* **20**, 2345–2371.

Bar-On, Y.M., Phillips, R., Milo, R., 2018. The biomass distribution on earth. *Proceedings of the National Academy of Sciences* **115**, 6506–6511.

Barrett, R.D., Laurent, S., Mallarino, R., Pfeifer, S.P., Xu, C.C., Foll, M., et al., 2019. Linking a mutation to survival in wild mice. *Science* **363**, 499–504.

Barton, N.H., Etheridge, A.M., Véber, A., 2017. The infinitesimal model: Definition, derivation, and implications. *Theoretical Population Biology* **118**, 50–73.

Berardi, A.E., Esfeld, K., Jäggi, L., Mandel, T., Cannarozzi, G.M., Kuhlemeier, C., 2021. Complex evolution of novel red floral color in *Petunia*. *The Plant Cell* **33**, 2273–2295.

Blázquez, M.A., Nelson, D.C., Weijers, D., 2020. Evolution of plant hormone response pathways. *Annual Review of Plant Biology* **71**, 327–353.

Boyle, E.A., Li, Y.I., Pritchard, J.K., 2017. An expanded view of complex traits: from polygenic to omnigenic. *Cell* **169**, 1177–1186.

Carroll, M.J., Schmelz, E.A., Meagher, R.L., Teal, P.E., 2006. Attraction of *Spodoptera frugiperda* larvae to volatiles from herbivore-damaged maize seedlings. *Journal of Chemical Ecology* **32**, 1911–1924.

Cortés Llorca, L., Li, R., Yon, F., Schäfer, M., Halitschke, R., Robert, C.A., et al., 2020. ZEITLUPE facilitates the rhythmic movements of *Nicotiana attenuata* flowers. *The Plant Journal* **103**, 308–322.

Crossa, J., Pérez-Rodríguez, P., Cuevas, J., Montesinos-López, O., Jarquín, D., Campos, G. de los, et al., 2017. Genomic selection in plant breeding: Methods, models, and perspectives. *Trends in Plant Science* **22**, 961–975.

Darwin, C., 1859. On the Origin of Species. Routledge.

Ehrlich, P.R., Raven, P.H., 1964. Butterflies and plants: A study in coevolution. *Evolution* 586–608.

Field, C.B., Behrenfeld, M.J., Randerson, J.T., Falkowski, P., 1998. Primary production of the biosphere: Integrating terrestrial and oceanic components. *Science* **281**, 237–240.

Fisher, R.A., 1919. The correlation between relatives on the supposition of Mendelian inheritance. *Earth and Environmental Science Transactions of the Royal Society of Edinburgh* **52**, 399–433.

Fonseca, S., Chini, A., Hamberg, M., Adie, B., Porzel, A., Kramell, R., et al., 2009. (+)-7-iso-Jasmonoyl-L-isoleucine is the endogenous bioactive jasmonate. *Nature Chemical Biology* **5**, 344–350.

Fraenkel, G.S., 1959. The Raison d'Etre of Secondary Plant Substances: These odd chemicals arose as a means of protecting plants from insects and now guide insects to food. *Science* **129**, 1466–1470.

Geng, X., Jin, L., Shimada, M., Kim, M.G., Mackey, D., 2014. The phytotoxin coronatine is a multifunctional component of the virulence armament of *Pseudomonas syringae*. *Planta* **240**, 1149–1165.

Glawe, G.A., Zavala, J.A., Kessler, A., Van Dam, N.M., Baldwin, I.T., 2003. Ecological costs and benefits correlated with trypsin protease inhibitor production in *Nicotiana attenuata*. *Ecology* **84**, 79–90.

Halitschke, R., Schittko, U., Pohnert, G., Boland, W., Baldwin, I.T., 2001. Molecular interactions between the specialist herbivore *Manduca sexta* (Lepidoptera, Sphingidae) and its natural host *Nicotiana attenuata*.

III. Fatty acid-amino acid conjugates in herbivore oral secretions are necessary and sufficient for herbivore-specific plant responses. *Plant Physiology* **125**, 711–717.

Hartmann, T., 2008. The lost origin of chemical ecology in the late 19th century. *Proceedings of the National Academy of Sciences* **105**, 4541–4546.

He, J., Fandino, R.A., Halitschke, R., Luck, K., Köllner, T.G., Murdock, M.H., et al., 2019. An unbiased approach elucidates variation in (S)-(+)-linalool, a context-specific mediator of a tri-trophic interaction in wild tobacco. *Proceedings of the National Academy of Sciences* **116**, 14651–14660.

Howe, G.A., Major, I.T., Koo, A.J., 2018. Modularity in jasmonate signaling for multistress resilience. *Annual Review of Plant Biology* **69**, 387–415.

Kang, J.-H., Wang, L., Giri, A., Baldwin, I.T., 2006. Silencing threonine deaminase and *JAR4* in *Nicotiana attenuata* impairs jasmonic acid–isoleucine–mediated defenses against *Manduca sexta*. *The Plant Cell* **18**, 3303–3320.

Katsir, L., Schilmiller, A.L., Staswick, P.E., He, S.Y., Howe, G.A., 2008. *COI1* is a critical component of a receptor for jasmonate and the bacterial virulence factor coronatine. *Proceedings of the National Academy of Sciences* **105**, 7100–7105.

Kessler, A., Baldwin, I.T., 2001. Defensive function of herbivore-induced plant volatile emissions in nature. *Science* **291**, 2141–2144.

Kessler, A., Halitschke, R., Baldwin, I.T., 2004. Silencing the jasmonate cascade: Induced plant defenses and insect populations. *Science* **305**, 665–668.

Kessler, A., Heil, M., 2011. The multiple faces of indirect defences and their agents of natural selection. *Functional Ecology* **25**, 348–357.

Kessler, A., Mueller, M.B., Kalske, A., Chautá, A., 2023. Volatile-mediated plant–plant communication and higher-level ecological dynamics. *Current Biology* **33**, R519–R529.

Kessler, D., Diezel, C., Baldwin, I.T., 2010. Changing pollinators as a means of escaping herbivores. *Current Biology* **20**, 237–242.

Knudsen, C., Gallage, N.J., Hansen, C.C., Møller, B.L., Laursen, T., 2018. Dynamic metabolic solutions to the sessile life style of plants. *Natural Product Reports* **35**, 1140–1155.

Li, D., Baldwin, I., Gaquerel, E., 2016. Beyond the canon: Within-plant and population-level heterogeneity in jasmonate signaling engaged by plant-insect interactions. *Plants* **5**, 14.

Li, D., Baldwin, I.T., Gaquerel, E., 2015. Navigating natural variation in herbivory-induced secondary metabolism in coyote tobacco populations using MS/MS structural analysis. *Proceedings of the National Academy of Sciences* **112**, E4147–E4155.

Li, R., Schuman, M.C., Wang, Y., Llorca, L.C., Bing, J., Bennion, A., et al., 2018. Jasmonate signaling makes flowers attractive to pollinators and repellant to florivores in nature. *Journal of Integrative Plant Biology* **60**, 190–194.

Li, R., Wang, M., Wang, Y., Schuman, M.C., Weinhold, A., Schäfer, M., et al., 2017. Flower-specific jasmonate signaling regulates constitutive floral defenses in wild tobacco. *Proceedings of the National Academy of Sciences* **114**, E7205–E7214.

Li, Z., Wang, B., Luo, W., Xu, Y., Wang, J., Xue, Z., et al., 2023. Natural variation of codon repeats in *COLD11* endows rice with chilling resilience. *Science Advances* **9**, eabq5506.

Lin, M., Qiao, P., Matschi, S., Vasquez, M., Ramstein, G.P., Bourgault, R., et al., 2022. Integrating GWAS and TWAS to elucidate the genetic architecture of maize leaf cuticular conductance. *Plant Physiology* **189**, 2144–2158.

Linnen, C.R., Poh, Y.-P., Peterson, B.K., Barrett, R.D., Larson, J.G., Jensen, J.D., et al., 2013. Adaptive evolution of multiple traits through multiple mutations at a single gene. *Science* **339**, 1312–1316.

Liu, X., Li, Y.I., Pritchard, J.K., 2019. Trans effects on gene expression can drive omnigenic inheritance. *Cell* **177**, 1022–1034.e6.

Meng, C., Zeleznik, O.A., Thallinger, G.G., Kuster, B., Gholami, A.M., Culhane, A.C., 2016. Dimension reduction techniques for the integrative analysis of multi-omics data. *Briefings in Bioinformatics* **17**, 628–641.

Niu, Y., Figueroa, P., Browse, J., 2011. Characterization of JAZ-interacting bHLH transcription factors that regulate jasmonate responses in *Arabidopsis*. *Journal of Experimental Botany* **62**, 2143–2154.

Oh, Y., Baldwin, I.T., Gális, I., 2012. NaJAZh regulates a subset of defense responses against herbivores and

spontaneous leaf necrosis in *Nicotiana attenuata* plants. *Plant Physiology* **159**, 769–788.

Paschold, A., Bonaventure, G., Kant, M.R., Baldwin, I.T., 2008. Jasmonate perception regulates jasmonate biosynthesis and JA-Ile metabolism: the case of COI1 in *Nicotiana attenuata*. *Plant & Cell Physiology* **49**, 1165–1175.

Paschold, A., Halitschke, R., Baldwin, I.T., 2007. Co (i)-ordinating defenses: NaCOI1 mediates herbivore-induced resistance in *Nicotiana attenuata* and reveals the role of herbivore movement in avoiding defenses. *The Plant Journal* **51**, 79–91.

Roda, A., Halitschke, R., Steppuhn, A., Baldwin, I.T., 2004. Individual variability in herbivore-specific elicitors from the plant's perspective. *Molecular Ecology* **13**, 2421–2433.

Rosenthal, G.A., Berenbaum, M.R., 2012. Herbivores: Their interactions with secondary plant metabolites: Ecological and evolutionary processes. Academic Press.

Schuman, M.C., 2023. Where, when, and why do plant volatiles mediate ecological signaling? The answer is blowing in the wind. *Annual Review of Plant Biology* **74**, 609–633.

Schuman, M.C., Barthel, K., Baldwin, I.T., 2012. Herbivory-induced volatiles function as defenses increasing fitness of the native plant *Nicotiana attenuata* in nature. *eLife* **1**, e00007.

Schweizer, F., Fernández-Calvo, P., Zander, M., Diez-Diaz, M., Fonseca, S., Glauser, G., et al., 2013. *Arabidopsis* basic helix-loop-helix transcription factors MYC2, MYC3, and MYC4 regulate glucosinolate biosynthesis, insect performance, and feeding behavior. *The Plant Cell* **25**, 3117–3132.

Scossa, F., Alseekh, S., Fernie, A.R., 2021. Integrating multi-omics data for crop improvement. *Journal of Plant Physiology* **257**, 153352.

Stahl, E., 1888. Pflanzen und schnecken. Jenaische Zeitschrift fuer Naturwissenschaften.

Stitz, M., Hartl, M., Baldwin, I.T., Gaquerel, E., 2014. Jasmonoyl-L-isoleucine coordinates metabolic networks required for anthesis and floral attractant emission in wild tobacco (*Nicotiana attenuata*). *The Plant Cell* **26**, 3964–3983.

Thines, B., Katsir, L., Melotto, M., Niu, Y., Mandaokar, A., Liu, G., et al., 2007. JAZ repressor proteins are targets of the SCF^{COI1} complex during jasmonate signalling. *Nature* **448**, 661–665.

Tini, G., Marchetti, L., Priami, C., Scott-Boyer, M.-P., 2019. Multi-omics integration—a comparison of unsupervised clustering methodologies. *Briefings in Bioinformatics* **20**, 1269–1279.

VanDoorn, A., Kallenbach, M., Borquez, A.A., Baldwin, I.T., Bonaventure, G., 2010. Rapid modification of the insect elicitor N-linolenoyl-glutamate via a lipoxygenase-mediated mechanism on *Nicotiana attenuata* leaves. *BMC Plant Biology* **10**, 1–11.

Von Marilaun, A.K., 1890. Pflanzenleben. Verlag des Bibliographischen instituts.

Wang, B., Lin, Z., Li, X., Zhao, Y., Zhao, B., Wu, G., et al., 2020. Genome-wide selection and genetic improvement during modern maize breeding. *Nature Genetics* **52**, 565–571.

Wang, M., Schäfer, M., Li, D., Halitschke, R., Dong, C., McGale, E., et al., 2018. Blumenols as shoot markers of root symbiosis with arbuscular mycorrhizal fungi. *eLife* **7**, e37093.

Wang, X., Liu, Y., Han, Z., Chen, Y., Huai, D., Kang, Y., et al., 2021. Integrated transcriptomics and metabolomics analysis reveal key metabolism pathways contributing to cold tolerance in peanut. *Frontiers in Plant Science* 2597.

Wasternack, C., Feussner, I., 2018. The oxylipin pathways: Biochemistry and function. *Annual Review of Plant Biology* **69**, 363–386.

Wasternack, C., Hause, B., 2013. Jasmonates: Biosynthesis, perception, signal transduction and action in plant stress response, growth and development. An update to the 2007 review in annals of botany. *Annals of Botany* **111**, 1021–1058.

Wu, J., Hettenhausen, C., Schuman, M.C., Baldwin, I.T., 2008. A comparison of two *Nicotiana attenuata* accessions reveals large differences in signaling induced by oral secretions of the specialist herbivore *Manduca sexta*. *Plant Physiology* **146**, 927–939.

Xie, D.-X., Feys, B.F., James, S., Nieto-Rostro, M., Turner, J.G., 1998. COI1: an *Arabidopsis* gene required for jasmonate-regulated defense and fertility. *Science* **280**, 1091–1094.

Xu, S., Brockmöller, T., Navarro-Quezada, A., Kuhl, H., Gase, K., Ling, Z., et al., 2017. Wild tobacco genomes reveal the evolution of nicotine biosynthesis. *Proceedings of the National Academy of Sciences* **114**, 6133–6138.

Zhao, N., Wang, W., Grover, C.E., Jiang, K., Pan, Z., Guo, B., et al., 2022. Genomic and GWAS analyses demonstrate phylogenomic relationships of *Gossypium barbadense* in China and selection for fibre length, lint percentage and *Fusarium* wilt resistance. *Plant Biotechnology Journal* **20**, 691–710.

Zhou, W., Kügler, A., McGale, E., Haverkamp, A., Knaden, M., Guo, H., et al., 2017. Tissue-specific emission of (E)-α-bergamotene helps resolve the dilemma when pollinators are also herbivores. *Current Biology* **27**, 1336–1341.

Using natural variation to achieve a whole-plant functional understanding of the responses mediated by jasmonate signaling

Rishav Ray, Dapeng Li, Rayko Halitschke, Ian T. Baldwin

Published in The Plant Journal 99.3 (2019): 414-425.

DOI: https://doi.org/10.1111/tpj.14331

In **Manuscript I**, we review the literature pertaining to JA-signaling, focusing on the *N. attenuata* system, and discuss the various layers of defense which it mediates. We argue that the diverse responses are best understood in the context of the organism and its ecological surroundings. We discuss the effects of JA signaling organism-level, specifically the responses that influence a plant's Darwinian fitness. Furthermore, analyzing the natural variation in JA signaling components within plants and populations, a comprehensive understanding of the functional role of this signaling cascade can be achieved, and we provide examples from the *Nicotiana attenuata* system to support this approach.

FORM 1

Manuscript No. I

Manuscript title: Using natural variation to achieve a whole-plant functional understanding of the responses mediated by jasmonate signaling

Authors: Rishav Ray, Dapeng Li, Rayko Halitschke, Ian T. Baldwin

Bibliographic information: The Plant Journal 99.3 (2019): 414-425.

The candidate is

☒ First author, ☐ Co-first author, ☐ Corresponding author, ☐ Co-author.

Status: Published

Authors' contributions (in %) to the given categories of the publication

Author	Conceptual	Writing the manuscript
Rishav Ray	10%	30%
Dapeng Li	15%	10%
Rayko Halitschke	20%	15%
Ian T. Baldwin	55%	45%
Total:	100%	100%

Signature candidate

Signature supervisor
(member of the Faculty)

the plant journal

SEB Society for Experimental Biology

The Plant Journal (2019) **99**, 414–425 doi: 10.1111/tpj.14331

FOCUSED REVIEW

Using natural variation to achieve a whole-plant functional understanding of the responses mediated by jasmonate signaling

Rishav Ray, Dapeng Li, Rayko Halitschke and Ian T. Baldwin*

Department of Molecular Ecology, Max Planck Institute for Chemical Ecology, Hans-Knöll-Straße 8, D-07745 Jena, Germany

Received 24 January 2019; revised 25 February 2019; accepted 27 February 2019; published online 29 March 2019.
*For correspondence (e-mail baldwin@ice.mpg.de).

SUMMARY

The dramatic advances in our understanding of the molecular biology and biochemistry of jasmonate (JA) signaling have been the subject of several excellent recent reviews that have highlighted the phytohormonal function of this signaling pathway. Here, we focus on the responses mediated by JA signaling which have consequences for a plant's Darwinian fitness, i.e. the organism-level function of JA signaling. The most diverse module in the signaling cascade, the JAZ proteins, and their interactions with other proteins and transcription factors, allow this canonical signaling cascade to mediate a bewildering array of traits in different tissues at different times; the functional coherence of these diverse responses are best appreciated in an organismal/ecological context. From published work, it appears that jasmonates can function as the 'Swiss Army knife' of plant signaling, mediating many different biotic and abiotic stress and developmental responses that allow plants to contextualize their responses to their frequently changing local environments and optimize their fitness. We propose that a deeper analysis of the natural variation in both within-plant and within-population JA signaling components is a profitable means of attaining a coherent whole-plant functional perspective of this signaling cascade, and provide examples of this approach from the *Nicotiana attenuata* system.

Keywords: Jasmonate signaling, natural variation, plant fitness, tissue specificity, MAGIC population, *Nicotiana attenuata*.

INTRODUCTION

Plants, perhaps as a consequence of being sessile organisms, have evolved to be master chemists, synthesizing a plethora of natural products that allow them to solve the ecological challenges posed by their immobility. These natural products shape plant growth, development and Darwinian fitness, and are frequently produced in response to signals from the environment. Jasmonate (JA) signaling plays a central role in orchestrating the environmental responsiveness of a plant's repertoire of natural products, particularly with regard to the sectors that mediate herbivore and pathogen resistance (Wasternack and Hause, 2013; Howe *et al.*, 2018; Wasternack and Feussner, 2018).

Most of the work to understand the JA pathway has been carried out in Arabidopsis, primarily due to the advances that have been made in understanding the physiology of this model plant, advances enabled by a well-annotated and comparatively simple genome and impressive genomic resources. Furthermore, the availability of mutants in Arabidopsis, tomato and rice has facilitated the detailed characterization of the individual enzymatic steps of JA biosynthesis (Li *et al.*, 2001; Browse, 2009; Dhakarey *et al.*, 2016). Through mutant screens, enzymes have been identified that provide the initial fatty acid substrates, catalyze the multiple biosynthetic steps in the octadecanoid pathway producing JA, conjugate JA to the active form, JA-Ile, or channel JA into degradation pathways that include methylation, glycosylation and hydroxylation or carboxylation reactions (Wasternack and Feussner, 2018). The availability of these biosynthesis and signaling mutants has fueled the discovery of an impressive catalog of traits which are regulated by JA signaling. However, the overall paucity of field studies with these JA signaling mutants has thwarted an organism-level functional understanding of these diverse traits, which is the objective of this review.

Amortizing natural variation in model species has proven to be one of the most powerful means of understanding the evolutionary significance of traits (Gasch *et al.*, 2016), and the considerable genetic resources available in Arabidopsis and other model crops, such as rice and tomato, have been leveraged to understand the responses mediated by JA signaling in genome-wide association studies (GWAS) and quantitative trait locus (QTL) mapping studies with JA-elicited plants, or more simply by comparing accessions with extreme phenotypes under the experimental conditions. In the next section, we review the traits that have been uncovered in these studies.

NATURAL VARIATION IN JA-MEDIATED RESPONSES

Interactions between JA and other phytohormones are crucial factors which plants are likely to regulate to minimize growth and defense trade-offs. Proietti *et al.* (2018) performed GWAS on 349 natural accessions of Arabidopsis to dissect the crosstalk of salicylic acid (SA) and abscisic acid (ABA) with JA. The magnitude of change in JA-induced expression levels of the *PLANT DEFENSIN1.2* (*PDF1.2*) gene was calculated for each accessions 24 h after treating the leaves with methyl jasmonate (MeJA) alone or a combination of MeJA and SA or ABA, respectively, as a readout for GWAS and interpreted as evidence of phytohormonal 'crosstalk', without specifying the nature of the interaction. Through fine mapping and transfer DNA insertion mutant analysis, two genes, encoding a glyoxalase protein and a response regulator involved in cytokinin signaling, were found to be involved in the JA–SA interaction and also in resistance against *Botrytis cinerea*. Similarly, an uncharacterized cation efflux family protein was shown to affect the interaction of JA–ABA signaling by suppressing MeJA-induced expression of *PDF1.2* and *VSP2* and resistance against *Mamestra brassicae* (Proietti *et al.*, 2018). Although these studies highlight potential players in JA–SA and JA–ABA 'crosstalk', their functional roles in the interaction remain unclear as the phytohormone levels were not analyzed when the plants were challenged with a pathogen or herbivore. In another study, ethylene–JA interactions were found to affect the growth and elongation of rice mesocotyls and coleoptiles. Using publically available resequencing data of 3000 rice accessions, the authors identified a gene, *gaoyao1* (*GY1*) which is homologous to two Arabidopsis lipases, *DONGLE* (*DGL*) and *defective in anther dehiscence1* (*DAD1*) (Xiong *et al.*, 2017). *DONGLE* is the first enzyme in JA biosynthesis, and an allelic difference in its homolog GY1 suppresses JA biosynthesis in rice and promotes the elongation of mesocotyls and coleoptiles with increased ethylene production. A GWAS was performed on JA levels for 221 rice varieties and identified two pectin-modifying genes, *OsPME1* and *OsTSD2*, which are epigenetically regulated by a NAD(+)-dependent histone deacetylase gene, *OsSRT1*, indicating the interaction of methanol and JA signaling in the regulation of senescence in rice (Fang *et al.*, 2016). These GWAS investigations identified previously uncharacterized genes and mechanisms that regulate JA signaling, presumably to maximize plant growth and fitness, with agronomic importance.

In another study, significantly elevated JA and sugar levels were found in eight *Arabis alpina* accessions in response to cold stress, suggesting an interaction of JA and other phytohormones with sugar signaling in response to altitude and other environmental characteristics of the plant's native habitat in the French Alps (Wingler *et al.*, 2014). Furthermore, JA levels across accessions were negatively correlated with chlorophyll content, which the authors interpreted as suggesting a role for JA in acclimation and mediating plant responses to abiotic stresses associated with altitude.

Jasmonate signaling plays a pivotal role in orchestrating plant inducible defenses to herbivory. The ability to synchronize increases in resistance with herbivore attack has clear fitness benefits for plants in nature (Baldwin, 1998), yet we still have little understanding of the causes and fitness consequences of population-level genotypic variation in JA signaling. In a recent study of seven Arabidopsis accessions elicited by either insect attack or JA treatment, the overall inducible herbivore resistance was found to be highly variable across accessions and negatively correlated with constitutive resistance (Rasmann *et al.*, 2015). Such apparent trade-offs between constitutive and induced resistance suggest that the JA-mediated expression of resistance traits is costly or otherwise physiologically or evolutionarily constrained, generating patterns of heterogeneity within populations. Similar heterogeneity was reported in two maize accessions that differ in their resistance to herbivory – one of the accessions, Mp708, had higher constitutive transcript levels of JA biosynthesis and response genes, and performed better under herbivory compared with the susceptible genotype Tx601 (Shivaji *et al.*, 2010). Interestingly, another study investigating herbivory by spider mites on two extreme Arabidopsis accessions in a time series analysis found the overall initial transcriptional responses to herbivory to be similar in the two accessions (Zhurov *et al.*, 2014). The differentially expressed genes (DEGs) clustered together irrespective of genotype at the first time point (1 h after feeding) while later time points (3, 6, 12, 24 h) clustered by genotype. When enriched by their Gene Ontology (GO) terms, the early time point DEGs were involved in perception, signaling and transcriptional activation processes, whereas the DEGs in the later time points were involved in enzymatic activities for the production and alteration of defensive metabolites in response to herbivory and JA elicitation. The results were further validated using JA signaling mutants that performed significantly worse than wild-type plants when challenged with the herbivore. This study

revealed that the different JA-elicited modules have different temporal dynamics in different accessions and suggested that the initial transcriptional reconfiguration in response to herbivory is broadly conserved across accessions. The evolution of this initial transcriptional reconfiguration was analyzed in a study of six *Nicotiana* species, in which plants were wounded and treated with oral secretion (OS) from specialist *Manduca sexta* or generalist *Spodoptera littoralis* larvae, respectively, and fatty acid–amino acid conjugates (FAC), a class of JA elicitors found in these larval OS (Halitschke *et al.*, 2001; Roda *et al.*, 2004). The study revealed different responses across species for the same elicitors, indicating their rapid evolution within the genus. The authors also reported a leucine-rich repeat receptor kinase, which functions independently of the JA signaling pathway but negatively regulates JA biosynthesis and the hydroxylation of JA-Ile. This modulation of JA signaling is likely to suppress defense elicitation effects, perhaps to regulate putative growth–defense trade-offs (Zhou *et al.*, 2016). It is tempting to speculate that similar mechanisms might be at play in the intra-species natural variation in JA signaling and hence would be testable with extant populations. In a meta-analysis, Bhosale *et al.* (2013) used 41 untreated leaves from three different Arabidopsis accessions originating from six different laboratories and used the residual expression, after removing the laboratory and accession effects, to uncover biologically relevant co-expression modules (Bhosale *et al.*, 2013). The residual variance accounted for an average of 52.5% for a single gene, which was substantially higher than the variance due to the accessions, lab and lab–accession interactions. When the gene modules were enriched for GO terms, 'response to JA stimulus' was one of the top-scoring GO modules in the network. As a proof of concept, the authors identified a previously uncharacterized component, ILL6 which acts as a negative regulator of JA accumulation and response, potentially as an amidohydrolase of JA-Ile. This result highlights the fact that variation in growing conditions alters regulatory mechanisms, and JA signaling is a top mediator of responses to subtle environmental changes. Whiteman *et al.* (2011) developed a plant–insect system with Arabidopsis and *Scaptomyza flava*, a drosophilid fly whose larvae feed on Arabidopsis in nature. Using different natural accessions, it was found that female flies caused significantly more feeding punctures and had higher oviposition rates on the Tsu-0 accession, which has been previously reported to be susceptible to attack from specialist herbivores (Pfalz *et al.*, 2007). Fly larvae also performed significantly better on the Tsu-0 accession than on the Col-0 accession. The leaf area mined by larvae on JA- and glucosinolate-deficient mutants was significantly greater than on Col-0 plants, indicating that the JA and glucosinolate defense pathways are important in mediating quantitative resistance of the plant against *S. flava* herbivory (Whiteman *et al.*, 2011).

These studies highlight the importance of JA as a central mediator of the responses of plants to environmental stresses but fall short of understanding whether the elicited responses benefit plants by increasing their fitness and do not illuminate the reasons why so much natural variation exists in this signaling pathway. This limitation is partly due to the overall paucity of mechanistic understanding of the observed natural variation coupled with the fact that evaluating the fitness effects of JA-elicited responses without a deep understanding of the plant's diverse natural histories is challenging.

Nicotiana attenuata, an ecological model plant, is a diploid tobacco native to the Great Basin Desert of North America. It enjoys a rather unique position scientifically, because hundreds of transgenic lines have been studied in the field over the past two decades to understand the fitness consequences of precisely defined changes in gene expression for plants growing in their native habitats. Jasmonate signaling was found to be important for this plant's performance in nature early in the research program (Baldwin *et al.*, 1994a, 1997; Baldwin, 1998). Several transgenic lines with impaired JA production through RNA interference (RNAi)-mediated silencing of JA biosynthetic genes (including *GLA1*, *LOX3*, *AOS*, *AOC*, *OPR3* and *JAR4/-6*) or by creating 'jasmonate sinks' (by silencing *JME* and overexpressing *JMT*) have been released in the plant's natural habitat to better understand the diverse functional consequences of JA signaling (see, for example, Kessler *et al.*, 2004; Stitz *et al.*, 2011; Kallenbach *et al.*, 2012; Machado *et al.*, 2016). Similarly, the function of signaling components up- and downstream of JA production have been characterized in field releases of plants silenced in the expression of *COI1* and *JAZ* genes, as well as in *WRKY* transcription factors and early signaling protein kinases (Skibbe *et al.*, 2008; Wu *et al.*, 2008; Kallenbach *et al.*, 2012; Oh *et al.*, 2012, 2013). This 'sledgehammer' reverse genetics approach has provided both mechanistic and functional understanding of within-plant JA signaling diversity in *N. attenuata* and has paved the way to map this diversity of responses at a population level to achieve a functionally coherent understanding of the pathway.

In this focused review, we discuss the within-plant diversity (tissue- and elicitation-specific changes with different dynamics) of JA signaling networks uncovered in *N. attenuata*, followed by within-population diversity (differences among individuals) and its ecological consequences. Finally, we propose how this multilevel variation can be utilized to attain a holistic functional perspective of JA signaling using sophisticated forward genetic tools that amortize the considerable natural variation in JA signaling that occurs in this species.

FUNCTIONAL DIVERSITY OF JA SIGNALING IN *N. ATTENUATA*

The JA biosynthesis pathway has been intensively reviewed (Wasternack, 2015; Wasternack and Feussner, 2018), thus it is not the main scope of this paper. Briefly, in response to herbivore attack, which triggers a burst of accumulation of JA-Ile, JAZs are recruited by the F-box protein COI1 that binds JA-Ile and are subsequently ubiquitinated and degraded by the 26S proteasome. When this occurs, the inhibition of MYC transcription factors is released and transcription of early JA-responsive genes is activated. Tissue-specific transcription factors, the 13 JAZ proteins, and the variants of NINJA in the *N. attenuata* genome make up the within-plant diversity that enables JA responses to be rendered tissue-specific to tailor responses to different attackers (Figure 1a). Jasmonate signaling is strongly amplified when herbivore-specific FAC elicitors are introduced into wounds (Halitschke *et al.*, 2001), which in turn activate mitogen-activated (SIPK and WIPK) and calcium-dependent (CDPK4/5) protein kinases and a lectin receptor kinase (LecRK1) which provide important context-dependent regulation of JA signaling and its outputs (Meldau *et al.*, 2009; Kallenbach *et al.*, 2010; Gilardoni *et al.*, 2011; Yang *et al.*, 2012). In this way, the JA signaling pathway can function with the versatility of a Swiss Army knife, providing context-dependent regulation for a host of different responses that function in direct and indirect defense, tolerance and avoidance responses (Figure 1b; Li *et al.*, 2016) that are hard to make sense of unless they are studied in a single species and in a plant's native environmental context. Broadly speaking, *N. attenuata* exhibits the following four classes of defense responses to herbivore attack, in which JA signaling plays a central role.

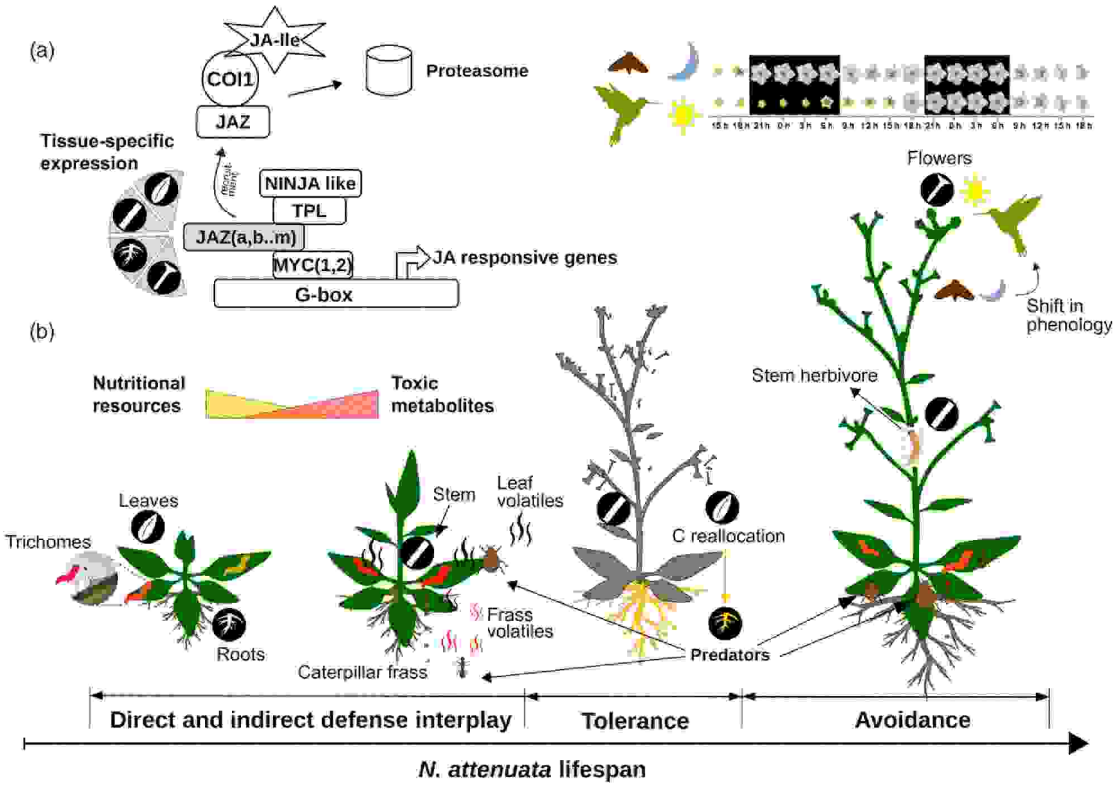

Figure 1. Schematic of the diversity of different defense responses mediated by jasmonate (JA) signaling in *Nicotiana attenuata*.
(a) The canonical JA-Ile signaling cascade, as largely revealed by work in Arabidopsis and tomato, is fully operational in *N. attenuata* and includes the structural and functional diversity mediated by 13 JAZ proteins, but also a NINJA-like protein which provides floral-specific defense signaling (Li *et al.*, 2017) in *N. attenuata*.
(b) Jasmonate signaling mediates a sophisticated six-layered suite of defense, tolerance and avoidance responses to herbivore attack in *N. attenuata* which are expressed at different times in the plant's life cycle and are described in the text. The up/down herbivory-regulated defensive and nutritional metabolites for the herbivore are shown as red and yellow bars indicating that as herbivore load increases the levels of defense-related metabolites generally increase while levels of nutritional metabolites for the herbivore decrease. However, when the attack comes from a specialized herbivore that can co-opt a plant defense mechanism for its own defense, as is the case with *Manduca sexta* attack and nicotine production, the production of defense metabolites can be strongly downregulated.

 The Plant Journal, (2019), **99**, 414–425

DIRECT DEFENSES

Direct defense against herbivory involves a host of different metabolites such as nicotine, trypsin protease inhibitors, phenolamides and diterpene glycosides, that impair the growth and digestive capabilities of the herbivores and act as deterrents, thus reducing the probability of further damage. A majority of these defensive metabolites are regulated by JA signaling in some tissues (Halitschke and Baldwin, 2003; Heiling *et al.*, 2010; Kaur *et al.*, 2010; Kallenbach *et al.*, 2012; Machado *et al.*, 2016). Different variants of the canonical JA signaling cascade will activate different metabolites in a tissue-specific manner. For example, chlorogenic acid is specifically upregulated in the pith of stems when larvae of the pith-feeding weevil *Trichobaris mucorea* attack stems of *N. attenuata*, the regulation of which is locally mediated by JA (Lee *et al.*, 2017). Interestingly, this phenolic is neither regulated by JA nor elicited by herbivory in tissues other than the pith, such as leaves, where it functions as a 'sun screen' that accumulates in response to UVB exposure (Ballaré *et al.*, 1996; Dinh *et al.*, 2013). By comparing the field performance of the wild type, JA-signaling mutants and plants silenced in the expression of pathway-specific biosynthetic genes, the direct defensive function of particular sectors of JA-regulated secondary metabolism has been rigorously demonstrated.

INDIRECT DEFENSES

Jasmonate signaling mediates different responses to herbivore attack in *N. attenuata* throughout the plant's life cycle. Glandular trichomes are one of the first physical barriers that the herbivore must overcome to feed on the leaves, and trichome development is regulated by JA signaling (Xu *et al.*, 2002; Paschold *et al.*, 2007; Yoshida *et al.*, 2009). The glandular trichomes of solanaceous taxa are also the sites of synthesis of many different secondary metabolites (Laue *et al.*, 2000; Kang *et al.*, 2010; Weinhold and Baldwin, 2011). One of the most abundant compound classes in *N. attenuata* glandular trichomes are the *O*-acyl sugars which are consumed by neonate caterpillars as their first meal after hatching. These ingested *O*-acyl sugars are rapidly saponified in the high-pH midguts of the larvae, releasing volatile short-chain fatty acids that impart a distinctive odor to larval bodies and frass. The fresh redolent caterpillar frass, as it falls to the ground, attracts the attention of ground-foraging predators, including ants (Weinhold and Baldwin, 2011) and possibly lizards (Stork *et al.*, 2011), and thereby functions as an indirect defense by tagging the larvae for predation. When herbivores attack leaves, plants employ other forms of indirect defenses by releasing herbivory-induced plant volatiles (HIPVs) which increase the foraging efficiency of higher trophic levels that prey upon herbivorous insects (Dicke and Baldwin, 2010). In *N. attenuata*, these HIPV blends include terpenes, such as linalool and (E)-α-bergamotene (Halitschke *et al.*, 2000; Kessler and Baldwin, 2001), that are thought to function as long-distance cues and are released systemically from plants and require JA signaling and a pair of WRKY transcription factors (WRKY3/6) for their activation (Kessler *et al.*, 2004; Skibbe *et al.*, 2008). Interestingly, green leaf volatiles, that are released independently of JA signaling, are amplified when JAZh is silenced (Oh *et al.*, 2012), are under circadian control (Joo *et al.*, 2018) and are thought to function as short-distance cues for the predators as they are released more from attacked leaves than the entire plant (Kessler and Baldwin, 2001; Halitschke *et al.*, 2008; Allmann and Baldwin, 2010; Schuman *et al.*, 2012; Allmann *et al.*, 2013; Zhou *et al.*, 2017).

TOLERANCE RESPONSES

When consumed by highly adapted specialist herbivores that are able to sequester toxic compounds for their own defense, plants may rapidly downregulate the production of these toxins (e.g. nicotine; Winz and Baldwin, 2001) and also activate tolerance responses that translocate nutrient or carbon resources from attacked tissues (shoots) to spatially isolated belowground root sinks protected from leaf-feeding herbivores. These bunkered reserves can be rapidly remobilized to support regrowth and flowering after the herbivore pressure has subsided, and allow plants to tolerate attack from folivores and optimize fitness in the face of predictably varying herbivore loads. The mechanism of this transient reallocation of photoassimilates from shoots to roots is known to be independent of JA and requires the activity of the GAL83 subunit of a SNF1-related kinase (Schwachtje *et al.*, 2006). However, the remobilization of reserves from roots back to shoots to support regrowth requires JA signaling with a particular role for root-sequestered JA signaling, as shown by micrografting experiments with JA-deficient lines (Machado *et al.*, 2013). Regrowth after herbivore attack involves a complex suite of responses mediated by the intersection of JA signaling with many other phytohormone signaling systems, and will require more work to fully understand it (Machado *et al.*, 2013). While roots play a central role in tolerance responses to herbivore attack, they are also important players in the leaf defense responses discussed above. For instance, in *N. attenuata*, JA levels are highly increased in both shoots and roots in response to folivory, which consequently activates the synthesis of nicotine in the roots that is subsequently mobilized to the shoot for defense. Micrografting experiments with *N. attenuata* have revealed that intact JA signaling in both shoot and root compartments is required for expression of the complete nicotine defense response (Fragoso *et al.*, 2014).

AVOIDANCE RESPONSES

Plants deficient in JA biosynthesis or perception are highly susceptible to attack from both invertebrate (Kessler *et al.*, 2004; Kallenbach *et al.*, 2012) (but not nematodes; Machado *et al.*, 2018) and vertebrate (Machado *et al.*, 2016) herbivores, as well as florivores (Li *et al.*, 2017). The floral tissues are a conduit of Darwinian fitness and hence are one of the most fitness-valuable tissues for plants in later developmental stages. Consequently, consistent with predictions of the optimal defense theory (McKey, 1974), flowers are highly provisioned with defenses. *Manduca sexta* moths commonly oviposit on leaves after pollinating and nectaring on flowers of *N. attenuata* (Kessler, 2012). The neonates hatching from these eggs grow into voracious leaf-eating caterpillars that can be devastating to the plant and against which most of the above-mentioned JA-regulated defenses are likely to have evolved. If these defenses are not effective and the larvae continue to consume leaf material, JA signaling activates a unique avoidance response, which entails interactions with components of the plant circadian clock, to switch the flowers' first opening time from night to day. This change in flower opening (and scenting) time allows the plant to switch pollinators from moths to hummingbirds, thereby avoiding the collateral damage that results from attracting this moth to function as a pollinator (Kessler *et al.*, 2010). Silencing the expression of *ZEITLUPE* (*ZTL*), a clock component gene, alters flowering time and phenocopies the flower movement pattern for the first night when flowers are open, as is observed after herbivory (Yon *et al.*, 2016). A number of lines of evidence suggest that JA signaling is directly involved in altering the function of this component of the clock. Seven of the thirteen JAZ proteins (JAZa, JAZb, JAZd, JAZe, JAZj, JAZk and JAZl; Figure 2a) in *N. attenuata* are known to interact with ZTL in yeast two-hybrid assays (Li *et al.*, 2017). Furthermore, silencing ZTL expression causes a phase-shift in expression pattern of JA-responsive *MYC2a* transcripts in roots (Li *et al.*, 2018), which interestingly interact with JAZi that is only expressed in flowers and known to regulate floral defense (Li *et al.*, 2017). From these results, we infer that JA signaling transiently highjacks the clock to allow plants to switch pollinators, and thereby reduce future herbivore loads. This inference, however, will require additional research to place it on a stronger experimental footing.

Why plants continue to rely on the pollination services of the highly nicotine-tolerant moths and suffer the

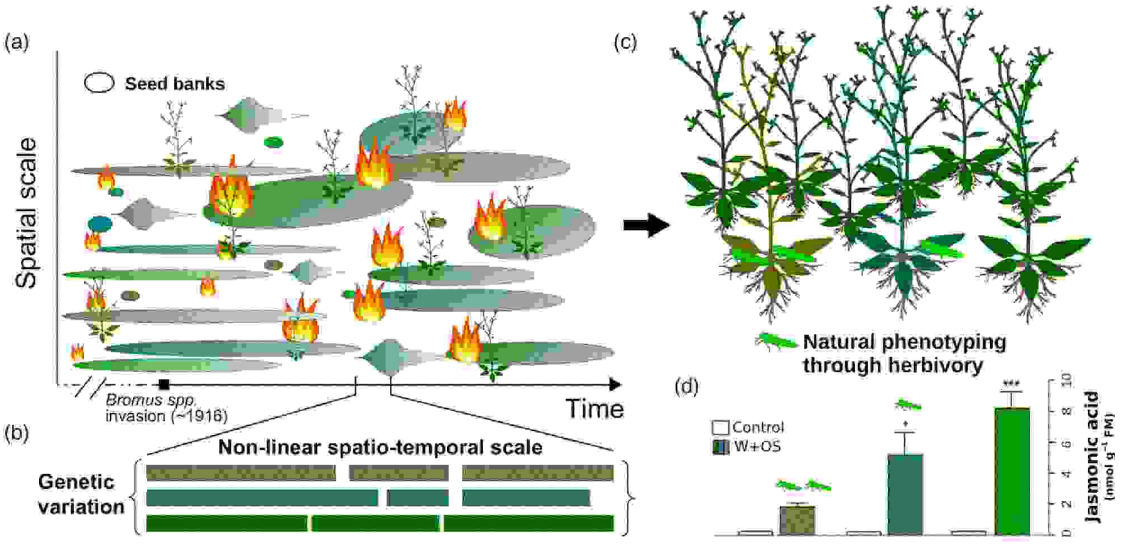

Figure 2. Natural variation in jasmonate (JA) signaling in *Nicotiana attenuata* enables the genetic dissection of the regulation of the pathway.
(a), (b) The post-fire germination behavior of *N. attenuata* recruits plants from long-lived seedbanks separated in both time and space, resulting in natural populations that harbor a substantial amount of genetic variation in JA signaling. The circled areas indicate the spatial distribution and longevity of the seedbanks of *N. attenuata*. The size of the fire icons is proportional to the size of the fires, which in turn determines the amount of opened habitat and the opportunity to stimulate the germination of *N. attenuata* seeds from the seedbanks in the subsequent one to three growing seasons post-fire before the burned habitat is again recolonized by perennial plants. The seedbank colors reflect different genotypes and the color gradients reflect the density of viable seeds that wanes as the seedbank ages with time. The genetic variance that results from plant recruitment from multi-generational seedbanks is shown for a small subset of a population.
(c), (d) High-throughput phenotyping of natural variation in JA signaling using *Empoasca* spp. leaf hoppers which preferentially attack JA-deficient plants. The data are adapted from Kallenbach *et al.* (2012).

collateral damage that comes with their oviposition behavior remains an open question which deserves further experimental work. It might be that these moths, due to the greater distances they travel, provide plants with pollen loads that harbor a greater diversity of pollen genotypes than the locally foraging hummingbird pollinators. This diversity allows plants to select amongst potential mates in mixed pollen loads to increase the genetic diversity of their seedbanks (Bhattacharya and Baldwin, 2012). For a self-compatible species with a very long-lived seedbank, processes that increase the genetic diversity of offspring are likely to increase the chances of surviving the long dormancy periods between fires. At the time of *N. attenuata* flowering in Utah, hummingbirds visit nectar sources in the local areas of their nests, resulting in low rates of outcrossing. Interestingly, the plant then utilizes another JA-mediated defense, nicotine, in floral nectar to disrupt the trap-lining foraging behavior of hummingbirds to increase outcrossing rates with this pollinator (Kessler *et al.*, 2012).

Jasmonate signaling clearly mediates a bewildering array of different responses in plants. When these responses are genetically dissected in a native plant which has not been subjected to rounds of artificial selection, and the genetically manipulated plants are released into the plant's native habitat, it is possible to obtain glimpses of a functionally coherent understanding of how these different responses work together to allow plants to contextualize their responses and maximize fitness. Clearly, JA signaling regulates responses that can be understood as functioning as direct and indirect defenses against current and future attackers, enhancing a plant's tolerance of herbivore attack and avoiding future attack. However, these variants in JA signaling and response that have been generated by RNAi approaches do not necessarily represent natural variation in JA signaling, and hence the raw material from which natural selection could sculpt functional responses. In the next section, we summarize what we know about natural variation in JA signaling in *N. attenuata* and point to a way forward that amortizes this natural variation in a forward genetics approach to understand how evolution has shaped JA signaling networks to optimize plant defense in the face of varying environments.

NATURAL VARIATION IN JA SIGNALING IN *N. ATTENUATA* POPULATIONS

Natural accessions of *N. attenuata* collected from across the species' range in the Great Basin Desert and grown in a common glasshouse environment exhibit highly variable OS-elicited JA profiles and responses (Figures 2d and 3a) indicating a high within-population diversity in the species. Recent advances in untargeted mass spectrometry (MS)-based metabolomics have started to reveal the consequences of this within-population diversity in the layers of specialized metabolism differentially regulated by the JA signaling pathway among accessions (Li *et al.*, 2015). Advances in the speed and decreases in the costs of high-resolution MS instruments have made such analyses a

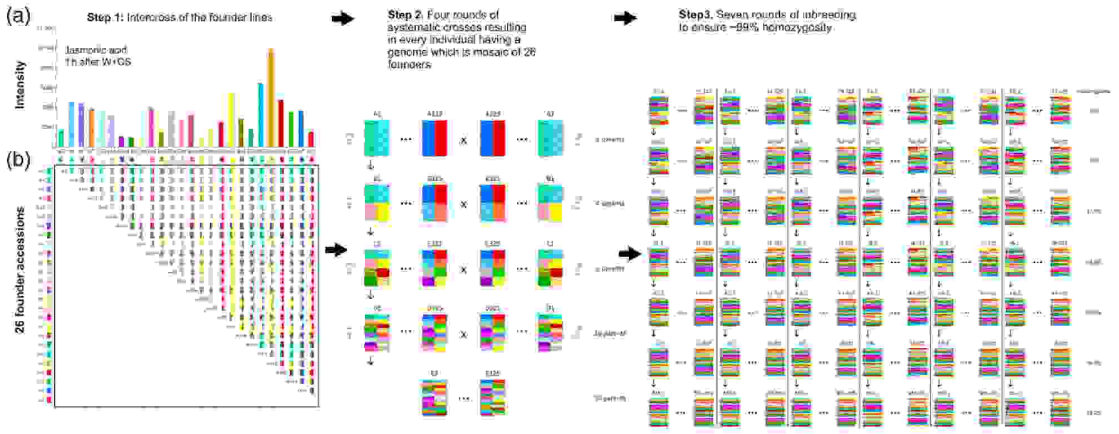

Figure 3. Creation of a Multiparent Advanced Generation Inter-Cross (MAGIC) recombinant inbred line (RIL) population for *Nicotiana attenuata* that captures the species' genetic variation in jasmonate (JA) signaling and other ecologically relevant traits.
(a) Natural variation in herbivory-elicited JA signaling in the 26 founder accessions that were used for the construction of the MAGIC population; leaf JA levels were quantified 1 h after leaf puncture wounds were immediately treated with the oral secretions of *Manduca sexta* larvae (data adapted from Li *et al.*, 2015).
(b)–(d) Construction of the MAGIC population. A complete unidirectional diallelic cross was performed with the 26 accessions, followed by four generations of systematic intercrossing to generate a 6 × 325 membered RIL population that was inbred for six generations to create the final MAGIC RIL population which is about 99% homozygous and harbors different alleles from the 26 founders.

powerful high-throughput (HTP) means of phenotyping natural variation in JA signaling. In addition to this laboratory-based HTP phenotyping, we can utilize native herbivores as accurate JA phenotyping tools in field studies. *Empoasca* spp. leafhoppers, for example, can provide a HTP 'insect-guided' phenotyping tool to rapidly and efficiently screen native populations. The piercing–sucking *Empoasca* spp. leafhoppers apparently 'eavesdrop' on the JA-mediated signaling capacities of their host plants, preferentially selecting those hosts that are deficient in JA accumulation (Kessler *et al.*, 2004; Kallenbach *et al.*, 2012). Intriguingly, this natural phenotyping 'bloodhound' specifically targets JA signaling independently of the known downstream defense metabolites that are regulated by JA signaling, and is thereby a phenotyping tool for rapidly identifying JA-deficient accessions in natural populations [Figure 2c,d, adapted from Kallenbach *et al.* (2012)].

This observation raises the following question: why is there such extensive genetic diversity in natural *N. attenuata* populations? One contributing factor is that the plants largely occur for 2–3 years after fires and time their germination from long-lived seedbanks to initiate growth in the first growing season after a natural burn. Seeds can remain dormant in these seedbanks for hundreds of years and synchronize germination in response to smoke cues that are produced during fires (Baldwin and Morse, 1994; Baldwin *et al.*, 1994b; Preston and Baldwin, 1999). Since the invasion and spread of cheat grass (*Bromus* spp.) into the Great Basin Desert, the size of wildfires has grown substantially, as the dry grass readily spreads lightning-started fires amongst the widely distributed woody species that dominate this habitat. These larger fires are likely to have increased the genetic structure of post-fire populations as these large fires stimulate the germination of seeds from multiple seedbanks of different ages at the same time (Figure 2a). The genetic heterogeneity of these populations is probably maintained by the rapidly changing selection regimes that occur after fires. As one of the first plants to colonize post-fire habitats, *N. attenuata* enjoys low herbivore loads and open and nutrient-rich habitats. As these post-fire habitats are recolonized, herbivore loads and competition from other plant species for fire-released resources dramatically increase, and thereby change the selection for traits that are associated with JA signaling (Lynds and Baldwin, 1998; Baldwin, 2001). The adaptive phenotypic diversity that is associated with JA signaling, coupled with the ability to escape in time that the post-fire germination behavior facilitates, has probably allowed *N. attenuata* to evade selective sweeps that result from strong natural selection in small populations (Bahulikar *et al.*, 2004) and thereby maintain high genetic and metabolic heterogeneity in its natural populations (Figure 2b) (Wu *et al.*, 2008; Schuman *et al.*, 2009; Li *et al.*, 2015).

Population geneticists have long utilized the genetic variance derived from natural populations to query the genetic architecture underlying traits of interest. Recently, the allelic diversity in the genome of two natural accessions collected from Utah and Arizona (Glawe *et al.*, 2003; Wu *et al.*, 2008) has been utilized to create an advanced intercross recombinant inbred line (AI-RIL) population to identify genetic components of indirect defense (Zhou *et al.*, 2017) and arbuscular mycorrhizal interactions (Wang *et al.*, 2018). This AI-RIL approach has recently been extended by creating a 26-parent Multiparent Advanced Generation Inter-Cross (MAGIC) population which we describe in the next section.

CAPTURING INTRA-SPECIES NATURAL VARIATION IN JA SIGNALING WITH A MAGIC POPULATION

Linkage mapping (or QTL mapping) and association mapping (or GWAS) are the two most commonly used statistical frameworks to query the genetic architecture underlying traits of interest. While GWAS can identify associative single nucleotide polymorphisms with 1-bp precision, the procedure has limitations that make it difficult to use with the highly structured natural populations of *N. attenuata*. One of the primary assumptions of GWAS is that there should be no structure in the population, that is, the population must interbreed freely. This is due to the fact that correlating patterns among loci and traits causing variation can create spurious associations between markers and traits where no actual causal relation exists. This problem has long been identified (Li, 1969; Lander and Schork, 1994) and statistical efforts help to address it (Devlin and Roeder, 1999; Pritchard *et al.*, 2000; Yu *et al.*, 2006). Given that *N. attenuata*'s post-fire germination behavior from long-lived seedbanks creates natural populations with substantial genetic structure (Figure 2b), thereby thwarting the use of GWAS, we started a 9-year effort to create a 26-parent MAGIC population that captures the natural variation of the species. MAGIC populations are one of the most powerful forward genetic tools but they also recapitulate aspects of natural *N. attenuata* populations and hence are ideal for planting into native habitats.

Approximately 400 natural accessions of *N. attenuata* have been collected over the past three decades of field work with this species. These accessions were grown in a glasshouse and screened for a panel of ecologically relevant traits for this species, which included JA signaling (Li *et al.*, 2015), *O*-acyl sugar content (Luu *et al.*, 2017) as well as volatile emissions. From this screening, 26 accessions that captured the majority of the phenotypic diversity of the approximately 400 accessions were selected as the founders of the MAGIC population (Figure 3a). Diallelic crossing was performed on the 26 founder lines (with each other) to obtain a set of intermediate crosses which had alleles from each of two parents (Figure 3b). Systematic

intercrossing of the intermediate lines was performed for four generations, resulting in a population of 325 lines, (26 × 25)/2, each harboring genetic contributions from all the 26 founder lines in their genome. Two of six replicate populations were selected and inbred for six subsequent generations to ensure approximately 99% homozygosity across all loci. While phenotyping this large MAGIC population for JA levels can be onerous, the job can be readily 'outsourced' to herbivores such as *Empoasca* leafhoppers, which can identify the JA-deficient lines in a HTP manner under field conditions as described earlier.

Once the variation is quantified, it can be mapped to the identified JA networks mentioned above, much like mapping genomic sequences onto a reference genome, allowing for the discovery of network variants that are of ecological significance. Although there is compelling evidence that the core JA signaling module has remained highly conserved throughout the evolution of vascular plants (Howe *et al.*, 2018; Monte *et al.*, 2018), the elicitation of the core JA module by environmental signals and the resulting physiological responses are highly variable (Li *et al.*, 2016), which in turn might help explain the heterogeneity maintained at the population level. Whether natural variation in the up- and downstream components of the core JA signaling pathway can explain the highly variable distribution of specialized metabolites in *N. attenuata* populations remains an open question. The natural variation in JA-mediated metabolites quantified within *N. attenuata* populations often exceeds the between-population diversity (Li *et al.*, 2015), a pattern consistent with the polymorphic genetic structure of the species (Bahulikar *et al.*, 2004). This coupled variation pattern in the natural populations suggests that the phenotypic variation results from genetic variation in JA accumulation and perception. These polymorphic genetic loci could include regulatory genes that shape downstream responses to JA, potentially including small and long non-coding RNAs. The genetic variation might also be involved in the JA activation/deactivation pathways through mechanisms such as hydroxylation, carboxylation, glycosylation or methylation, which in turn could be subjected to layers of regulation, fine tuning the amplitude, duration and timing of JA-mediated responses. This fine-tuned JA signaling readout, which includes both spatial and temporal variations, mediates various physiological trade-offs and interactions with other signaling pathways.

Given the quantitative variation in JA-induced metabolic profiles and defense phenotypes, it is likely that a transcriptomic analysis of these natural accessions would provide excellent opportunities for identifying previously uncharacterized genes associated with various ecological traits regulated by JA signaling and extending our understanding of JA signaling networks. Moreover, with current advances in unbiased metabolomic techniques the previously inaccessible layers of JA-regulated defense metabolites that are central to plant fitness are now readily accessible and quantifiable. These processes can be conceptualized as adding extra dimensions to existing biological networks at the organism level, dimensions that can be extended to the level of populations. In addition to JA-related traits, the MAGIC RIL population presents an excellent tool with which to uncover the genetic underpinnings of other important ecological traits, including, for example, the recruitment of the plant's root microbiome, mate selection, etc.

We propose that such an unbiased forward genetic approach will pave the way towards a coherent understanding of the molecular mechanisms responsible for plant fitness in natural environments. The approach does not obviate the need for reverse genetic tools, as it is essential to dissect imputed genetic loci to manipulate these molecular mechanisms and evaluate their fitness consequences, both under field and more controlled laboratory conditions. The objective would be an organism-level understanding of the function of this 'Swiss Army knife' of phytohormones.

Summary Box

- Within-plant variation in JA signaling is mediated by a diverse array of proteins such as JAR/JIH which activate/deactivate the bioactive form of JA (JA-Ile), JAZ, NINJA-like proteins, transcription factors, etc. that can mediate various growth and defense phenotypes in a tissue-specific manner when challenged with various abiotic and biotic stress factors.
- Within-population variation in JA occurs when plants face heterogeneous environments and evolve the ability to contextualize their response to these varying factors in order to maximize their fitness; we know very little about the mechanisms responsible for this type of variation.
- The population-level variation can be leveraged to genetically map these variable traits, using increasingly complex AI-RIL and MAGIC mapping populations that harness the power of forward genetics for a species.
- Identifying the genetic components harboring the variable traits in JA signaling that can be dissected from genetically linked QTLs and genomic islands extracted from QTL mapping and GWAS studies will greatly advance our understanding of the evolutionary processes that maintain the natural variation in this important signaling pathway.

Open Questions

- What are the genetic mechanisms responsible for natural variation in JA signaling, particularly in the control of JA-Ile levels?
- How does natural variation in JA signaling at the molecular level influence phenotypic variation and Darwinian fitness at the organismal level?
- Despite the clear advantages of strong JA signaling, which selective forces maintain variation in JA signaling in natural populations of *N. attenuata*?
- If fitness costs of JA-mediated responses are at play in maintaining the natural variation, can these costly responses be uncoupled from the advantageous defenses mediated by JA signaling?
- To what extent do environmentally mediated epigenetic factors affect the genetic configuration and evolution of JA signaling networks?

ACKNOWLEDGEMENTS

The authors thank the Max Planck Society, and the Deutsche Forschungsgemeinschaft Grant, 'Chemical Mediators in Complex Biosystems – ChemBioSys' (SFB 1127) for funding.

CONFLICT OF INTEREST

The authors declare no conflict of interest.

AUTHOR CONTRIBUTIONS

All authors contributed to the writing and revising of the paper.

REFERENCES

Allmann, S. and Baldwin, I.T. (2010) Insects betray themselves in nature to predators by rapid isomerization of green leaf volatiles. *Science*, **329**, 1075–1078.

Allmann, S., Spathe, A., Bisch-Knaden, S., Kallenbach, M., Reinecke, A., Sachse, S., Baldwin, I.T. and Hansson, B.S. (2013) Feeding-induced rearrangement of green leaf volatiles reduces moth oviposition. *eLife*, **2**, e00421.

Bahulikar, R.A., Stanculescu, D., Preston, C.A. and Baldwin, I.T. (2004) ISSR and AFLP analysis of the temporal and spatial population structure of the post-fire annual, *Nicotiana attenuata*, in SW Utah. *BMC Ecol.* **4**, 12.

Baldwin, I.T. (1998) Jasmonate-induced responses are costly but benefit plants under attack in native populations. *Proc. Natl Acad. Sci. USA*, **95**, 8113–8118.

Baldwin, I.T. (2001) An ecologically motivated analysis of plant-herbivore interactions in native tobacco. *Plant Physiol.* **127**, 1449–1458.

Baldwin, I.T. and Morse, L. (1994) Up in smoke: II. Germination of *Nicotiana attenuata* in response to smoke-derived cues and nutrients in burned and unburned soils. *J. Chem. Ecol.* **20**, 2373–2391.

Baldwin, I.T., Schmelz, E.A. and Ohnmeiss, T.E. (1994a) Wound-induced changes in root and shoot jasmonic acid pools correlate with induced nicotine synthesis in *Nicotiana sylvestris* Spegazzini and Comes. *J. Chem. Ecol.* **20**, 2139–2157.

Baldwin, I.T., Staszak-Kozinski, L. and Davidson, R. (1994b) Up in smoke: I. Smoke-derived germination cues for postfire annual, *Nicotiana attenuata* Torr. Ex. Watson. *J. Chem. Ecol.* **20**, 2345–2371.

Baldwin, I.T., Zhang, Z.-P., Diab, N., Ohnmeiss, T.E., McCloud, E.S., Lynds, G.Y. and Schmelz, E.A. (1997) Quantification, correlations and manipulations of wound-induced changes in jasmonic acid and nicotine in *Nicotiana sylvestris*. *Planta*, **201**, 397–404.

Ballaré, C.L., Scopel, A.L., Stapleton, A.E. and Yanovsky, M.J. (1996) Solar ultraviolet-B radiation affects seedling emergence, DNA integrity, plant morphology, growth rate, and attractiveness to herbivore insects in *Datura ferox*. *Plant Physiol.* **112**, 161–170.

Bhattacharya, S. and Baldwin, I.T. (2012) The post-pollination ethylene burst and the continuation of floral advertisement are harbingers of non-random mate selection in *Nicotiana attenuata*. *Plant J.* **71**, 587–601.

Bhosale, R., Jewell, J.B., Hollunder, J., Koo, A.J., Vuylsteke, M., Michoel, T., Hilson, P., Goossens, A., Howe, G.A. and Maere, S. (2013) Predicting gene function from uncontrolled expression variation among individual wild-type *Arabidopsis* plants. *Plant Cell*, **25**, 2865–2877, tpc–113.

Browse, J. (2009) The power of mutants for investigating jasmonate biosynthesis and signaling. *Phytochemistry*, **70**, 1539–1546.

Devlin, B. and Roeder, K. (1999) Genomic control for association studies. *Biometrics*, **55**, 997–1004.

Dhakarey, R., Kodackattumannil Peethambaran, P. and Riemann, M. (2016) Functional analysis of jasmonates in rice through mutant approaches. *Plants*, **5**, 15.

Dicke, M. and Baldwin, I.T. (2010) The evolutionary context for herbivore-induced plant volatiles: beyond the "cry for help". *Trends Plant Sci.* **15**, 167–175.

Dinh, S.T., Galis, I. and Baldwin, I.T. (2013) UV radiation and 17-hydroxygeranyllinalool diterpene glycosides provide durable resistance against mirid (*Tupiocoris notatus*) attack in field-grown *Nicotiana attenuata* plants. *Plant, Cell Environ.* **36**, 590–606.

Fang, C., Zhang, H., Wan, J. *et al.* (2016) Control of leaf senescence by an MeOH-jasmonates cascade that is epigenetically regulated by *OsSRT1* in rice. *Mol. Plant*, **9**, 1366–1378.

Fragoso, V., Rothe, E., Baldwin, I.T. and Kim, S.-G. (2014) Root jasmonic acid synthesis and perception regulate folivore-induced shoot metabolites and increase *Nicotiana attenuata* resistance. *New Phytol.* **202**, 1335–1345.

Gasch, A.P., Payseur, B.A. and Pool, J.E. (2016) The power of natural variation for model organism biology. *Trends Genet.* **32**, 147–154.

Gilardoni, P.A., Hettenhausen, C., Baldwin, I.T. and Bonaventure, G. (2011) *Nicotiana attenuata LECTIN RECEPTOR KINASE1* suppresses the insect-mediated inhibition of induced defense responses during *Manduca sexta* herbivory. *Plant Cell*, **23**, 3512–3532.

Glawe, G.A., Zavala, J.A., Kessler, A., Van Dam, N.M. and Baldwin, I.T. (2003) Ecological costs and benefits correlated with trypsin protease inhibitor production in *Nicotiana attenuata*. *Ecology*, **84**, 79–90.

Halitschke, R. and Baldwin, I.T. (2003) Antisense LOX expression increases herbivore performance by decreasing defense responses and inhibiting growth-related transcriptional reorganization in *Nicotiana attenuata*. *Plant J.* **36**, 794–807.

Halitschke, R., Keßler, A., Kahl, J., Lorenz, A. and Baldwin, I.T. (2000) Ecophysiological comparison of direct and indirect defenses in *Nicotiana attenuata*. *Oecologia*, **124**, 408–417.

Halitschke, R., Schittko, U., Pohnert, G., Boland, W. and Baldwin, I.T. (2001) Molecular interactions between the specialist herbivore *Manduca sexta* (Lepidoptera, Sphingidae) and its natural host *Nicotiana attenuata*. III. Fatty acid-amino acid conjugates in herbivore oral secretions are necessary and sufficient for herbivore-specific plant responses. *Plant Physiol.* **125**, 711–717.

Halitschke, R., Stenberg, J.A., Kessler, D., Kessler, A. and Baldwin, I.T. (2008) Shared signals–"alarm calls" from plants increase apparency to herbivores and their enemies in nature. *Ecol. Lett.* **11**, 24–34.

Heiling, S., Schuman, M.C., Schoettner, M., Mukerjee, P., Berger, B., Schneider, B., Jassbi, A.R. and Baldwin, I.T. (2010) Jasmonate and ppHsystemin regulate key malonylation steps in the biosynthesis of 17-hydroxygeranyllinalool diterpene glycosides, an abundant and effective direct defense against herbivores in *Nicotiana attenuata*. *Plant Cell*, **22**, 273–292.

Howe, G.A., Major, I.T. and Koo, A.J. (2018) Modularity in jasmonate signaling for multistress resilience. *Annu. Rev. Plant Biol.* **69**, 387–415.

Joo, Y., Schuman, M.C., Goldberg, J.K., Kim, S.-G., Yon, F., Brütting, C. and Baldwin, I.T. (2018) Herbivore-induced volatile blends with both "fast"

and "slow" components provide robust indirect defence in nature. *Funct. Ecol.* **32**, 136–149.

Kallenbach, M., Alagna, F., Baldwin, I.T. and Bonaventure, G. (2010) *Nicotiana attenuata* SIPK, WIPK, NPR1, and fatty acid-amino acid conjugates participate in the induction of jasmonic acid biosynthesis by affecting early enzymatic steps in the pathway. *Plant Physiol.* **152**, 96–106.

Kallenbach, M., Bonaventure, G., Gilardoni, P.A., Wissgott, A. and Baldwin, I.T. (2012) *Empoasca* leafhoppers attack wild tobacco plants in a jasmonate-dependent manner and identify jasmonate mutants in natural populations. *Proc. Natl Acad. Sci. USA*, **109**, E1548–E1557.

Kang, J.-H., Liu, G., Shi, F., Jones, A.D., Beaudry, R.M. and Howe, G.A. (2010) The tomato *odorless-2* mutant is defective in trichome-based production of diverse specialized metabolites and broad-spectrum resistance to insect herbivores. *Plant Physiol.* **154**, 262–272.

Kaur, H., Heinzel, N., Schöttner, M., Baldwin, I.T. and Gális, I. (2010) R2R3-NaMYB8 regulates the accumulation of phenylpropanoid-polyamine conjugates, which are essential for local and systemic defense against insect herbivores in *Nicotiana attenuata*. *Plant Physiol.* **152**, 1731–1747.

Kessler, D. (2012) Context dependency of nectar reward-guided oviposition. *Entomol. Exp. Appl.* **144**, 112–122.

Kessler, A. and Baldwin, I.T. (2001) Defensive function of herbivore-induced plant volatile emissions in nature. *Science*, **291**, 2141–2144.

Kessler, A., Halitschke, R. and Baldwin, I.T. (2004) Silencing the jasmonate cascade: induced plant defenses and insect populations. *Science*, **305**, 665–668.

Kessler, D., Diezel, C. and Baldwin, I.T. (2010) Changing pollinators as a means of escaping herbivores. *Curr. Biol.* **20**, 237–242.

Kessler, D., Bhattacharya, S., Diezel, C., Rothe, E., Gase, K., Schottner, M. and Baldwin, I.T. (2012) Unpredictability of nectar nicotine promotes outcrossing by hummingbirds in *Nicotiana attenuata*. *Plant J.* **71**, 529–538.

Lander, E. and Schork, N. (1994) Genetic dissection of complex traits. *Science*, **265**, 2037–2048.

Laue, G., Preston, C.A. and Baldwin, I.T. (2000) Fast track to the trichome: induction of *N*-acyl nornicotines precedes nicotine induction in *Nicotiana repanda*. *Planta*, **210**, 510–514.

Lee, G., Joo, Y., Kim, S.-G. and Baldwin, I.T. (2017) What happens in the pith stays in the pith: tissue-localized defense responses facilitate chemical niche differentiation between two spatially separated herbivores. *Plant J.* **92**, 414–425.

Li, C. (1969) Population subdivision with respect to multiple alleles. *Ann. Hum. Genet.* **33**, 23–29.

Li, L., Li, C. and Howe, G.A. (2001) Genetic analysis of wound signaling in tomato. Evidence for a dual role of jasmonic acid in defense and female fertility. *Plant Physiol.* **127**, 1414–1417.

Li, D., Baldwin, I.T. and Gaquerel, E. (2015) Navigating natural variation in herbivory-induced secondary metabolism in coyote tobacco populations using MS/MS structural analysis. *Proc. Natl Acad. Sci. USA*, **112**, E4147–E4155.

Li, D., Baldwin, I. and Gaquerel, E. (2016) Beyond the canon: within-plant and population-level heterogeneity in jasmonate signaling engaged by plant-insect interactions. *Plants*, **5**, 14.

Li, R., Wang, M., Wang, Y., Schuman, M.C., Weinhold, A., Schäfer, M., Jiménez-Alemán, G.H., Barthel, A. and Baldwin, I.T. (2017) Flower-specific jasmonate signaling regulates constitutive floral defenses in wild tobacco. *Proc. Natl Acad. Sci. USA*, **114**, E7205–E7214.

Li, R., Llorca, L.C., Schuman, M.C., Wang, Y., Wang, L., Joo, Y., Wang, M., Vassão, D.G. and Baldwin, I.T. (2018) ZEITLUPE in the roots of wild tobacco regulates jasmonate-mediated nicotine biosynthesis and resistance to a generalist herbivore. *Plant Physiol.* **177**, 833–846.

Luu, V.T., Weinhold, A., Ullah, C., Dressel, S., Schoettner, M., Gase, K., Gaquerel, E., Xu, S. and Baldwin, I.T. (2017) *O*-acyl sugars protect a wild tobacco from both native fungal pathogens and a specialist herbivore. *Plant Physiol.* **174**, 370–386.

Lynds, G.Y. and Baldwin, I.T. (1998) Fire, nitrogen, and defensive plasticity in *Nicotiana attenuata*. *Oecologia*, **115**, 531–540.

Machado, R.A., Ferrieri, A.P., Robert, C.A., Glauser, G., Kallenbach, M., Baldwin, I.T. and Erb, M. (2013) Leaf-herbivore attack reduces carbon reserves and regrowth from the roots via jasmonate and auxin signaling. *New Phytol.* **200**, 1234–1246.

Machado, R.A., McClure, M., Herve, M.R., Baldwin, I.T. and Erb, M. (2016) Benefits of jasmonate-dependent defenses against vertebrate herbivores in nature. *eLife*, **5**, e13720.

Machado, R.A., Arce, C.C., McClure, M.A., Baldwin, I.T. and Erb, M. (2018) Aboveground herbivory induced jasmonates disproportionately reduce plant reproductive potential by facilitating root nematode infestation. *Plant, Cell Environ.* **41**, 797–808.

McKey, D. (1974) Adaptive patterns in alkaloid physiology. *Am. Nat.* **108**, 305–320.

Meldau, S., Wu, J. and Baldwin, I.T. (2009) Silencing two herbivory-activated MAP kinases, SIPK and WIPK, does not increase *Nicotiana attenuata*'s susceptibility to herbivores in the glasshouse and in nature. *New Phytol.* **181**, 161–173.

Monte, I., Ishida, S., Zamarreño, A.M. *et al.* (2018) Ligand-receptor co-evolution shaped the jasmonate pathway in land plants. *Nat. Chem. Biol.* **14**, 480.

Oh, Y., Baldwin, I.T. and Gális, I. (2012) NaJAZh regulates a subset of defense responses against herbivores and spontaneous leaf necrosis in *Nicotiana attenuata* plants. *Plant Physiol.* **159**, 769–788.

Oh, Y., Baldwin, I.T. and Galis, I. (2013) A jasmonate ZIM-domain protein NaJAZd regulates floral jasmonic acid levels and counteracts flower abscission in *Nicotiana attenuata* plants. *PLoS One*, **8**, e57868.

Paschold, A., Halitschke, R. and Baldwin, I.T. (2007) Co(i)-ordinating defenses: NaCOI1 mediates herbivore-induced resistance in *Nicotiana attenuata* and reveals the role of herbivore movement in avoiding defenses. *Plant J.* **51**, 79–91.

Pfalz, M., Vogel, H., Mitchell-Olds, T. and Kroymann, J. (2007) Mapping of QTL for resistance against the crucifer specialist herbivore *Pieris brassicae* in a new *Arabidopsis* inbred line population, Da (1)-12xEi-2. *PLoS One*, **2**, e578.

Preston, C.A. and Baldwin, I.T. (1999) Positive and negative signals regulate germination in the post-fire annual, *Nicotiana attenuata*. *Ecology*, **80**, 481–494.

Pritchard, J.K., Stephens, M. and Donnelly, P. (2000) Inference of population structure using multilocus genotype data. *Genetics*, **155**, 945–959.

Proietti, S., Caarls, L., Coolen, S., Van Pelt, J.A., Van Wees, S.C. and Pieterse, C.M. (2018) Genome-wide association study reveals novel players in defense hormone crosstalk in *Arabidopsis*. *Plant, Cell Environ.* **41**, 2342–2356.

Rasmann, S., Chassin, E., Bilat, J., Glauser, G. and Reymond, P. (2015) Trade-off between constitutive and inducible resistance against herbivores is only partially explained by gene expression and glucosinolate production. *J. Exp. Bot.* **66**, 2527–2534.

Roda, A., Halitschke, R., Steppuhn, A. and Baldwin, I.T. (2004) Individual variability in herbivore-specific elicitors from the plant's perspective. *Mol. Ecol.* **13**, 2421–2433.

Schuman, M.C., Heinzel, N., Gaquerel, E., Svatos, A. and Baldwin, I.T. (2009) Polymorphism in jasmonate signaling partially accounts for the variety of volatiles produced by *Nicotiana attenuata* plants in a native population. *New Phytol.* **183**, 1134–1148.

Schuman, M.C., Barthel, K. and Baldwin, I.T. (2012) Herbivory-induced volatiles function as defenses increasing fitness of the native plant *Nicotiana attenuata* in nature. *eLife*, **1**, e00007.

Schwachtje, J., Minchin, P.E., Jahnke, S., van Dongen, J.T., Schittko, U. and Baldwin, I.T. (2006) SNF1-related kinases allow plants to tolerate herbivory by allocating carbon to roots. *Proc. Natl Acad. Sci. USA*, **103**, 12935–12940.

Shivaji, R., Camas, A., Ankala, A., Engelberth, J., Tumlinson, J.H., Williams, W.P., Wilkinson, J.R. and Luthe, D.S. (2010) Plants on constant alert: elevated levels of jasmonic acid and jasmonate-induced transcripts in caterpillar-resistant maize. *J. Chem. Ecol.* **36**, 179–191.

Skibbe, M., Qu, N., Galis, I. and Baldwin, I.T. (2008) Induced plant defenses in the natural environment: *Nicotiana attenuata* WRKY3 and WRKY6 coordinate responses to herbivory. *Plant Cell*, **20**, 1984–2000.

Stitz, M., Baldwin, I.T. and Gaquerel, E. (2011) Diverting the flux of the JA pathway in *Nicotiana attenuata* compromises the plant's defense metabolism and fitness in nature and glasshouse. *PLoS One*, **6**, e25925.

Stork, W.F., Weinhold, A. and Baldwin, I.T. (2011) Trichomes as dangerous lollipops: do lizards also use caterpillar body and frass odor to optimize their foraging?. *Plant Signal. Behav.* **6**, 1893–1896.

Wang, M., Schäfer, M., Li, D. *et al.* (2018) Blumenols as shoot markers of root symbiosis with arbuscular mycorrhizal fungi. *eLife*, **7**, e37093.

Wasternack, C. (2015) How jasmonates earned their laurels: past and present. *J. Plant Growth Regul.* **34**, 761–794.

Wasternack, C. and Feussner, I. (2018) The oxylipin pathways: biochemistry and function. *Annu. Rev. Plant Biol.* **69**, 363–386.

Wasternack, C. and Hause, B. (2013) Jasmonates: biosynthesis, perception, signal transduction and action in plant stress response, growth and development. An update to the 2007 review in annals of botany. *Ann. Bot.* **111**, 1021–1058.

Weinhold, A. and Baldwin, I.T. (2011) Trichome-derived *O*-acyl sugars are a first meal for caterpillars that tags them for predation. *Proc. Natl Acad. Sci. USA*, **108**, 7855–7859.

Whiteman, N.K., Groen, S.C., Chevasco, D., Bear, A., Beckwith, N., Gregory, T.R., Denoux, C., Mammarella, N., Ausubel, F.M. and Pierce, N.E. (2011) Mining the plant–herbivore interface with a leafmining *Drosophila* of *Arabidopsis*. *Mol. Ecol.* **20**, 995–1014.

Wingler, A., Juvany, M., Cuthbert, C. and Munné-Bosch, S. (2014) Adaptation to altitude affects the senescence response to chilling in the perennial plant *Arabis alpina*. *J. Exp. Bot.* **66**, 355–367.

Winz, R.A. and Baldwin, I.T. (2001) Molecular interactions between the specialist herbivore *Manduca sexta* (Lepidoptera, Sphingidae) and its natural host *Nicotiana attenuata*. IV. Insect-induced ethylene reduces jasmonate-induced nicotine accumulation by regulating putrescine *N*-methyltransferase transcripts. *Plant Physiol.* **125**, 2189–2202.

Wu, J., Hettenhausen, C., Schuman, M.C. and Baldwin, I.T. (2008) A comparison of two *Nicotiana attenuata* accessions reveals large differences in signaling induced by oral secretions of the specialist herbivore *Manduca sexta*. *Plant Physiol.* **146**, 927–939.

Xiong, Q., Ma, B., Lu, X. *et al.* (2017) Ethylene-inhibited jasmonic acid biosynthesis promotes mesocotyl/coleoptile elongation of etiolated rice seedlings. *Plant Cell*, **29**, 1053–1072.

Xu, L., Liu, F., Lechner, E., Genschik, P., Crosby, W.L., Ma, H., Peng, W., Huang, D. and Xie, D. (2002) The SCF^{COI1} ubiquitin-ligase complexes are required for jasmonate response in *Arabidopsis*. *Plant Cell*, **14**, 1919–1935.

Yang, D.-H., Hettenhausen, C., Baldwin, I.T. and Wu, J. (2012) Silencing *Nicotiana attenuata* calcium-dependent protein kinases, *CDPK4* and *CDPK5*, strongly up-regulates wound- and herbivory-induced jasmonic acid accumulations. *Plant Physiol.* **159**, 1591–1607.

Yon, F., Joo, Y., Cortés Llorca, L., Rothe, E., Baldwin, I.T. and Kim, S.-G. (2016) Silencing *Nicotiana attenuata LHY* and *ZTL* alters circadian rhythms in flowers. *New Phytol.* **209**, 1058–1066.

Yoshida, Y., Sano, R., Wada, T., Takabayashi, J. and Okada, K. (2009) Jasmonic acid control of GLABRA3 links inducible defense and trichome patterning in *Arabidopsis*. *Development*, **136**, 1039–1048.

Yu, J., Pressoir, G., Briggs, W.H. *et al.* (2006) A unified mixed-model method for association mapping that accounts for multiple levels of relatedness. *Nat. Genet.* **38**, 203.

Zhou, W., Brockmoller, T., Ling, Z., Omdahl, A., Baldwin, I.T. and Xu, S. (2016) Evolution of herbivore-induced early defense signaling was shaped by genome-wide duplications in *Nicotiana*. *eLife*, **5**, e19531.

Zhou, W., Kugler, A., McGale, E. *et al.* (2017) Tissue-specific emission of (*E*)-α -bergamotene helps resolve the dilemma when pollinators are also herbivores. *Curr. Biol.* **27**, 1336–1341.

Zhurov, V., Navarro, M., Bruinsma, K.A. *et al.* (2014) Reciprocal responses in the interaction between *Arabidopsis* and the cell-content-feeding chelicerate herbivore spider mite. *Plant Physiol.* **164**, 384–399.

A persistent major mutation in canonical jasmonate signaling is embedded in an herbivory-elicited gene network

Rishav Ray, Rayko Halitschke, Klaus Gase, Sabrina M. Leddy, Meredith C. Schuman, Nathalie Rodde, Ian T. Baldwin

Published in Proceedings of the National Academy of Sciences, 120 (35) (2023): e2308500120.

DOI: https://doi.org/10.1073/pnas.2308500120

In **Manuscript II**, we identified a mutation in the JA-Ile biosynthetic gene, *NaJAR4*, in *N. attenuata* natural populations using high resolution GWAS, which was then associated with higher fitness but relatively compromised foliar defenses indicating a growth defense trade-off. However, the floral defense was buffered by a homologous gene, *NaJAR6*, which complemented *NaJAR4* in coordinating the overall defense responses in a spatio-temporal manner within the plant. We estimated the frequency of this variant allele in the seed collection of *N. attenuata* natural populations over several decades, revealing its presence at variable frequencies, implying that a balancing selection through spatio-temporal variation in populations is acting on the loci. Moreover, by analyzing the transcriptomes and metabolomes of different natural accessions, we uncovered a complex gene co-expression network which co-ordinated plant defense response against herbivory. Silencing certain hub genes within this network using RNAi technique, revealed their pleiotropic role in mediating the induced metabolic responses against herbivory, closely following the omnigene model. The findings suggest that compensatory responses from a large gene network, together with environmental variation can allow mutations with significant fitness consequences to persist in natural populations.

FORM 1

Manuscript No. II

Manuscript title: A persistent major mutation in canonical jasmonate signaling is embedded in an herbivory-elicited gene network

Authors: Rishav Ray, Rayko Halitschke, Klaus Gase, Sabrina M. Leddy, Meredith C. Schuman, Nathalie Rodde, Ian T. Baldwin

Bibliographic information: Proceedings of the National Academy of Sciences, 120 (35) (2023): e2308500120.

The candidate is

☒ First author, ☐ Co-first author, ☐ Corresponding author, ☐ Co-author.

Status: Published

Authors' contributions (in %) to the given categories of the publication

Author	Conceptual	Data analysis	Experimental	Writing the manuscript	Provision of material
Rishav Ray	20%	70%	50%	44%	-
Rayko Halitschke	20%	10%	10%	5%	-
Klaus Gase	-	-	15%	2%	-
Sabrina M. Leddy	-	-	10%	-	-
Meredith C. Schuman	20%	-	5%	5%	-
Nathalie Rodde	-	-	-	-	2%
Ian T. Baldwin	40%	20%	10%	44%	98%
Total:	100%	100%	100%	100%	100%

Signature candidate

Signature supervisor
(member of the Faculty)

PNAS RESEARCH ARTICLE | PLANT BIOLOGY OPEN ACCESS

A persistent major mutation in canonical jasmonate signaling is embedded in an herbivory-elicited gene network

Rishav Ray[a], Rayko Halitschke[a], Klaus Gase[b], Sabrina M. Leddy[†], Meredith C. Schuman[a,b], Nathalie Rodde[†], and Ian T. Baldwin[a,1]

Edited by Anne Osbourn, John Innes Centre, Norwich, United Kingdom; received May 21, 2023; accepted July 19, 2023

When insect herbivores attack plants, elicitors from oral secretions and regurgitants (OS) enter wounds during feeding, eliciting defense responses. These generally require plant jasmonate (JA) signaling, specifically, a jasmonoyl-L-isoleucine (JA-Ile) burst, for their activation and are well studied in the native tobacco *Nicotiana attenuata*. We used intraspecific diversity captured in a 26-parent MAGIC population planted in nature and an updated genome assembly to impute natural variation in the OS-elicited JA-Ile burst linked to a mutation in the JA-Ile biosynthetic gene *NaJAR4*. Experiments revealed that *NaJAR4* variants were associated with higher fitness in the absence of herbivores but compromised foliar defenses, with two *NaJAR* homologues (4 and 6) complementing each other spatially and temporally. From decade-long seed collections of natural populations, we uncovered enzymatically inactive variants occurring at variable frequencies, consistent with a balancing selection regime maintaining variants. Integrative analyses of OS-induced transcriptomes and metabolomes of natural accessions revealed that *NaJAR4* is embedded in a nonlinear complex gene coexpression network orchestrating responses to OS, which we tested by silencing four hub genes in two connected coexpressed networks and examining their OS-elicited metabolic responses. Lines silenced in two hub genes (*NaGLR* and *NaFB67*) co-occurring in the *NaJAR4/6* module showed responses proportional to JA-Ile accumulations; two from an adjacent module (*NaERF* and *NaFB61*) had constitutively expressed defenses with high resistance. We infer that mutations with large fitness consequences can persist in natural populations due to compensatory responses from gene networks, which allow for diversification in conserved signaling pathways and are generally consistent with predictions of an omnigene model.

jasmonate signaling | plant defense | MAGIC populations | *NaJAR4* | natural mutations with large fitness effects

Significance

Single-gene mutations with large fitness effects are found in natural populations, contrary to theoretical expectations: understanding how these fitness effects are buffered would complement the functional explanations of balancing selection for their maintenance. Jasmonate (JA) signaling mediates many environmental responses in higher plants; the formation of its central ligand, jasmonoyl-L-isoleucine (JA-Ile), was thought to be invariable. In natural populations of native tobacco plants, we uncover a major mutation in forming JA-Ile; demonstrate its molecular basis, biochemical function, fitness consequences, and find it maintained in several populations over a decade of sampling. When highly connected hub genes were silenced from a coexpression network, JA-mediated defense responses varied with distance from the mutation, consistent with its embedding in a gene regulatory network.

Fisher in his seminal 1930 book proposed the geometric model of adaptation to reconcile Darwinian and Mendelian views on genetics, predicting that most mutations are pleiotropic and that evolutionary adaptations, which drive populations to realize fitness optima, result from changes in many genes of small fitness effects (1–3). Yet recent empirical research has identified several examples of single-gene mutations with large fitness effects in natural populations, from genes that influence coat color and burrowing behavior of mice and in flower color that mediates pollination syndromes (4–6). In natural accessions of the model plant, *Arabidopsis thaliana*, major mutations in several genes in the aliphatic glucosinolate defense pathway (7) and in the salicylate (SA)-mediated pathogen resistance locus, *ACD6* (8), are known to influence plant fitness in context- and season-specific manners. Balancing selection regimes, mediating temporally and spatially varying and conflicting selection pressures from different biotic and abiotic selective agents, are thought to maintain these major mutations in natural populations. For example, attack from seasonally variable herbivores and pathogens engage different and sometimes incompatible defense responses (9), and the growth costs associated with some of these defense responses can impair competitive abilities to produce frequency-dependent selection regimes (10). While direct empirical evidence of these balancing selection regimes, particularly from natural environments, is challenging to obtain, patterns of allelic diversity at mutated loci provide compelling population genetic evidence for the existence of these balancing selection regimes, as elegantly shown for the *ACD6* locus (8).

While balancing selection provides an explanation for the maintenance of major mutations at an evolutionary level of analysis (11), other processes operating at a mechanistic level of analysis can buffer the fitness effects of these major mutations at the level of the individual. This phenotypic buffering is commonly explored by examining the potential compensatory effects of paralogs of the mutated loci, or when the mutation occurs in well-characterized pathways, other elements of the pathway are explored for potential fitness-buffering effects. Genome wide association (GWA) studies have consistently found

The authors declare no competing interest.

This article is a PNAS Direct Submission.

[1]To whom correspondence may be addressed. Email: baldwin@ice.mpg.de.

This article contains supporting information online at https://www.pnas.org/lookup/suppl/doi:10.1073/pnas.2308500120/-/DCSupplemental.

Published August 22, 2023.

low heritabilities for most traits, even those associated with large fitness effects, such as complex diseases (12), likely due to pleiotropic effects of the mutated loci. These pleiotropic effects are frequently explored within the context of presumed balancing selection regimes, such as for growth-related traits in defense pathway mutants (7, 8). However, when examined more globally, the pleiotrophy is often found to extend more widely, often to traits not clearly related to the proposed balancing selection regime, presumably through gene regulatory networks (GRNs) (7, 13, 14).

Recently, the "omnigene" model (15), framed at the mechanistic level of analysis, was proposed to reconcile the low heritabilities observed in most GWA studies, by proposing that large-effect mutations in a core pathway have additional nonzero effects from "peripheral" genes in the larger GRNs in which traits are embedded. These highly interconnected networks have the "small world" property in which most nodes are connected by few steps, even the "hub" genes in these nodes (16, 17). These tightly coregulated gene networks have modular topologies that distribute phenotypic effects to peripheral nodes and could account for the low heritabilities (18). The omnigene model has been applied to explain genetic and epigenetic bases of several human diseases (19–21) and tested in populations of *Populus nigra* trees (22) using transcriptomic analyses, but manipulative tests of the model are rare. The fine-grained modularity of GRN architecture was demonstrated with perturbation experiments of the different subunits of the conserved Mediator transcriptional coregulator of *Saccharomyces cerevisiae* (23). We note that knocking down the expression of *ACD6* in different *Arabidopsis* accessions results in phenotypes that extend beyond the protein's canonical function as a transmembrane, ankyrin-repeat domain protein regulating the pathogenesis phytohormone, SA, to another phytohormone, jasmonic acid (JA) (8, 24). Hence, in studies that provide some of the strongest support for balancing selection-maintaining mutations with large fitness effects, the known pleiotropic interactions are generally consistent with the predictions of the omnigene model. Here, we identify a major mutation in the JA signaling pathway in a non-model plant and take inspiration from the omnigene model to explore how this major mutation's fitness effects could be buffered.

In natural environments, plants are continuously attacked by heterotrophs and compete with each other for fitness-limiting resources; these primary environmental challenges have selected for growth–defense tradeoffs largely mediated by the JA phytohormonal signaling systems that plants use to recognize herbivore attack (25–30). When lepidopteran insect herbivores attack the native tobacco plant, *Nicotiana attenuata*, fatty acid–amino acid conjugates in the herbivores' oral secretions and regurgitants (OS) are introduced into wounds during feeding to elicit the JA-signaling cascade (31–34), through its most active metabolite, JA-Ile (35, 36) acting as a ligand for coronatine-insensitive 1 (COI1), an FBox protein (37–39) which forms a receptor complex with hypervariable jasmonate ZIM-domain (JAZ) proteins and inositol pentakisphosphate (40–45). Most higher plants deploy this signaling system in response to many environmental challenges (26, 45–48). JA-induced responses activate the production of a plant's arsenal of diverse specialized metabolites that function as direct and indirect defenses and are well studied in the *N. attenuata-Manduca sexta* natural model plant–herbivore system (48–52) (*SI Appendix*, *Supplemental text*).

At the heart of JA signaling, sits the conserved JA-Ile COI1 receptor system, the evolutionary history of which has illuminated the GRN architecture of JA signaling. The nonvascular liverwort, *Marchantia polymorpha*, neither produces nor perceives JA-Ile but uses a JA-Ile precursor, dinor-*cis/iso*-12-oxo-10,15(Z)-phytodienoic acid, as a ligand for its MpCOI1 receptor (53, 54). A single-residue substitution in MpCOI1 switches ligand specificity to JA-Ile, a more polar metabolite that is more readily transported through the vasculature (53), a trait lacking in liverworts. The JA-Ile receptor complex is thought to be highly conserved among vascular land plants, consistent with the observation that many biotrophic pathogens, such as the model plant pathogen, *Pseudomonas syringae*, produce coronatine, a structural mimic of JA-Ile that activates the COI1-JAZ receptor system and functions a key virulence factor by dampening SA signaling responses (55, 56).

Two decades ago, when we released *NaLOX3*-silenced, JA-deficient *N. attenuata* plants into natural habitats, they attracted an entirely new herbivore species, an *Empoasca* leaf hopper (57), which subsequent research revealed to be a natural insect "bloodhound" for JA mutants (58). This insect guild is prevented from using tobacco plants with intact JA signaling as hosts by a combination of direct and indirect defensive chemistry that is elicited in response to leafhopper probing and provides a rarely documented mechanism for non-host resistance against insect herbivores (59). Furthermore, when *N. attenuata* plants, silenced in *NaMYC2* expression, a major JA-responsive hub gene, were released during two field seasons that differed dramatically in their herbivory pressures, the *NaMYC2*-silenced plants realized a significant growth advantage in the year when herbivore pressure was low but were severely compromised during the season of high herbivory pressure and did not survive to reproductive maturity (60). These natural history interactions suggested that natural populations of *N. attenuata* would harbor natural JA-signaling mutants that balance the JA-mediated growth/defense trade-off. Yet our understanding of how the fitness effects of such putative JA-signaling mutants could have been buffered by OS-elicited GRNs was hampered because previous attempts to understand OS-mediated signaling in the *Nicotiana* genus using closely related species did not resolve JA signaling within the OS-elicited GRN (61, 62). We hypothesized that the failure of this previous attempt using interspecific variation was due to the lack of shared OS-mediated JA-signaling GRNs among these closely related species; in other words, we had underestimated the speed with which OS-elicited GRNs evolve (62).

Here, we revisit the OS-elicited gene network with an intraspecific approach harnessing natural variation within *N. attenuata*. Together with a chromosome-length contiguous genome assembly (N50 82 Mb), and a 26-parent Multiparent Advanced Generation Inter Cross (MAGIC) Recombinant Inbred Line (RIL) population of *N. attenuata* (*SI Appendix*, *Materials and Methods*, Figs. S1 and S2, and Table S1), we imputed a locus associated with variation in OS-elicited JA-Ile bursts. We screened for candidate genes using RNAi-silenced lines of genes in the pathway and, with stable-isotope labeling experiments, confirmed *NaJAR4* as the causal gene. We estimated the frequency of this variant locus in natural populations and characterized the whole-plant fitness consequences of harboring these variants in environments lacking herbivores. After failing to find compensatory buffering effects in jasmonate resistant (JAR) and COI paralogs, we undertook a broader multiomics integrative approach and identified a putative GRN from a gene coexpression network in which the mutation resides, and by manipulating gene expression of four hub genes in two topologically connected modules, we characterized the OS-induced metabolic responses to examine predictions inferred from the omnigene framework (15, 18).

Results and Discussion

MAGIC Population and *NaJAR4* Natural Variation. We constructed a 26-parent MAGIC RIL population capturing a large fraction of *N. attenuata*'s total natural variation to identify the genetic bases of various ecological traits. The selection of 19 of the parental lines was based on the accessions' metabolic diversity in response

to *M. sexta* OS elicitation (*SI Appendix*, Fig. S3*A*; see *SI Appendix*, *Materials and Methods*) and to dissect the genetic basis of traits involved in plant–herbivore interactions. A Principal component analysis of the Single-nucleotide polymorphisms (SNP) of the parents shows a distinct population structure, partly correlating with their geographic origins (*SI Appendix*, Fig. S4*D*), and the two replicate inbred MAGIC RIL populations, L1 and L2 (sixth generation) form a tight cluster, indicating a homogeneous admixture. This genetic homogeneity allowed for the use of high-resolution quantitative GWA trait mapping without population-structure corrections (63) and after correcting for kinship effects, the model delivered robust trait mappings. Given the importance of the JA-signaling cascade, through its most active metabolite, JA-Ile, in orchestrating this plant's response to herbivory (64), we quantified JA and its conjugates at 1 h after the OS elicitation of a single leaf from two replicates of 650 MAGIC population RILs and parents growing in a field plantation in Arizona in 2019. Interestingly, JA-Ile and JA-Val levels showed greater variation in the RILs compared to the parental lines (*SI Appendix*, Fig. S3*C*), consistent with the loss of regulatory activity of the OS-regulated gene networks on these phytohormones, which had been lost in the creation of the RILs. The subsequent GWA analysis of OS-elicited JA-Ile and JA-Valine (JA-Val) bursts imputed a significant QTL at the same region of chromosome 5, consistent with the two amino acids being conjugated to JA by the same biochemical mechanism (Fig. 1 *A* and *B*) (65, 66). Results from a replicate glasshouse (GH) screen of the same MAGIC RIL population imputed the same locus but at a marginal level of significance (*SI Appendix*, Fig. S5), underscoring the importance of screening plants in their native habitats to elicit ecologically relevant signals.

Mining the assembled genome at chromosome 5, we identified candidate genes, and further eQTL analyses of 350 RILs from the same experiment identified jasmonoyl-L-amino acid synthetase (*NaJAR4*) as a candidate (*SI Appendix*, Fig. S6), a known enzyme conjugating Ile and Val to JA (66). The two SNPs showing the highest association with the JA-Ile QTL, and JAR4 eQTL lie adjacent to each other and show strong linkage (*SI Appendix*, Fig. S6*E*). A phylogenetic analysis of the *NaJAR4* region delineating the variation found in the 26 parents of the MAGIC RIL population (*SI Appendix*, Fig. S4*B*), revealed that six variant (V) lines form a monophyletic clade, and the variant allele correlated with a strong reduction in *NaJAR4* expression (*SI Appendix*, Fig. S6 *B* and *D*). Additionally, phylogenetic analysis of all *NaJAR* genes in *N. attenuata* and well-studied taxa in the Solanaceae placed *NaJAR4* in a clade distinct from the other *NaJARs* in the genome (*SI Appendix*, Fig. S7) and the OS-elicited expression of *NaJAR4* was highest among the *NaJARs* (*SI Appendix*, Fig. S6*F*). We then randomly selected six other lines from the other clades with high *NaJAR4* expression and used these as non-variant (NV) lines for further comparisons. Sequence analysis and additional PCRs confirmed a deletion in *NaJAR4*'s 5′ untranslated region (UTR) in the V lines, which renders the gene inactive (Fig. 1*C* and *SI Appendix*, Fig. S6 *A*, *B*, and *D*).

We next scrutinized the geographic origins of V and NV lines to evaluate whether the *NaJAR4* mutation was a spatially limited phenomenon. Clustering the accessions based on their genetic distance captured only minor associations with their respective geographic origin (*SI Appendix*, Fig. S4*D*); the V lines did not form a distinct cluster but were distributed along the tree (Fig. 1*D*). This indicates a lack of population substructure associated with the

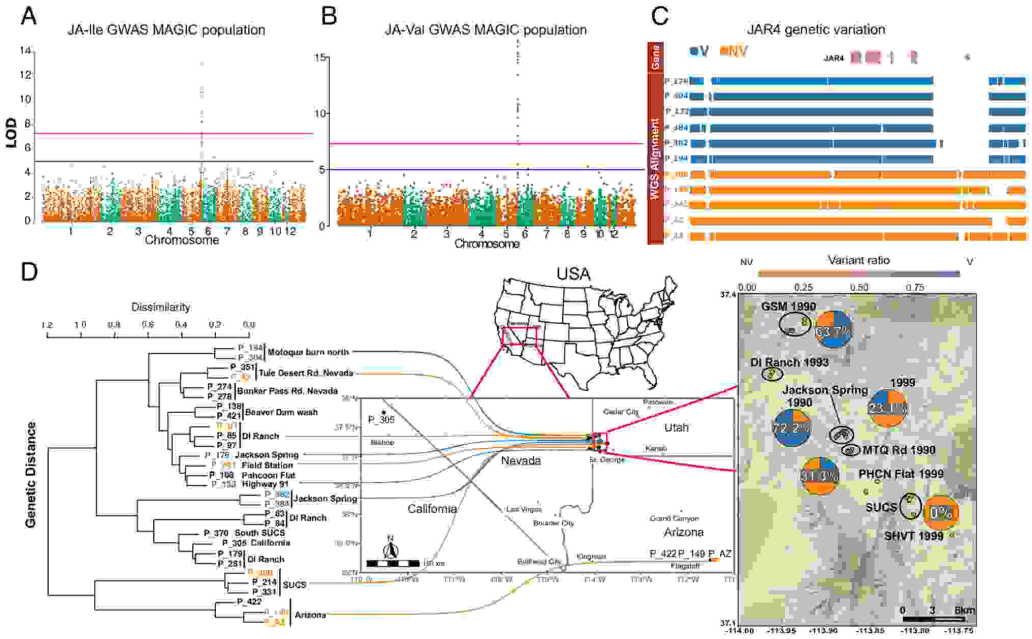

Fig. 1. GWA trait mapping of OS-elicited JA-Ile and JA-Val in MAGIC RIL populations and locations of the *NaJAR4* mutation in *N. attenuata* natural populations (*A* and *B*) GWA analysis of OS-elicited JA-Ile and JA-Val bursts. (*C*) The structures of the JAR4 gene showing Whole Genome Sequence (WGS) alignments of V and NV lines and the deletion in the 5′ UTR region of *NaJAR4* in the V lines. (*D*) Genetic distance of natural accessions of *N. attenuata* originating in the SW USA. Blue accessions indicate V lines and orange accessions indicate NV lines. Locations of seed collections in the SW Utah region over 9 y from 32 natural populations that were genotyped for the *NaJAR4* variant (blue): Pie diagrams are genotype ratios of either bulked or averages of individual genotypes in each location represented by the black circles, while points reflect each genotyped collection. Details of each collection are listed in *SI Appendix*, Table S2.

NaJAR4 locus and is consistent with considerable gene flow among the different populations. We focused on a small region in SW Utah from where some V lines originate and examined the frequencies of the variant allele (Fig. 1*D* and *SI Appendix*, Table S2) to examine how their distributions changed over time in this annual plant. Using DNA extracted directly from individual or bulk seed collections, we quantified allele frequencies from multiple seed collections made over 9 y from this 400 km^2 area. The allele frequencies were highly variable both spatially and temporally, with no clear patterns of fixation (Fig. 1*D* and *SI Appendix*, Table S2). In the Jackson Spring (JS) population, for example, 8 of 11 (72%) individuals sampled in 1990 harbored the variant allele. However, in a 1999 bulk collection from the same location, this ratio dropped to 23%. Populations within the 6 km^2 Gold Strike Mine (GSM) area also harbored high frequencies of the variant allele, whereas the variant allele was not found in seeds from several years of collections at the DI ranch (the origin of the Utah (UT) genotype) located just 5 km downstream from the GSM. From these results, we infer that balancing selection through spatiotemporal variation (67) is acting on the *NaJAR4* loci, which maintains this allele in natural populations (see *SI Appendix, Supplemental text* for additional discussion of this point).

To evaluate whether this *NaJAR4* mutation could be maintained in natural populations through gene duplication/neofunctionalizations of canonical JA-signaling genes, we used a candidate gene approach to evaluate whether other *NaJARs* or *NaCOIs* could provide *NaJAR4* mutants with compensatory responses (*SI Appendix, Supplemental text*). As *N. attenuata* is an annual plant that rapidly transitions from vegetative to reproductive growth as its habitat dries out (68), the priority of defending leaves rapidly switches to one of defending reproductive parts as plants transition into flowering. Prior research had established that constitutive JA-Ile levels in flower buds are typically 10x higher than those of OS-elicited leaves and that floral defense engages a floral-specific NaJAZi repressor that physically interacts with the NINJA-like protein rather than the canonical NINJA (44). Floral JA-Ile levels were dramatically lower (by 20-fold) in a previously characterized *NaJAR6*-RNAi line (69) compared to those of wild type (WT) plants, indicating additional tissue-specific conjugation activity of NaJAR6 (*SI Appendix*, Fig. S9). We then asked whether *N. attenuata* has evolved a tissue-specific JA-Ile receptor through the second COI in its genome, NaCOI2. We tested this hypothesis in floral tissues by silencing *NaCOI2* expression by stable RNAi (*SI Appendix*, Fig. S10*A*); however, phytohormone and metabolic profiles of ir*NaCOI2* lines revealed that *NaCOI2* did not buffer the likely fitness consequences of the JA-Ile variation (*SI Appendix, Supplemental text* and Fig. S11).

Taken together, these results establish a causal association between natural genetic variation in the *NaJAR4* locus of the *N. attenuata* MAGIC population with OS-elicited JA-Ile levels in leaf tissues and a genomic deletion in the *NaJAR4* 5′ UTR that lowers OS-elicited JA-Ile levels in the V lines. Additionally, the effect of silencing *NaJAR4* in floral tissues was much less than that of silencing *NaJAR6*, and thus the loss of *NaJAR4* function could potentially be buffered by intact NaJAR6 activity in floral tissues. However, we needed to evaluate both the biochemical and fitness consequences of the NaJAR4 mutation in greater detail.

OS-Elicited JA-Ile Conjugation Kinetics. *NaJAR4* adenylates JA for conjugation with Ile and Val (66). To determine whether the V lines have lower Ile conjugation rates compared to the NV lines due to abrogated NaJAR4 activity, we conducted in vivo JA-conjugation kinetic experiments with isotopically labeled ^{13}C-Ile. We utilized previously published *NaJAR4*- and *NaJAR6*-RNAi lines produced in the UT genetic background (an NV line) as positive controls for the experiments and quantified JA and its conjugates at 45 and 90 min after simulated herbivory, just before and exactly when OS-elicited JA-Ile peaks (Fig. 2 *A* and *B*) (35, 65, 69). We reasoned that if the JA-Ile levels are lower in the V lines due to lower conjugation activity and not the lack of Ile substrate, then supplementing puncture wounds with ^{13}C-Ile in OS and subsequently quantifying the ^{13}C-labeled JA-Ile levels should reflect activity differences between the two groups. Additionally, to rule out the effect of JA variation, we analyzed the JA-Ile levels with respect to the JA levels, estimating conjugation rates from the slopes of JA-Ile vs. JA regressions (*SI Appendix*, Table S3).

Both ^{13}C-JA-Ile and endogenous JA-Ile conjugation rate estimates at 90 min were significantly lower in *NaJAR4* and *NaJAR4x6*-RNAi lines compared to those of EV plants (Fig. 2 *G* and *H*). The V lines phenocopied the *NaJAR4*-RNAi line in both their ^{13}C-JA-Ile and endogenous JA-Ile conjugation rate estimates and had lower conjugation rates compared to NV lines (Fig. 2 *I* and *J*). The estimated ^{13}C-JA-Ile conjugation rates of *NaJAR6*-RNAi plants were significantly higher than those of EV plants, which suggests that NaJAR4 activity dominates Ile-conjugating activity at 90 min in leaves. Moreover, the conjugation estimates of *NaJAR4*- and *NaJAR4x6*-RNAi plants did not differ, suggesting that NaJAR6 activity contributes little to the total Ile-conjugation activity at 90 min. The similarity of the response in the V lines and the *NaJAR4*-RNAi lines is consistent with the inference that the deletion in the 5′ UTR of their NaJAR4 gene (Fig. 1*C*) is responsible for their lower conjugation rates.

Interestingly, at 45 min after OS elicitation, ^{13}C-JA-Ile conjugation rate estimates of all *NaJAR*-RNAi lines were significantly lower compared to those of EV; however, no difference was observed in the endogenous JA-Ile conjugation rate estimate at this early time point (Fig. 2 *C* and *D*). The opposite pattern was observed in V vs. NV lines (Fig. 2 *E* and *F*) where endogenous JA-Ile conjugation estimates differed but not the exogenous ^{13}C-JA-Ile conjugation estimates. From these results, we inferred that a larger apoplastic flux of ^{13}C-Ile conjugated by NaJAR6, as opposed to NaJAR4, was responsible, as the former is intact in these lines and dominates the conjugation activity at 45 min. This is in contrast to the lower flux of endogenously synthesized Ile (*SI Appendix*, Fig. S12*A*), possibly conjugated by basal NaJAR4 activity which showed a significantly lower conjugation rate in V compared to NV lines. We quantified levels of Ile and its precursor, threonine, and found no evidence of substrate limitations at either time point (*SI Appendix*, Fig. S12*B*). In summary, silencing *NaJAR4* had a stronger effect on OS-elicited JA-Ile accumulations than did silencing *NaJAR6*, consistent with previous work (69), and the two enzymes contribute to conjugation activity at different times following OS elicitation in leaves.

Fitness Consequences of the *NaJAR4* Variation. We next quantified the whole-plant fitness consequences associated with the *NaJAR4* natural variant. Since *N. attenuata* is a self-fertilizing annual plant, we used life-time seed set as an ecologically relevant proxy for its fitness and MeJA-induced trypsin proteinase inhibitor (TPI) activity was used as a proxy for quantifying defense (*SI Appendix, Supporting Information Text*). Moreover, JA-signaling is preserved in floral tissues, the fitness consequences of *NaJAR4* variation can be accurately estimated in this currency. Additionally, after germination in nature, *N. attenuata* plants compete for ephemeral resources with conspecifics, which can be either full-siblings or unrelated plants, and relative growth rates are another important parameter in determining fitness outcomes, depending on genetic ancestry. Therefore, we used a two-plant/pot competitive growth system that facilitates the quantification of fitness differences

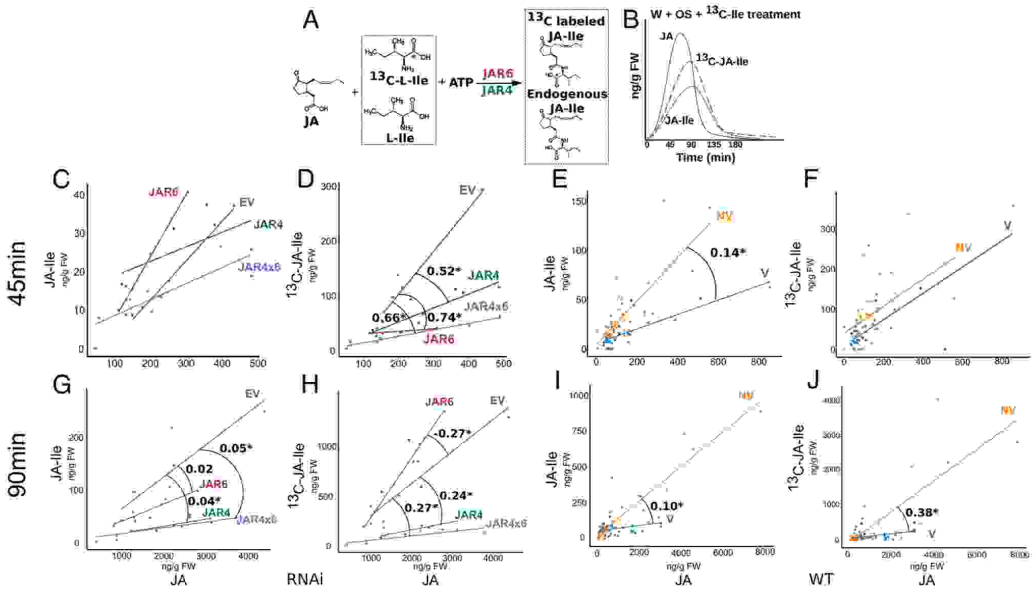

Fig. 2. JA-Ile synthesis and accumulation kinetics in OS-elicited leaves. (*A*) *NaJAR4* and/or *NaJAR6* catalyzes the conjugation step of JA-Ile synthesis, conjugating either free endogenously produced isoleucine (Ile) or exogenously applied ^{13}C-labeled Ile to JA in response to OS elicitation. (*B*) Schematic representation of typical JA and JA-Ile bursts in *N. attenuata* leaves immediately after simulated herbivory (OS elicitation). (*C* and *D*) Endogenous JA-Ile and ^{13}C-JA-Ile vs. endogenous JA accumulations at 45 min after OS elicitation in three RNAi knockdown lines and empty vector (EV) as controls (*E* and *F*) Endogenous JA-Ile and ^{13}C-JA-Ile vs. JA accumulation in 6 V and 6 NV MAGIC parental accessions at 45 min after OS elicitation. (*G* and *H*) Endogenous JA-Ile and ^{13}C-JA-Ile vs. JA accumulations at 90 min after OS elicitation in the different RNAi lines. (*I* and *J*) Endogenous JA-Ile and ^{13}C-JA-Ile vs. JA accumulations in 6 V and 6 NV MAGIC parental accessions at 90 min after OS elicitation. The values are the differences in the slopes of regression lines calculated with the emmeans package in R and are listed in *SI Appendix*, Table S3; an asterisk denotes significant differences.

under ecologically realistic conditions (70). The two plant/pot experimental setup allowed us to quantify the relative growth/defense trade-off incurred through TPI by the different genotypes associated with *NaJAR4* variation (10, 71). We expected that if plants deficient in *NaJAR4* activity (Fig. 3 *A* and *B*) are trading off their investment in defense toward growth and fitness, they would acquire more resources than slower-growing but well-defended competitors and be clearly distinguishable in the defense-fitness trait space. In the case of plants harboring the intact *NaJAR4* copy, their growth/defense trajectory would be the same as that of their well-defended neighbor.

The MeJA-elicited *NaJAR4*-deficient V lines (X position in Fig. 3) produced significantly greater seed set (by 37%), while the MeJA-induced TPI activity was significantly lower (by 50%) compared with NV lines (Fig. 3*A*), which is quantitatively consistent with previously reported results (50). In line with these expectations, the competing UT counterparts (inbred NV line used as a standard wild-type in decades of *N. attenuata* research, Y) showed MeJA-induced trends similar to those of the NV lines in the fitness-defense trait space. However, in unelicited pairs, their realized fitness matched that of their competitors. These data indicate that the realized fitness gain of the V lines did not come at the expense of the competing (Y) plants, as the MeJA-induced fitness of UT competitors did not differ between the V and NV pairs. The fitness benefit of the V lines is rather a direct consequence of the NaJAR4 deficiency, which reduced TPI activity by 50%, indicating a reduced investment in plastic defenses resulting in a 37% gain in seed set. Previous research with this species in a 2 plant/pot competition setup found that when competing with non-kin, plants dramatically increased their growth rates when not induced with MeJA (70), a result consistent with Hamilton's rule (72) (see *SI Appendix*, *Supporting Information Text* for additional discussion of this point). Furthermore, the relative defense/fitness trade-off effect for V lines is likely underestimated due to the inclusion of two NV lines (AZ and P-149) originating from Arizona, which are impaired in their ability to produce TPIs due to an evolutionarily recent Nonsense Mediated Decay pseudogenation of the TPI gene (73).

The *NaJAR*-RNAi lines did not show significantly lower capsule counts in response to MeJA treatments (Fig. 3*B*). Both silenced lines accumulated two-fold lower TPI activity (Fig. 3*B*) compared to NV plants (Fig. 3*A*). When compared to their isogenic UT competitors, the *NaJAR*-RNAi lines produced significantly more (by 42%) capsules. Final stalk lengths, providing a quantitative proxy for growth, revealed that V lines phenocopied the *NaJAR4*-RNAi lines with comparable effect sizes, together with strong growth reductions in MeJA-induced Y competitors in comparison to the JAR-deficient plants in both groups (Fig. 3*C*). The estimated standardized effect size between uninduced X and Y plants in V and *NaJAR4*-RNAi lines remained small (0.32 and 0.26) but increased to 0.84 and 1.56 in response to MeJA-induction, respectively. In contrast, the effect size remained negative in the NV group, reducing to −0.45 upon MeJA-induction, indicating strong competition for resources between X and Y plants. In comparison to the *NaJAR4*-RNAi line, the MeJA-induced growth reduction was stronger in the *NaJAR4/6*-RNAi group, where under both control and induced conditions, Y plants were significantly shorter than X plants, as revealed by the larger effect sizes that likely result from the additive effect of silencing *NaJAR6*.

These findings reveal that abrogating NaJAR activity through RNAi in the UT WT genotype disrupts JA-induced regulation of

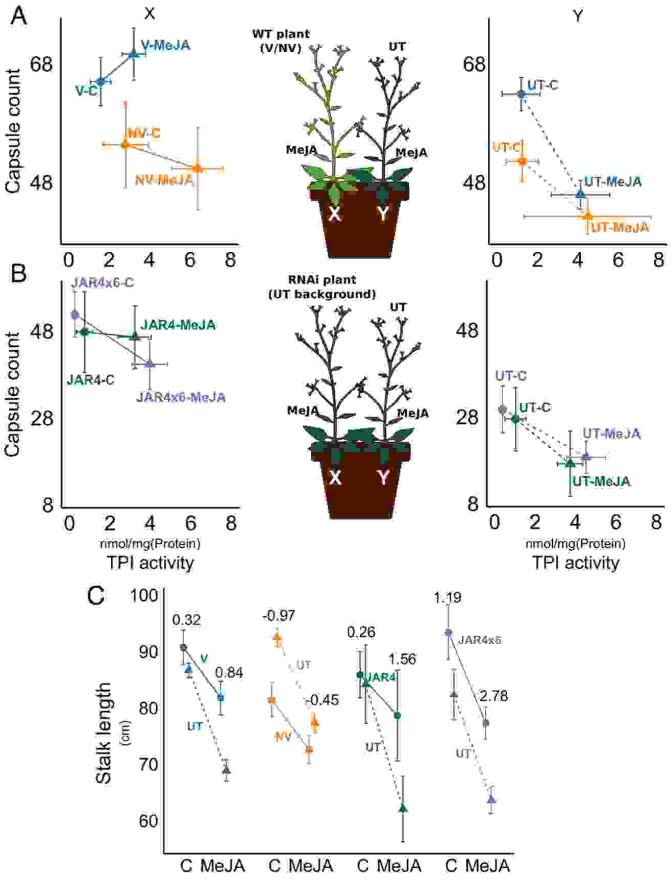

Fig. 3. Growth and fitness consequences of the *NaJAR4* natural variation. (*A* and *B*) An ecologically realistic competition experiment was used to estimate fitness-defense consequences of the *NaJAR4* variant. The middle schematics describes two size-matched 10-d-old seedlings that were planted in a single pot (n = 10), of which one (Y-plant) was always a UT-WT plant, with the other competing neighbor (X-plant) being, either (*A*) a non-isogenic V or NV WT plant; or (*B*) an isogenic RNAi-line silenced in either *NaJAR4* or both *NaJAR4* and *NaJAR6* (*NaJAR4/6*). Bivariate plots describe the fitness/defense consequences of methyl jasmonate (MeJA)-elicitation during reproductive maturation in fitness (lifetime capsule numbers: *Y* axis) and leaf defense (fitness-costly trypsin proteinase inhibitor (TPI) defenses: *X* axis). Traits of the X competitors are shown in the left-side panels while those of the Y competitors are shown in the right-side panels. (*C*) Flowering stalk lengths of X (solid lines) and Y plants (dashed lines) measured at the final harvest, 37 d after treatments. Error bars indicate ± 95% CIs. The numbers on top of error bars indicate standardized effect sizes estimated by Cohen's D method.

growth/defense responses. The V lines have presumably adapted to their NaJAR deficient JA-signaling and, when MeJA-induced, maximize their seed set by exploiting this deficiency (Fig. 3*A*). In contrast, MeJA induction of *NaJAR*-RNAi lines in the NV UT background did not increase seed set despite consistently displaying a NaJAR deficient growth/defense phenotype, suggesting that their metabolic configurations are not adapted to this deficiency (Fig. 3*B*). Recombination, as evidenced by gene flow patterns (Fig. 1) and sporadic outcrossing in *N. attenuata* populations (74, 75), both processes that antagonize selective sweeps, makes it unlikely that these adaptations are in linkage disequilibrium with the NaJAR4 loci. It is more likely that the beneficial adaptations are dispersed across the genome. Overall, V lines lacking NaJAR4 activity realize higher fitness when induced in herbivore-free environments compared to NV lines, displaying similar effects on defense/growth-fitness trade-offs in magnitude, but not induction patterns, as the *NaJAR4*-RNAi line. From these results, we infer that other unknown compensatory responses have evolved in the V lines, enabling their survival in natural populations. To better understand these compensatory responses, we next characterized the OS-elicited coexpression network in the natural accessions.

Multi-omic Integration of OS-Elicited *N. attenuata* Natural Accessions. In higher plants, JA-Ile is the critical bioactive hormone that allows plants to contextualize an impressive array of physiological and developmental processes to environmental contingencies. The canonical model of JA-signaling posits that responses will be proportional to the amounts of JA-Ile elicited by environmental signals above some thresholds, and the diversity of responses elicited emerges from the spatiotemporal diversity of JA-Ile accumulations, their turnover, and specific JAZ/transcription factor complexes that regulate downstream responses (40). The mutation we identified dramatically lowers JA-Ile accumulations in leaves and significantly affects JA-Ile-associated traits. Previous studies showed that coexpression modules can deliver mechanistically insightful genes, regulating specialized metabolic responses (76, 77). Extending our search from a canonical JA-signaling candidate gene approach, we wanted to identify a conserved OS-induced coexpression network and other hub genes within it, that might be buffering the effect of the *NaJAR4* variation in natural accessions. This would enable us to gain mechanistic insights at a molecular level into how the mutation is maintained in these populations, which can otherwise be explained by balancing selection at a functional level of analysis (11). We note that the coexpression network structure regulating effector-triggered immunity can be largely conserved even in JA/SA-deficient *Arabidopsis* plants (78), where only the amplitude of the network was delayed, due to abrogation of the phytohormonal network.

To this end, we analyzed the OS-elicited leaf transcriptomes of 29 *N. attenuata* natural accessions, including 25 of the 26 the

MAGIC parental lines (*SI Appendix*, Table S4), using gene coexpression analysis and constructed a putative OS-elicited network. The analysis revealed seven major topologically connected modules of coexpressed genes in which both *NaJAR4* and *NaJAR6* clustered in the same M7 module (Fig. 4*A*). Gene ontology (GO) term enrichment analysis for each module revealed the M7 module was enriched for terms like "defense response," whereas another module, M5, was enriched in terms like "jasmonic acid metabolic process," "modulation of process of another organism," and "response to biotic stimuli," indicating that a defense-response-related gene network was captured in these two modules (*SI Appendix*, Fig. S13), which additionally, based on gene expression similarity, were also functionally closely related (Fig. 4*B*).

We focused on the M5 and M7 modules (Fig. 4*A*) to identify potential hub genes that could be targeted for gene silencing to test the effect on JA-Ile-associated traits with respect to the canonical JA-signaling embedded in the gene network. Hub genes were identified by ranking the genes by 11 network connectivity metrics, and further manual curation of the GO term enrichment results led to a selection of four genes, namely, Ethylene Response Factor 1B (*NaERF*) and F-BoxAt61340 (*NaFB61*) from the M5 module, and Glutamate receptor (*NaGLR*), and F-BoxAt67340 (*NaFB67*) from the M7 module. These selections were based on the observations that ethylene signaling is strongly elicited by OS in *N. attenuata* and fine-tunes JA-Ile responses (79, 80); glutamate receptors are likely involved in systemic JA signaling through Ca^{2+} signaling (81); the F-Box *NaFB67* contains a conserved Tetratrico Peptide Repeats motif which is involved in protein–protein interactions and has been shown to be essential for phytohormone-mediated signaling (82, 83); and the *Arabidopsis* homologue of *NaFB61* is known to regulate multiple JA- and ABA-responsive genes in stress situations (84). This suggested that the two selected F-Box genes could be involved in OS-elicited hormone sensing, albeit by different mechanisms than that of the canonical COI1. Furthermore, none of these genes co-localized with *NaJAR4* loci; thus, it is unlikely that their role in the JA-signaling pathway would be confounded by selection pressures acting on the *NaJAR4* locus.

To further understand the correlation patterns between gene expression and downstream metabolite accumulations, we conducted an integrative analysis using multiblock sPLSDA of the OS-elicited transcriptomes, metabolomes, and phytohormones of the 29 natural accessions. This dimension reduction (or latent variable approach) to data integration helps to highlight correlations across multiple datasets, parse-out outliers, or batch effects

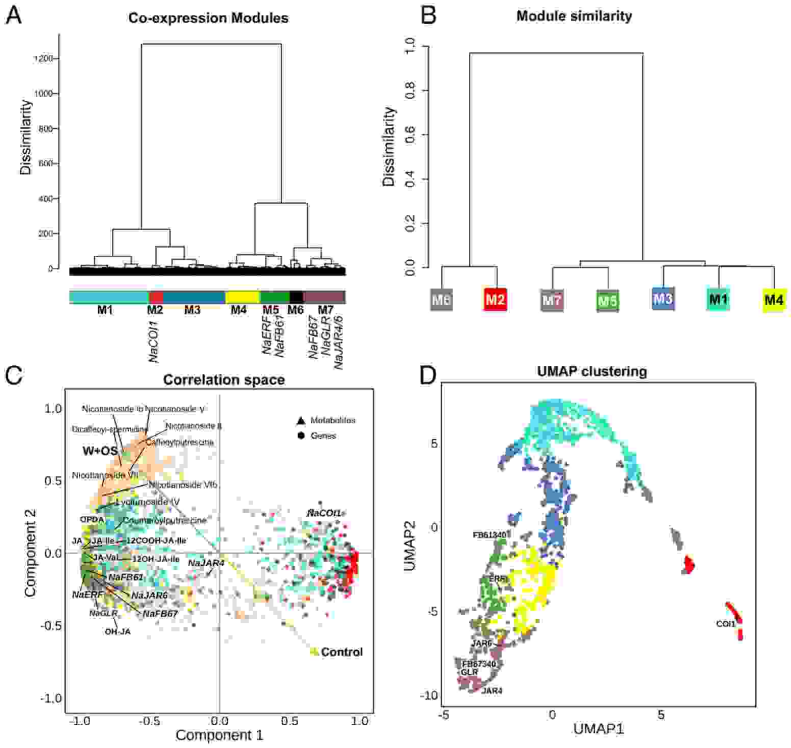

Fig. 4. Coexpression analysis of OS-elicited transcriptomes, metabolomes, and phytohormones of *N. attenuata* natural accessions (*A*) Coexpression analysis of OS-elicited transcriptomes of *N. attenuata* natural accessions revealed seven gene modules. Each node in the dendrogram represents a single gene, and the number of genes in each module is M1 = 499, M2 = 93, M3 = 392, M4 = 214, M5 = 187, M6 = 89, and M7 = 259. (*B*) Module similarity was computed using the eigen-gene expression of each module and by calculating the Pearson correlation coefficient similarity matrix. Hierarchical clustering was performed on the (1-similarity) matrix obtained in the previous step. (*C*) Correlation plot of integrative analysis of the transcriptome, metabolome, and phytohormones performed using multiblock sparse partial least squares discriminant analysis (sPLSDA), showing the correlation of each feature against two latent variables, namely components 1 and 2. The two vectors C and W+OS are diametrically opposite, indicating that these two components adequately captured the variation due to the OS elicitation. (*D*) UMAP clustering was performed on the OS-induced transcriptomes of *N. attenuata* natural accessions, and colored based on the modules returned by the coexpression analysis in panel *A*.

in individual sets, and provides a robust selection (of genes and metabolites) to facilitate further downstream analyses (85). The analysis revealed that major defense metabolites were linearly correlated with the expression of the four selected hub genes and *NaJAR6* (Fig. 4*C*). *NaCOI1* in the M2 module was negatively correlated with component 1 and distinct from the two selected F-Box genes that correlated positively with component 1, consistent with the inference that the selected F-Box genes are not functionally similar to the canonical JA-Ile/COI1 receptor complex. Interestingly, *NaJAR4* was not strongly correlated with JA or JA-Ile, or with JA-induced metabolites along the first two sPLSDA components, representing linear dimensionality reduction. This suggested that *NaJAR4* expression may share a more complex nonlinear relation within the network, not captured by the sPLSDA. Indeed, Uniform Manifold Approximation and Projection (UMAP) clustering of the module gene expression, which is a nonlinear dimensionality reduction technique, revealed that *NaJAR4* clusters well within the M7 module (Fig. 4*D*) in a two-dimensional space. Taken together, these results indicate that although the *NaJAR4* variation has major fitness consequences as observed in glasshouse experiments (Fig. 3), the variation itself is embedded in a complex gene network in which other interconnected genes could compensate for the deleterious effects of this major mutation on *N. attenuata*'s OS-elicited defense responses.

Metabolomic Analysis of Silenced Hub Genes. To test the effects of hub genes on OS-elicited defense responses, we silenced the expression of the four hub genes from the M5 and M7 modules by transforming *N. attenuata* plants with inverted repeat (ir) RNAi constructs. We conducted the transformations in the UT genetic background (an NV genotype) to produce lines that function with an intact *NaJAR4* allele and are thus not confounded by compensatory responses from the connected genes in the network (Fig. 3). Two homozygous T_2 plants were generated harboring a single T-DNA insertion effectively silencing the expression (*SI Appendix*, Figs. S10*B*, S14, and S15) of *NaERF* and *NaFB61* (M5), *NaGLR*, and *NaFB67* (M7) genes in individual lines, showing consistent elicitation patterns of induced metabolites in both lines. Thus, one replicate per construct was chosen for comparisons with the V, NV, and *NaJAR4/6*-RNAi lines. Rosette-stage leaves were elicited with *M. sexta* OS and sampled after 1 h for phytohormone analyses, and untargeted liquid chromatography–mass spectrometry (LC-MS) analyses were used to characterize their defense responses (Fig. 5).

The OS-elicited JA-Ile levels in V lines were significantly lower (two-fold) than those of the NV lines (Fig. 5*B*). The lower JA conjugation efficiency in V lines was likely responsible for significantly higher JA levels (1.7-fold) compared to NV (Fig. 5*A*). The same trend was seen in the *NaJAR4*- and *NaJAR4x6*-RNAi lines (Fig. 5*B*) which also had significantly reduced basal (2.6-fold for both lines) and induced JA-Ile levels (4.4-fold and 8.3-fold, respectively) and tended to have higher induced JA levels compared to those of WT plants (Fig. 5*A*). JA-induced metabolites, CP, DCS (51), and total diterpene glycosides (DTGs), sectors of specialized metabolism which are strongly regulated by JA-Ile (52) (*SI Appendix*, Fig. S16), were proportionally down-regulated in the *NaJAR4x6*-RNAi line, but the defense reductions in the V lines were not as dramatic. Moreover, PLS-DA of mass features revealed that OS-elicited V lines clustered differently than those of the *NaJAR4* and *NaJAR4x6*-RNAi lines, despite all of these lines being comparably impaired in their NaJAR4 activity (Fig. 5*F*).

Both the ir*NaGLR* and ir*NaFB67* lines, silenced in genes of the topologically proximal M7 module, had significantly reduced basal JA and JA-Ile levels (Fig. 5 *A* and *B*), but did not differ from WT in their OS-elicited levels. Consistent with the canonical role of JA-signaling in defense responses, basal levels of CP and DCS were significantly lower in these lines (2.5-fold and 1.5-fold, respectively). Interestingly, OS-elicited levels were also low (by 1.5-fold and 1.7-fold) and hence not proportional to the lines' induced JA/JA-Ile levels. Moreover, no effect was observed in total DTGs in these lines, with the JA-Ile-elicited DTG, dimalonylated nicotianoside II, also not being affected (*SI Appendix*, Fig. S16). PLS-DA of the OS-induced mass features and the relative contributions of the targeted compounds confirmed that ir*NaGLR* and ir*NaFB67* lines had low constitutive and induced metabolite levels that clustered separately from WT along component 1 (Fig. 5*G* and *SI Appendix*, Fig. S17), revealing that variations correlated with canonical JA-signaling in uninduced leaves, but not with the expected induced changes.

For the genes of the topologically distal M5 module, both RNAi-silenced lines showed WT or higher JA/JA-Ile levels after OS elicitation (Fig. 5 *A* and *B*). OS-elicited JA-Ile in ir*NaFB61* plants were significantly higher (1.3-fold), and given that the JA-Ile degradation products (OH-JA, OH-JA-Ile, and COOH-JA-Ile) (86) of both lines were dramatically higher than those of WT plants after OS elicitation (*SI Appendix*, Figs. S18 and S19), it is likely that the flux of oxylipins through JA-signaling was significantly up-regulated in both lines. Surprisingly, basal levels of JA-regulated DCS (by 5.9-fold and 3.3-fold) and DTG (by 2.6-fold and 2.3-fold) were dramatically up-regulated (Fig. 5 *D* and *E*) and PLS-DA analysis of the LC-MS mass features revealed that ir*NaERF* and ir*NaFB61* lines displayed a "constitutively-on" defense phenotype along component 1 (Fig. 5*H* and *SI Appendix*, Fig. S16), which was not proportional to constitutive JA/JA-Ile levels, a complete departure from the canonical JA-signaling model. Furthermore, OS elicitation did not increase the levels of these metabolites. To test the putative constitutively defended phenotype of ir*NaERF* and ir*NaFB61* plants, we conducted a caterpillar bioassay, in which *M. sexta* larvae were fed razor-excised leaves from these plants (cut at the base of petioles to minimize wound-induced responses) and larval weight was measured as a proxy for herbivore performance over 10 d. The mass of larvae fed ir*NaERF* and ir*NaFB61* leaves was significantly lower (by 54 and 53%) than those feeding on WT leaves (*SI Appendix*, Fig. S20). In summary, disrupting hub genes in a topologically distal module resulted in larger disruptions of the canonical model of JA-elicited defenses.

Overall, these results reveal that OS-elicited defense responses in V lines show minor deviations compared to the NV lines, which are likely buffered by the larger OS-elicited gene network. In contrast, the *NaJAR4/6*-RNAi lines in the NV background, which have not had the opportunity to evolve a compensatory gene network, exhibit significant differences. While both V lines and *NaJAR4/6*-RNAi lines exhibit significantly reduced OS-elicited JA-Ile levels and V lines phenocopy the *NaJAR4*-RNAi in specific defense metabolites controlled by *NaJAR4*, subtle differences between V lines and *NaJAR4*-RNAi line are evident in the entire OS-induced metabolome (Fig. 5*F*). Interestingly, these results closely follow the quantitative predictions of the "omnigene" model (18), where the OS-elicited defense responses in V lines are perhaps buffered by the larger gene network, and that the *NaJAR4* variation only affects the proximal M7 module, resulting in minor deviations from the NV lines. In contrast, deviations resulting from silencing of the hub genes of the network, particularly those from module M5, topologically most distal (Fig. 4*A*) from the module harboring *NaJAR4*, leads to the most aberrant patterns of OS-elicited metabolites. This can be explained by the amplifying effect of the M7 module, where perturbations in hub

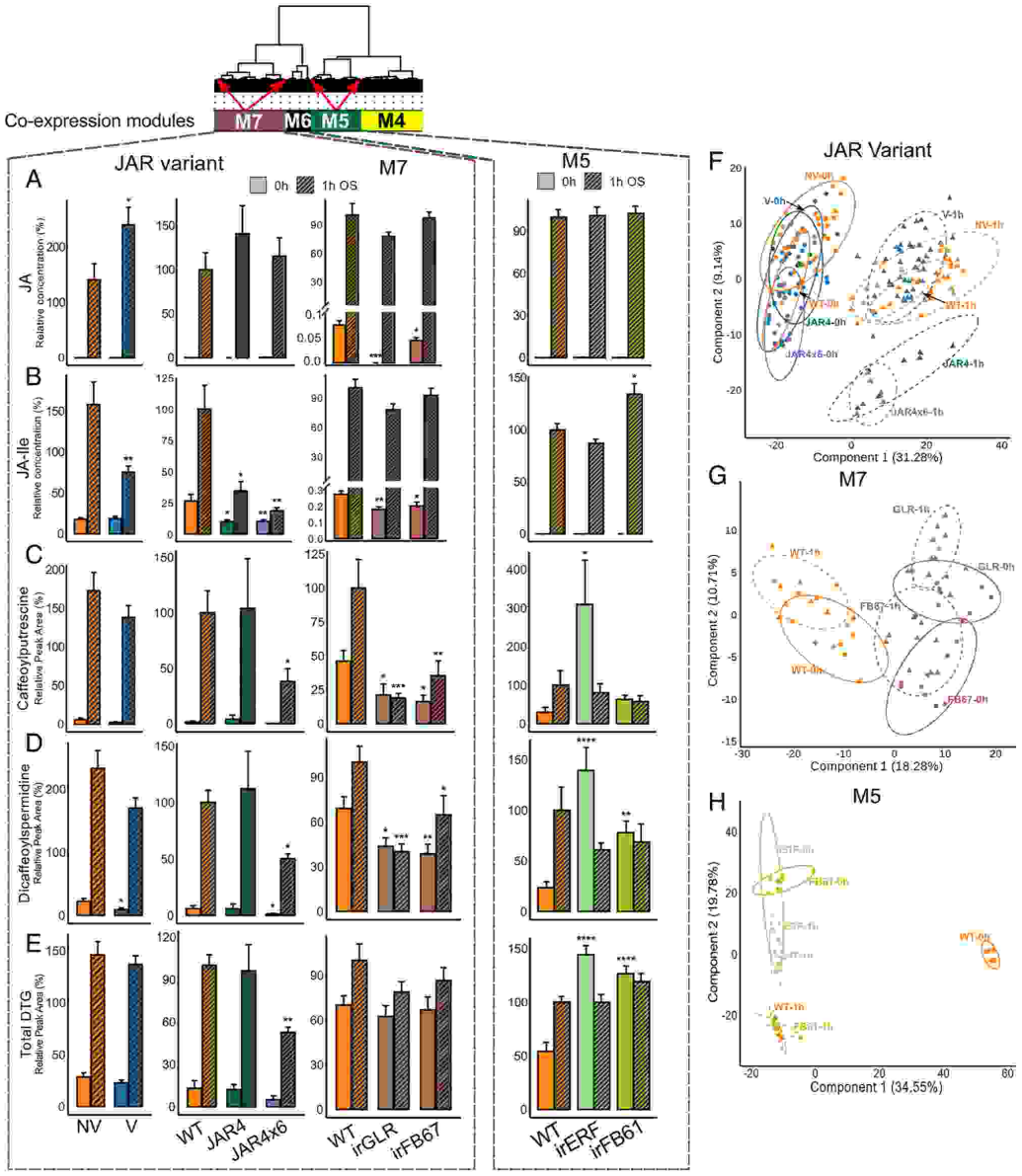

Fig. 5. Metabolic characterization of four RNAi lines silenced in the expression of hub genes, two *NaJAR*-RNAi lines, V and NV plants (*A–E*) JA, JA-Ile, caffeoylputrescine (CP), dicaffeoylspermidine (DCS), and total diterpene glycoside (DTG) levels in unelicited (0 h) control plants and 1 h after OS elicitation in ir*NaERF*, ir*NaFB61*, ir*NaGLR*, and ir*NaFB67*, *NaJAR4/6*-RNAi and the NV and V lines. Metabolite levels were normalized against the common UT genotype that was included in all experiments and used as a genotypic control for all RNAi lines. The module dendrogram on the top is a subset of the coexpression clustering from Fig. 4*A* (with reversed branch ordering for better visualization), indicating the relationships of the genes within their modules and their respective silenced lines. (*F*) Partial least square discriminant analysis (PLS-DA) projection in two components of control and OS-elicited metabolomes of the *NaJAR4* variant group. The WT lines are circled within the larger NV group. (*G*) PLS-DA biplot of control and OS-elicited module 7 lines. (*H*) PLS-DA biplot of control and OS-elicited metabolomes of module 5 lines. See *SI Appendix*, Fig. S16 for quantifications of the JA-regulated sector of the potent HG-DTG defense metabolites. Error bars are SEs. Significance was calculated by ANOVAs followed by Tukey's Honestly significant difference tests comparing against WT in the M5 and M7 groups and the *NaJAR*-RNAi group, and NV in natural variant, across two treatment groups (*P-values < 0.05; ** < 0.01; *** < 0.001; **** < 0.0001).

genes of the distal M5 module cascade through the highly interconnected gene network, causing large cumulative effects directly on the proximal M7 module resulting in a dramatic change in metabolic response (18). Moreover, the flux of oxylipins through JA-signaling became increasingly unregulated with the topological distance of perturbed genes from *NaJAR4*, as revealed by the

OS-elicited OH-JA-Ile and COOH-JA-Ile levels across the 3 groups (*SI Appendix*, Fig. S19). The M5 lines exhibit the highest JA-Ile degradation levels, followed by ir*GLR* in the M7 and the JAR variant group. Thus, silencing hub genes in the OS-elicited network results in major aberrations in defense responses, proportional to their topological distance in the network from a major mutation in a core gene of the pathway. This result provides insight into how a gene network can buffer OS-induced defense traits through phenotypic plasticity, allowing JA-Ile natural mutants to maintain their chemical defense when faced with herbivory. This interpretation complements the functional explanation at a different level of analysis, where varying degrees of herbivory or other environmental factors facilitate balancing selection regimes maintaining *NaJAR4* variants in natural populations.

Proximate and Ultimate Levels of Explanation of Major Mutations. This work provides an example of how a single gene mutation in a major signaling pathway can be buffered by a robust GRN and provides the outlines of a mechanistic explanation for how the mutants are able to persist in nature. In such cases, the GRN likely evolve toward a stable state where a single gene mutation becomes less likely to affect individual fitness (87). This robustness however does not come at a cost of polygenic selection, as it can facilitate accumulation of other loss-of-function mutations, thereby increasing genetic diversity and providing additional mechanisms for adaptation in changing environments, elegantly described as "evolutionary capacitance" (88). Thus, a mechanistic understanding of a trait in the context of its larger GRN can provide evolutionary insights into organismal fitness. For example, when grown under laboratory conditions, *Arabidopsis JAR1*-mutants display an early flowering phenotype but are also hypersensitive to drought, which suggests the hypothesis that the mutation could maximize fitness under drought conditions (89). Whether *N. attenuata* V lines are similarly adapted to dryer sites, and whether the GRN minimizes the V line's likely drought susceptibility, are testable hypotheses that could inform the analysis of potential balancing selection regimes.

The melding of evolutionary and molecular biology approaches is leading to a new era of consilience between these disciplines, where the focus is shifting from gene-first to interaction-first models (14). Molecular biology has primarily focused on understanding the genetic bases of a trait, often using model systems to characterize signaling pathways. We have learned that these systems are often complex, with multiple levels of fine-tuning and cross-talk among signaling pathways (90). This complexity can be amortized through an omnigene model, which emphasizes the interconnectedness of genes and their role in shaping complex phenotypes (18). The integration of molecular and evolutionary approaches can furthermore provide a more nuanced understanding of the relationship between genes and phenotypes and the genetic bases underlying complex traits in the context of evolutionary outcomes. This framework accommodates both mechanistic and functional explanations for trait evolution in an organismic context (14). However, it is still critical to examine alternative hypotheses in the same level of analysis to holistically understand biological systems (11). Our inference of both spatiotemporal balancing selection and the OS-elicited gene network facilitating the maintenance of the *NaJAR4* mutation are not alternative hypotheses as they are posed at different levels of analysis. Thus, the analysis of the four hub genes from the OS-elicited gene network presented here should be viewed in the context of this broader perspective, as part of a larger network of interacting players that contribute to plant defense and fitness.

Conclusions

The identification of natural variation in JA-signaling in *N. attenuata* brings full circle two-decades of research with this system in which these natural mutants were anticipated based on the herbivore community's response to field releases of lines from a reverse-genetics toolbox (57). The dramatic response of leafhoppers to field releases of JA-deficient RNAi lines, combined with sporadic observations of leafhopper damage in wild populations (seemingly corresponding to JA deficiency in damaged plants, (58)) suggested that natural populations of *N. attenuata* must harbor JA-signaling mutants. This is what we report here by developing a forward-genetics toolbox that captured most of the species genetic variability in ecological traits. An updated contiguous reference genome allowed natural variation in OS-elicited JA-Ile bursts in field plantings of the MAGIC RIL population to be imputed to the *NaJAR4* locus. We mined our extensive seed collections of natural *N. attenuata* populations to describe the spatial and temporal persistence of the mutation in natural populations and its fitness effects in controlled environments. We further show how this large-effect single-gene mutation could be maintained in natural populations as a consequence of being embedded in stabilizing layers of an OS-induced coexpression network, which, together with overlapping homolog functions, allow mutants to maximize their fitness in varying environments.

It is likely that natural populations of other plant species harbor such major mutations in other canonical signaling cascades, despite large fitness effects of these mutations. Indeed, two commonly used models in plant biology are consistent with this inference: The laboratory strain of *N. benthamiana*, a workhorse for plant biotechnology and synthetic biology, is a natural *RdR1* mutant, highly deficient in the RNAi mechanisms required for viral resistance (91–93); the reference strain of *A. thaliana*, Col-0, is a natural hydroperoxide lyase mutant (94, 95) deficient in green leaf volatile production. The coarse-grained perturbation analysis presented here of an herbivory-induced gene network stabilizing a natural mutation in canonical JA-signaling reveals how much more remains to be discovered in the complex signaling systems that plants use to optimize their fitness in heterogeneous natural environments.

The results of this work also harmonize with recent work on *Caenorhabditis elegans* natural populations (96). Interindividual metabolic variation in amino acid (again, Ile and Val) conjugation to 3-hydroxypropionate in the species, resulting from mutations in propionyl-CoA carboxylase activity, which in humans causes a rare, but severe, metabolic disorder—propionic acidemia—is maintained on a small spatial scale in Hawaiian island populations of worms. It is likely that the compensatory transcriptomic and metabolic responses result from the pleiotropic effect of "peripheral" genes, which maintain these large-effect mutations in the Ile/Val conjugation steps in both natural populations of plants and nematodes. In nematodes, the biochemical details of these compensatory responses, elegantly characterized as "shunts within shunts" are known; in plants, these mechanisms remain unresolved in the complicated regulatory circuits of the 446-gene OS-elicited gene network that buffers canonical JA-signaling from perturbations. Clearly, more fine-grained perturbations of network topologies, as pioneered in *S. cerevisiae* (23), are needed to evaluate whether and how these complex gene networks and metabolic networks maintain large-effect mutations in natural populations.

The commonalities of metabolic variation uncovered in natural populations of nematodes and plants suggest that the concepts of precision medicine (97) apply equally well to animals and plants. In plants, such concepts have been in practice through "precision" pest

control and disease resistance for eons. These similarities also provide valuable guidance to the conservation stewards of a planet rapidly losing its unexplored biodiversity (98): Identifying and preserving hotspots of genetic variance should be of the highest priority.

Materials and Methods

The description of plant materials, cultivation, plant treatment and sampling in the GH together with subsequent transcriptome sequencing and analysis, metabolite analyses, genetic, genomic analyses, and larval growth assays are all based on published procedures and detailed in *SI Appendix*. As the MAGIC population and the field screening and its analysis motivated our focus on *NaJAR4* variation and its characterization, those methods are briefly described here, with additional details in *SI Appendix*.

Creation of MAGIC RIL Population. The founder lines for 26-parent MAGIC RIL population were selected by screening 422 plants from 74 different natural accessions for various ecologically relevant traits, focusing on metabolic response to herbivory (99). The 24 plants with the most extreme phenotypes (*SI Appendix*, Fig. S3*A*) plus the well-characterized Utah (UT, 30× inbred line) and Arizona (AZ, 22× inbred line) accessions were chosen as MAGIC founder lines. This is a common selection criterion for founder lines for multiparent plant population, when the primary focus is to dissect the genetic basis of agronomic traits and improve them (100) and not specifically to sample spatially stratified populations to conduct population genetic analyses. Five rounds of systematic intercrossing ensured the resulting population of 325 plants had genetic contribution from all 26 parents and were subsequently inbred for six generation to achieve approximately 99% homozygosity. Detailed methods and technical considerations are given in *SI Appendix*, *Materials and Methods*. A graphical overview of the creation of this MAGIC population is given in ref. 64. All the plants for all crosses were grown in GH of Max Planck Institute for Chemical Ecology (MPI-CE), Jena, Germany, under the conditions described earlier.

Field Experiments and RNA-Seq from Field Samples. Two replicates of the 650 MAGIC RILs population and the 26 parental lines were planted at the Walnut Creek Center for Education and Research (WCCER) in Prescott, AZ. Smoke- and GA_3-treated *N. attenuata* seeds were germinated in Jiffy-7® peat pellets hydrated with a native soil extract to provide plants with an appropriate microbiome during germination (101) and then planted in the field plot. A standardized *M. sexta*-specific response in a kinetically defined manner was elicited in the second and third stem leaves of every plant by wounding and applying 20 µL of 1:5 diluted *M. sexta* OS. The first (lowest) stem leaf was left untreated and harvested as an unelicited control leaf immediately before the elicitation. Leaf samples were harvested at 0 h, 1 h, and 72 h, respectively, and immediately frozen on dry ice, transported on dry ice in dry-ice shipping containers to the MPI-CE, where they were stored in −80 °C freezers until further processing. Ground frozen leaf tissue (1 h OS-elicited) aliquots from 350 plants were shipped to Novogene (HK) Company Ltd. for RNA-Seq and sequenced on Illumina Novaseq.

The details of the field watering and planting scheme as well as experimental and harvesting protocols along with library preparations for sequencing are given in *SI Appendix*.

Data, Materials, and Software Availability. All raw sequence and optical map data were deposited in the NCBI SRA database. The Whole Genome project has been deposited at DDBJ/ENA/GenBank under the accession JAPQWU000000000 with BioProject id PRJNA900029 (102). The version described in this paper is version JAPQWU010000000. The MAGIC parents and RIL WGS are available under BioProject id PRJNA907539 (103). The two transcriptome datasets are available under BioProject PRJNA898122(104) and PRJNA911202 (105).

ACKNOWLEDGMENTS. We thank all the members of the Department of Molecular Ecology who contributed to the decade-long MAGIC project. Detailed acknowledgments with individual contributions are listed in *SI Appendix*. This work was supported by the Max Planck Society's core funding of I.T.B.'s department, Advanced grant no. 293926 of the European Research Council to I.T.B., and the Deutsche Forschungsgemeinschaft–SFB 1127/2 ChemBioSys–239748522 grant to I.T.B.

Author affiliations: [a]Department of Molecular Ecology, Max Planck Institute for Chemical Ecology, 07745 Jena, Germany; [b]Department of Natural Product Biosynthesis, Max Planck Institute for Chemical Ecology, 07745 Jena, Germany; [c]Department of Molecular Biology and Genetics, Cornell University, Ithaca, NY 14850; [d]Department of Geography, University of Zurich, 8006 Zurich, Switzerland; [e]Department of Chemistry, University of Zurich, 8006 Zurich, Switzerland; and [f]Institut national de recherche pour l'agriculture, l'alimentation et l'environnement, Centre National de Resources Génomiques Végétales, French Plant Genomic Resource Center, Castanet Tolosan F-31326, France

Author contributions: R.R., R.H., M.C.S., and I.T.B. designed research; R.R., R.H., K.G., S.M.L., M.C.S., and I.T.B. performed research; K.G., N.R., and I.T.B. contributed new reagents/analytic tools; R.R., R.H., S.M.L., M.C.S., and I.T.B. analyzed data; and R.R. and I.T.B. wrote the paper, with contributions from R.H., K.G., and M.C.S.

1. R. A. Fisher, *The Genetical Theory of Natural Selection* (Oxford University Press, 1930).
2. C. Darwin, *On the Origin of Species* (Routledge, 1859).
3. N. H. Barton, A. M. Etheridge, A. Véber, The infinitesimal model: Definition, derivation, and implications. *Theor. Popul. Biol.* **118**, 50–73 (2017).
4. R. D. Barrett *et al.*, Linking a mutation to survival in wild mice. *Science* **363**, 499–504 (2019).
5. C. R. Linnen *et al.*, Adaptive evolution of multiple traits through multiple mutations at a single gene. *Science* **339**, 1312–1316 (2013).
6. A. E. Berardi *et al.*, Complex evolution of novel red floral color in *Petunia*. *Plant Cell* **33**, 2273–2295 (2021).
7. R. Kerwin *et al.*, Natural genetic variation in *Arabidopsis thaliana* defense metabolism genes modulates field fitness. *eLife* **4**, e05604. (2015).
8. M. Todesco *et al.*, Natural allelic variation underlying a major fitness trade-off in *Arabidopsis thaliana*. *Nature* **465**, 632–636 (2010).
9. C. Ponzio, B. T. Weldegergis, M. Dicke, R. Gols, Compatible and incompatible pathogen–plant interactions differentially affect plant volatile emissions and the attraction of parasitoid wasps. *Funct. Ecol.* **30**, 1779–1789 (2016).
10. T. Züst, A. A. Agrawal, Trade-offs between plant growth and defense against insect herbivory: An emerging mechanistic synthesis. *Annu. Rev. Plant. Biol.* **68**, 513–534 (2017).
11. P. W. Sherman, The levels of analysis. *Anim. Behav.* **36**, 616–619 (1988).
12. T. A. Manolio *et al.*, Finding the missing heritability of complex diseases. *Nature* **461**, 747–753 (2009).
13. I. Barrio-Hernandez *et al.*, Network expansion of genetic associations defines a pleiotropy map of human cell biology. *Nat. Genet.* **55**, 1–10 (2023).
14. M. Fagny, F. Austerlitz, Polygenic adaptation: Integrating population genetics and gene regulatory networks. *Trends Genet.* **37**, 631–638 (2021).
15. E. A. Boyle, Y. I. Li, J. K. Pritchard, An expanded view of complex traits: From polygenic to omnigenic. *Cell* **169**, 1177–1186 (2017).
16. D. J. Watts, S. H. Strogatz, Collective dynamics of "small-world" networks. *Nature* **393**, 440–442 (1998).
17. S. H. Strogatz, Exploring complex networks. *Nature* **410**, 268–276 (2001).
18. X. Liu, Y. I. Li, J. K. Pritchard, Trans effects on gene expression can drive omnigenic inheritance. *Cell* **177**, 1022–1034.e6 (2019).
19. E. Q. Paull *et al.*, A modular master regulator landscape controls cancer transcriptional identity. *Cell* **184**, 334–351 (2021).
20. J. Peedicayil, D. R. Grayson, An epigenetic basis for an omnigenic model of psychiatric disorders. *J. Theor. Biol.* **443**, 52 (2018).
21. P. Van Der Harst, N. Verweij, Identification of 64 novel genetic loci provides an expanded view on the genetic architecture of coronary artery disease. *Circ. Res.* **122**, 433–443 (2018).
22. A. Chateigner *et al.*, Gene expression predictions and networks in natural populations supports the omnigenic theory. *BMC Genomics* **21**, 1–16 (2020).
23. P. Kemmeren *et al.*, Large-scale genetic perturbations reveal regulatory networks and an abundance of gene-specific repressors. *Cell* **157**, 740–752 (2014).
24. D. N. Rate, J. V. Cuenca, G. R. Bowman, D. S. Guttman, J. T. Greenberg, The gain-of-function *Arabidopsis acd6* mutant reveals novel regulation and function of the salicylic acid signaling pathway in controlling cell death, defenses, and cell growth. *Plant Cell* **11**, 1695–1708 (1999).
25. M. Erb, D. J. Kliebenstein, Plant secondary metabolites as defenses, regulators, and primary metabolites: The blurred functional trichotomy. *Plant Physiol.* **184**, 39–52 (2020).
26. A. Kessler, I. T. Baldwin, Plant responses to insect herbivory: The emerging molecular analysis. *Annu. Rev. Plant. Biol.* **53**, 299–328 (2002).
27. D. Cipollini, D. Walters, C. Voelckel, "Costs of resistance in plants: from theory to evidence" in *Annual Plant Reviews, Insect-Plant Interactions*, C. Voelckel, G. Jander, Eds. (John Wiley & Sons, Ltd, 2014), pp. 263–307.
28. P. D. Coley, J. P. Bryant, F. S. Chapin III, Resource availability and plant antiherbivore defense. *Science* **230**, 895–899 (1985).
29. D. A. Herms, W. J. Mattson, The dilemma of plants: To grow or defend. *Q. Rev. Biol.* **67**, 283–335 (1992).
30. M. Dicke, I. T. Baldwin, The evolutionary context for herbivore-induced plant volatiles: Beyond the 'cry for help'. *Trends Plant Sci.* **15**, 167–175 (2010).
31. N. Yoshinaga *et al.*, Fatty acid-amino acid conjugates diversification in lepidopteran caterpillars. *J. Chem. Ecol.* **36**, 319–325 (2010).
32. R. Halitschke, U. Schittko, G. Pohnert, W. Boland, I. T. Baldwin, Molecular interactions between the specialist herbivore *Manduca sexta* (Lepidoptera, Sphingidae) and its natural host *Nicotiana attenuata*. III. Fatty acid-amino acid conjugates in herbivore oral secretions are necessary and sufficient for herbivore-specific plant responses. *Plant Physiol.* **125**, 711–717 (2001).

33. A. Roda, R. Halitschke, A. Steppuhn, I. T. Baldwin, Individual variability in herbivore-specific elicitors from the plant's perspective. *Mol. Ecol.* **13**, 2421–2433 (2004).
34. A. VanDoorn, M. Kallenbach, A. A. Borquez, I. T. Baldwin, G. Bonaventure, Rapid modification of the insect elicitor N-linolenoyl-glutamate via a lipoxygenase-mediated mechanism on *Nicotiana attenuata* leaves. *BMC Plant Biol.* **10**, 1–11 (2010).
35. J.-H. Kang, L. Wang, A. Giri, I. T. Baldwin, Silencing threonine deaminase and *JAR4* in *Nicotiana attenuata* impairs jasmonic acid–isoleucine–mediated defenses against *Manduca sexta*. *Plant Cell* **18**, 3303–3320 (2006).
36. S. Fonseca *et al.*, (+)-7-iso-Jasmonoyl-L-isoleucine is the endogenous bioactive jasmonate. *Nat. Chem. Biol.* **5**, 344–350 (2009).
37. D.-X. Xie, B. F. Feys, S. James, M. Nieto-Rostro, J. G. Turner, COI1: An *Arabidopsis* gene required for jasmonate-regulated defense and fertility. *Science* **280**, 1091–1094 (1998).
38. A. Paschold, R. Halitschke, I. T. Baldwin, Co (i)-ordinating defenses: NaCOI1 mediates herbivore-induced resistance in *Nicotiana attenuata* and reveals the role of herbivore movement in avoiding defenses. *Plant J.* **51**, 79–91 (2007).
39. A. Paschold, G. Bonaventure, M. R. Kant, I. T. Baldwin, Jasmonate perception regulates jasmonate biosynthesis and JA-Ile metabolism: The case of COI1 in *Nicotiana attenuata*. *Plant Cell Physiol.* **49**, 1165–1175 (2008).
40. A. Chini, S. Gimenez-Ibanez, A. Goossens, R. Solano, Redundancy and specificity in jasmonate signalling. *Curr. Opin. Plant. Biol.* **33**, 147–156 (2016).
41. B. Thines *et al.*, JAZ repressor proteins are targets of the SCF^{COI1} complex during jasmonate signalling. *Nature* **448**, 661–665 (2007).
42. Y. Yan *et al.*, A downstream mediator in the growth repression limb of the jasmonate pathway. *Plant Cell* **19**, 2470–2483 (2007).
43. Y. Oh, I. T. Baldwin, I. Gális, NaJAZh regulates a subset of defense responses against herbivores and spontaneous leaf necrosis in *Nicotiana attenuata* plants. *Plant Physiol.* **159**, 769–788 (2012).
44. R. Li *et al.*, Flower-specific jasmonate signaling regulates constitutive floral defenses in wild tobacco. *Proc. Natl. Acad. Sci. U.S.A.* **114**, E7205–E7214 (2017).
45. G. A. Howe, I. T. Major, A. J. Koo, Modularity in jasmonate signaling for multistress resilience. *Annu. Rev. Plant. Biol.* **69**, 387–415 (2018).
46. C. Wasternack, B. Hause, Jasmonates: Biosynthesis, perception, signal transduction and action in plant stress response, growth and development. An update to the 2007 review in annals of botany. *Ann. Bot.* **111**, 1021–1058 (2013).
47. G. Bonaventure, I. T. Baldwin, New insights into the early biochemical activation of jasmonic acid biosynthesis in leaves. *Plant Signal Behav.* **5**, 287–289 (2010).
48. J. Wu, I. T. Baldwin, New insights into plant responses to the attack from insect herbivores. *Annu. Rev. Genet.* **44**, 1–24 (2010).
49. H. Kaur, N. Heinzel, M. Schöttner, I. T. Baldwin, I. Gális, R2R3-NaMYB8 regulates the accumulation of phenylpropanoid-polyamine conjugates, which are essential for local and systemic defense against insect herbivores in *Nicotiana attenuata*. *Plant Physiol.* **152**, 1731–1747 (2010).
50. J. A. Zavala, A. G. Patankar, K. Gase, I. T. Baldwin, Constitutive and inducible trypsin proteinase inhibitor production incurs large fitness costs in *Nicotiana attenuata*. *Proc. Natl. Acad. Sci. U.S.A.* **101**, 1607–1612 (2004).
51. N. Onkokesung *et al.*, MYB8 controls inducible phenolamide levels by activating three novel hydroxycinnamoyl-coenzyme A: Polyamine transferases in *Nicotiana attenuata*. *Plant Physiol.* **158**, 389–407 (2012).
52. S. Heiling *et al.*, Jasmonate and ppHsystemin regulate key malonylation steps in the biosynthesis of 17-hydroxygeranyllinalool diterpene glycosides, an abundant and effective direct defense against herbivores in *Nicotiana attenuata*. *Plant Cell* **22**, 273–292 (2010).
53. I. Monte *et al.*, Ligand-receptor co-evolution shaped the jasmonate pathway in land plants. *Nat. Chem. Biol.* **14**, 480–488 (2018).
54. S. Kneeshaw *et al.*, Ligand diversity contributes to the full activation of the jasmonate pathway in *Marchantia polymorpha*. *Proc. Natl. Acad. Sci. U.S.A.* **119**, e2202930119 (2022).
55. X. Geng, L. Jin, M. Shimada, M. G. Kim, D. Mackey, The phytotoxin coronatine is a multifunctional component of the virulence armament of *Pseudomonas syringae*. *Planta* **240**, 1149–1165 (2014).
56. L. Katsir, A. L. Schilmiller, P. E. Staswick, S. Y. He, G. A. Howe, *COI1* is a critical component of a receptor for jasmonate and the bacterial virulence factor coronatine. *Proc. Natl. Acad. Sci. U.S.A.* **105**, 7100–7105 (2008).
57. A. Kessler, R. Halitschke, I. T. Baldwin, Silencing the jasmonate cascade: Induced plant defenses and insect populations. *Science* **305**, 665–668 (2004).
58. M. Kallenbach, G. Bonaventure, P. A. Gilardoni, A. Wissgott, I. T. Baldwin, *Empoasca* leafhoppers attack wild tobacco plants in a jasmonate-dependent manner and identify jasmonate mutants in natural populations. *Proc. Natl. Acad. Sci. U.S.A.* **109**, E1548–E1557 (2012).
59. Y. Bai *et al.*, Natural history-guided omics reveals plant defensive chemistry against leafhopper pests. *Science* **375**, eabm2948 (2022).
60. C. Yang *et al.*, Exploring the metabolic basis of growth/defense trade-offs in complex environments with *Nicotiana attenuata* plants cosilenced in *NaMYC2a* expression. *New Phytol.* **238**, 349–366 (2023).
61. S. Xu, W. Zhou, S. Pottinger, I. T. Baldwin, Herbivore associated elicitor-induced defences are highly specific among closely related *Nicotiana* species. *BMC Plant Biol.* **15**, 1–13 (2015).
62. W. Zhou *et al.*, Evolution of herbivore-induced early defense signaling was shaped by genome-wide duplications in *Nicotiana*. *eLife* **5**, e19531 (2016).
63. A. L. Price *et al.*, Principal components analysis corrects for stratification in genome-wide association studies. *Nat. Genet.* **38**, 904–909 (2006).
64. R. Ray, D. Li, R. Halitschke, I. T. Baldwin, Using natural variation to achieve a whole-plant functional understanding of the responses mediated by jasmonate signaling. *Plant J.* **99**, 414–425 (2019).
65. L. Wang, S. Allmann, J. Wu, I. T. Baldwin, Comparisons of LIPOXYGENASE3-and JASMONATE-RESISTANT4/6-silenced plants reveal that jasmonic acid and jasmonic acid-amino acid conjugates play different roles in herbivore resistance of *Nicotiana attenuata*. *Plant Physiol.* **146**, 904–915 (2008).
66. P. E. Staswick, I. Tiryaki, The oxylipin signal jasmonic acid is activated by an enzyme that conjugates it to isoleucine in *Arabidopsis*. *Plant Cell* **16**, 2117–2127 (2004).
67. L. F. Delph, J. K. Kelly, On the importance of balancing selection in plants. *New Phytol.* **201**, 45–56 (2014).
68. J. Schwachtje *et al.*, SNF1-related kinases allow plants to tolerate herbivory by allocating carbon to roots. *Proc. Natl. Acad. Sci. U.S.A.* **103**, 12935–12940 (2006).
69. L. Wang *et al.*, Independently silencing two JAR family members impairs levels of trypsin proteinase inhibitors but not nicotine. *Planta* **226**, 159–167 (2007).
70. G. A. Glawe, J. A. Zavala, A. Kessler, N. M. Van Dam, I. T. Baldwin, Ecological costs and benefits correlated with trypsin protease inhibitor production in *Nicotiana attenuata*. *Ecology* **84**, 79–90 (2003).
71. O. L. Cope, K. Keefover-Ring, E. L. Kruger, R. L. Lindroth, Growth-defense trade-offs shape population genetic composition in an iconic forest tree species. *Proc. Natl. Acad. Sci. U.S.A.* **118**, e2103162118 (2021).
72. A. L. File, G. P. Murphy, S. A. Dudley, Fitness consequences of plants growing with siblings: Reconciling kin selection, niche partitioning and competitive ability. *Proc. R. Soc. Lond. B Biol. Sci.* **279**, 209–218 (2012).
73. J. Wu, J.-H. Kang, C. Hettenhausen, I. T. Baldwin, Nonsense-mediated mRNA decay (NMD) silences the accumulation of aberrant trypsin proteinase inhibitor mRNA in *Nicotiana attenuata*. *Plant J.* **51**, 693–706 (2007).
74. R. A. Bahulikar, D. Stanculescu, C. A. Preston, I. T. Baldwin. ISSR and AFLP analysis of the temporal and spatial population structure of the post-fire annual, *Nicotiana attenuata*, SW Utah. *BMC Ecol.* **4**, 1–13 (2004).
75. K. R. Sime, I. T. Baldwin, Opportunistic out-crossing in *Nicotiana attenuata* (Solanaceae), a predominantly self-fertilizing native tobacco. *BMC Ecol.* **3**, 1–9 (2003).
76. E. Katz *et al.*, Genetic variation underlying differential ammonium and nitrate responses in *Arabidopsis* thaliana. *Plant Cell* **34**, 4696–4713 (2022).
77. J. H. Wisecaver *et al.*, A global coexpression network approach for connecting genes to specialized metabolic pathways in plants. *Plant Cell* **29**, 944–959 (2017).
78. A. Mine *et al.*, The defense phytohormone signaling network enables rapid, high-amplitude transcriptional reprogramming during effector-triggered immunity. *Plant Cell* **30**, 1199–1219 (2018).
79. C. C. von Dahl *et al.*, Tuning the herbivore-induced ethylene burst: The role of transcript accumulation and ethylene perception in *Nicotiana attenuata*. *Plant J.* **51**, 293–307 (2007).
80. N. Onkokesung *et al.*, Jasmonic acid and ethylene modulate local responses to wounding and simulated herbivory in *Nicotiana attenuata* leaves. *Plant Physiol.* **153**, 785–798 (2010).
81. S. A. Mousavi, A. Chauvin, F. Pascaud, S. Kellenberger, E. E. Farmer, GLUTAMATE RECEPTOR-LIKE genes mediate leaf-to-leaf wound signalling. *Nature* **500**, 422–426 (2013).
82. A. L. Schapire, V. Valpuesta, M. A. Botella, TPR proteins in plant hormone signaling. *Plant Signal Behav.* **1**, 229–230 (2006).
83. A. Rosado *et al.*, The *Arabidopsis* tetratricopeptide repeat-containing protein TTL1 is required for osmotic stress responses and abscisic acid sensitivity. *Plant Physiol.* **142**, 1113–1126 (2006).
84. L. E. Gonzalez, K. Keller, K. X. Chan, M. M. Gessel, B. C. Thines, Transcriptome analysis uncovers *Arabidopsis* F-BOX STRESS INDUCED 1 as a regulator of jasmonic acid and abscisic acid stress gene expression. *BMC Genomics* **18**, 1–15 (2017).
85. C. Meng *et al.*, Dimension reduction techniques for the integrative analysis of multi-omics data. *Brief. Bioinform.* **17**, 628–641 (2016).
86. A. J. Koo, F. F. Cooke, G. A. Howe, Cytochrome P450 CYP94B3 mediates catabolism and inactivation of the plant hormone jasmonoyl-L-isoleucine. *Proc. Natl. Acad. Sci. U.S.A.* **108**, 9298–9303 (2011).
87. A. Wagner, Does evolutionary plasticity evolve? *Evolution* **50**, 1008–1023 (1996).
88. A. Bergman, M. L. Siegal. Evolutionary capacitance as a general feature of complex gene networks. *Nature* **424**, 549–552 (2003).
89. S. Mahmud *et al.*, Constitutive expression of JASMONATE RESISTANT 1 induces molecular changes that prime the plants to better withstand drought. *Plant Cell Environ* **45**, 2906–2922 (2022).
90. N. Aerts, M. Pereira Mendes, S. C. Van Wees, Multiple levels of crosstalk in hormone networks regulating plant defense. *Plant J.* **105**, 489–504 (2021).
91. J. Bally *et al.*, The extremophile *Nicotiana benthamiana* has traded viral defence for early vigour. *Nat. Plants* **1**, 1–6 (2015).
92. S.-J. Yang, S. A. Carter, A. B. Cole, N.-H. Cheng, R. S. Nelson, A natural variant of a host RNA-dependent RNA polymerase is associated with increased susceptibility to viruses by *Nicotiana benthamiana*. *Proc. Natl. Acad. Sci. U.S.A.* **101**, 6297–6302 (2004).
93. X.-B. Ying *et al.*, RNA-dependent RNA polymerase 1 from *Nicotiana tabacum* suppresses RNA silencing and enhances viral infection in *Nicotiana benthamiana*. *Plant Cell* **22**, 1358–1372 (2010).
94. H. Duan, M.-Y. Huang, K. Palacio, M. A. Schuler, Variations in *CYP74B2* (hydroperoxide lyase) gene expression differentially affect hexenal signaling in the Columbia and Landsberg erecta ecotypes of *Arabidopsis*. *Plant Physiol.* **139**, 1529–1544 (2005).
95. J. P. Yactayo-Chang, C. T. Hunter, H. T. Alborn, S. A. Christensen, A. K. Block, Production of the green leaf volatile (Z)-3-hexenal by a *Zea mays* hydroperoxide lyase. *Plants* **11**, 2201 (2022).
96. B. W. Fox *et al.*, *C. elegans* as a model for inter-individual variation in metabolism. *Nature* **607**, 571–577 (2022).
97. E. A. Ashley, Towards precision medicine. *Nat. Rev. Genet.* **17**, 507–522 (2016).
98. M. Exposito-Alonso *et al.*, Genetic diversity loss in the Anthropocene. *Science* **377**, 1431–1435 (2022).
99. D. Li, I. T. Baldwin, E. Gaquerel, Navigating natural variation in herbivory-induced secondary metabolism in coyote tobacco populations using MS/MS structural analysis. *Proc. Natl. Acad. Sci. U.S.A.* **112**, E4147–E4155 (2015).
100. M. F. Scott *et al.*, Multi-parent populations in crops: A toolbox integrating genomics and genetic mapping with breeding. *Heredity (Edinb)* **125**, 396–416 (2020).
101. R. Santhanam *et al.*, Native root-associated bacteria rescue a plant from a sudden-wilt disease that emerged during continuous cropping. *Proc. Natl. Acad. Sci. U.S.A.* **112**, E5013–E5020 (2015).
102. R. Ray *et al.*, *Nicotiana attenuata* isolate: UT31x Genome sequencing and assembly. NCBI Sequence Read Archive https://www.ncbi.nlm.nih.gov/bioproject/PRJNA900029 Deposited 11 November 2022.
103. R. Ray *et al.*, Whole Genome Sequence of MAGIC parents and RIL population. NCBI Sequence Read Archive. https://www.ncbi.nlm.nih.gov/bioproject/PRJNA907539. Deposited 2 December 2022.
104. R. Ray *et al.*, Natural variation of OS elicitation in *Nicotiana attenuata*. NCBI Sequence Read Archive. https://www.ncbi.nlm.nih.gov/bioproject/PRJNA898122. Deposited 4 November 2022.
105. R. Ray *et al.*, *Nicotiana attenuata* AZ-2019 MAGIC eQTL. NCBI Sequence Read Archive. https://www.ncbi.nlm.nih.gov/bioproject/PRJNA911202. Deposited 12 December 2022.

PNAS

Supporting Information for
A persistent major mutation in canonical jasmonate signaling is embedded in an herbivory-elicited gene network

Rishav Ray[a], Rayko Halitschke[a], Klaus Gase[b], Sabrina M. Leddy[c], Meredith C. Schuman[d,e], Nathalie Rodde[f], Ian T. Baldwin[a,*]

[a]Department of Molecular Ecology, Max Planck Institute for Chemical Ecology, 07745 Jena, Germany
[b]Department of Natural Product Biosynthesis, Max Planck Institute for Chemical Ecology, 07745 Jena, Germany
[c]Department of Molecular Biology and Genetics, Cornell University, Ithaca, NY 14850
[d]Department of Geography, University of Zurich, 8006 Zurich, Switzerland
[e]Department of Chemistry, University of Zurich, 8006 Zurich, Switzerland
[f]Institut national de recherche pour l'agriculture, l'alimentation et l'environnement (INRAE), Le Centre National de Ressources Génomiques Végétales (CNRGV), French Plant Genomic Resource Center, Castanet Tolosan, F-31326 France

*Author for correspondence: Ian T. Baldwin
Email: baldwin@ice.mpg.de

This PDF file includes:

Supporting text
Figures S1 to S20
Tables S1 to S5
SI References

Supporting Information Text

Jasmonate (JA) signaling in *N. attenuata*

The JA signaling cascade in *N. attenuata* is triggered and strongly amplified when fatty acid amino acid elicitors in the oral secretions (OS) of Lepidopteran larvae are introduced into wounds during feeding (1–3). Both JA signaling and the resulting metabolic and transcriptomic responses are well-characterized in the *N. attenuata-M. sexta* model plant-herbivore system, and are known to be mediated by JA-Ile (4) acting as a ligand for COI1 (5, 6) which forms a receptor complex with hyper-variable jasmonate ZIM-domain (JAZ) proteins (7–10).

The JA signaling pathway provides context-dependent responses in form of diverse specialized metabolites that function as direct and indirect defenses. This metabolic reconfiguration accompanies changes in flowering behaviors that function as herbivore avoidance responses for this plant-herbivore system (11, 12). The metabolic flux into specialized metabolism used for chemical defenses can command substantial fractions of a plant's fitness-limiting resources (13–15) and in combination with the inherent toxicity of many defensive metabolites (16), is ultimately responsible for growth/defense trade-offs mediated by JA signaling (17–19). The remarkable diversity of the often tissue-specific metabolic and developmental responses regulated by this conserved pathway is largely mediated by the diversification of downstream modules, including the JAZ family of transcription factors (10, 20, 21). Experiments performed under unconstrained resources in the laboratory have shown that *Arabidopsis thaliana* mutants, lacking five JAZ proteins and the photoreceptor, phytochrome B, can avoid the ubiquitous growth/-defense trade-off faced by most plants (22). Hence, JA signaling likely anticipates the ultimate resource-based and (auto)toxicity costs of elicited defense metabolites, allowing plants to dampen or avoid these.

In the ABA phytohormone signaling system, which shares many structural similarities with the JA-signaling system, ABA degradation products have evolved signaling functions through duplications of the canonical receptors (23). We were particularly interested in evaluating if similar signaling innovations had evolved in JA-signaling in *N. attenuata*, and hence examined correlations with JA-degradation products (OH-JA, OH-JA-Ile, COOH-JA-Ile: Fig. S18 - S19) and silenced the expression of *NaCOI2*.

Balancing selection acting on the *NaJAR4* allele

The spatio-temporal variation of *NaJAR4* variant allele is consistent with previous unsuccessful attempts at identifying population and geographical structure of *N. attenuata* using ISSR and AFLP markers (24), likely resulting from the species' long-lived seedbanks and long-distance seed dispersal patterns from seasonal water flow and ancestral humans, who valued the plant for smoking purposes (25). In natural populations, germination from long-lived seedbanks is synchronized by smoke from wildfires (26, 27), where co-occurring plants commonly span a 10-fold size range at flowering time. This substantial variability in an individual's size can be attributed to water availability at the micro-site of the germinating seed, adding an additional layer of complexity to the underlying selection regime. From this natural history context, it is evident that there is considerable mobility of *N. attenuata* populations in different niches, either naturally or through anthropogenic means, which are a pre-requisite for the persistence of genetic polymorphisms through spatial variation (28, 29). We infer that balancing selection regimes resulting from environmental stochasticity and phenotypic plasticity, rather than frequency dependent niche adaptations, maintain this mutation in natural populations. This inference is consistent with field studies of glucosinolate mutants in *A. thaliana* and *Boechera stricta*, where fitness varied more by site and season than by genotype (30, 31), and provides another example of "protected polymorphism" in plants through spatio-temporal variation (28). In order to analyze the precise selection mechanism at play in this system, a more rigorous stratified sampling of *N. attenuata* population would be required, which was not our objective in selecting the MAGIC parents ((32) and Materials and Methods).

NaCOI2 does not buffer the *NaJAR4* mutation in floral tissues

Research in the *M. polymorpha* system has revealed that the COI receptor complex has been evolutionarily labile (33–35). Although *Arabidopsis* has only one copy of COI, other higher plant genomes, such as corn and rice, harbor multiple COIs (36–38); the *N. attenuata* genome has two: *NaCOI1*, *NaCOI2*. We hypothesized that *NaCOI2* could be an alternate JA-Ile receptor in floral tissues, and silenced *NaCOI2* expression by stable RNAi to test this inference (Fig. S10A). Previous research with *NaCOI1*-RNAi lines revealed strong feedback between receptor function and ligand (JA-Ile) accumulation: the lack of JA-Ile perception results in elevated accumulation of JA-Ile and its degradation products (6, 8). However, JA and JA-Ile levels did not differ between ir*NaCOI2* and WT plants, but the levels in ir*NaCOI1* plants differed dramatically from WT, as previously published (5, 6, 8) (Fig. S11A-B). Additionally, JA-Ile dependent total diterpene glycosides (DTG) (39) levels which are significantly downregulated (by 51%) in ir*NaCOI1* were at WT levels in ir*NaCOI2* plants (Fig. S11E). We thus discounted the possibility of an alternate JA-Ile receptor system in *N. attenuata* floral tissues, and *NaCOI2* as a viable candidate that buffers the fitness consequences of the JA-Ile variation (Fig. 3).

MeJA induced TPI as a proxy for defense

MeJA treatment was used to induce defense responses in a standardized manner without leaf damage, tissue loss, or inducing other phytohormone signaling; however, it elevates endogenous JA levels for conjugation by NaJARs (17, 40). MeJA-induced trypsin proteinase inhibitor (TPI) activity was used as a quantitative proxy for defense; TPI activity has been shown to be both a potent anti-herbivore defense acting synergistically with other deterrents such as nicotine (41), and to accrue significant fitness costs when plants are grown in competition with other plants (13). Although nicotine, which is synthesized in the roots, commands almost 6% of *N. attenuata*'s nitrogen budget (14), nicotine pools are remarkably stable and are not reused for metabolism and growth. In contrast, costs accrued due to TPI production in leaves likely reflect changes in metabolism required to support their production (42) as well as other co-regulated induced defenses and hence TPI activity is a reliable proxy for induced defense costs.

Kin-recognition and competitive outcomes

Under kin-recognition assumptions formulated by Hamilton's rule (43), genetically-related individuals such as the RNAi lines created in the UT-WT background paired with UT-WT plants, can forgo their individual fitness toward others to maximize mean genotypic fitness, whereas genetically-distant individuals would compete for the shared resources and through other means maximize their own fitness. We reasoned that if the X plants (Fig. 3A-B) are trading-off their investment in defense towards growth and fitness, they would be expected to acquire more resources than the slower-growing but well-defended Y plants and be clearly distinguishable in the defense-fitness trait space. Furthermore, the RNAi lines paired with UT-WT plants represent full-sibling pairings that are homozygous at all loci but the one harboring the T-DNA insertion. Under the assumption of kin-recognition, the *NaJAR*-RNAi lines are expected to perform better than UT-WT, irrespective of the treatment, as the former will accrue lower defense costs owing to the NaJAR deficiency. The results are consistent with kin-recognition expectations, where the isogenic RNAi lines competing with UT-WT, did not show significantly lower capsule counts when MeJA-induced although they accumulated 2-fold lower TPI activity compared to NV plants (Fig. 3B). However, when compared to their well-defended UT competitors, the *NaJAR*-RNAi lines produced significantly more (by 42%) capsules. While these results are consistent with the predictions of kin-recognition theory, further research is needed to resolve these putative kin-recognition mechanisms.

Materials and Methods

Plant material

The *N. attenuata* WT plants used for all the sequencing and optical mapping were from a 31st generation inbred line referred to as the UT accession, which originated from a collection from a native population at the Desert Inn (DI) ranch in Washington County, Utah, USA. The collection

locations of the other natural accessions were described in (32) and are shown in Fig. S4. The other natural accessions used in this study are listed in in table S4. All plants were grown with a day/night cycle of 16 h (22-26 °C) /8 h 22-24 °C at a relative humidity of 40-60% in a glasshouse (GH) of Max Planck Institute for Chemical Ecology (MPI-CE), Jena, Germany.

Creation of MAGIC RIL population

To create the 26-parent Multiparent Advanced Generation Inter-Cross (MAGIC) recombinant inbred line (RIL) population, 422 plants from 74 different natural accessions were germinated and characterized with respect to morphological, biochemical and ecologically relevant traits (32). The 24 plants with the most extreme phenotypes (Fig. S3A) plus the well-characterized Utah (UT, 30x inbred line) and Arizona (AZ, 22x inbred line) accessions were chosen as MAGIC founder lines. This allowed us to capture a large proportion of the diverse quantitative ecological traits from genotypically diverse natural accessions of this native plant.

To structure this genetic diversity in the MAGIC RIL population, we developed a crossing scheme with the 26-parental lines that entailed five rounds of systematic inter-crosses from which the offspring would each have all of the 26 parental lines as ancestors. In each round of these crosses, the following 3 criteria were fulfilled: (1) no reciprocal crosses, (2) each plant served as a maternal line, and (3) each plant served as a paternal line if possible. In the first round, diallelic crossing of each of the 26 parental lines with each other was performed, resulting in an F_1 or A-generation of (26 x 26 - 26)/2 or 325 different crosses. Five plants per founder line were grown and one plant per line was used as a maternal line; the other 4 served as paternal lines (pollen donors). To prevent self-pollination, all flowers on each maternal-line plant that would open in a given night were antherectomized between 4:30 AM and the start of the light cycle (sunrise or 6:00 AM when GH lights were switched on), before anthesis, which normally occurred just before corollas fully opened the following evening. For hand-pollinations, one freshly dehisced anther was used to pollinate one maternal-line stigma in an antherectomized flower with approximately 4000 pollen grains (44). Five antherectomized flowers per line were pollinated. All seeds were collected from each crossed capsule and were pooled per plant to represent one line of the A-generation, numbered A1 to A325. This numbering scheme was maintained in all subsequent crosses, which allowed tracking of the maternal lines; subsequent generations were given different letters. For example, seeds of the A1 generation were germinated to produce plant A1, which produced seeds B1, which were germinated to produce plant B1, which produced seeds C1 and so forth.

The 2nd to 5th rounds of crosses generated the B- to E-generations. All 325 lines created in the F_1 were continued in the B-, C-, D- and E-generations, where in each step, each plant had 4, 8, 16 and all 26 MAGIC founders, respectively, as parents. In each generation, one plant per line was grown, which served as both maternal and paternal lines. About 5 flowers per plant were antherectomized as described above, and used for pollination and seed production in the 2nd and 3rd rounds of crosses; in the 4th cross, 27 lines were used twice as pollen donors to produce the complete set of offspring with 16-founder parents. For the 5th round of crosses, a script was developed to optimize the crossing scheme. Accordingly, 86 additional crosses were performed in the 4th round. The additional offspring served as pollen donors (in one case, DX8, as a maternal line) in the 5th round of crosses. Since the plant DX8 produced no pollen, it was used as a maternal line and pollinated with D189 pollen and hence line E189 was the only exception to the rule of numbering lines according to the maternal plant. The complete crossing scheme is provided as a supplemental file, Crosses_A-E.xlsx. These five generations of systematic crosses were followed by 6 generations of inbreeding to create Recombinant Inbred Lines (RILs) with ~99% homozygosity. To achieve this, two lines from each of the 325 E-lines were inbred for 6 generations (lines F1-1 to F1-325 and F2-1 to F2-325, continued to lines L1-1 to L1-325 and L2-1 to L2-325). In each generation, one plant per line was grown, and after flowering and self-pollination, seeds were collected from multiple capsules of each plant. The resulting L generation represented a MAGIC RIL population consisting of 650 different RILS with approximately 99% homozygosity.

DNA sequencing of *N. attenuata* MAGIC population and reference accession

For the reference genome sequencing, plants were grown in the GH as described above. Sequence data were generated using Pacific Biosciences SMRT sequencing (PacBio) and 10x Chromium linked-read sequencing (10x) technology. The genomic DNA (gDNA) used for both PacBio and 10x sequencing originated from the same individual plant. PacBio sequencing was performed on RSII PacBio sequencers using the RSII P6/C4 chemistry at DRESDEN-concept Genome Center. High molecular weight gDNA for PacBio sequencing was isolated by Amplicon Express (https://ampliconexpress.com) and three libraries were prepared and 192 SMRT cells were sequenced. About 60x coverage was achieved during sequencing. 10x sequencing including gDNA isolation was performed at the Max Planck Genome Centre, Cologne.
The MAGIC parental accessions were grown under the same GH conditions and high molecular weight gDNA was isolated from ca. 2 x 300mg of frozen leaf tissue. The gDNA was isolated using a modified CTAB method (45), using leaf material from late-rosette-stage plants, collected and ground with mortar and pestle in liquid N_2. Briefly, for each parental line, two 2-mL Eppendorf tubes were filled each with 0.3 g of finely-ground leaf material. Per tube, gDNA was extracted by adding 800 µL of hot (65°C) 2% CTAB buffer (2% CTAB w/v, 100 mM Tris pH 8.0, 20 mM EDTA pH 8.0, 1.4 mM NaCl, 1% PVP MW 40000, 1% β-mercaptoethanol). After 1 h incubation at 65°C, 500 µL of chloroform/isoamyl alcohol (24:1, v:v) was added. Incubations at room temperature (10 min) were followed by 1 min centrifugations at 5,900 x g. The supernatant was mixed with 0.1 V of 10% CTAB (w/v) and 1 mL of chloroform/isoamyl alcohol (24:1, v:v) was added. After repeating incubation and centrifugation, 1 V of isopropanol was added. gDNA was precipitated overnight at 4°C and pelleted for 2 min at 16,100 x g. The pellet was dissolved in 800 µL of high-salt TE buffer (10 mM Tris pH 8.0, 1 mM EDTA pH 8.0, 1 M NaCl, 100 ng/µL RNaseA; Macherey-Nagel, www.mn-net.com) and incubated for 30 min at 37°C. After phase separation with chloroform/isoamyl alcohol (24:1, v:v) and centrifugation for 1 min at 5900 x g, the supernatant was mixed with 750 µL of isopropanol. The precipitated gDNA was pelleted by centrifugation for 1 min at 9300 x g. The pellet was washed twice with 800 µL of 80% ethanol and finally dissolved in 50 µL of nuclease-free water. The sequencing was then performed at BGI TECH SOLUTIONS (HONGKONG) CO on Hiseq 3000 sequencers.

For the sequencing of the 650 MAGIC RILs, seedlings of L1 and L2 (6th generation) plants were grown in the GH as described above, in Jiffy peat pellets (Jiffy-7®, https://jiffygroup.com/) and Tekus (Teku tray JP 3050/104 T black 95 box, Pöppelmann GmbH & Co. KG Kunststoffwerk – Werkzeugbau) planting pellets until plants were 2-3 weeks old. Frozen tissue was shipped to Novogene and gDNA extraction and sequencing was performed at Novogene HK. A total amount of 1.0 µg DNA per sample was used as input material for the DNA sample preparation. Sequencing libraries were generated using the NEBNext® DNA Library Prep Kit following the manufacturer's recommendations, and indices were added to each sample. The genomic DNA was randomly fragmented to a size of 350bp by shearing, then DNA fragments were end-polished, A-tailed, and ligated with the NEBNext adapter for Illumina sequencing, and further PCR-enriched by P5 and indexed P7 oligos. The PCR products were purified (AMPure XP system) and resulting libraries were analyzed for size distribution by Agilent 2100 Bioanalyzer and quantified using real-time PCR. The qualified libraries were sequenced by Illumina Hiseq X after pooling according to their effective concentration and expected data volumes.

BioNano Optical map generation

Leaves from 20 4-week old GH-grown plants of the 30th *N. attenuata* Utah inbred generation were harvested and transported on cooling packs (4 °C) to INRAE. One gram of these leaves was treated according to the Plant DNA Isolation Kit protocol (Bionano Genomics) to isolate high molecular-weight DNA. DNA quantity and size were estimated using Qubit (Invitrogen) and PFGE (24 h; 6 V cm–1; angle, 120 °C; initial switch time, 60 s; final switch time, 120 s; linear ramping; Biorad). DNA was labeled using the DLE-1 enzyme following the DLS protocol (Bionano Genomics). Labeled molecules were produced using the Saphyr System (Saphyr Chip G1.2). Data processing was performed using the Bionano Solve v.3.3 software (https://bionanogenomics.com/support/software-downloads).

Genome assembly and annotation

The genome assembly steps are summarized in a flowchart in Fig. S1. Briefly, Canu v1.8 assembler (46) was used to correct, trim and assemble the raw PacBio reads with default parameters and the genome size set as 2.5Gb from previous size estimates (47). The resultant assembly size was 2.18 Gb with an N50 of 3.5 Mb and a total of 2721 contigs. The raw assembly was further polished using Racon (48) in two iterations using the corrected PacBio reads by Canu. The polished assembly was further polished using the BWA + Freebayes pipeline as outlined in Rhie et. al (49). For this step, we utilized Illumina based short reads to correct for small indels and SNPs that potentially occur due to sequencing errors from the long PacBio reads. The polished assembly was then super-scaffolded using the SSPACE-Longread tool (50). The scaffolded assembly was further scaffolded using the BioNano Optical map, which resulted in near chromosome level assembly with an N50 of 81.9 Mb and an L50 of 9, and a total of 1378 contigs (table S1).

To further anchor this assembly on pseudo-chromosomes, we constructed a genetic map of *N. attenuata* based on a biparental mapping population of 256 individuals constructed from two geographically distinct genotypes originating from Utah and Arizona named UT and AZ respectively (47). The sequenced reads were downloaded from NCBI (PRJNA378521) and aligned using minimap2 (51). Genome Analysis Toolkit (GATK v4.1.4.1) (52) was used to call SNPs and indels using the Haplotype caller following the recommended best practice workflow and the resultant VCF file was generated. All the SNPs were initially filtered based on the mapping quality and low-coverage individuals were removed. Further filtering was performed using GATK to filter and remove non-informative markers with the following criteria: minimum and maximum allele frequency of 5% and 95% respectively, minimum mean depth of 0.5, "QUAL < 30.0", "QD < 5.0", "FS>60.0", "MQ < 40.0" and –cluster-window-size 10. This resulted in a total of 6028 high quality markers and 252 individuals. The linkage map was constructed using R/qtl (53) following the recommended workflow (54). The resultant map consists of 12 linkage groups, which were then used to anchor the scaffolds using Chromonomer (55). Benchmarking of the genome was performed using BUSCO (56) against the Embryophyta lineage at both the genome and protein levels (Fig. S2).

Annotation of the genome was done similar to (57). Briefly, publicly available RNA-Seq data (PRJNA317743) was aligned to the genome using HISAT2 (58) and transcripts were generated using StringTie (59). RNA-Seq based transcriptomes were combined and selected using Mikado (60). StringTie transcriptomes were provided to Mikado along with reliable splice junctions obtained by Portcullis (61). Blast alignments to SwissProt plant proteins (62) were also provided to the Mikado pipeline. Based on homology and identification of protein domains, transcripts were classified as protein-coding and non-coding genes. Protein-coding transcripts identified from expression data through Mikado were then integrated in the MAKER annotation pipeline. MAKER (version 3.1) annotation pipeline (63) was employed iteratively to improve previous version gene models and to predict novel gene models. For protein evidence, curated proteins from SwissProt were provided to the MAKER annotation pipeline. For transcript evidence, a Mikado generated transcriptome was provided to MAKER comprising of publicly available RNA-Seq data. Functional annotations were assigned with TAIR11, SwissProt and TrEMBL plant databases using DIAMOND (64) which is faster than legacy blast. Blast results were imported to Automated Assignment of Human Readable Descriptions (AHRD) (https://github.com/groupschoof/AHRD) to produce functional descriptions along with GO annotations.

GH experiments and RNA-seq from GH samples

For the OS-elicited transcriptome co-expression analysis, rosette stage leaves of 29 *N. attenuata* natural accessions (listed in table S4) were wounded with a pattern wheel and treated with 20 µL of 1:5 diluted *M. sexta* OS (diluted with distilled water) or distilled water at +2 and +3 positions, respectively, and the +1 leaves were harvested as controls immediately before elicitation (65). The OS-elicited leaves were harvested and flash frozen in liquid N_2 after 30 min to capture unsaturated co-expression signals (66), which typically peak at 1 h post-OS-elicitation in this species. Due to the challenges of harvesting and shipping leaf material from a remote field station

and meeting the sample preparation requirements for high-quality RNA samples, together with the need to have completely undamaged control samples as well as samples precisely OS-elicited at 30 min, the 29 parental lines were regrown in a spatially randomized planting in the GH, and one replicate per treatment group per accession was sent for sequencing. Leaf material excluding the midrib was ground under liquid N_2 and shipped to NOVOGENE (HK) COMPANY LIMITED for RNA-Seq. Briefly, mRNA from leaf tissue was enriched using oligo(dT) beads and was then fragmented randomly by adding fragmentation buffer, and subsequently cDNA was synthesized using mRNA template and random hexamers primer, after which a custom second-strand synthesis buffer (Illumina, dNTPs, RNase H and DNA polymerase I) was added to initiate the second-strand synthesis. After a series of terminal repair, and sequencing adaptor ligations, the double-stranded cDNA library was completed through size selection and PCR enrichment and sequenced by Illumina HiSeq.

For the kinetic experiments with ^{13}C-labeled Ile, +2 and +3 leaves of GH-grown plants were wounded with a pattern wheel and the resulting puncture wounds were immediately treated with 20 µL of 1:5 diluted *M. sexta* OS (diluted with distilled water) or OS containing 0.625 µmol of ^{13}C-labeled Ile (Cambridge Isotope Laboratories), following the procedure previously validated by Kang et al. (4). Given the source-sink relationship in *N. attenuata* (67), the youngest +1 leaf was harvested as a control from each plant and flash frozen under liquid N_2 immediately before OS elicitation, avoiding any systemic signals from younger source leaves reaching the older leaves due to elicitation. The oldest elicited +3 leaves were harvested at 45min after the treatment to minimize systemic effects on the +2 leaf, which was then harvested at 90 min into liquid N_2. Since OS-elicited JA-Ile usually peaks at 90min after elicitation, the sampling window of 45 and 90 min were chosen to accurately capture the conjugation rate of Ile to JA just before JA-Ile pools attain peak values. The extraction and quantification of ^{13}C-labeled JA-Ile is further detailed in the *Metabolite, TPI, and protein extractions and analysis* section.

For methyl jasmonate (MeJA) treatments, size-matched seedlings were planted in 2 L pots with a UT genotype as a neighbor in the GH. Leaf petioles of +1, +2, and +3 position leaves of rosette-stage plants were treated with 20 µL lanolin paste containing 100 µg MeJA (Sigma-Aldrich, USA), or with 20 µL of pure lanolin as controls, for six days. Leaves at standardized nodal positions across treatment groups were chosen and leaf discs were harvested using a size 6 hole-punch (10 mm diameter) at the specified time points for metabolite extraction and immediately frozen with liquid N_2. All plants were grown for 21 days post-treatment under the normal watering regimes, and for an additional 22-day attenuating watering-regime described in Schwachtje *et. al.* (68) which mimics the natural soil-drying environment that these plants experience in their natural habitats and ensures the synchronized ripening of fertilized flowers representing the total seed set. Following the drying regime, plants were harvested and fitness correlates, i.e., the capsule count data was collected. Previous studies have shown that seed number per capsule, seed mass, viability and dormancy of selfed seeds show only minor variations as a function of location along the inflorescence (69), and lifetime capsule production is thus a reasonable proxy for its Darwinian fitness. *N. attenuata* is a fire-chasing plant that germinates synchronously from long-lived seedbanks after fires in the Great Basin Desert in North America; selfed-seeds do not differ in their primary or secondary dormancy (26, 27).

Field experiments and RNA-seq from field samples

The field plot at the Walnut Creek Center for Education and Research (WCCER) in Prescott, Arizona, USA was prepared with a customized drip watering system. It consisted of 8 main 1-inch diameter water pipes, each containing four splitters for irrigating the plants. Each splitter was further subdivided into 18 drippers, which each watered four individual plants. The four plants in a cluster at each dripper were 50 cm apart from each other, and the four-plant clusters were 150 cm apart. The two replicates of the 650 MAGIC RILs population and the 26 parental lines were subsequently planted randomly in this plot, with each cluster containing a UT genotype as control. Oral secretions (OS) from *M. sexta* larvae when reared on *N. attenuata* plants contain several fatty acid-amino acid conjugates (FACs), which when applied to mechanical wounds on *N. attenuata* leaves, closely mimics the amplified JA burst and its associated response observed during actual feeding of the larvae (1, 70, 71). Thus, to elicit a standardized *M. sexta*-specific response in a kinetically defined manner, 2nd and 3rd stem leaves of every plant (counting from the

rosette (67)) were wounded with three rows of puncture wounds on each side of the midrib with a fabric pattern wheel (Dritz, Spartanburg, SC), and the resulting puncture wounds were immediately treated with 20 µL of 1:5 diluted *M. sexta* OS (diluted in distilled water). The 1st (lowest) stem leaf was left untreated and harvested as an unelicited control leaf immediately before the elicitation, while the 2nd and 3rd stem leaves were harvested at 1 h, and 72 h, respectively. Leaves were harvested by excision with a clean razor at the base of the petiole to minimize wounding. Samples were wrapped in aluminum foil, immediately frozen on dry ice and transported on dry ice in dry-ice shipping containers to the MPI-CE, where samples were stored in -80°C freezers until further processing.

Ground frozen leaf tissue (1 h OS-elicited) aliquots from 350 plants from the field experiment were shipped to NOVOGENE (HK) COMPANY LIMITED for RNA-Seq. Briefly, mRNA was enriched using oligo(dT) beads and for long-non-coding libraries, rRNA was removed using the Ribo-Zero kit which retains the mRNA. First, the mRNA was fragmented randomly by adding fragmentation buffer, then the cDNA was synthesized by using mRNA template and random hexamers primers, after which a custom second-strand synthesis buffer (Illumina), dNTPs (dUTP, dATP, dGTP and dCTP), RNase H and DNA polymerase I were added to initiate the second-strand synthesis. This was followed by purification using AMPure XP beads, terminal repair, polyadenylation, sequencing adapter ligation, size selection and degradation of second-strand U-containing cDNA by the USER enzyme. The strand-specific cDNA library was generated after the final PCR enrichment and was sequenced on Illumina Novaseq.

RNA-Seq and co-expression analysis

RNA-Seq data was aligned to the genome using HISAT2 (58) and transcripts were generated using StringTie (59). The expressions of the annotated coding transcripts were aggregated at the gene-level using the *tximport* package in R (72). Differential gene expression analysis was carried out using DESeq2 (73) and all downstream analyses was carried out on variance-stabilized expression matrices obtained from DESeq2. For co-expression analyses, pairwise Euclidean distances were used as gene similarity indices, and hierarchical clustering was performed using the ward.D method. Subsequent trees were produced using the Dynamic Tree Cut package in R (74).

Hub gene selection was performed in Cytoscape v3.9.1 using the Cytohubba plugin. The geometric means of the individual ranks from 11 metrics were calculated and used for hub gene selection. The ranks are available as an additional data file, M5_M7_Hub_ranks.xlsx.

eQTL and GWA pipeline

RILs from both the biparental population and the MAGIC population were aligned using minimap2 (51) on the newly scaffolded genome. SNPs were called as described previously, and subsequently filtered. For the MAGIC population GAPIT (75) was used for GWA analysis. For the MAGIC GWA analysis, we included the maternal information of each RIL, i.e, which parental accession was the mother, as an additional covariate to correct for maternally inherited plastidial effects (76). The model also corrected for kinship effects in the population. A Generalized Linear Model was used for the GWA analysis in GAPIT. eQTL analysis was performed using the *Matrix eQTL* package in R (77).

RNAi-silencing by plant transformation

RNAi-silenced lines were produced by the published *Agrobacterium tumefaciens* mediated transformation method (78) using a pRESC8 (79) or a pSOL8 binary transformation vector (80) containing an inverted repeat (ir) fragment (about 0.3 kb) of the *NaCOI2* (Niat3g_36487; in pRESC8), *NaERF* (*Niat3g_79923*), *NaFB61* (*Niat3g_00376*), *NaFB67* (*Niat3g_20607*), *NaGLR* (*Niat3g_14989*) sequences each in separate vectors (table S5). The transgenic lines were screened following previously described procedures (80). The number of insertion copies and the fidelity of the insertions (over-reads and truncations) were evaluated by NanoString N-counter technology (Fig. S10) (81). For each construct, the T_2 generation of two individual diploid, homozygous line harboring a single completely integrated T-DNA was screened, and due to consistent elicitation patterns in both lines (Fig. S14), the first line from each construct is subsequently used in this study. The line numbers are ir*NaERF*: A-19-020-5, A-19-032-3

ir*NaFB61*: A-19-026-2, A-19-025-1 ir*NaGLR*: A-19-028-5, A-19-065-3 ir*NaFB67*: A-19-043-5, A-19-130-5 ir*NaCOI2*: A-12-768-5. Silencing efficiency of each line was determined using quantitative real time PCR (qRT-PCR) (Fig. S15).

M. sexta performance assay

M. sexta eggs were obtained from an in-house colony supported by Department of Evolutionary Neuroethology at the Max Planck Institute for Chemical Ecology, Jena, Germany, as previously described (82). To measure the performance of *M. sexta* larvae, an excised-leaf feeding assay was conducted. To avoid activating induced defenses from larval feeding, young stem leaves were excised with sterile razor blades from the base of the petiole with minimal cellular damage and a single neonate *M. sexta* larvae was introduced in enclosed humidified containers placed in the same GH conditions as the plants. The containers were cleaned, and leaves were replenished at regular intervals. The larvae were weighed at 4, 6, 8, and 10 days after introduction. The excised-leaf assay was critical to test the "Constitutive Induction" hypothesis of ir*NaERF* and ir*NaFB61* lines without inducing resistance traits that are known to spread systemically throughout attacked plants. This assay would not be appropriate for larval performance evaluations on ir*NaGLR* and ir*NaFB67* lines, which showed constitutively lower basal defense levels.

Metabolite, TPI, and protein extractions and analysis

For phytohormone and specialized metabolite extraction, *circa* 100 mg of ground leaf or floral tissue (n = 7-10 replicates in each experiment) was aliquoted into Eppendorf tubes. One mL of extraction buffer (80% MeOH) containing internal standards (D_6-ABA, D_4-SA, D_6-JA, D_6-JA-Ile) was added and samples were homogenized in a GenoGrinder 2000 (SPEX SamplePrep) for 60 seconds at 1,150 strokes min^{-1}. After two centrifugations at 1600g, 800 µL of the supernatant was used for both phytohormone and metabolite analysis as described previously (83, 84). Briefly, the phytohormone quantification was performed via liquid chromatography coupled to a triple quadrupole MS (Bruker EVO-Q Elite) equipped with a heated electrospray ionization source. The MS was operated in negative ionization mode using multiple reactions monitoring (MRM). To quantify ^{13}C-JA-Ile, the existing method (83) was extended with an MRM setting to detect ^{13}C-JA-Ile ($[M-H]^-$ parental ion at *m/z* 328.2, fragment ion at *m/z* 136.0, collision energy 19V). The ratios of the ion intensities of all the endogenous compounds and internal standards, together with the fresh mass of the samples, as a normalization factor, were then used to calculate the phytohormone levels of each sample.

Protein was extracted from *circa*. 100 mg leaf or floral tissue using cold extraction buffer (0.1 M Tris-C1, pH 7.6, 5% polyvinylpolypyrrolidone, 2 mg/mL phenylthiourea, 5 mg/mL diethyldithiocarbamate, 0.05 M Na_2EDTA). Bradford assays were conducted to quantify protein contents which were used to normalize TPI activity measures, as previously described in Van Dam et al. (67).

DNA extraction from seeds and PCR

To quantify the allele frequency, we selected a template region (chr5:157084070-157084168) of the *NaJAR4* gene deleted in the V lines (Fig. 1), and an adjacent region (chr5:157079856-157079950) which showed no evidence of deletion from any accession, as a normalizing control. Allele frequency was determined as a ratio of the deleted region and the adjacent region. As a test of the procedure, an experiment was conducted using the parental accessions (V and NV) of known genotypes (Fig. S8) where the ratio was 0 for the V lines. Approximately 40 mg (ca. 400 seeds) of each *N. attenuata* accession was ground using mortar and pestle after flash-freezing with liquid N_2. DNA was extracted from the ground seeds using QIAGEN DNeasy Plant Kits according to the manufacturer's instruction. DNA was quantified using a Nanodrop spectrophotometer (Peqlab, ND-1000) and a total of 15ng DNA was used for PCR amplification. Taq DNA Polymerase 2x Master Mix (Thermo Scientific) was used for PCR amplification according to the manufacturer's instructions. Finally, qPCR runs were performed using Taykon™ No ROX SYBR® Master Mix (Eurogente, UF-NSMT-B0701) on a Stratagene MX3005P. All the primers used are listed in table S5.

Statistical and bioinformatic analysis

All statistical analyses were carried out in R version 3.6.3 (85). The JA vs JA-Ile slopes from the isotope labeling experiment were initially fitted using the *lm* function in base R, where the dependent variable was JA-Ile, and the respective genotype groups were considered as independent variables with JA levels as a covariate. Cook's distance was calculated for each fit, and outliers were removed before fitting the final model again. *Post hoc* slope difference estimates and *p*-values were calculated using the *emtrends* function in the *emmeans* package keeping JA fixed in the function (table S3).

NaJAR4 locus-specific sequences for each of the 25 accessions were reconstructed from the reference genome by adding the indels and SNPs from the VCF files generated previously. For the JAR phylogeny, protein sequences similar to *NaJAR4* in the *Solanaceae* taxa were retrieved from NCBI. For the phylogenies, either DNA or protein sequences were aligned using MAFFT (86) and phylogenetic trees were constructed using RAxML (87) with 1000 bootstraps. Integrative analysis was performed using the mixOmics package in R (88). GO term enrichment was performed using the universal *enricher* function and the GO network was generated using the *cnetplot* from clusterProfiler R package (89) in R version 4.2.1. SNP PCA was computed using PLINK v1.90b5.3 64-bit, and plotted in R.

Acknowledgments

We thank W. Zhou, A. Kügler, and S. Xu for arranging the sequencing of MAGIC parental lines; W. Seibt, and E. Claussen for help with RNAi screening and together with E. Rothe and members of the Molecular Ecology department for generation of the MAGIC population; M. Stitz and E. Gaquerel for their roles in generating the *NaCOI2* transgenic line; Prescott College, Northern Arizona University, the Arboretum at Flagstaff, Prescott National Forest, and the Southwest Experimental Garden Array for the use of a field plot at the Walnut Creek Center for Education and Research; Brigham Young University (BYU) for the use of its Lytle Ranch Preserve; R. Carlson and N. Carlson for logistics support of the 2019 field team; G. Baldwin for sowing the MAGIC population and plant transformations; the 2019 MPI-CE field team (E. McGale, H. Valim, J. Li, P. Harary, K. Burkard, C. Mahadevan, and M. Smith) for planting, screening, and OS-eliciting the MAGIC population; C. Mahadevan and Y. Bai for help with the mRNA isolation of MAGIC RILs; R. Rossouw, S. Lorenz, L. Olsen, and K. Christensen for help with MAGIC sample preparation; C. Rocha for help with metabolite runs and analyses, M. Niebergall for the script that optimized the MAGIC crossing scheme, and T. Hahn for technical support of the analytical equipment; and J. Gershenzon and S. O'Connor for comments on an early draft, and P. Wigge, Y. You, S. Xu and five anonymous reviewers for their helpful comments on the manuscript.

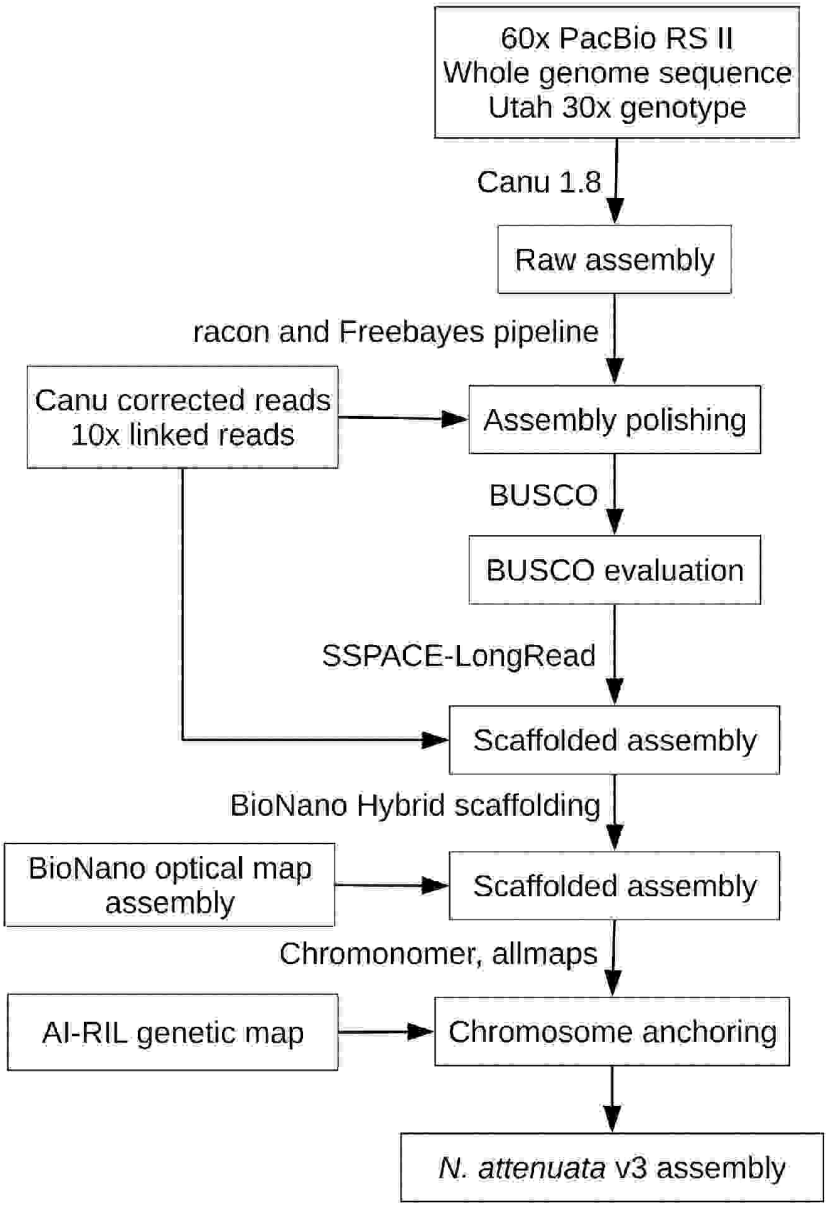

Fig. S1. Flowchart depicting the steps used in the *N. attenuata* genome assembly. DNA sequences attaining 60x coverage were generated by PacBio RS II of Utah31x accession which were used for the raw assembly by Canu v1.8. The raw assembly was then polished using racon and Freebayes protocol utilizing the 10x linked reads of the same accession. The polished assembly was then evaluated using BUSCO and further scaffolded using the SSPACE-LongRead program. The scaffolded assembly was further scaffolded at chromosomal arm length using a separate BioNano optical DNA map of the same accession. Finally, the hybrid scaffolded assembly was anchored to the pseudo-chromosomes using an AI-RIL genetic map. This resulted in an assembly with 12 pseudo-chromosomes with all unassigned scaffolds concatenated as a single contig designated as chr0.

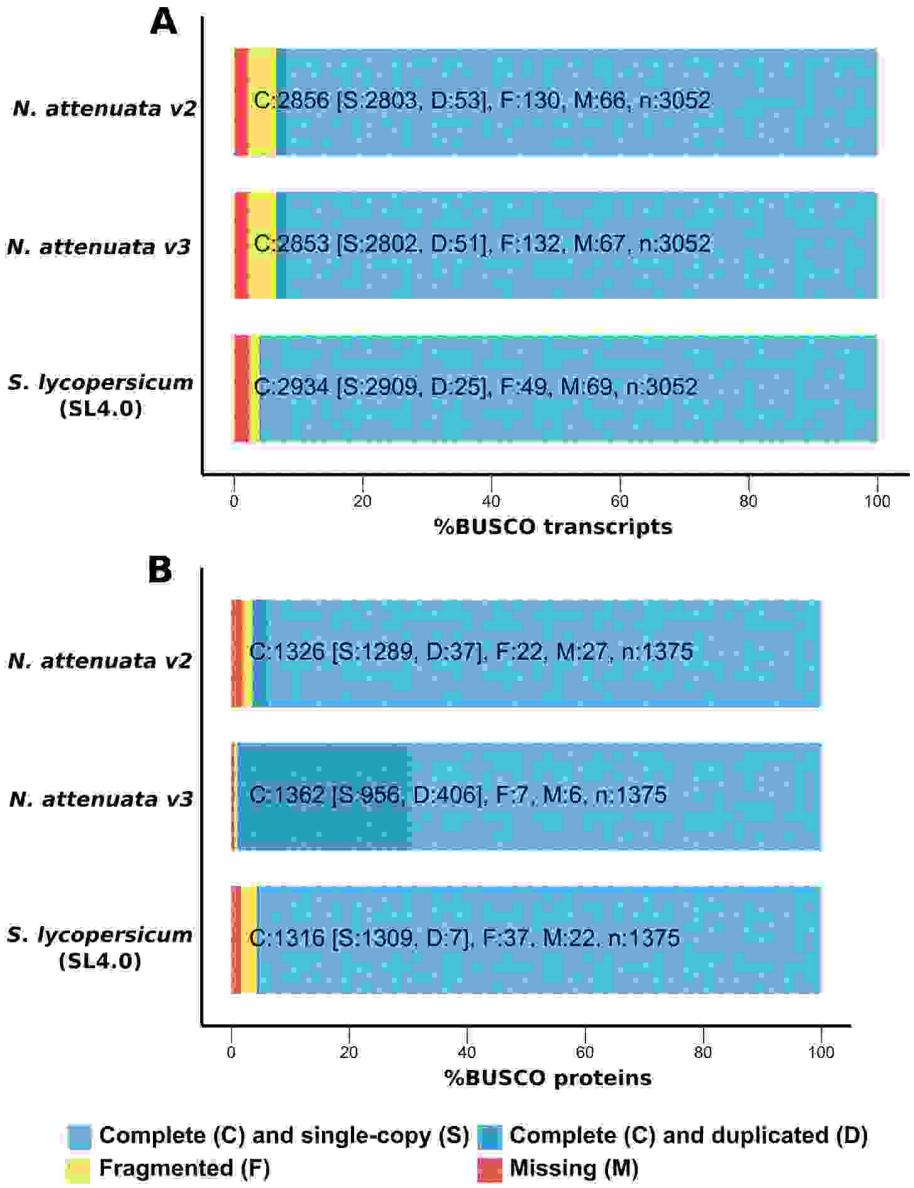

Fig. S2. Benchmarking Universal Single-Copy Orthologues (BUSCO) scores of the *N. attenuata* genomes version 2, version 3 and the latest *Solanum lycopersicum* genome, SL4.0. (**A**) BUSCO transcript scores are comparable between the two versions of the *N. attenuata* genomes when compared with the *S. lycopersicum* genome. There was no significant improvement in the new assembly in terms of the number of novel transcripts compared against the BUSCOs, but genome contiguity was significantly improved (Supplementary Table 1). (**B**) BUSCO scores of the same assemblies at the protein level compared against the more conserved Embryophyta lineage. The *N. attenuata* v3 genome shows a slight improvement at the protein level, which might be due to the combined effects of updated protein annotation databases and the improved genome contiguity.

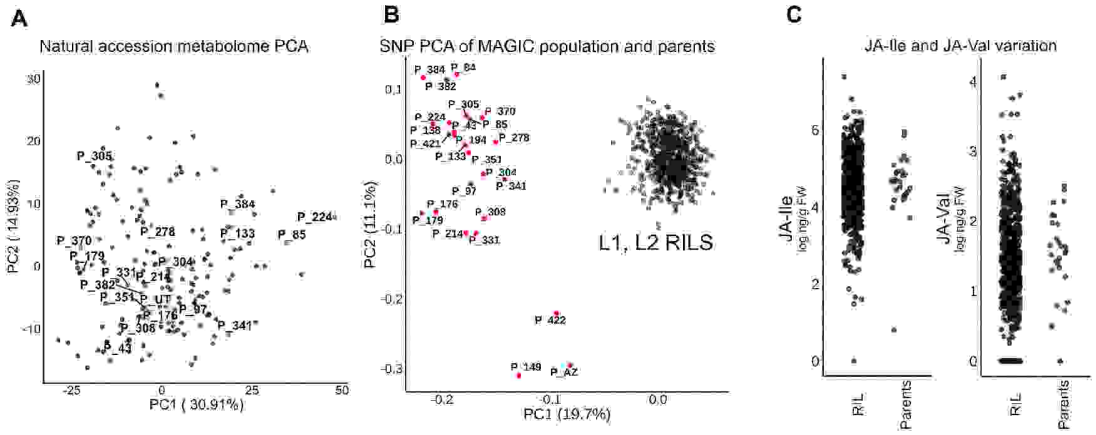

Fig. S3. Genetic and metabolic characterization of *N. attenuata* natural accessions (A) Selection of progenitor lines for the *N. attenuata* MAGIC population based on the metabolic diversity upon elicitation by *M. sexta* oral secretion (OS). The red points denote the accessions chosen to create the MAGIC RIL population based on their spread across the two principal components capturing the maximum metabolic variability. **(B)** PCA plot of the Single Nucleotide Polymorphisms (SNP)s in the MAGIC RIL population and the 26 parental lines. **(C)** JA-Ile and JA-Val levels in the MAGIC RIL and parental lines 1 h post-OS elicitation.

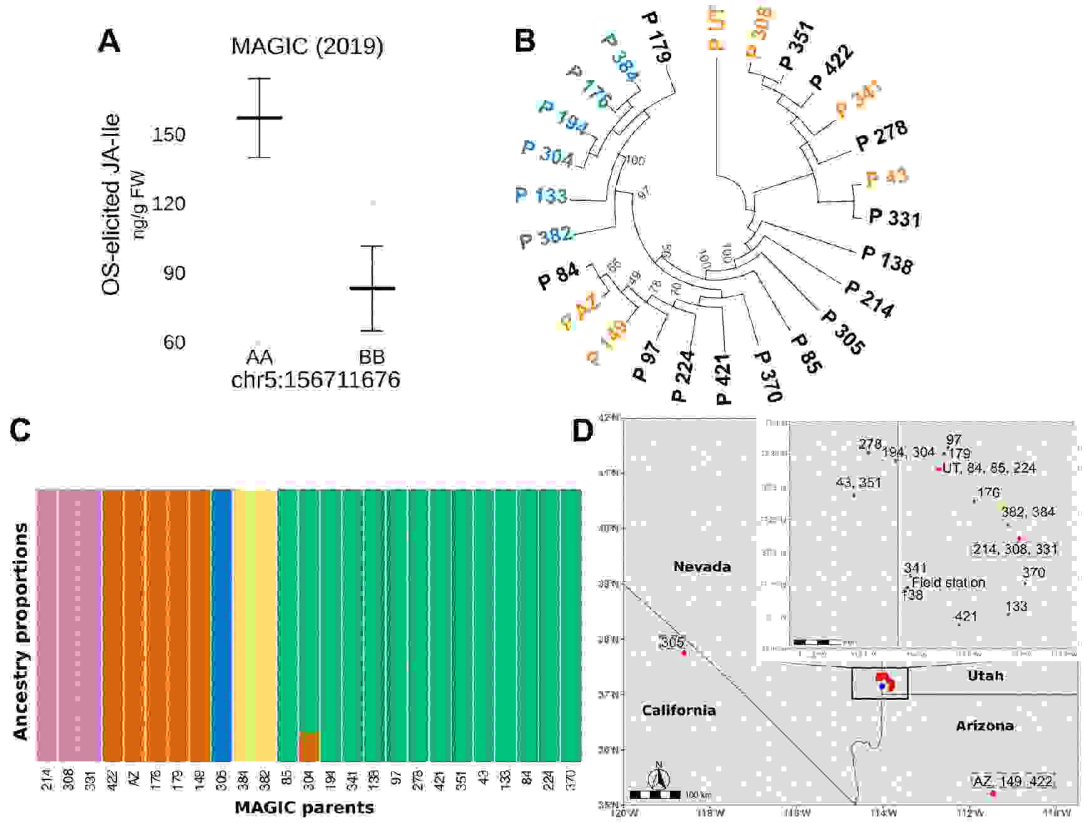

Fig. S4. The JAR4 sequence phylogeny and *N. attenuata* MAGIC parental analysis. (**A**) The effect plot of the JA-Ile QTL in the 26-parent MAGIC population planted in the AZ field plot in 2019. The effect plot of the QTL in the MAGIC population shows the presence of an alternate allele that is associated with reduced OS-elicited JA-Ile levels. (**B**) Phylogenetic analysis of the JAR4 locus among the 26-parental lines of the MAGIC population. A 21kb region of DNA sequence encompassing the *NaJAR4* gene (Fig. 1C) was extracted from the newly assembled UT30x (node labeled as P-UT in orange) genome. By introducing indels and SNPs obtained from variant calls from the parent-specific whole-genome sequences, the *NaJAR4* genomic loci of the 25 accessions were reconstructed from the UT reference sequence. Six of 7 accessions forming a monophyletic group (blue color) had the most significant effect on the JA-Ile QTL of the MAGIC population and are called “Variant (V)” accessions. We randomly selected six from the remaining accessions, including UT and called them “Non-Variant (NV)” accessions (orange color). (**C**) Ancestry proportions in the parental lines inferred by the fastSTRUCTURE algorithm with *a priori* number of population (*K*) set to 5 (**D**) Geographic origins of the 26 parental lines, some of which correlate with their inferred ancestry.

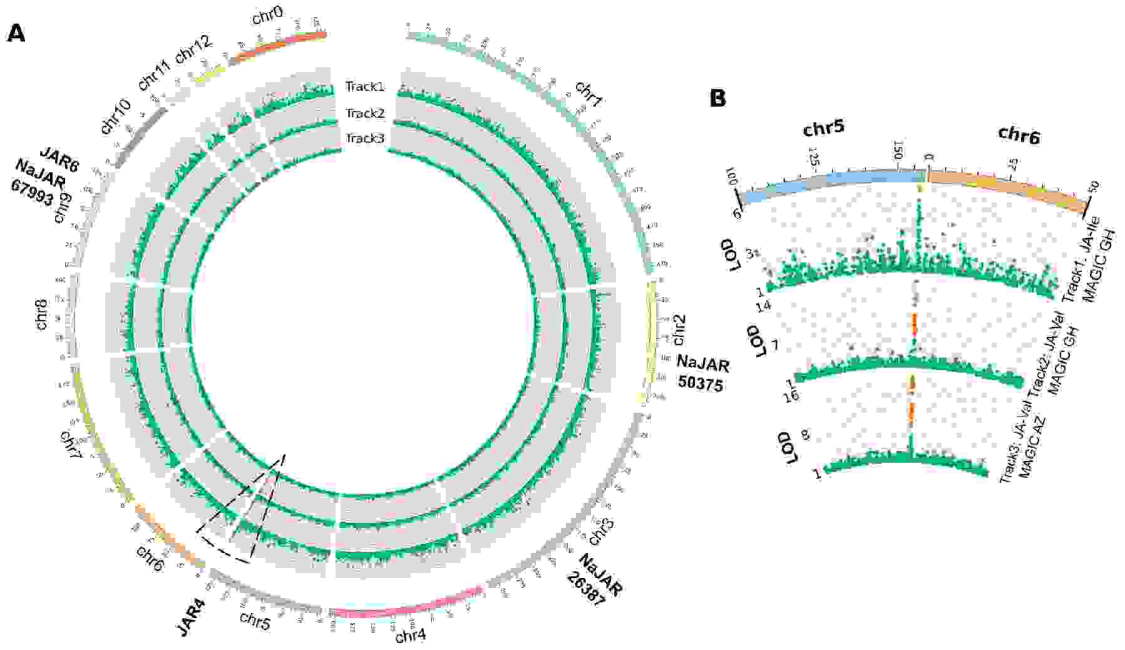

Fig. S5. Genome-wide Manhattan plots of OS-elicited JA-Ile and JA-Val bursts in a MAGIC population of *N. attenuata* planted in both field (AZ) and glasshouse (GH). (**A**) Orange dots represent markers with significance levels, *p*-values < 0.05. The outermost two tracks (1, 2) show genome-wide tests of significance level for OS-elicited JA-Ile and JA-Val bursts, respectively, at 1 h after the treatment of the MAGIC population planted in a GH experiment. The next track (3) shows the significance level for the OS-elicited JA-Val burst from a MAGIC population grown at the Arizona (AZ) field site during the 2019 field season. Additionally, the chromosomal locations of all *NaJAR*s are shown in the outer track. (**B**) A magnified slice of chromosome 5 and 6 shows that all OS-elicited JA-Ile and JA-VAL bursts returned the same loci on chromosome 5.

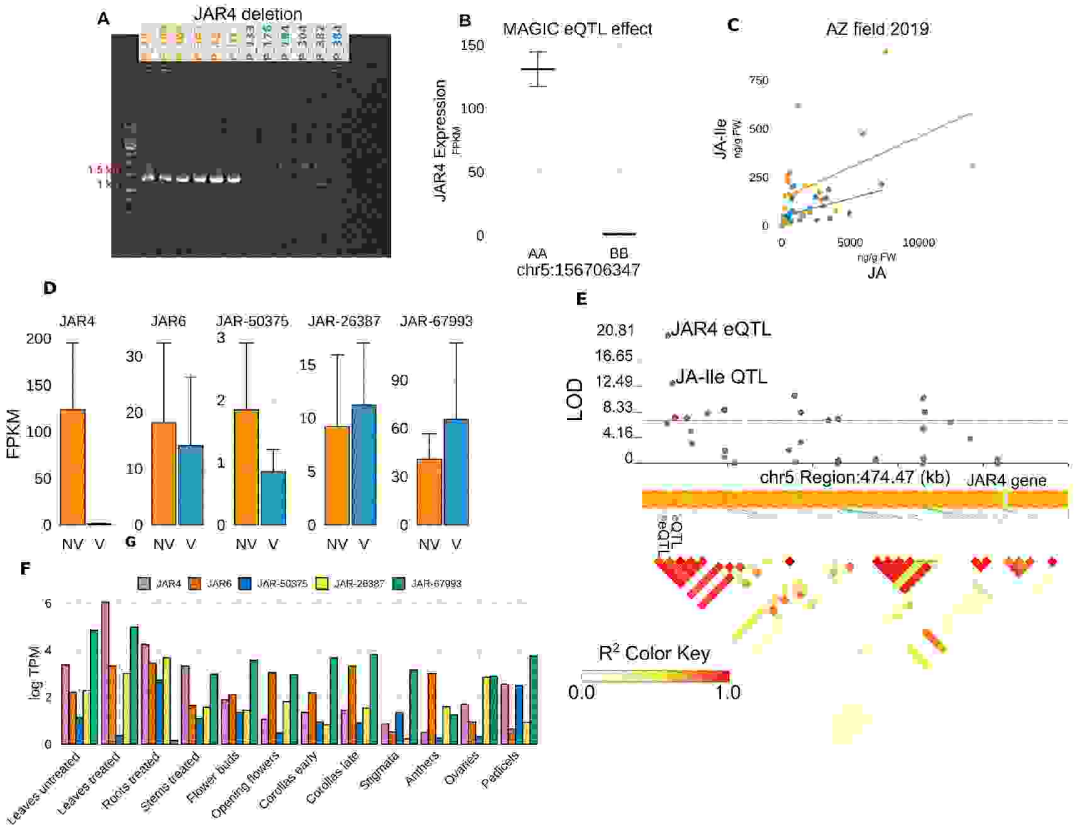

Fig. S6. JAR4 deletion and eQTL analysis. (**A**) A 1.3kb genomic region around the JAR4 deletion region (Fig. 1C) was amplified by PCR in 12 *N. attenuata* natural accessions. The V accessions (blue) showed a clear deletion where no band was present compared to the NV accessions (orange) which showed an amplified product of expected length. (**B**) The JAR4 gene shows a significant eQTL in the MAGIC RILS between alleles near the location where the OS-elicited JA-Ile QTL was found. (**C**) JA vs JA-Ile levels from the Arizona 2019 field experiment among the 12 V and NV parental lines. Significant association of JA-Ile with the two groups is observed ($F_{(1,42)}$ = 8.202, *p*-value = 0.00650) when accounting for the effect of JA ($F_{(1,42)}$ = 12.5340, *p*-value = 0.000993). (**D**) Abundances of five JAR genes in the *N. attenuata* genome in fragments per kilobase of exon per million mapped fragments (FPKM). The JAR4 and JAR6 are the two characterized genes in this family, and the rest are annotated with their gene IDs in the new genome. (**E**) Linkage Disequilibrium (LD) heatmap showing the locations of the JAR4 eQTL and the JA-Ile QTL position with respect to the JAR4 gene. The QTL positions lie adjacent to each other on the genome and have high LD values. (**F**) *NaJAR* abundance in 12 tissues of the *N. attenuata* UT accession in transcript per million (TPM). *NaJAR-67993* shows similar levels of expression compared to *NaJAR4* in OS-elicited leaves, but in the phylogenetic analysis (Fig. S7), was most closely related to *AtGH3.10*, which potentially plays a redundant role in JA conjugation to the more dominant *AtJAR1* in *Arabidopsis* (*90*).

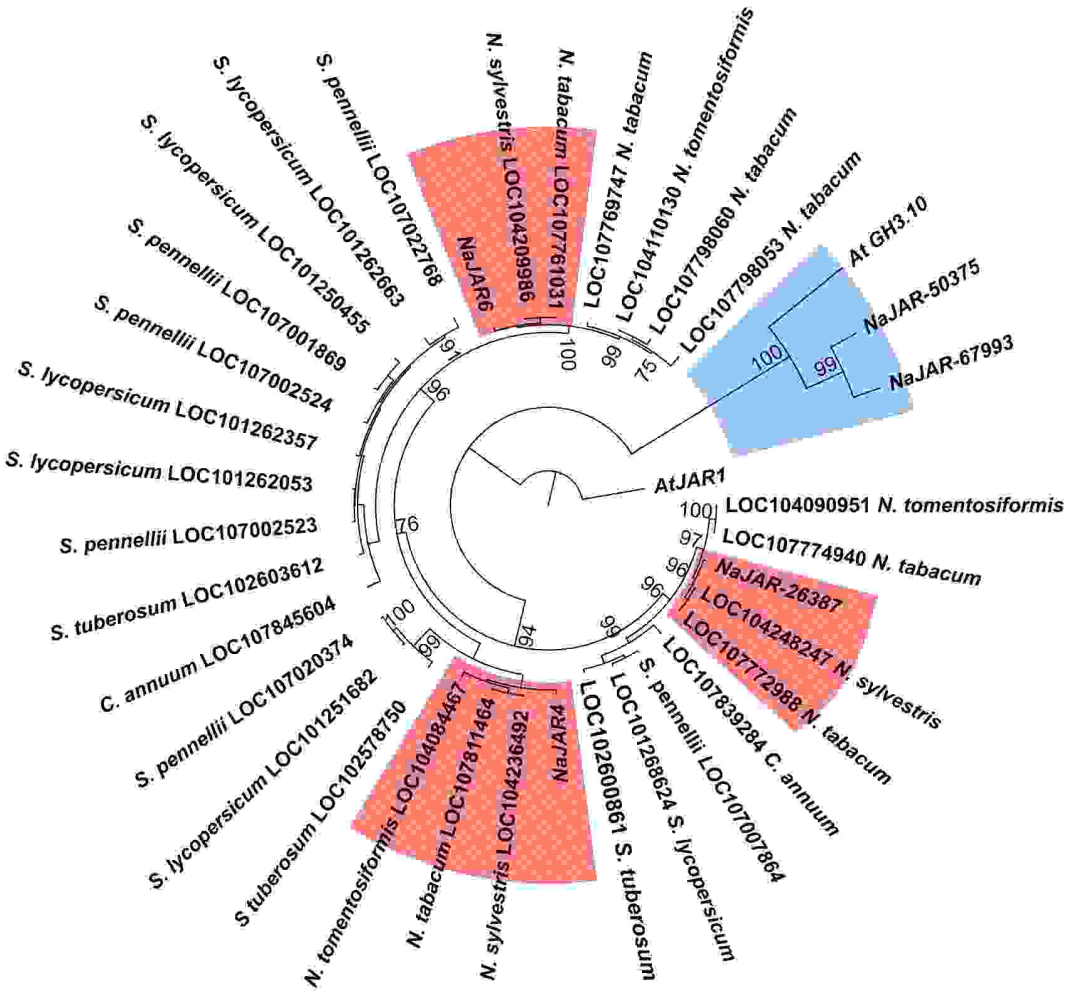

Fig. S7: Phylogentic analysis of *NaJAR* genes in *N. attenuata* and well-studied taxa in the Solanaceae family, with *A. thaliana* as outgroup. The highlighted clades include the five JAR genes in the *N. attenuata* genome. The blue highlighted clade forms a distinct monophyletic group with a recently discovered JAR, *AtGH3.10*, in *A. thaliana* (*90*). Numbers on the branches reflect the bootstrap confidence levels.

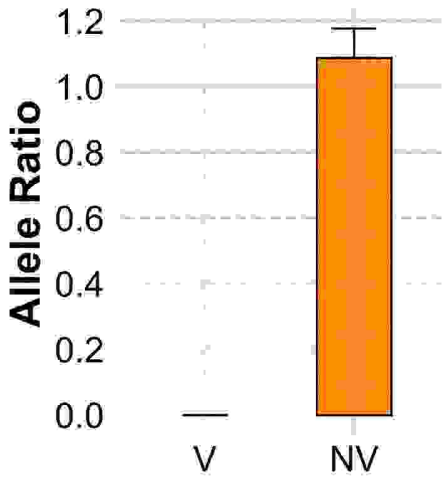

Fig. S8. Allele ratio of the *NaJAR4* variant locus in V and NV lines. (**A**) Allele ratio was determined from DNA extracted from the seeds of each of the parental accessions, and subsequently using qPCR, the ratio of the C_t values of the deletion region and an intact adjacent region, was calculated. The ratio of all the V lines was effectively 0, indicating the accuracy of this method. Error bars are 95% confidence intervals (n = 6).

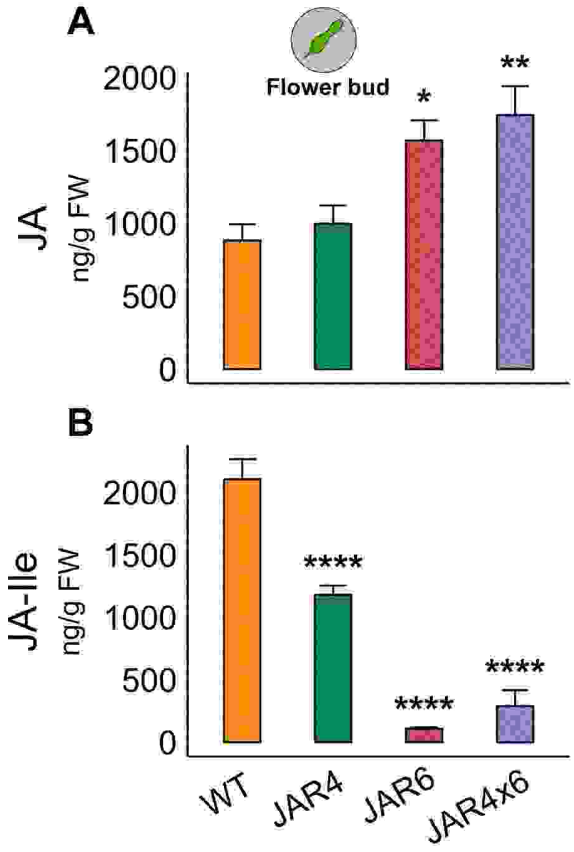

Fig. S9. Constitutive jasmonate levels in flower buds. (**A-B**) JA and JA-Ile levels in the WT and the *NaJAR*-RNAi lines (n = 6). The JA-Ile levels were reduced 20-fold in the *NaJAR6*–silenced line, suggesting a tissue-specific conjugation activity of NaJAR6. Error bars are standard errors in both panels. Significance was calculated by ANOVA followed by Tukey's HSD test comparing against WT (*: *p*-values < 0.05; **: < 0.01; ***: < 0.001; ****: < 0.0001).

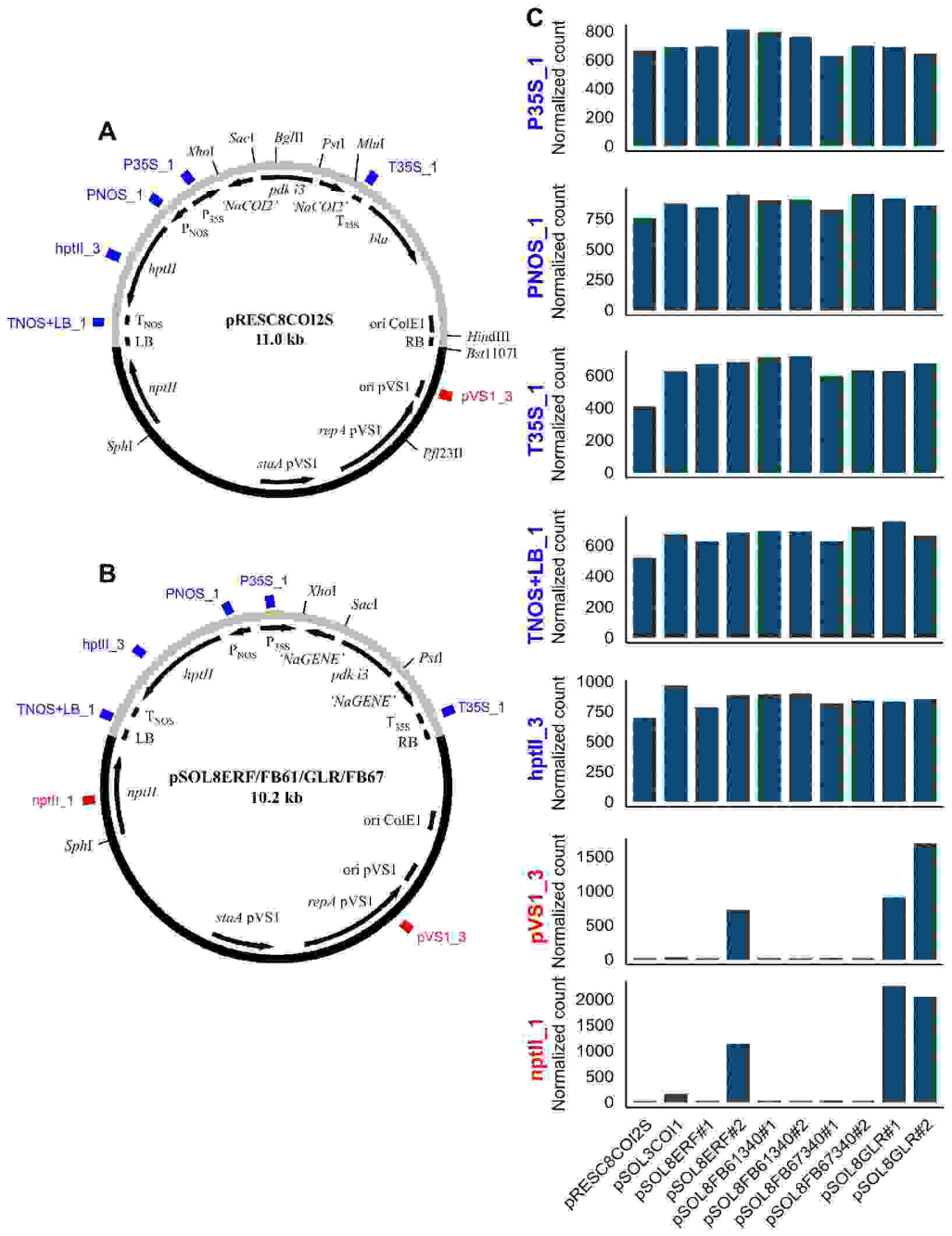

Fig. S10. Characterization of the RNAi-silenced lines of *N. attenuata* plants. (**A-B**) Vector map of pRESC8COI2S, pSOL8ERF, pSOL8FB61, pSOL8GLR, and pSOL8FB67 lines. The blue highlighted regions were selected for the confirmation of a single copy insertion. (**C**) TNOS+LB_1, hptII_3, PNOS_1, P35S_1, and T35S_1 (blue) were used to evaluate single and complete T-DNA insertions. pVS1_3 and nptII_1 (red) probe indicates over-reads of the plasmid sequences outside of the T-DNA borders, which do not affect the plant phenotype or its stable inheritance. The lack of signal from these probes indicate that over-reads did not occur during the transformation process.

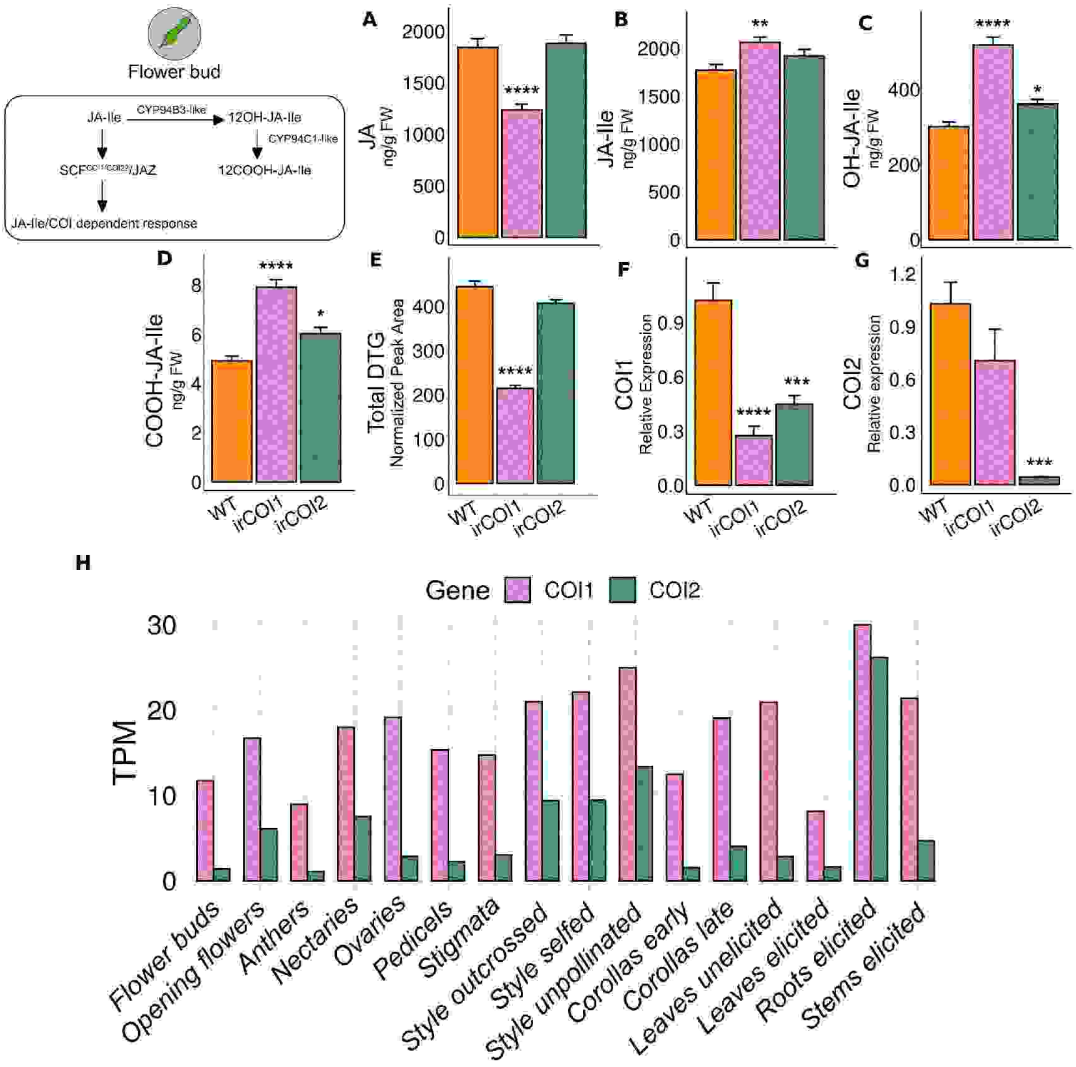

Fig. S11. Jasmonate, defense metabolite levels and COI gene expressions in the two COI-silenced lines of *N. attenuata*. (**A-D**) Constitutive levels of JA, JA-Ile, and its degradation products (OH-JA-Ile and COOH-JA-Ile) in the flower buds of UT-WT and ir*COI1* and ir*COI2* silenced lines (n = 10). COI1 is a known receptor of JA-Ile and both the irCOI-silenced lines show significantly elevated pools of these phytohormones, due to the inactivation of this receptor. However, ir*COI1* accumulates 72% more OH-JA-Ile and 60% more COOH-JA-Ile compared to modest 20% and 22% increases in ir*COI2,* respectively. (**E**) Total DTG levels were significantly downregulated only in ir*COI1* (by 51%) but not in ir*COI2* lines. (**F-G**) Relative transcript abundances of of *NaCOI1* and *NaCOI2* lines compared to UT-WT. (**H**) Transcript abundance in Transcript per million (TPM) units in different tissues of *N. attenuata*. Error bars are standard errors in all panels. Significance was calculated by ANOVA followed by Tukey's HSD test comparing against UT-WT (*: *p*-values < 0.05; **: < 0.01; ***: < 0.001; ****: < 0.0001).

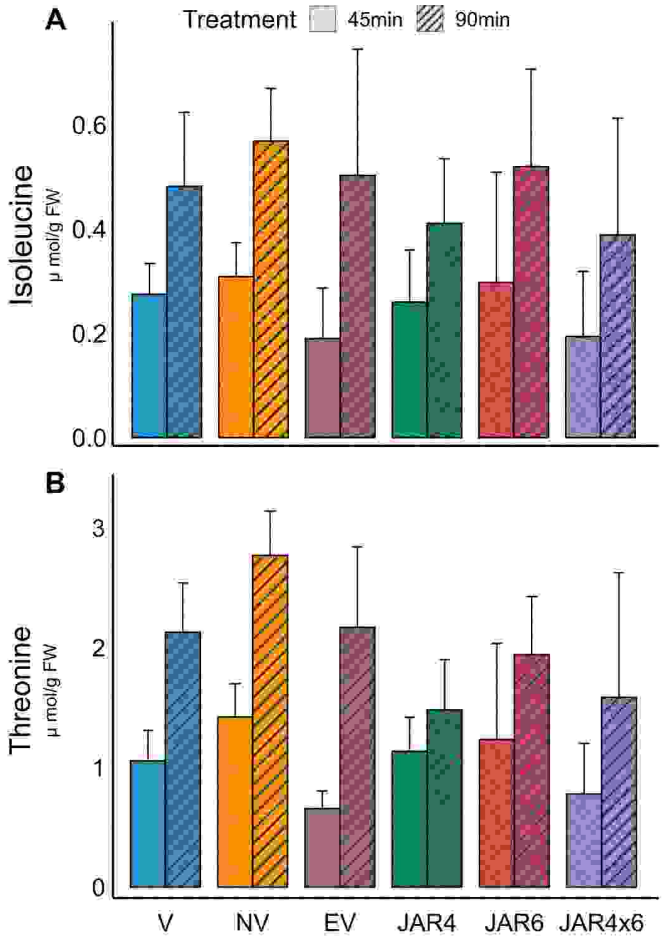

Fig. S12. Threonine and isoleucine levels in *N. attenuata* at 45 and 90min post OS-elicitation in V, NV, and 4 RNAi lines. (**A**) No significant difference is observed in isoleucine pools at either of the time points across all the lines (ANOVA *p*-value = 0.54, *p*-value = 0.75 at 45 and 90 min, respectively). This result makes the possibility that JA-Ile variation results from differential availability of isoleucine for conjugation unlikely, and suggests that the JA-Ile difference are primarily driven by the variation in JAR4 conjugation activity. Error bars indicate 95% confidence intervals in both panels. (**B**) Threonine, a precursor of isoleucine is also not significantly different at 45 min (ANOVA with $\alpha = 0.05$, *p*-value = 0.091). However, we observed marginally higher pools of threonine at 90min between the V and NV lines (ANOVA, *p*-value = 0.02) which might be driven by the higher isoleucine conjugation rate to JA in the NV lines. This difference is not reflected in downstream isoleucine pools, which might be explained by the isoleucine feedback inhibition mechanism maintaining threonine-isoleucine homeostasis. This trend is mirrored in the EV and JAR4-RNAi comparison (ANOVA, *p*-value = 0.05).

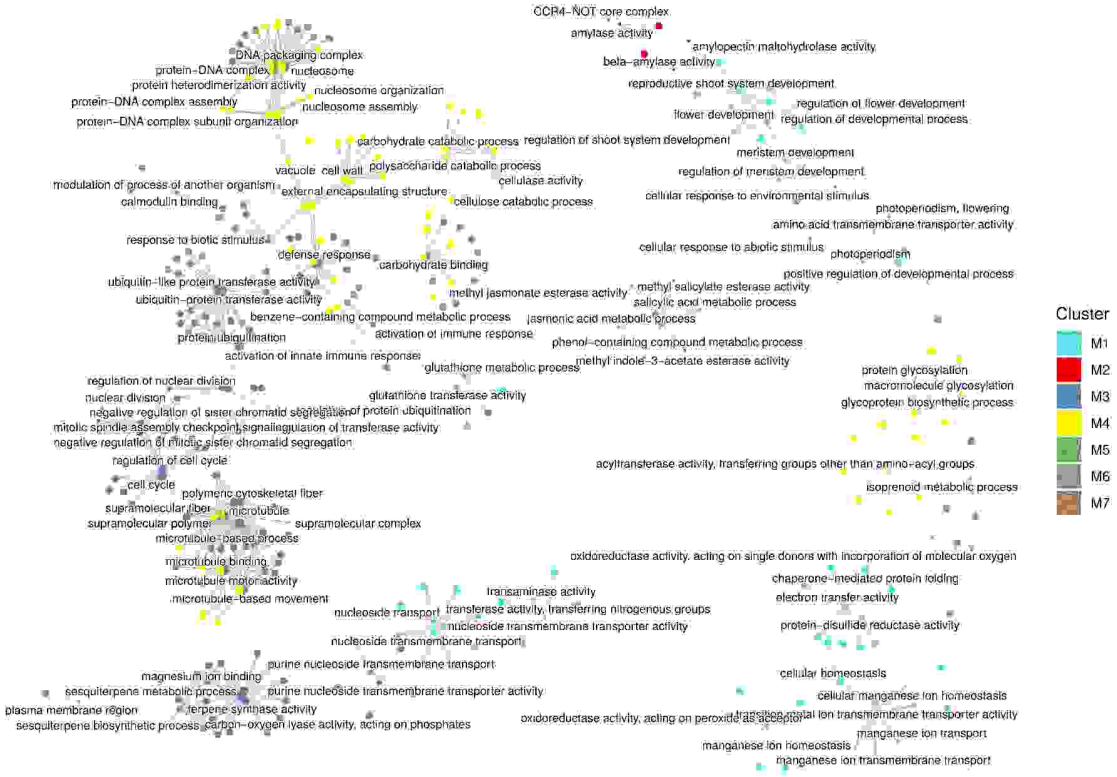

Fig. S13. GO term enrichment of the co-expressed modules. GO term enrichment was performed for all modules simultaneously using the clusterProfiler R package with *p*-value cutoff of $P = 0.05$.

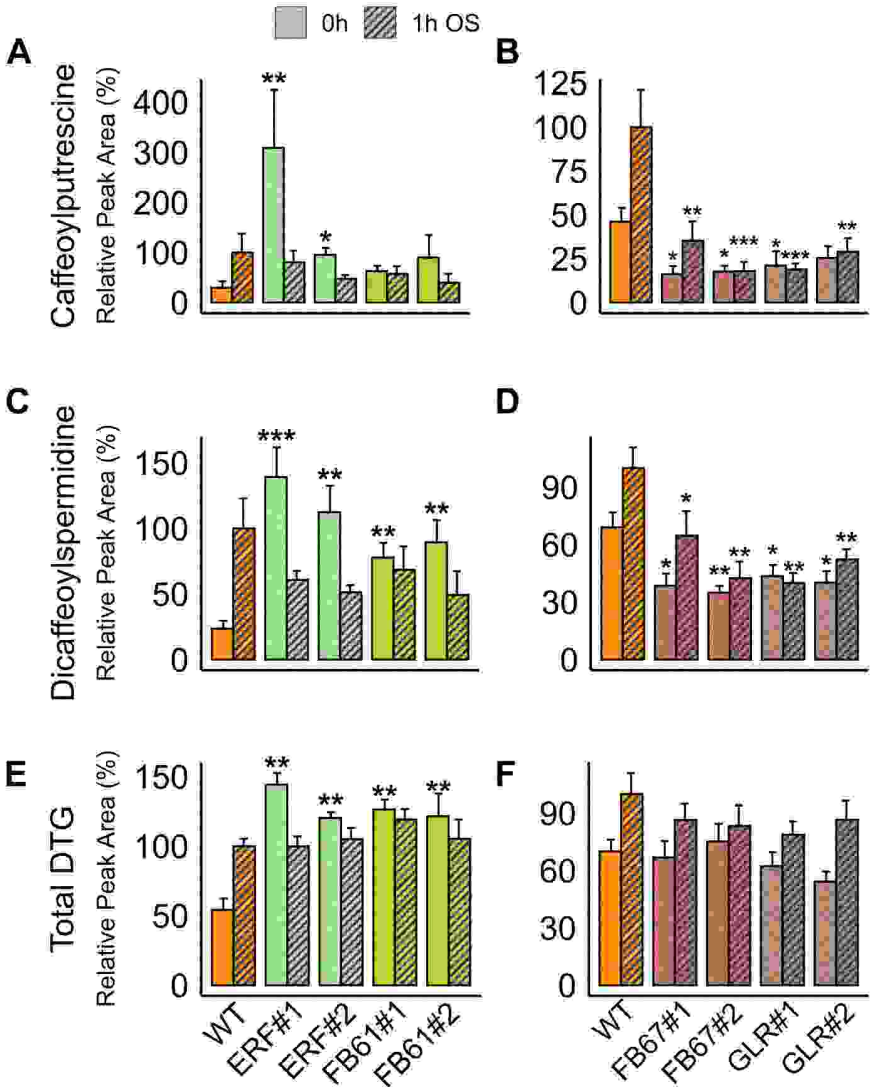

Fig. S14. Metabolite screening of 4 RNAi lines. (A-F) Caffeoylputrescine (CP), dicaffeoylspermidine (DCS), and total diterpene glycoside (DTG) levels in unelicited (0 h) control plants and 1 h post OS-elicitation in 2 replicate lines of ir*NaERF*, ir*NaFB61*, ir*NaGLR*, and ir*NaFB67*. Metabolite levels were normalized against the common UT genotype which was included in all experiments as the genotypic control for all RNAi lines. Due to overall consistent elicitation patterns in all the replicate lines, line 1 for each construct is shown in subsequent results. Error bars are standard errors. Significance was calculated by ANOVAs followed by Tukey's HSD tests comparing against WT in M5 and M7 group (n = 10) across 2 treatment group (*: *p*-values < 0.05; **: < 0.01; ***: < 0.001; ****: < 0.0001).

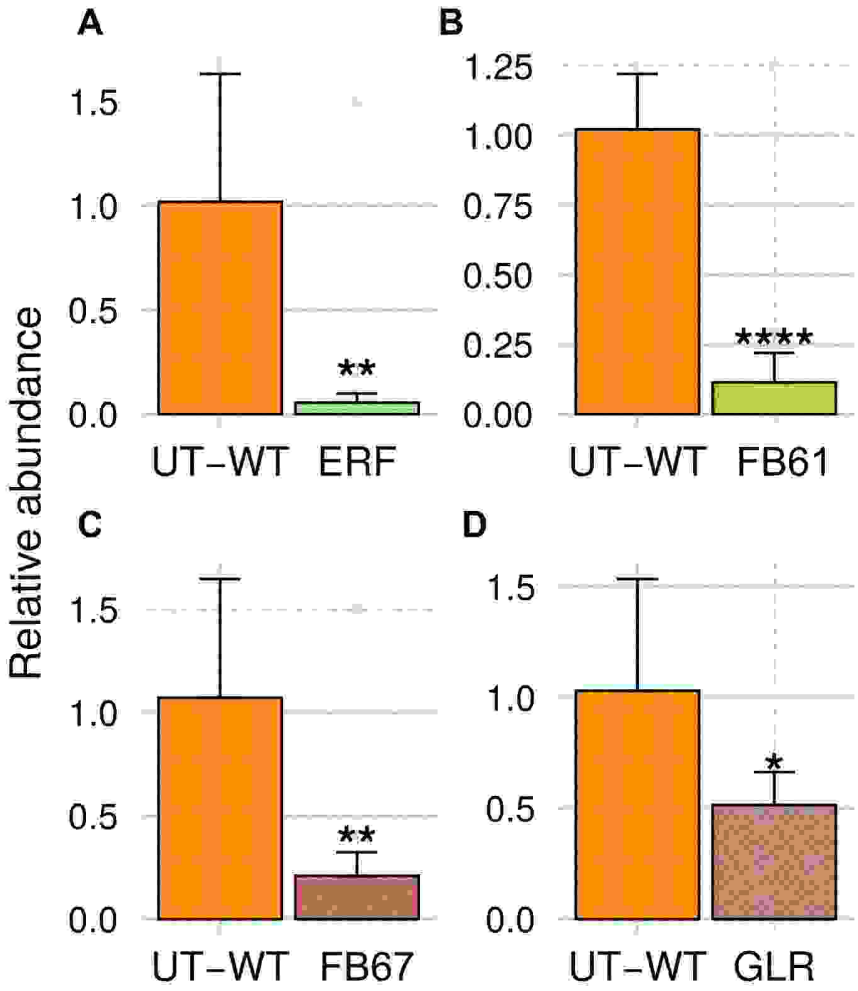

Fig. S15. Silencing efficiency of the "hub"-gene RNAi lines. (A-D) Relative transcript abundances of *NaERF*, *NaFB61*, *NaFB67*, *NaGLR* genes in the RNAi-silenced lines compared to UT-WT 1 h after OS-elicitation (n = 6). Asterisks denote t-test p-values (*: *p*-values < 0.05; **: < 0.01; ***: < 0.001; ****: < 0.0001).

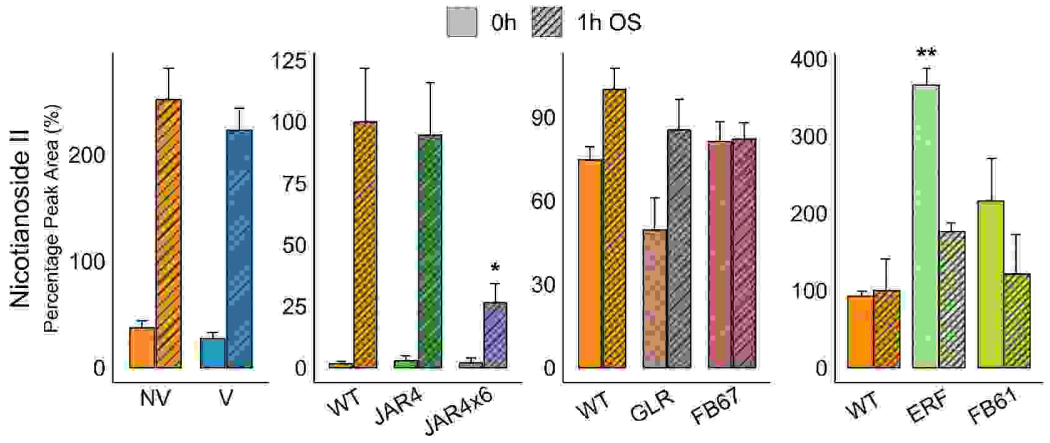

Fig. S16. Nicotianoside II levels in 4 RNAi lines silenced in the expression of "peripheral" hub genes, namely *NaERF, NaFB61, NaGLR, NaFB67,* 2 RNAi lines silenced in *NaJAR4/6* and the NV and V lines. Nicotianoside II, a JA-regulated DTG (39), in unelicited (0 h) plants and 1 h post OS-elicitation in the RNAi and WT lines. Metabolite levels were normalized against the common UT genotype which was included in all experiments, and was the genotypic control for all RNAi lines. Error bars are standard errors. Significance was calculated by ANOVAs followed by Tukey's HSD tests comparing against WT in M5 and M7 group (n = 10) and the *NaJAR*-silenced group, and NV in the natural variant group (n = 42), across 2 treatment group (*: *p*-values < 0.05; **: < 0.01; ***: < 0.001; ****: < 0.0001).

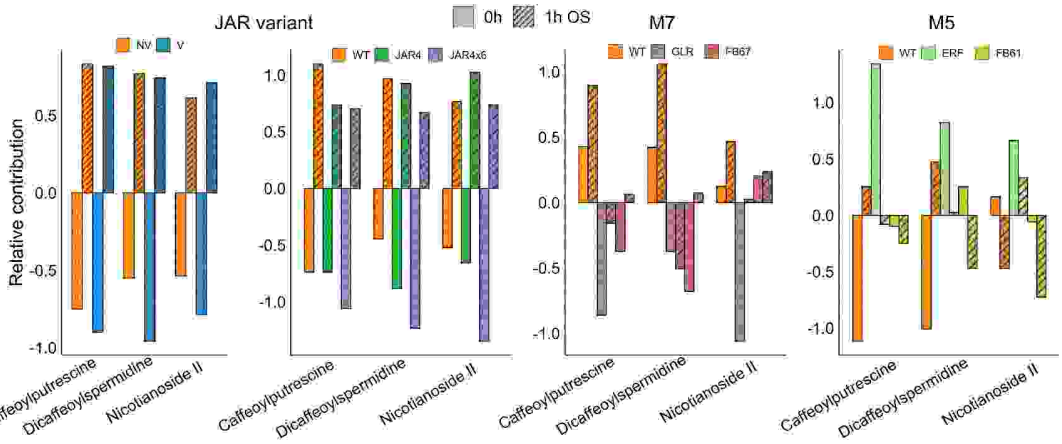

Fig. S17. Relative PLS-DA loading scores of caffeoylputrescine, dicaffeoylspermidine, and nicotianoside II in ir*NaERF*, *irNaFB61*, ir*NaGLR*, ir*NaFB67*, 2 RNAi lines silenced in *NaJAR4/6* and the NV and V lines. The relative contribution from the loading scores of caffeoylputrescine, dicaffeoylspermidine, and nicotianoside, the JA-regulated sector of HG-DTGs was calculated from the LC-MS mass features along component 1 from the PLS-DA results shown in Fig. 5F-H. The targeted loading scores of these JA-regulated metabolites in each group are consistent with the predictions of the overall "omnigene" model.

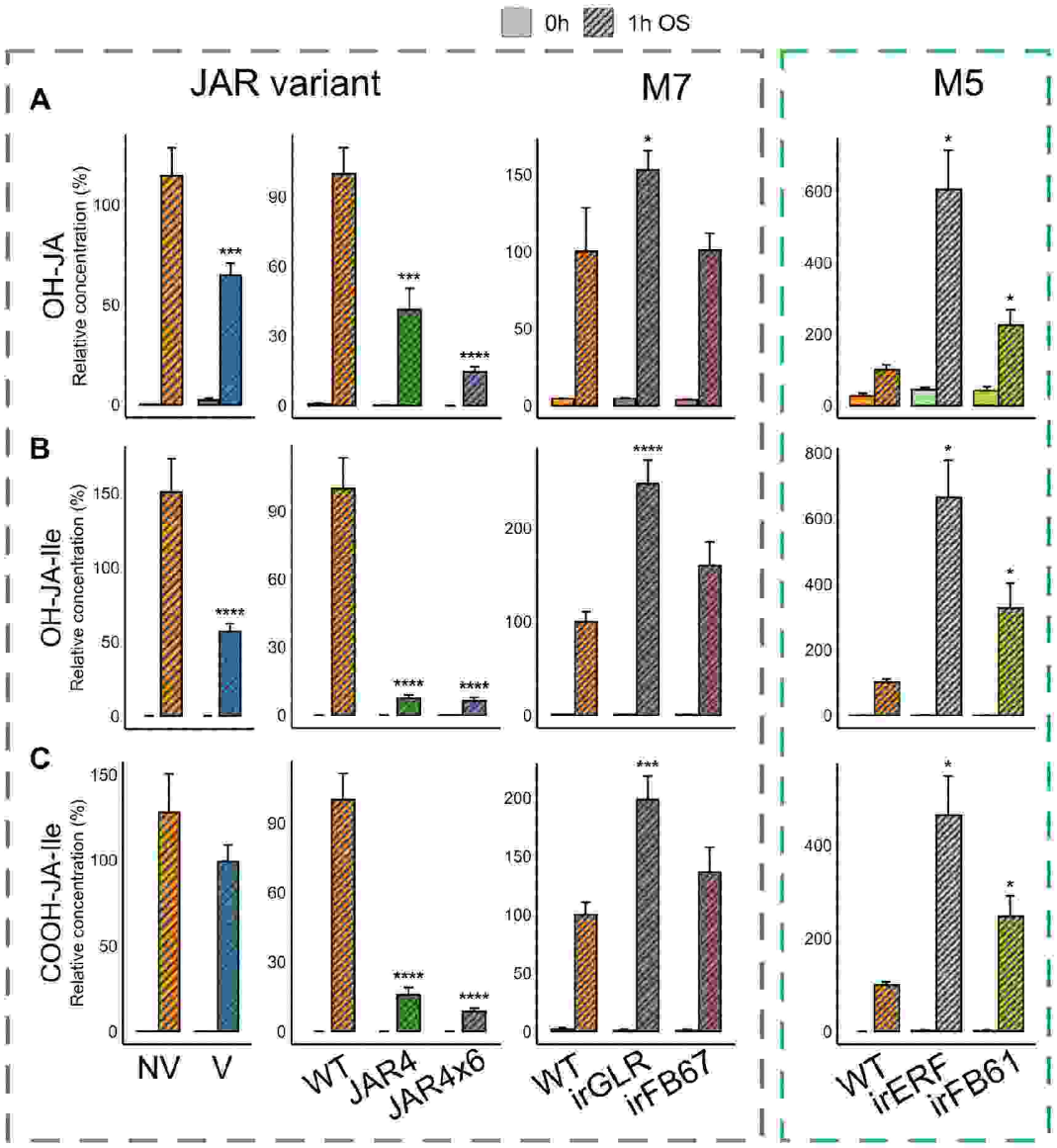

Fig. S18. JA-signaling degradation products in 4 RNAi lines silenced in the expression of "peripheral" hub genes, *NaERF, NaFB61, NaGLR, NaFB67,* 2 RNAi lines silenced in *NaJAR4/6* and the NV and V lines. (**A-C**) OH-JA, OH-JA-Ile, and COOH-JA-Ile levels in unelicited (0 h) plants and 1 h post OS-elicitation in the RNAi and WT lines. Phytohormone levels were normalized against the common UT genotype, which was included in all experiments, and was the genotypic control for all RNAi lines. Error bars are standard errors. Significance was calculated by ANOVAs followed by Tukey's HSD tests comparing against WT in the M5 and M7 group and the *NaJAR*-silenced group, and NV in the natural variant group, across 2 treatment groups (*: *p*-values < 0.05; **: < 0.01; ***: < 0.001; ****: < 0.0001).

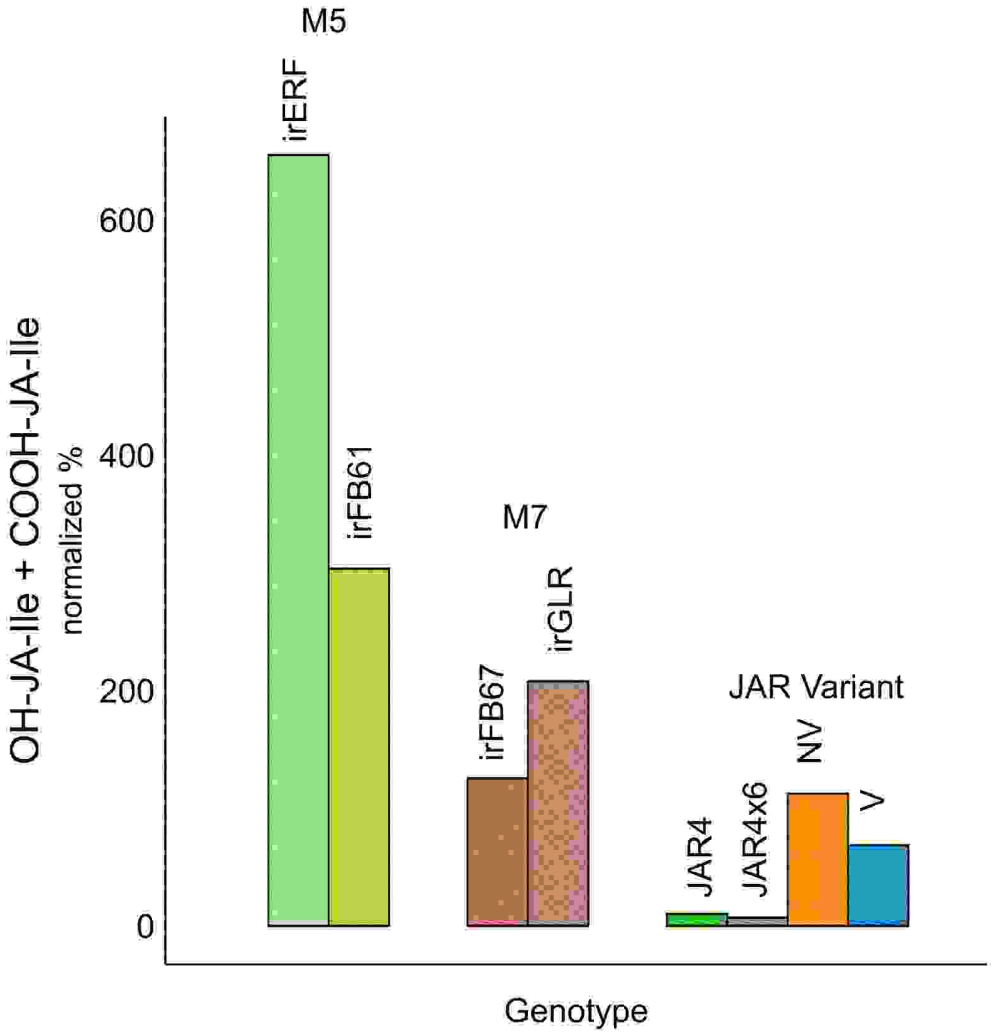

Fig. S19. Relative OS-elicited JA-Ile degradation products, OH-JA-Ile and COOH-JA-Ile in each of the 3 nodal groups of the OS-elicited GRN. The absolute levels of OS-elicited OH-JA-Ile and COOH-JA-Ile from Fig. S17 were summed and normalized against the WT in each experiment. The M5 group had the highest levels, followed by the M7, and the JAR variant group.

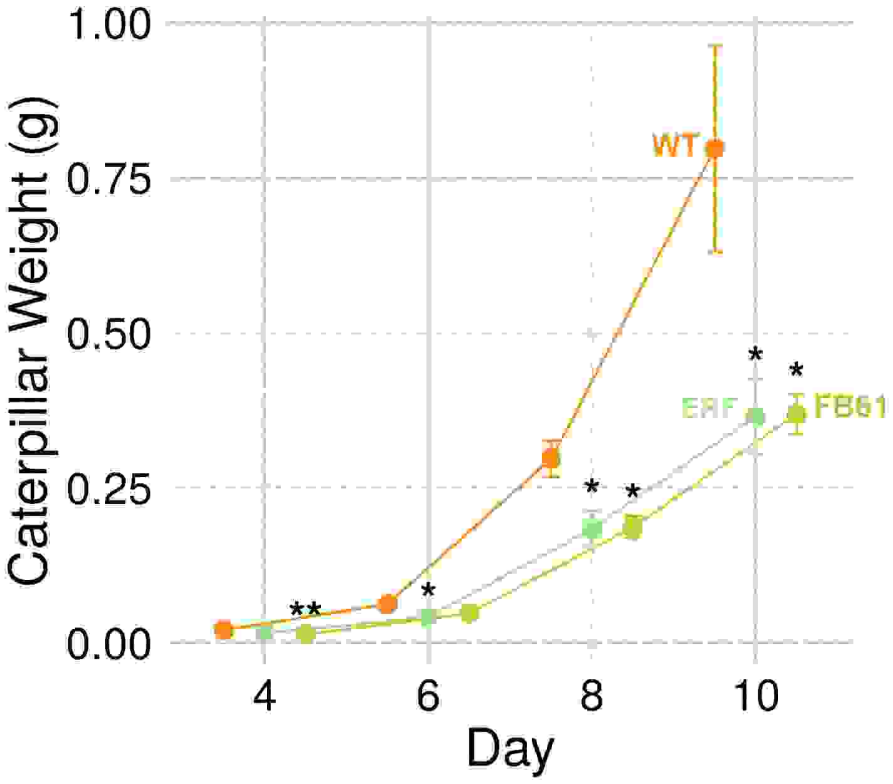

Fig. S20. Caterpillar feeding bioassay testing the constitutively-induced hypothesis of *NaERF*- and *NaFB61*-RNAi lines. The excised leaf feeding assay was conducted using neonate *M. sexta* caterpillars whose weight was recorded for 10 days as a proxy of constitutive resistance. To avoid activating induced defenses from larval feeding, leaves were excised with sterile razor blades from the base of the petiole with minimal cellular damage, and fed to larvae individually housed in enclosed humidified containers. Error bars indicate standard error (n= 8 plants/ line). Statistical significance was computed using ANOVA followed by Tukey's HSD at each day against WT plants. Asterisks denote *p*-values (*: *p*-values < 0.05; **: < 0.01; ***: < 0.001; ****: < 0.0001).

Table S1. *N. attenuata* genome assembly statistics. Various assembly statistics calculated on the different stages of the new *N. attenuata* assembly together with the previously published version 2 assembly and the *S. lycopersicum* assembly.

Assembly	Total length (bp)	Contigs	N_count	Gaps	N50 (bp)	N50n	N90 (bp)	N90n
N. attenuata v3 polished + scaffolded	2201964433	1378	14897441	1302	81992919	9	20517335	30
N. attenuata v3 unpolished	2185972991	2564	0	0	3528542	189	896276	638
N. attenuata v3 10x assembly	2090745855	133870	173879790	95623	251763	2329	3889	25452
N. attenuata v2	2365682703	37194	275168947	119817	524499	420	50394	5951
S. lycopersicum SL4	782520033	13	44731	435	65269487	6	53473368	11

Table S2. Variant allele ratios in various *N. attenuata* natural populations and individual plants. Values were estimated from DNA isolated from seed collections shown in Fig. 1D. DNA was isolated from ~40mg of each seed collection (representing approximately 400 seeds) and allele ratio was quantified using real-time qPCR. Probes were designed to amplify the deleted region shown in Fig. 1D, and an adjacent region in which there was no deletion. The respective deletion C_t values were normalized against the adjacent region to obtain the allele ratio. A value of 1 indicates no deletion and a value of 0 indicates the presence of pure variant allele. Intermediate values provide quantitative proxies of the proportion of variant alleles present in a population or in an individual plant's reproductive output.

Location	Code	Mean	CI	Latitude	Longitude
Before shot-up CAN site #2 20.8.95		0.889	0.082	37.201	-113.800
DI ranch past spring caves 7/8/93		0.891	0.396	37.331	-113.961
Goldstrike mine Bulk	GSM	0.519	0.064	37.365	-113.942
Goldstrike #1 bulk 1990		0.749	1.856	37.376	-113.928
Goldstrike #5 bulk 1990		0.001	0.002	37.365	-113.942
Goldstrike #5 bulk 5 miles from water line		0.546	0.268	37.376	-113.928
Goldstrike #1 bulk from 1 plant		0.002	0.002	37.365	-113.942
Bulk Grate 1,2,3,4,6 6/93		0.855	0.066	37.231	-113.844
Jackson springs bulk 1999		0.769	0.232	37.274	-113.880
Jackson springs Individual 1 1990		0.006	0.002	37.274	-113.880
Jackson springs Individual 2 1990		0.01	0.01	37.274	-113.880
Jackson springs Individual 3 1990		0.001	0	37.274	-113.880
Jackson springs Individual 4 1990		0.462	0.235	37.274	-113.880
Jackson springs Individual 5 1990		0.009	0.007	37.274	-113.880
Jackson springs Individual 6 1990		0.965	0.151	37.274	-113.880
Jackson springs Individual 7 1990		0.906	0.087	37.274	-113.880
Jackson springs Individual 8 1990		0.006	0.003	37.274	-113.880
Jackson springs Individual 9 1990		0.006	0.003	37.274	-113.880
1 Individual plant little house Motoqua road		0.001	0.003	37.271	-113.889
1 Individual plant little house Motoqua road		0.012	0.005	37.271	-113.889
Motoqua road night sample 1 1990	MTQ Rd	0.427	0.23	37.260	-113.874
Motoqua road night sample 2 1990		0.835	0.614	37.260	-113.874
Motoqua road night sample 3 1990		0.8	0.659	37.260	-113.874
Motoqua road night sample 4 1990		0.685	0.34	37.260	-113.874
Pahcoon flat Aug 2 1999	PHCN Flat	1.04	1.602	37.222	-113.854
Shivwit Wash Aug 1 1999	SHVWT	1.006	0.543	37.182	-113.757
Bulk collection from SUCS utah 7/9/93		1.151	0.023	37.215	-113.806
3 plant bulk SUCS site 21/8/95		0.993	0.051	37.215	-113.806
5 individual plants SUCS 6/93		1.071	0.431	37.215	-113.806
5 individual plants SUCS 6/93		1.072	0.095	37.215	-113.806

Location	Code	Mean	CI	Latitude	Longitude
5 individual plants SUCS 6/93		1.11	0.096	37.215	-113.806
UT accession 30x inbred		1.053	0.17	37.327	-113.965

Table S3. Pairwise comparison statistics of Fig. 2 indicating the contrasts and the respective statistics. Pairwise statistics for each of the panels in Fig. 2 calculated using the *emmeans* package in R, indicating the estimates of difference of slopes of JA-Ile vs JA and the associated *p*-values of the contrasts.

Timepoint comparison	contrast	estimate	SE	df	t.ratio	*p*-value
RNAi 45min JA vs JA-Ile	EV - JAR4	0.064	0.029	16	2.247	0.039
	EV - JAR6	-0.060	0.039	16	-1.563	0.138
	EV - JAR4x6	0.060	0.025	16	2.389	0.030
	JAR4 - JAR6	-0.125	0.036	16	-3.417	0.004
	JAR4 - JAR4x6	-0.004	0.022	16	-0.177	0.861
	JAR6 - JAR4x6	0.121	0.034	16	3.561	0.003
RNAi 45min JA vs 13C-JA-Ile	EV - JAR4	0.528	0.088	16	5.972	1.952e-05
	EV - JAR6	0.738	0.119	16	6.207	1.254e-05
	EV - JAR4x6	0.665	0.078	16	8.517	2.437e-07
	JAR4 - JAR6	0.210	0.113	16	1.870	0.080
	JAR4 - JAR4x6	0.137	0.068	16	2.020	0.060
	JAR6 - JAR4x6	-0.073	0.105	16	-0.701	0.493
RNAi 90min JA vs JA-Ile	EV - JAR4	0.047	0.018	20	2.59	0.02
	EV - JAR6	0.028	0.017	20	1.68	0.11
	EV - JAR4x6	0.050	0.012	20	4.21	4.27E-04***
	JAR4 - JAR6	-0.019	0.021	20	-0.89	0.38
	JAR4 - JAR4x6	0.003	0.018	20	0.15	0.88
	JAR6 - JAR4x6	0.022	0.016	20	1.33	0.20
RNAi 90min JA vs ^{13}C-JA-Ile	EV - JAR4	0.240	0.107	20	2.23	0.04*
	EV - JAR6	-0.272	0.098	20	-2.77	0.01*
	EV - JAR4x6	0.273	0.070	20	3.92	8.47E-04***
	JAR4 - JAR6	-0.512	0.126	20	-4.05	6.32E-04***
	JAR4 - JAR4x6	0.034	0.106	20	0.32	0.75
	JAR6 - JAR4x6	0.546	0.097	20	5.65	1.57E-05***
WT 45min JA vs JA-Ile	NV - V	0.148	0.027	71	5.52	5.16E-07***
WT 45min JA vs ^{13}C-JA-Ile	NV - V	0.010	0.097	71	0.10	0.92
WT 90min JA vs JA-Ile	NV - V	0.102	0.014	72	7.28	3.35E-10***
WT 90min JA vs ^{13}C-JA-Ile	NV - V	0.384	0.077	72	4.95	4.64E-06***

Table S4. *N. attenuata* natural accessions. A list of natural accessions used in this study. The column MAGIC parents indicates the accessions that were a part of the MAGIC parent crossing, and the 29 transcriptome accession column indicates the ones used for transcriptome co-expression analysis. P-UT or WT is the UT genotype sequenced and used as reference.

Accession ID	MAGIC parents	Transcriptome 29 accession
P-108	No	Yes
P-133	Yes	Yes
P-138	Yes	Yes
P-149	Yes	Yes
P-176	Yes	Yes
P-179	Yes	Yes
P-194	Yes	Yes
P-214	Yes	Yes
P-224	Yes	No
P-274	No	Yes
P-278	Yes	Yes
P-281	No	Yes
P-304	Yes	Yes
P-305	Yes	Yes
P-308	Yes	Yes
P-331	Yes	Yes
P-341	Yes	Yes
P-351	Yes	Yes
P-370	Yes	Yes
P-382	Yes	Yes
P-384	Yes	Yes
P-421	Yes	Yes
P-422	Yes	Yes
P-43	Yes	Yes
P-83	No	Yes
P-84	Yes	Yes
P-85	Yes	Yes
P-97	Yes	Yes
P-AZ	Yes	Yes
P-UT	Yes	Yes

Table S5. Primer list. Primer sequences used for qPCR and PCR amplifications and for RNAi plasmid construction. The restriction sites used for cloning are underlined.

Primer Name	Sequence 5' to 3'	Purpose
JAR4_DEL F	GACAGGAGGGAGCAGTAATATACA	qPCR
JAR4_DEL R	AAAGGTTTAATCGTCGTGTTTCA	qPCR
JAR4_CTRL F	GACTTGAACCTCATCGCGGA	qPCR
JAR4_CTRL R	GCAATGCAGACCCCTTGTTG	qPCR
JAR4_DEL 2 F	GCTCGTAAACCACACAAGAAATG	PCR
JAR4_DEL 2 R	TGTATATTACTGCTCCCTCCTGTC	PCR
ERF F	CAGCTCAAGAAACAACGTCGG	qPCR
ERF R	GATCTTGAACTAACTTCCTCTTCCT	qPCR
FB61F	ACTGCAGCGCAAATTAAGGA	qPCR
FB61 R	TTCTCACTAGACCCGACCCA	qPCR
FB67 F	AGAACTGGTCGGAATCTGCTC	qPCR
FB67 R	GCAGTAGAATCGAATCATGCCAA	qPCR
GLR F	ATAGACCCCCAGCATCCTTC	qPCR
GLR R	AGACAAGAGGGGTTGCTCTG	qPCR
COI1 F	GGCTTGACGTACTTGGGGAA	qPCR
COI1 R	CCCAACAACATTCCTTGTCTCA	qPCR
COI2 F	GGAATTCGGTGGGGGTTCAT	qPCR
COI2 R	CCAACAACATTCCTTGCCTCA	qPCR
COI2-S-P	GCGGCGCTGCAGTTACAAGTGTTTTTTTTAAACTATG	RNAi
COI2-S-M	GCGGCGACGCGTGCGCGTGGCTTCCCCTTGAGCTTG	RNAi
COI2-AS-S	GCGGCGGAGCTCGTTACAAGTGTTTTTTTTAAACTATG	RNAi
COI2-AS-X	GCGGCGCTCGAGCGCGTGGCTTCCCCTTGAGCTTG	RNAi
ERF-S-P	GCGGCGCTGCAGGATTCTACTAGGAATGGTGTTAG	RNAi
ERF-S-H	GCGGCGAAGCTTCAACATTTACATTCTCCATTTTTACTTC	RNAi
ERF-AS-S	GCGGCGGAGCTCGATTCTACTAGGAATGGTGTTAG	RNAi
ERF-AS-X	GCGGCGCTCGAGCAACATTTACATTCTCCATTTTTACTTC	RNAi
FB61-S-N	GCGGCGATGCATGAGGCTTTTTCATGTATCAAGGAC	RNAi
FB61-S-H	GCGGCGAAGCTTCAAAAACTCTGATGTCTGGCTCAGC	RNAi
FB61-AS-S	GCGGCGGAGCTCAGAGGCTTTTTCATGTATCAAGGAC	RNAi
FB61-AS-X	GCGGCGCTCGAGCAAAAACTCTGATGTCTGGCTCAGC	RNAi
GLR-S-P	GCGGCGCTGCAGCGCAACTGCCATCCCAGAAGTCAAG	RNAi
GLR-S-H	GCGGCGAAGCTTCCTAGTTGCTTATTATTACTCTTAGCTG	RNAi
GLR-AS-S	GCGGCGGAGCTCGCAACTGCCATCCCAGAAGTCAAG	RNAi
GLR-AS-X	GCGGCGCTCGAGCCTAGTTGCTTATTATTACTCTTAGCTG	RNAi
FB67-S-P	GCGGCGCTGCAGCGAGGGTCGCCGGTTCCTCGTCCAAG	RNAi
FB67-S-H	GCGGCGAAGCTTGTCTCCTAGTTTCGGGTCTTCCAC	RNAi
FB67-AS-S	GCGGCGGAGCTCCGAGGGTCGCCGGTTCCTCGTCCAAG	RNAi
FB67-AS-X	GCGGCGCTCGAGGTCTCCTAGTTTCGGGTCTTCCAC	RNAi

SI References

1. R. Halitschke, U. Schittko, G. Pohnert, W. Boland, I. T. Baldwin, Molecular interactions between the specialist herbivore *Manduca sexta* (Lepidoptera, Sphingidae) and its natural host *Nicotiana attenuata*. III. Fatty acid-amino acid conjugates in herbivore oral secretions are necessary and sufficient for herbivore-specific plant responses. *Plant Physiol.* **125**, 711–717 (2001).
2. A. Roda, R. Halitschke, A. Steppuhn, I. T. Baldwin, Individual variability in herbivore-specific elicitors from the plant's perspective. *Mol. Ecol.* **13**, 2421–2433 (2004).
3. A. VanDoorn, M. Kallenbach, A. A. Borquez, I. T. Baldwin, G. Bonaventure, Rapid modification of the insect elicitor N-linolenoyl-glutamate via a lipoxygenase-mediated mechanism on *Nicotiana attenuata* leaves. *BMC Plant Biol.* **10**, 1–11 (2010).
4. J.-H. Kang, L. Wang, A. Giri, I. T. Baldwin, Silencing threonine deaminase and *JAR4* in *Nicotiana attenuata* impairs jasmonic acid–isoleucine–mediated defenses against *Manduca sexta*. *Plant Cell* **18**, 3303–3320 (2006).
5. A. Paschold, R. Halitschke, I. T. Baldwin, Co (i)-ordinating defenses: NaCOI1 mediates herbivore-induced resistance in *Nicotiana attenuata* and reveals the role of herbivore movement in avoiding defenses. *Plant J.* **51**, 79–91 (2007).
6. A. Paschold, G. Bonaventure, M. R. Kant, I. T. Baldwin, Jasmonate perception regulates jasmonate biosynthesis and JA-Ile metabolism: the case of COI1 in *Nicotiana attenuata*. *Plant Cell Physiol.* **49**, 1165–1175 (2008).
7. Y. Oh, I. T. Baldwin, I. Gális, NaJAZh regulates a subset of defense responses against herbivores and spontaneous leaf necrosis in *Nicotiana attenuata* plants. *Plant Physiol.* **159**, 769–788 (2012).
8. R. Li, *et al.*, Flower-specific jasmonate signaling regulates constitutive floral defenses in wild tobacco. *Proc. Natl. Acad. Sci. U.S.A.* **114**, E7205–E7214 (2017).
9. Y. Bai, *et al.*, Natural history–guided omics reveals plant defensive chemistry against leafhopper pests. *Science* **375**, eabm2948 (2022).
10. D. Li, I. T. Baldwin, E. Gaquerel, Beyond the canon: within-plant and population-level heterogeneity in jasmonate signaling engaged by plant-insect interactions. *Plants* **5**, 14 (2016).
11. D. Kessler, C. Diezel, I. T. Baldwin, Changing pollinators as a means of escaping herbivores. *Current Biology* **20**, 237–242 (2010).
12. L. Cortés Llorca, *et al.*, ZEITLUPE facilitates the rhythmic movements of *Nicotiana attenuata* flowers. *Plant J.* **103**, 308–322 (2020).
13. J. A. Zavala, A. G. Patankar, K. Gase, I. T. Baldwin, Constitutive and inducible trypsin proteinase inhibitor production incurs large fitness costs in *Nicotiana attenuata*. *Proc. Natl. Acad. Sci. U.S.A.* **101**, 1607–1612 (2004).
14. I. T. Baldwin, D. Gorham, E. A. Schmelz, C. A. Lewandowski, G. Y. Lynds, Allocation of nitrogen to an inducible defense and seed production in *Nicotiana attenuata*. *Oecologia* **115**, 541–552 (1998).
15. I. T. Baldwin, M. Karb, T. Ohnmeiss, Allocation of ^{15}N from nitrate to nicotine: production and turnover of a damage-induced mobile defense. *Ecology* **75**, 1703–1713 (1994).
16. J. Li, *et al.*, Controlled hydroxylations of diterpenoids allow for plant chemical defense without autotoxicity. *Science* **371**, 255–260 (2021).
17. I. T. Baldwin, Jasmonate-induced responses are costly but benefit plants under attack in native populations. *Proc. Natl. Acad. Sci. U.S.A.* **95**, 8113–8118 (1998).
18. T. Züst, A. A. Agrawal, Trade-offs between plant growth and defense against insect herbivory: an emerging mechanistic synthesis. *Annu. Rev. Plant. Biol.* **68**, 513–534 (2017).
19. O. L. Cope, K. Keefover-Ring, E. L. Kruger, R. L. Lindroth, Growth–defense trade-offs shape population genetic composition in an iconic forest tree species. *Proc. Natl. Acad. Sci. U.S.A.* **118**, e2103162118 (2021).
20. A. Chini, S. Gimenez-Ibanez, A. Goossens, R. Solano, Redundancy and specificity in jasmonate signalling. *Curr. Opin. Plant. Biol.* **33**, 147–156 (2016).
21. G. A. Howe, I. T. Major, A. J. Koo, Modularity in jasmonate signaling for multistress resilience. *Annu. Rev. Plant. Biol.* **69**, 387–415 (2018).
22. M. L. Campos, *et al.*, Rewiring of jasmonate and phytochrome B signalling uncouples plant growth-defense tradeoffs. *Nat. Commun.* **7**, 1–10 (2016).

23. J.-K. Weng, M. Ye, B. Li, J. P. Noel, Co-evolution of hormone metabolism and signaling networks expands plant adaptive plasticity. *Cell* **166**, 881–893 (2016).
24. R. A. Bahulikar, D. Stanculescu, C. A. Preston, I. T. Baldwin, ISSR and AFLP analysis of the temporal and spatial population structure of the post-fire annual, *Nicotiana attenuata*, in SW Utah. *BMC Ecol* **4**, 1–13 (2004).
25. A. Charlton, Medicinal uses of tobacco in history. *J R Soc Med* **97**, 292–296 (2004).
26. I. T. Baldwin, L. Morse, Up in smoke: II. germination of *Nicotiana attenuata* in response to smoke-derived cues and nutrients in burned and unburned soils. *J. Chem. Ecol.* **20**, 2373–2391 (1994).
27. I. T. Baldwin, L. Staszak-Kozinski, R. Davidson, Up in smoke: I. Smoke-derived germination cues for postfire annual, *Nicotiana attenuata* torr. Ex. Watson. *J. Chem. Ecol.* **20**, 2345–2371 (1994).
28. L. F. Delph, J. K. Kelly, On the importance of balancing selection in plants. *New Phytol.* **201**, 45–56 (2014).
29. P. W. Hedrick, M. E. Ginevan, E. P. Ewing, Genetic polymorphism in heterogeneous environments. *Annual Review of Ecology and Systematics* **7**, 1–32 (1976).
30. E. Katz, *et al.*, Genetic variation underlying differential ammonium and nitrate responses in *Arabidopsis* thaliana. *Plant Cell* **34**, 4696–4713 (2022).
31. K. V. S. K. Prasad, *et al.*, A gain-of-function polymorphism controlling complex traits and fitness in nature. *Science* **337**, 1081–1084 (2012).
32. D. Li, I. T. Baldwin, E. Gaquerel, Navigating natural variation in herbivory-induced secondary metabolism in coyote tobacco populations using MS/MS structural analysis. *Proc. Natl. Acad. Sci. U.S.A.* **112**, E4147–E4155 (2015).
33. I. Monte, *et al.*, Ligand-receptor co-evolution shaped the jasmonate pathway in land plants. *Nat. Chem. Biol.* **14**, 480–488 (2018).
34. I. Monte, *et al.*, An ancient COI1-independent function for reactive electrophilic oxylipins in thermotolerance. *Current Biology* **30**, 962–971 (2020).
35. J. L. Bowman, *et al.*, Insights into land plant evolution garnered from the *Marchantia polymorpha* genome. *Cell* **171**, 287–304 (2017).
36. L. An, R. M. Ahmad, H. Ren, J. Qin, Y. Yan, Jasmonate signal receptor gene family ZmCOIs restore male fertility and defense response of *Arabidopsis* mutant coi1-1. *Journal of Plant Growth Regulation* **38**, 479–493 (2019).
37. H. Y. Lee, *et al.*, Oryza sativa COI homologues restore jasmonate signal transduction in *Arabidopsis* coi1-1 mutants. *PLoS One* **8**, e52802 (2013).
38. D.-L. Yang, *et al.*, Plant hormone jasmonate prioritizes defense over growth by interfering with gibberellin signaling cascade. *Proc. Natl. Acad. Sci. U.S.A.* **109**, E1192–E1200 (2012).
39. S. Heiling, *et al.*, Jasmonate and ppHsystemin regulate key malonylation steps in the biosynthesis of 17-hydroxygeranyllinalool diterpene glycosides, an abundant and effective direct defense against herbivores in *Nicotiana attenuata*. *Plant Cell* **22**, 273–292 (2010).
40. W. E. Pluskota, N. Qu, M. Maitrejean, W. Boland, I. T. Baldwin, Jasmonates and its mimics differentially elicit systemic defence responses in *Nicotiana attenuata*. *J. Exp. Bot.* **58**, 4071–4082 (2007).
41. A. Steppuhn, I. T. Baldwin, Resistance management in a native plant: nicotine prevents herbivores from compensating for plant protease inhibitors. *Ecol. Lett.* **10**, 499–511 (2007).
42. N. M. Van Dam, I. T. Baldwin, Competition mediates costs of jasmonate-induced defences, nitrogen acquisition and transgenerational plasticity in *Nicotiana attenuata*. *Functional Ecology* **15**, 406–415 (2001).
43. A. L. File, G. P. Murphy, S. A. Dudley, Fitness consequences of plants growing with siblings: reconciling kin selection, niche partitioning and competitive ability. *Proc. R. Soc. Lond. B Biol. Sci.* **279**, 209–218 (2012).
44. S. Bhattacharya, I. T. Baldwin, The post-pollination ethylene burst and the continuation of floral advertisement are harbingers of non-random mate selection in *Nicotiana attenuata*. *Plant J.* **71**, 587–601 (2012).
45. B. Bubner, K. Gase, I. T. Baldwin, Two-fold differences are the detection limit for determining transgene copy numbers in plants by real-time PCR. *BMC Biotechnol.* **4**, 1–11 (2004).

46. S. Koren, *et al.*, Canu: scalable and accurate long-read assembly via adaptive k-mer weighting and repeat separation. *Genome Res* **27**, 722–736 (2017).
47. S. Xu, *et al.*, Wild tobacco genomes reveal the evolution of nicotine biosynthesis. *Proc. Natl. Acad. Sci. U.S.A.* **114**, 6133–6138 (2017).
48. R. Vaser, I. Sović, N. Nagarajan, M. Šikić, Fast and accurate de novo genome assembly from long uncorrected reads. *Genome Res* **27**, 737–746 (2017).
49. A. Rhie, *et al.*, Towards complete and error-free genome assemblies of all vertebrate species. *Nature* **592**, 737–746 (2021).
50. M. Boetzer, W. Pirovano, SSPACE-LongRead: scaffolding bacterial draft genomes using long read sequence information. *BMC Bioinformatics* **15**, 1–9 (2014).
51. H. Li, Minimap2: pairwise alignment for nucleotide sequences. *Bioinformatics* **34**, 3094–3100 (2018).
52. G. A. Van der Auwera, B. D. O'Connor, *Genomics in the Cloud: Using Docker, GATK, and WDL in Terra* (O'Reilly Media, 2020).
53. K. W. Broman, H. Wu, Ś. Sen, G. A. Churchill, R/qtl: QTL mapping in experimental crosses. *Bioinformatics* **19**, 889–890 (2003).
54. K. W. Broman, Genetic map construction with R/qtl. *University of Wisconsin-Madison, Department of Biostatistics & Medical Informatics* (2010).
55. J. Catchen, A. Amores, S. Bassham, Chromonomer: a tool set for repairing and enhancing assembled genomes through integration of genetic maps and conserved synteny. *G3: Genes, Genomes, Genetics* **10**, 4115–4128 (2020).
56. R. M. Waterhouse, *et al.*, BUSCO applications from quality assessments to gene prediction and phylogenomics. *Mol. Biol. Evol.* **35**, 543–548 (2018).
57. P. S. Hosmani, *et al.*, An improved de novo assembly and annotation of the tomato reference genome using single-molecule sequencing, hi-c proximity ligation and optical maps. *bioRxiv* (2019) https:/doi.org/10.1101/767764.
58. D. Kim, J. M. Paggi, C. Park, C. Bennett, S. L. Salzberg, Graph-based genome alignment and genotyping with HISAT2 and HISAT-genotype. *Nat. Biotechnol.* **37**, 907–915 (2019).
59. M. Pertea, *et al.*, StringTie enables improved reconstruction of a transcriptome from RNA-seq reads. *Nat. Biotechnol.* **33**, 290–295 (2015).
60. L. Venturini, S. Caim, G. G. Kaithakottil, D. L. Mapleson, D. Swarbreck, Leveraging multiple transcriptome assembly methods for improved gene structure annotation. *Gigascience* **7**, giy093 (2018).
61. D. Mapleson, L. Venturini, G. Kaithakottil, D. Swarbreck, Efficient and accurate detection of splice junctions from RNA-seq with Portcullis. *Gigascience* **7**, giy131 (2018).
62. G. P. Rédei, *Encyclopedia of genetics, genomics, proteomics, and informatics* (Springer Science & Business Media, 2008).
63. M. S. Campbell, C. Holt, B. Moore, M. Yandell, Genome annotation and curation using MAKER and MAKER-P. *Current Protocols in Bioinformatics* **48**, 4–11 (2014).
64. B. Buchfink, K. Reuter, H.-G. Drost, Sensitive protein alignments at tree-of-life scale using DIAMOND. *Nat Methods* **18**, 366–368 (2021).
65. A. P. Giri, *et al.*, Molecular interactions between the specialist herbivore *Manduca sexta* (Lepidoptera, Sphingidae) and its natural host *Nicotiana attenuata*. VII. Changes in the plant's proteome. *Plant Physiol.* **142**, 1621–1641 (2006).
66. H. Cai, D. L. Des Marais, Revisiting regulatory coherence: accounting for temporal bias in plant gene co-expression analyses. *New Phytol.* (2023).
67. N. M. Van Dam, M. Horn, M. Mareš, I. T. Baldwin, Ontogeny constrains systemic protease inhibitor response in *Nicotiana attenuata*. *J. Chem. Ecol.* **27**, 547–568 (2001).
68. J. Schwachtje, *et al.*, SNF1-related kinases allow plants to tolerate herbivory by allocating carbon to roots. *Proc. Natl. Acad. Sci. U.S.A.* **103**, 12935–12940 (2006).
69. I. T. Baldwin, C. Preston, M. Euler, D. Gorham, Patterns and consequences of benzyl acetone floral emissions from *Nicotiana attenuata* plants. *J. Chem. Ecol.* **23**, 2327–2343 (1997).
70. E. S. McCloud, I. T. Baldwin, Herbivory and caterpillar regurgitants amplify the wound-induced increases in jasmonic acid but not nicotine in *Nicotiana sylvestris*. *Planta* **203**, 430–435 (1997).

71. U. Schittko, C. A. Preston, I. T. Baldwin, Eating the evidence? *Manduca sexta* larvae can not disrupt specific jasmonate induction in *Nicotiana attenuata* by rapid consumption. *Planta* **210**, 343–346 (2000).
72. C. Soneson, M. I. Love, M. D. Robinson, Differential analyses for RNA-seq: transcript-level estimates improve gene-level inferences. *F1000Res* **4** (2015).
73. M. I. Love, W. Huber, S. Anders, Moderated estimation of fold change and dispersion for RNA-seq data with DESeq2. *Genome Biol.* **15**, 1–21 (2014).
74. P. Langfelder, B. Zhang, S. Horvath, Defining clusters from a hierarchical cluster tree: the Dynamic Tree Cut package for R. *Bioinformatics* **24**, 719–720 (2008).
75. A. E. Lipka, *et al.*, GAPIT: genome association and prediction integrated tool. *Bioinformatics* **28**, 2397–2399 (2012).
76. B. Joseph, J. A. Corwin, B. Li, S. Atwell, D. J. Kliebenstein, Cytoplasmic genetic variation and extensive cytonuclear interactions influence natural variation in the metabolome. *eLife* **2**, e00776 (2013).
77. A. A. Shabalin, Matrix eQTL: ultra fast eQTL analysis via large matrix operations. *Bioinformatics* **28**, 1353–1358 (2012).
78. T. Krügel, M. Lim, K. Gase, R. Halitschke, I. T. Baldwin, *Agrobacterium*-mediated transformation of *Nicotiana attenuata*, a model ecological expression system. *Chemoecology* **12**, 177–183 (2002).
79. K. Gase, I. T. Baldwin, Transformational tools for next-generation plant ecology: manipulation of gene expression for the functional analysis of genes. *Plant Ecol. Divers.* **5**, 485–490 (2012).
80. K. Gase, A. Weinhold, T. Bozorov, S. Schuck, I. T. Baldwin, Efficient screening of transgenic plant lines for ecological research. *Mol Ecol Resour* **11**, 890–902 (2011).
81. J. He, *et al.*, An unbiased approach elucidates variation in (S)-(+)-linalool, a context-specific mediator of a tri-trophic interaction in wild tobacco. *Proc. Natl. Acad. Sci. U.S.A.* **116**, 14651–14660 (2019).
82. C. Koenig, *et al.*, A reference gene set for chemosensory receptor genes of *Manduca sexta*. *Insect Biochem. Mol. Biol.* **66**, 51–63 (2015).
83. M. Schäfer, C. Brütting, I. T. Baldwin, M. Kallenbach, High-throughput quantification of more than 100 primary-and secondary-metabolites, and phytohormones by a single solid-phase extraction based sample preparation with analysis by UHPLC–HESI–MS/MS. *Plant Methods* **12**, 1–18 (2016).
84. E. Gaquerel, S. Heiling, M. Schoettner, G. Zurek, I. T. Baldwin, Development and validation of a liquid chromatography- electrospray ionization- time-of-flight mass spectrometry method for induced changes in *Nicotiana attenuata* leaves during simulated herbivory. *J. Agric. Food. Chem.* **58**, 9418–9427 (2010).
85. R Core Team, R: A language and environment for statistical computing (R Foundation for Statistical Computing, 2020).
86. K. Katoh, D. M. Standley, MAFFT multiple sequence alignment software version 7: improvements in performance and usability. *Mol. Biol. Evol.* **30**, 772–780 (2013).
87. A. Stamatakis, RAxML version 8: a tool for phylogenetic analysis and post-analysis of large phylogenies. *Bioinformatics* **30**, 1312–1313 (2014).
88. F. Rohart, B. Gautier, A. Singh, K.-A. Lê Cao, mixOmics: An R package for 'omics feature selection and multiple data integration. *PLoS Comput. Biol.* **13**, e1005752 (2017).
89. G. Yu, L.-G. Wang, Y. Han, Q.-Y. He, clusterProfiler: an R package for comparing biological themes among gene clusters. *OMICS* **16**, 284–287 (2012).
90. J. C. Delfin, *et al.*, AtGH3.10 is another jasmonic acid-amido synthetase in *Arabidopsis thaliana*. *Plant J.* **110**, 1082–1096 (2022).

An unbiased approach elucidates variation in (S)-(+)-linalool, a context-specific mediator of a tri-trophic interaction in wild tobacco

Jun He, Richard A. Fandino, Rayko Halitschke, Katrin Luck, Tobias G. Köllner, Mark H. Murdock, Rishav Ray, Klaus Gase, Markus Knaden, Ian T. Baldwin, and Meredith C. Schuman

Published in Proceedings of the National Academy of Sciences 116.29 (2019): 14651-14660.

DOI: https://doi.org/10.1073/pnas.1818585116

In **Manuscript III**, we focused on the role of volatile organic compounds (VOC) in mediating plant interactions in *N. attenuata* system, particularly in the context of ecological variations. We utilized two natural accessions from Arizona and Utah and a bi-parental mapping population with these two accessions as parents, to investigate the genetic factors controlling VOC variation. From field experiments we show that the emission of linalool significantly correlated with the predation of *M. sexta* larvae and eggs by native predators. Using QTL analysis, genetic mapping, and genome analysis, we identified the causal gene, *NaLIS*, and the genetic variation that was associated with the variation in linalool emission. By manipulating linalool emissions and its chemistry *in vivo*, we show that the effects of different linalool enantiomers on *M. sexta* oviposition depended on both the genetic background of the plant and the complexity of the environment.

FORM 1

Manuscript No. III

Manuscript title: An unbiased approach elucidates variation in (S)-(+)-linalool, a context-specific mediator of a tri-trophic interaction in wild tobacco

Authors: Jun He, Richard A. Fandino, Rayko Halitschke, Katrin Luck, Tobias G. Köllner, Mark H. Murdock, Rishav Ray, Klaus Gase, Markus Knaden, Ian T. Baldwin, and Meredith C. Schuman

Bibliographic information: Proceedings of the National Academy of Sciences 116.29 (2019): 14651-14660.

The candidate is

☐ First author, ☐ Co-first author, ☐ Corresponding author, ☒ Co-author.

Status: Published

Authors' contributions (in %) to the given categories of the publication

Author	Conceptual	Data analysis	Experimental	Writing the manuscript	Provision of material
Jun He	20%	40%	30%	25%	-
Richard A. Fandino	15%	-	15%	10%	-
Rayko Halitschke	10%	10%	10%	10%	-
Katrin Luck	-	-	10%	-	-
Tobias G. Köllner	5%	10%	5%	5%	-
Mark H. Murdock	-	10%	10%	-	-
Rishav Ray	-	20%	10%	5%	10%
Klaus Gase	5%	5%	5%	5%	10%
Markus Knaden	10%	5%	-	10%	30%
Ian T. Baldwin	15%	-	-	10%	50%
Meredith C. Schuman	20%	-	5%	20%	-
Total	100%	100%	100%	100%	100%

Signature candidate

Signature supervisor
(member of the Faculty)

An unbiased approach elucidates variation in (*S*)-(+)-linalool, a context-specific mediator of a tri-trophic interaction in wild tobacco

Jun He[a], Richard A. Fandino[b], Rayko Halitschke[a], Katrin Luck[c], Tobias G. Köllner[c], Mark H. Murdock[a,d,1], Rishav Ray[a], Klaus Gase[a], Markus Knaden[b], Ian T. Baldwin[a,2], and Meredith C. Schuman[a,e,2]

[a]Department of Molecular Ecology, Max Planck Institute for Chemical Ecology, 07745 Jena, Germany; [b]Department of Evolutionary Neuroethology, Max Planck Institute for Chemical Ecology, 07745 Jena, Germany; [c]Department of Biochemistry, Max Planck Institute for Chemical Ecology, 07745 Jena, Germany; [d]College of Life Sciences, Brigham Young University, Provo, UT 84606; and [e]Department of Geography, University of Zurich, 8057 Zürich, Switzerland

Edited by John G. Hildebrand, University of Arizona, Tucson, AZ, and approved June 4, 2019 (received for review October 29, 2018)

Plant volatile organic compounds (VOCs) mediate many interactions, and the function of common VOCs is especially likely to depend on ecological context. We used a genetic mapping population of wild tobacco, *Nicotiana attenuata*, originating from a cross of 2 natural accessions from Arizona and Utah, separated by the Grand Canyon, to dissect genetic variation controlling VOCs. Herbivory-induced leaf terpenoid emissions varied substantially, while green leaf volatile emissions were similar. In a field experiment, only emissions of linalool, a common VOC, correlated significantly with predation of the herbivore *Manduca sexta* by native predators. Using quantitative trait locus mapping and genome mining, we identified an (*S*)-(+)-linalool synthase (*NaLIS*). Genome resequencing, gene cloning, and activity assays revealed that the presence/absence of a 766-bp sequence in *NaLIS* underlies the variation of linalool emissions in 26 natural accessions. We manipulated linalool emissions and composition by ectopically expressing linalool synthases for both enantiomers, (*S*)-(+)- and (*R*)-(−)-linalool, reported to oppositely affect *M. sexta* oviposition, in the Arizona and Utah accessions. We used these lines to test ovipositing moths in increasingly complex environments. The enantiomers had opposite effects on oviposition preference, but the magnitude of the effect depended strongly both on plant genetic background, and complexity of the bioassay environment. Our study reveals that the emission of linalool, a common VOC, differs by orders-of-magnitude among geographically interspersed conspecific plants due to allelic variation in a linalool synthase, and that the response of a specialist herbivore to linalool depends on enantiomer, plant genotype, and environmental complexity.

Nicotiana attenuata | *Manduca sexta* | enantiomer-specific linalool synthase | tri-trophic interactions | oviposition preference

Plants use a variety of volatile organic compounds (VOCs) to mediate interactions with other organisms. VOC emissions from different tissues, such as leaves, flowers, fruit, and roots help to attract pollinators and seed dispersers, or defend against abiotic or biotic stress, including that from heat, ozone, herbivores, and pathogens (1, 2). However, herbivores also use plant VOCs as host location cues and feeding stimulants (1, 2). Two ubiquitous groups of plant VOCs are green leaf volatiles (GLVs) and terpenoids. GLVs comprise C_6 aldehydes, alcohols, and esters derived from fatty acids via the lipoxygenase (LOX)/hydroperoxide lyase (HPL) pathway, which are released upon damage from green tissues. The composition of GLV blends varies among plants and due to different causes of wounding (3–5). GLVs seem to be produced by all plants: the LOX/HPL pathway is also known from algae (6, 7). In contrast, while the general pathways of terpenoid biosynthesis are also conserved in higher plants (8), the production of specific terpenoid VOCs among the thousands of possible structures varies greatly from plant to plant (4, 9). Terpenoid VOCs include hemiterpenes (C_5), monoterpenes (C_{10}), sesquiterpenes (C_{15}), and a few diterpenes (C_{20}), and their derivatives, synthesized from the mevalonate (MVA) or the 2-C-methyl-D-erythritol 4-phosphate/1-deoxy-D-xylulose 5-phosphate (MEP/DOXP) pathway (10). Terpenoid VOCs directly synthesized by terpene synthases (TPSs) (8) are often emitted in response to stresses, and could have many functions in stress responses and interactions (11). Both GLVs and terpenoids have been shown to attract predators or parasitoids of herbivores, a phenomenon termed indirect defense, and some directly deter herbivore oviposition (12, 13). Considering the diverse interactions mediated by VOCs and their structural diversity, their functions may be highly specific. Interestingly, common VOCs, such as linalool, are also known to have multiple functions in different interaction systems (14).

Linalool is a monoterpenoid alcohol with 2 enantiomeric forms, (*R*)-(−)-linalool and (*S*)-(+)-linalool; both occur frequently in nature. In plants, linalool has been detected from many species (15). One plant species may produce only 1 enantiomer, but others can produce both enantiomers with dynamic composition, for example across individuals or development stages (16–18). Linalool has

Significance

The monoterpene alcohol linalool, occurring as 2 enantiomers, is made by many organisms and mediates diverse ecological interactions, including the attraction of both herbivores and their predators to plants. The specific effect of linalool differs by enantiomer and across interactions. Here, we used a forward genetics approach, which identified linalool as a candidate indirect defense compound produced by the wild tobacco *Nicotiana attenuata* against the specialist herbivore *Manduca sexta*. Linalool emission varied by orders-of-magnitude across 26 *N. attenuata* accessions, due to geographically interspersed allelic variation of a linalool synthase gene. We identified specific effects of the enantiomer, but also plant genotype and ecological context, which determined linalool's effect on *M. sexta* behavior within this plant–insect interaction.

Author contributions: J.H., R.A.F., R.H., T.G.K., K.G., M.K., I.T.B., and M.C.S. designed research; J.H., R.A.F., R.H., K.L., T.G.K., M.H.M., R.R., K.G., and M.C.S. performed research; R.R. and K.G. contributed new reagents/analytic tools; J.H., T.G.K., M.H.M., R.R., K.G., and M.K. analyzed data; and J.H., R.A.F., R.H., T.G.K., K.G., M.K., I.T.B., and M.C.S. wrote the paper.

The authors declare no conflict of interest.

This article is a PNAS Direct Submission.

Data deposition: The sequences reported in this paper have been deposited in the GenBank database (accession nos. LOC109240002 and LOC109235079). Source data are available at https://edmond.mpdl.mpg.de/imeji/collection/KpsiwBPSKETsPdQV.

[1]Present address: Department of Surgery, University of Pittsburgh, Pittsburgh, PA 15213.

[2]To whom correspondence may be addressed. Email: Baldwin@ice.mpg.de or meredith.schuman@geo.uzh.ch.

This article contains supporting information online at www.pnas.org/lookup/suppl/doi:10.1073/pnas.1818585116/-/DCSupplemental.

Published online July 1, 2019.

been documented to have several functions in plants: as a common component of floral scent (15), it is correlated with pollinator attraction, especially for hawkmoths (19–22). Linalool emitted from *Datura wrightii* (angel's trumpet) flowers stimulates visiting and feeding by *Manduca sexta* (tobacco hornworm) moths and, interestingly, mated female moths were attracted only by (*S*)-(+)-linalool but repelled by (*R*)-(−)-linalool (23). However, in some cases floral linalool and its derivatives do not attract pollinators but function as repellents of floral antagonists (24). Linalool is also often found in foliar VOCs, especially in herbivory-induced plant volatiles. For example, linalool accumulates in the trichomes of *Solanum lycopersicum* cv. Moneymaker (tomato) leaves and stems and is induced by wounding, jasmonic acid application, and herbivory by *Tetranychus urticae* (red spider mites) (25). (*S*)-(+)-Linalool is the most abundant herbivory-induced VOC in *Oryza sativa* (rice) plants attacked by *Spodoptera frugiperda* (fall armyworm) larvae, and the application of synthetic racemic linalool to rice plants attracted *Cotesia marginiventris* parasitic wasps, which are also attracted to *S. frugiperda*-damaged plants (26, 27). Linalool was also found in herbivory-induced VOCs from *Vicia faba* (broad bean) plants damaged by *Acyrthosiphon pisum* (pea aphids) and was attractive to the aphid parasitoid *Aphidius ervi* in wind-tunnel assays (28). Linalool in insects may function as a pheromone (29) and an antipathogen defense compound (30), and has been reported in multiple bacteria and fungi where its functions have not been revealed (31). Because linalool is ubiquitous in the biosphere, with contrasting functions in different interaction systems, its role has been recognized as highly context-dependent (14). However, few studies have addressed the essential question of how context affects linalool function.

The wild tobacco *Nicotiana attenuata* has been established as an ecological model plant for which interactions with many insects in its native environment, including the specialist Lepidopteran pollinator and herbivore *M. sexta* and predatory *Geocoris* spp. (big-eyed bugs), have been well characterized. Previous studies showed that complex blends of terpenoids, including (*E*)-β-ocimene, linalool, and (*E*)-α-bergamotene, can be detected in the headspace of *N. attenuata* plants and that these compounds vary among natural accessions (9, 12). The addition of racemic linalool, but also (*E*)-α-bergamotene and several other herbivory-induced VOCs, to wild *N. attenuata* plants in a natural population in Utah (UT) significantly increased the predation of *M. sexta* eggs; linalool further decreased oviposition by adult moths (12). Two *N. attenuata* genotypes originating in Arizona (AZ) and Utah, which vary in many traits (32–34), were used to develop an advanced intercross recombinant inbred line (AI-RIL) population (34). With this population, the gene encoding the (*E*)-α-bergamotene synthase was mapped and characterized and this compound was found to function both in attracting *M. sexta* moths to pollinate flowers, and indirectly defending leaves from *M. sexta* larvae (34).

Here, we used an integrated approach to dissect natural variation in herbivory-induced foliar VOCs and their function in tritrophic interactions in *N. attenuata*. Field predation assays using the AI-RIL population derived from the AZ and UT accessions revealed that linalool is a key attractant for native predators in Arizona. Quantitative trait locus (QTL) mapping and genome mining, together with gene cloning and expression, was used to identify and characterize a linalool synthase gene, *NaLIS*. The *NaLIS* gene displayed allelic variation, which explained variation in linalool production among 26 *N. attenuata* accessions collected from a selection of habitats within the range of the species. Natural accessions and RILs produced only the (*S*)-(+)-linalool enantiomer, and we used ectopic expression of enantiomer-specific linalool synthase (LIS) genes to either enhance the production of (*S*)-(+)-linalool, or introduce foreign (*R*)-(−)-linalool into the AZ and UT *N. attenuata* accessions. Oviposition assays using mated *M. sexta* females in increasingly complex and realistic environments demonstrated that the enhancement of (*S*)-(+)-linalool and introduction of (*R*)-(−)-linalool affect the oviposition preference of *M. sexta* moths differently depending on the enantiomer and plant accession. Furthermore, we found that ectopic expression of these linalool enantiomers did not affect the growth of *M. sexta* larvae. Together, these results provide evidence for context-dependent functions of a ubiquitous VOC, linalool, and imply local selection operating on plant signals mediating tritrophic interactions.

Results

Terpenoid VOC Emissions Are Highly Variable in Natural Accessions and a Derived Genetic Mapping Population. The AZ and UT accessions differ in many traits, including the release of individual VOCs from leaves and flowers (32–34). Here, we show that the differences in leaf headspace composition are extensive and primarily due to differences in terpenoid VOCs. We detected 33 VOCs emitted by at least 1 accession after leaves were treated with wounding and application of *M. sexta* regurgitant (W+R). These compounds comprised 17 GLVs and 14 terpenoids, as well as nicotine and benzyl alcohol (Fig. 1*A* and *SI Appendix*, Fig. S1*A* and Table S1). While the release of GLVs was similar, most terpenoids were enriched in one or the other accession. Abundance of the monoterpenoids (*E*)-β-ocimene and linalool were 36- and 3.5-fold higher, respectively, in the AZ versus the UT headspace, while sesquiterpenoids—including (*E*)-α-bergamotene, α-farnesene, sesquiphellandrene, and 5 unidentified terpenoids—were much more abundant in the UT versus the AZ headspace (Fig. 1*A* and *SI Appendix*, Table S1). Only 2 terpenoids, α-duprezianene and an unidentified sesquiterpene (retention time 27.3 min), were similar in relative abundance in the 2 accessions.

We further profiled foliar VOCs from plants in an AI-RIL population generated from crossing Arizona and Utah (34), after leaves were treated by W+R. Variation of terpenoid emissions among the 261 RILs was large and extended beyond the differences between the parental accessions (Fig. 1*B* and *SI Appendix*, Fig. S1*B*). For example, the range of (*E*)-α-bergamotene and linalool emission was 522- and 115-fold in the AI-RILs, compared with a 38- and 3.5-fold difference in the parents, respectively. Across the 261 RILs, the relative amount of (*E*)-α-bergamotene in the leaf headspace was correlated with the relative amount of (*E*)-β-ocimene, but not linalool (Fig. 1*B*).

Among Variable Leaf VOCs, Linalool Is Correlated with Predation Rates of *M. sexta* by Native Predators in the Field. We selected 6 RILs with large differences in terpenoid composition for a field predation assay. These RILs represented extremes in the emission of 6 terpenoids, including (*E*)-β-ocimene, α-farnesene, linalool, (*E*)-α-bergamotene, and 2 unknown sesquiterpenes with retention times of 22.8 and 23.8 min (*SI Appendix*, Fig. S1). The randomly distributed RILs and both parental lines were tested for predation rates of experimentally distributed *M. sexta* eggs and larvae. This experiment was conducted in a field plot at the Walnut Creek Center for Education and Research (WCCER) (Fig. 1*C*) near Prescott, Arizona. During the experimental period, we observed *Geocoris* spp. predators on several plants in the field and most of the predation occurred during the daytime, when *Geocoris* spp. are active (35). In total, predation rates on *M. sexta* eggs and larvae during the whole assay ranged from 3 to 19% (Fig. 1*C*). The predation rates on different genotypes were positively correlated with the relative abundance of linalool, but not of the 5 other terpenoids, which varied in the headspace of these lines (Fig. 1*D*).

Natural Variation of Linalool Is Driven by Allelic Variation in an Identified Linalool Synthase, *NaLIS*. We used QTL mapping and genome mining to determine the genetic components underlying

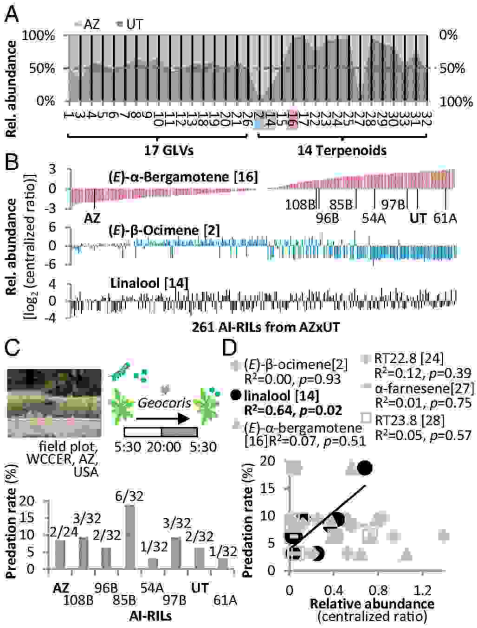

Fig. 1. *N. attenuata* accessions from Utah and Arizona differ in terpenoid emissions and among these, linalool is correlated with predation rates on *M. sexta*. (*A*) Relative abundance of VOCs in headspace of AZ and UT leaves. For each peak, the sum of the mean peak areas in AZ and UT, shown in *SI Appendix*, Table S1, is set to 100% (see *SI Appendix*, Table S1 for compound IDs). Boxed IDs indicate the compounds shown in *B*. (*B*) The distribution of relative abundances of (*E*)-α-bergamotene (34), (*E*)-β-ocimene, and linalool within the AI-RIL population. Numbers in brackets indicate the compound IDs (*SI Appendix*, Table S1). (*C*) Selected lines with large differences in terpenoid composition (*SI Appendix*, Fig. S1*B*) received different predation rates on *M. sexta* larvae and eggs in a field plot in Arizona. Numbers of predated larvae and eggs and numbers of total larvae and eggs placed on the plants are shown on top of the bars. The 2 parental lines are indicated by bold text. The assay lasted 72 h. Larvae and eggs were placed onto leaves at around 0500 hours and predated eggs and larvae were counted and supplemented at around 2000 hours. The following morning they were counted again and all larvae and eggs were replaced. Counting was repeated at dusk and the next morning. *Geocoris* spp. appeared in the field during the assay. Field plot image courtesy of R. Carlson (photographer). (*D*) Among 6 variable terpenoids, only linalool is correlated with predation rate across the assayed lines. Numbers in brackets indicate the compound IDs (*SI Appendix*, Table S1).

the variation of foliar VOCs in *N. attenuata* accessions. The published QTL for (*E*)-α-bergamotene was successfully reidentified in our dataset, with a higher LOD value than originally published (*SI Appendix*, Fig. S2) (34). In total, 8 terpenoids were mapped to the same locus or nearby loci (*SI Appendix*, Fig. S2). In contrast, a dominant single locus for linalool was mapped to a different linkage group (Fig. 2*A*). Because only the genome of UT has been well sequenced (36), we first analyzed the linalool locus in the UT genome. The corresponding region was located on the short arm of chromosome VIII, with a length of around 316 kb. In the parallel region of the *S. lycopersicum* genome, there are 4 putative *TPS* genes (*SI Appendix*, Fig. S3). However, NIATv7_g00838 is the only *TPS* at this region in the *N. attenuata* genome and no other genes share collinearity with the *SlTPS*s. We further mined data for the whole *NaTPS* family in *N. attenuata* (sequences in Dataset S1, and see refs. 37, 38). Aligning the sequences of all putative *TPS* genes, we found that the putative CDS of NIATv7_g00838 (later confirmed by sequencing) could be classified as a single member of the subclade *TPS*-g (*SI Appendix*, Fig. S4), possibly encoding a linalool/nerolidol synthase. NIATv7_g00838 was later renamed *NaLIS*.

Using the *Nicotiana attenuata* Data Hub (http://nadh.ice.mpg.de/NaDH/) (39), we found that the transcript abundance of *NaLIS* was relatively high in leaves, and present at lower levels in some floral organs, such as anthers and the stigma, ovary, and pedicel, but not detectable in the corolla or calyx. This is in agreement with the fact that linalool is abundant as a foliar VOC in some accessions, but not detected in floral VOCs of *N. attenuata* (*SI Appendix*, Fig. S5*A*). Using qPCR, we found the transcript abundance of *NaLIS* was strongly correlated with the amount of internal extractable linalool in leaves of transgenic plants in the UT background [ir*MPK4* (40), which emits greater amounts of most VOCs (*SI Appendix*, Table S2) and empty vector (EV) controls] for plants under different treatments, including light deprivation or abscisic acid treatment (Fig. 2*C* and *SI Appendix*, Fig. S5). Additionally, we identified 2 genes putatively encoding geranyl diphosphate (GPP) synthase (responsible for biosynthesis of the monoterpenoid substrate GPP), one of which was also highly correlated with the abundance of internal linalool (*SI Appendix*, Fig. S5), indicating coregulation of *NaLIS* and *NaGPPS2*.

NaLIS displays allelic variation between AZ and UT, both in the genomic DNA and cDNA. Alignment of the genome region bearing *NaLIS* in AZ and UT (sequences in Dataset S1) showed that a 766-bp sequence is present in AZ but missing in UT (Fig. 2*D*). Comparing putative transcripts of *NaLIS*-AZ and *NaLIS*-UT to reported homologous genes in relatives such as *S. lycopersicum*, *Solanum tuberosum*, and *Nicotiana tomentosiformis* revealed that *NaLIS*-AZ has a similar *TPS* exon–intron structure to these relatives, while *NaLIS*-UT does not. *NaLIS*-AZ has 6 exons and 5 introns. The missing sequence of *NaLIS*-UT is part of intron 5 and exon 6. Leaf transcriptome data (http://nadh.ice.mpg.de/NaDH/) from the 2 accessions revealed that the remnant sequence of intron 5 and exon 6 of *NaLIS*-UT was still transcribed, but the right border of exon 5 (left border of intron 5) was not spliced. Therefore, the *NaLIS*-UT transcript was 168-bp longer than *NaLIS*-AZ. However, we identified an in-frame TAG stop codon transcribed from intron 5 in the *NaLIS*-UT transcript. This resulted in the ORF of *NaLIS*-UT not only lacking exon 6 (278 bp) of *NaLIS*-AZ, but also including a 110-bp sequence from intron 5, and thus the full-length CDS is 168-bp shorter than that of *NaLIS*-AZ. Based on the different genome and transcriptome information, we designed primers and amplified the full-length ORFs of both *NaLIS*-AZ and *NaLIS*-UT from cDNA prepared from leaves of AZ and UT, respectively (Fig. 2*E*). Sequencing of the amplicons confirmed the expected sequence variation in the *NaLIS* alleles from AZ and UT.

We tested the activities of the 2 *NaLIS* variants in vitro (Fig. 2*F*). The putative plastid-targeting signal peptide was truncated and the remaining sequence from each allele was heterologously expressed in *Escherichia coli*. The extracted enzymes showed different activities depending on the terpenoid precursor supplied. When GPP was used as substrate, NaLIS-AZ produced approximately 10-fold as much linalool as NaLIS-UT under identical assay conditions (Fig. 2*F*). NaLIS-AZ also produced nerolidol from (*E*,*E*)-farnesyl diphosphate (FPP) and geranyllinalool from (*E*,*E*,*E*)-geranylgeranyl diphosphate (GGPP), whereas NaLIS-UT did not produce detectable terpenoids from these 2 precursors (*SI Appendix*, Fig. S6). The full-length protein of NaLIS-AZ showed similar activity as the truncated protein when expressed in *E. coli*, but with lower efficiency, while the full-length protein of NaLIS-UT did not convert any of the substrates in the in vitro assay.

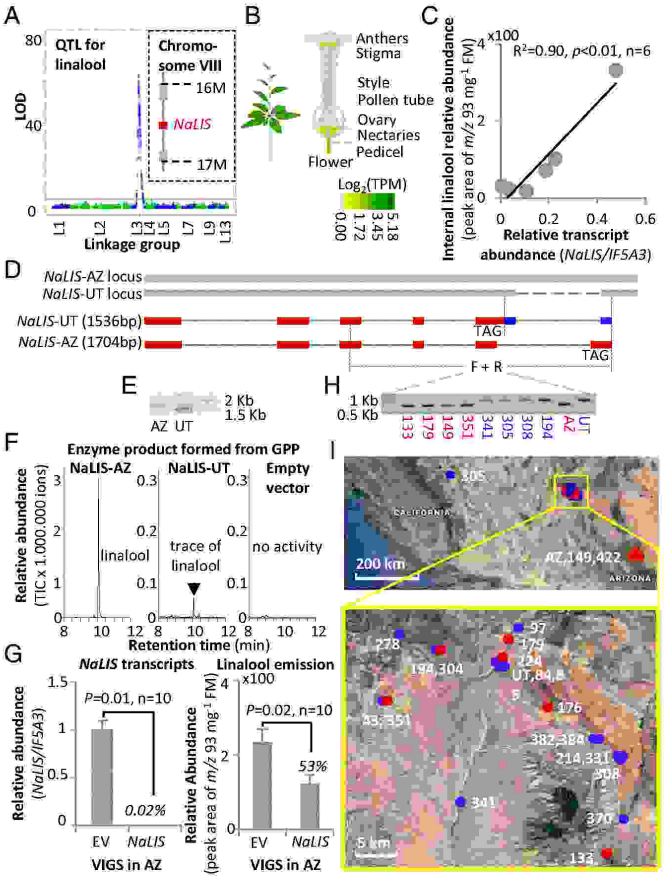

Fig. 2. *NaLIS* underlies variation in linalool emission among *N. attenuata* accessions. (*A*) A single QTL was mapped for linalool using the AI-RIL population and a single TPS was found within the mapped locus. The putative *TPS* gene is shown as a red bar, other proximate genes in gray. (*B*) *NaLIS* in the UT accession is constitutively expressed in leaves, and in some floral tissues (no data are available for stem and root tissue). The relative transcript abundance of *NaLIS* among different tissues was extracted from the *N. attenuata* Data Hub (http://nadh.ice.mpg.de/NaDH/) (39). TPM, transcripts per million. (*C*) In transgenic plants of the UT background (ir*MPK4*, which emits greater amounts of most VOCs, and EV controls), abundance of internal free linalool extracted from leaves is highly correlated with relative transcript abundance of *NaLIS* under different treatments shown in *SI Appendix*, Fig. S5 (mean + SE, $n = 3$). *IF5A3* was used as reference gene. (*D*) Alignment of the *NaLIS* genome region and different transcripts in AZ and UT shows splicing variation between the 2 accessions at the last exon of the gene. Gray bars represent sequences of the *NaLIS* genome locus. The dashed line represents a sequence of 766 bp missing in the UT genome compared with AZ. Red bars indicate exons of *NaLIS* in UT and AZ. Blue bars indicate transcribed sequence after the stop codon (TAG) in UT. *NaLIS*-UT has a longer transcript that includes a 110-bp sequence on the fifth exon, which is present in the intron region of the AZ variant (and also homologous genes in other relative species including tomato, potato, and *N. tomentosiformis*). A stop codon at the end of this 110-bp sequence makes the ORF of *NaLIS*-UT smaller than that of *NaLIS*-AZ. The sequence information on the transcripts of *NaLIS*-UT and *NaLIS*-AZ was extracted from the *N. attenuata* Data Hub (http://nadh.ice.mpg.de/NaDH/) (39) and later confirmed by cloning and sequencing. (*E*) ORFs of *NaLIS*-AZ and *NaLIS*-UT amplified from cDNA of the 2 accessions. (*F*) Heterologously expressed *NaLIS* ORFs produce linalool from GPP. NaLIS-AZ has much higher activity than NaLIS-UT in paralleled assays (note difference in scales of *y* axes). NaLIS-AZ can also accept (*E*,*E*)-FPP and (*E*,*E*,*E*)-GGPP to produce nerolidol and geranyllinalool, respectively, as shown in *SI Appendix*, Fig. S6. (*G*) VIGS of *NaLIS* in AZ caused reduced emission of linalool from leaves (mean + SE, $n = 10$). AZ was used here because it has higher emission of linalool as shown in Fig. 1*A* and a more active NaLIS. Relative abundance of transcript: *NaLIS*/*IF5A3*, relative abundance of linalool: peak area of *m*/*z* 93 mg^{-1} FM. (*H*) Amplified different 3′ ends of *NaLIS* in 10 natural accessions. The *NaLIS*-UT variant is correlated with nondetectable or extremely low linalool emissions (peak area of *m*/*z* 93 mg^{-1} FM < 30 counts/s in measurements, accession ID in blue) and the *NaLIS*-AZ variant is correlated with high linalool emission (peak area of *m*/*z* 93 mg^{-1} FM > 300 counts/s in measurements, accession in red). For relative abundance of linalool sampled in the headspace of these accessions, see *SI Appendix*, Fig. S7. (*I*) Geographic distribution of 26 natural accessions (including the 10 shown in *H*) and their linalool emission. Dots in blue indicate where the low linalool accessions were collected, and dots in red indicate where the high linalool accessions were collected from *N. attenuata*'s native range. For relative abundance of the linalool emission, *NaLIS* alleles and transcript accumulation in these accessions see *SI Appendix*, Fig. S7. Satellite images courtesy of Google Earth.

Subsequently, the activity of *NaLIS* was studied in vivo. We inserted a 205-bp gene-specific sequence of *NaLIS*-AZ into the pTV00 vector in an antisense orientation, and used the resulting construct for virus-induced gene silencing (VIGS) in AZ plants. VIGs nearly eliminated transcripts of *NaLIS* and significantly decreased the emission of linalool from W+R-treated leaves compared with control plants, which were infiltrated with an EV control (Fig. 2*G*); residual linalool emission may be due to existing levels of NaLIS protein before VIGS took effect, but see the discussion of linalool conjugates in *Discussion*.

Linalool is also highly variable among 24 other natural accessions of *N. attenuata* collected from different parts of *N. attenuata*'s native range, in addition to Arizona and Utah (*SI Appendix*, Fig. S7*A*). We classified 16 of these 26 accessions as low-linalool emitters (peak area of *m/z* 93 mg^{-1} FM < 30 counts/s) and 9 accessions as high-linalool emitters (peak area of *m/z* 93 mg^{-1} FM > 300 counts/s) based on linalool emission from W+R-treated leaves. Between the highest of the low emitters, accession 331, and the lowest of the high emitters, accession 179, there is a 19-fold difference, indicating a qualitative difference separating the low- and high-emitter groups. In contrast, the highest linalool emitter, accession 133, only emitted approximately 11-fold as much linalool as accession 179. We selected 4 accessions from each category and analyzed the length of *NaLIS* transcripts at the 3′ end. The 4 low-emitting accessions produce the UT variant of *NaLIS*, while the 4 high-emitting accessions produce the AZ variant of the *NaLIS* transcript (Fig. 2*H*).

We mapped the reads to chromosome VIII carrying *NaLIS* and manually assembled the genomic sequence of *NaLIS* for the 26 accessions (sequences in Dataset S1, and see refs. 37, 38). All of the high linalool emitters had the functional *NaLIS*-AZ allele, while all low linalool emitters had the deletion on intron 5 and exon 6 of the gene (*SI Appendix*, Fig. S7*B*). In contrast to the tight correlation with the allelic variation, the linalool emission did not correlate with *NaLIS* transcript abundance assayed by RNA-seq across the 26 accessions (*SI Appendix*, Fig. S7*C*).

The analyzed accessions were collected from different locations in the natural range of *N. attenuata* (Fig. 2*I*). The greatest distance between collection sites was 696 km between California (low-linalool emitter 305) and Arizona (high-linalool emitters AZ, 149 and 422). The remaining accessions, including 4 low-linalool emitters and 3 high-linalool emitters, were from a region covering approximately 448 km^2 near the border between Utah and Nevada. These accessions are all less than 33.5 km from each other, where high- and low-linalool emitters were interspersed (Fig. 2*I*).

Expressing Foreign *LIS* Genes in *N. attenuata* Plants Alters Emission of the Endogenous Enantiomer (*S*)-(+)-Linalool or the Foreign Enantiomer (*R*)-(−)-Linalool. There are 2 natural enantiomers of linalool, and both occur in plants and are reported to be perceived differently and elicit different behavioral responses in *M. sexta* (23, 41, 42). We analyzed W+R-induced foliar VOC samples from Arizona, Utah, and 50 RILs, along with racemic linalool, a pure (*R*)-(−)-linalool standard and enzyme products of NaLIS-AZ from (*E,E*)-FPP using a chiral GC column. Only (*S*)-(+)-linalool was detected in the NaLIS-AZ products and in all of the tested *N. attenuata* genotypes (Fig. 3*A*).

We altered the enantiomer-specific linalool production in *N. attenuata* plants via ectopic expression of 2 foreign *LIS* genes, *CbLIS*, from *Clarkia breweri* for (*S*)-(+)-linalool and *ObLIS* from *Ocimum basilicum* for (*R*)-(−)-linalool (42, 44). Each *LIS* under control of the CaMV35 promoter was separately introduced into AZ and UT plants, respectively, resulting in 4 different types of ectopic expression lines (Fig. 3*B*). AZ-(*S*) and UT-(*S*) lines are AZ or UT plants expressing *CbLIS*, which enhances emission of (*S*)-(+)-linalool, while AZ-(*R*) and UT-(*R*) lines express *ObLIS* in the AZ or UT background and emit (*R*)-(−)-linalool, which is absent in *N. attenuata* WT accessions. We subsequently screened transgenic lines for diploidy and homozygosity of transgene insertions, and used T2 plants of each line. We then measured linalool emission from unelicited plants, because we aimed to select plants for *M. sexta* oviposition assays (see below), and many W+R-induced VOCs have been shown to reduce *M. sexta* oviposition (12); moths lay only one or a few eggs per *N. attenuata* plant (12, 45) and seem to avoid plants already damaged by conspecifics.

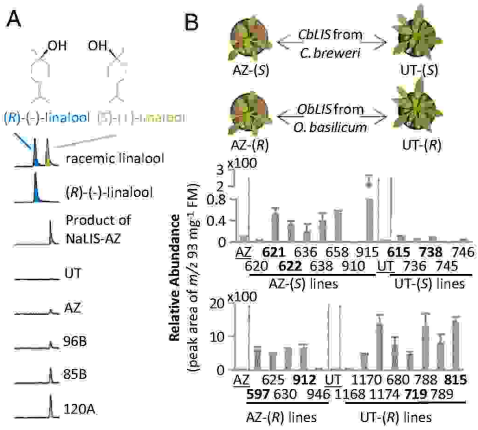

Fig. 3. Enantiomer identification of linalool produced in *N. attenuata* and linalool emission from transgenic plants with ectopic overexpression of different linalool enantiomer synthase genes. (*A*) Chromatogram for racemic linalool, standard (*R*)-(−)-linalool, major enzyme product of NaLIS-AZ from (*E,E*)-FPP, and linalool produced by UT, AZ, and 3 of 50 tested RILs. No (*R*)-(−)-linalool was found in any tested WT lines. (*B*) Profile of linalool in AZ and UT WT plants and in different ectopic expression lines expressing either *CbLIS* from *C. breweri* (produces (*S*)-(+)-linalool) or *ObLIS* from *O. basilicum* (produces (*R*)-(−)-linalool) in either the AZ or UT background (mean + SE, $n = 3$). Numbers in bold indicate the lines selected for further study. Shown here are the sum of 2 enantiomers measured using a standard nonpolar GC column. Different enantiomers were identified later in representative lines using a chiral column. In UT-(*S*) and AZ-(*S*) lines only (*S*)-(+)-linalool was found. In UT-(*R*) lines only (*R*)-(−)-linalool was found. Both enantiomers were detected in AZ-(*R*) lines; the ratios of the 2 enantiomers in the selected lines are shown at the top of the bars. Data from WT plants are from an independent experiment and are shown for comparison. Notice the different scales in every chart. Photo of *C. breweri* is from Wikipedia, by Eric in SF; *O. basilicum* picture: J.H.; *N. attenuata* images courtesy of A. Kügler (photographer).

We found that the ectopic lines as well as the corresponding WT genotypes emitted linalool constitutively (Fig. 3). The (*S*)-linalool emission from ectopic lines was within the range of natural variation among accessions of *N. attenuata* (*SI Appendix*, Fig. S9 and Dataset S2). Of 8 AZ-(*S*) lines, 6 emitted significantly more linalool than AZ WT plants, with increases ranging from 1.9- to 21.3-fold. Of 5 UT-(*S*) lines, 3 emitted 2.4- to 7.3-fold higher linalool levels than UT WT plants. Five AZ-(*R*) lines emitted 3.7- to 64.4-fold as much total linalool as AZ WT, while linalool emissions from 8 UT-(*R*) lines were 18.9- to 1,149.3-fold higher than the UT WT emission. While AZ-(*S*) lines produced on average 18-fold higher linalool emissions than the corresponding UT-(*S*) lines, the release of linalool was on average 1.8-fold higher in UT-(*R*) compared with AZ-(*R*) lines. Besides the differences in linalool emissions, other terpenoid VOCs measured from these ectopic expression lines were similar to the corresponding WT plants (*SI Appendix*, Fig. S8 and Dataset S3; lines used for further experiments are highlighted in *SI Appendix*). None of the transgenic lines except AZ-915(*S*) showed any

morphological or developmental differences from germination to the flowering stage, and line AZ-915(*S*) was not used in further experiments.

Enantiomer-specific linalool production was verified in representative ectopic expression lines using a chiral GC column. Only (*S*)-(+)-linalool was found in UT-(*S*) and AZ-(*S*) lines and only (*R*)-(−)-linalool was found in UT-(*R*). Both enantiomers were detected in AZ-(*R*) lines, with (*S*)-(+)-linalool only 0.3% as abundant as the (*R*)-(−)-linalool isomer (Fig. 3*B*).

Based on linalool emission, we selected 2 lines of each background–foreign gene combination (Fig. 3*B*) for further study. Among the 8 selected lines, UT-738(*S*) and UT-719(*R*) were confirmed to have a single insertion of T-DNA using Southern blotting by hybridizing an hptII probe to genomic DNA digested with XbaI or EcoRI (*SI Appendix*, Fig. S10*A*). For the remaining 6 selected lines, a single and complete T-DNA insertion was demonstrated using NanoString's nCounter technology. Multiple probes (sequences in Dataset S1) with different fluorescent barcodes were hybridized to sheared genomic DNA of each line to be tested, and scanned and counted in an nCounter Sprint instrument. Hybridization of 5 probes designed from transgene promotor (P_{NOS}, P_{35S}) and terminator (T_{NOS}, T_{35S}), as well as the selective marker gene (*hptII*) sequences indicated a single and complete insertion of the transformation cassette in all 6 lines (*SI Appendix*, Fig. S10*B*). Moreover, 2 probes designed from the transformation vector backbone outside the right and left transfer borders (nptII, pVS1) showed that only 3 lines harbor T-DNA overreads, which did not affect the transgenic phenotype or stability of inheritance. Very little background signal was observed for the 2 hybridization probes (nptIII, sat-1) designed from sequences not present on the pSOL9*CbLIS*/*ObLIS* plasmids (*SI Appendix*, Fig. S10*B*). Transgenic lines screened in this study are listed in *SI Appendix*, Table S2.

Linalool emissions from natural accessions of *N. attenuata* show a diurnal rhythm, with higher emissions during daytime and low emissions at nighttime (9). In the UT accession used in our experiments, linalool was emitted in greater abundance from W+R-treated leaves during the day, and this was light-dependent (*SI Appendix*, Fig. S11*A*). In the transgenic plants, both enantiomers followed a similar rhythm with greater emissions during day than night (*SI Appendix*, Fig. S11*B*). However, there were still considerable amounts of linalool of both enantiomers detected in the headspace during the dusk and night periods when *M. sexta* moths are active. This allowed us to compare behavioral responses to the specific linalool enantiomers, which are perceived differently by *M. sexta* adults (23, 41, 42).

Enhancement of Linalool Enantiomers in *N. attenuata* Leaves Alters Oviposition Preferences of *M. sexta* in an Accession-Specific Manner. We tested the oviposition preference of mated female *M. sexta* moths for AZ and UT WT plants versus transgenic plants with altered linalool emissions. Thus, AZ and UT WT plants and 4 ectopic expression lines—AZ-621(*S*), AZ-597(*R*), UT-738(*S*), and UT-1174(*R*)—were used to assay oviposition by *M. sexta* moths. Assays were conducted in 3 increasingly complex and realistic environments (Fig. 4). Because these ectopic expression plants constitutively emit linalool, and many *M. sexta*-elicited VOCs have been shown to deter *M. sexta* moth oviposition (12), we used unelicited plants for these assays.

First, binary choice assays were performed in a wind tunnel, where the input air was filtered through activated charcoal to remove background odors and wind speed and directions were strictly regulated. For each trial, a single mated female moth was released downwind of the plant pair in the tunnel during a standardized time window in which moths are known to actively oviposit, and allowed to choose between paired plants of AZ WT and UT WT, or an ectopic expression line and the corresponding WT. The moth was observed for the first 10 touches (any part of the moth body contacting the plant) and then removed; the order

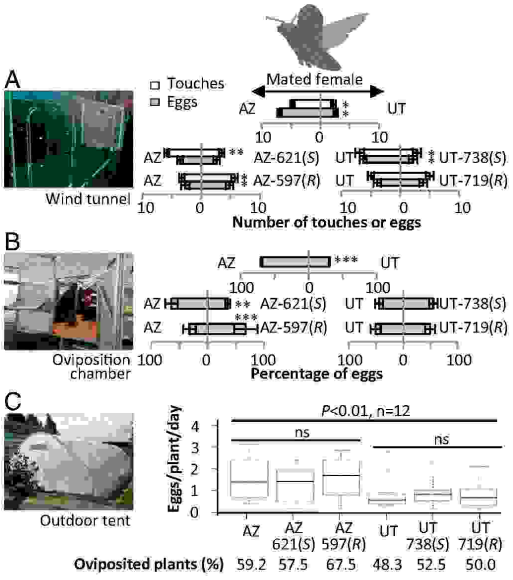

Fig. 4. Ectopic expression of (*S*)-(+)-linalool and (*R*)-(−)-linalool in UT and AZ accessions differently affect oviposition preference of mated female *M. sexta* moths. (*A*) First 10 touches of moths and the corresponding eggs laid on plants in binary choice assays in a wind tunnel (mean + SE, sign tests; $*P < 0.05$; $**P < 0.01$, $***P < 0.001$, $n = 20$). Wind tunnel picture: R.A.F. (*B*) Percentage of eggs laid on plants overnight in a climate chamber. Asterisks (*) indicate statistically significant differences (mean + SE, sign tests; $*P < 0.05$; $**P < 0.01$, $n = 20$). Oviposition chamber picture: J.H. (*C*) Eggs oviposited per plant per night by 1 single mated female moth in the tent. (Friedman tests for overall difference, Tukey–Kramer multiple comparison tests for comparisons of interest, $P < 0.05$, $n = 12$). Percentages of plants of each type receiving at least 1 egg (summed across all assays) are shown below the plot. Tent image courtesy of D. Kessler (photographer).

and number of visitations and the corresponding number of eggs laid on each plant were recorded (Fig. 4*A*). AZ WT plants, which have higher (*S*)-(+)-linalool emission, were touched more often and received more eggs than UT WT plants. However, compared with AZ WT plants, the (*S*)-(+)-linalool-enhanced AZ-621(*S*) were touched significantly fewer times, and tended to receive fewer eggs ($P = 0.18$). Similarly, UT-738(*S*) plants were touched fewer times and received fewer eggs than UT WT. In contrast, (*R*)-(−)-linalool–emitting AZ-597(*R*) plants were visited more often than AZ WT plants and received more eggs, while UT-1174(*R*) was visited and received a similar number of eggs as the UT WT. In all assays, the numbers of touches on each plant were correlated to the number of eggs oviposited.

We subsequently tested the same binary combinations of lines in a free-flying climate chamber where a colony of moths could oviposit overnight on plants of paired genotypes (Fig. 4*B*). In the chamber, air was not filtered and airflow was not controlled. Similar to the results from wind-tunnel assays, more eggs were oviposited on AZ WT than on UT WT in this more complex environment. AZ-621(*S*) received fewer, and AZ-597(*R*) received more eggs than AZ WT, respectively. However, neither UT-738(*S*) nor UT-1174(*R*) received significantly different numbers of eggs compared with UT WT plants.

Finally, all 4 ectopic expression lines and both WTs were tested simultaneously in a large outdoor tent, which represented a semi-

natural environment (Fig. 4*C*). In the tent, 10 plants of each genotype (60 plants in total) were placed at random positions at standardized distances (1.5 m from each other). A single newly mated moth was released into the tent and kept overnight for oviposition. Of a total of 16 moths tested, 12 oviposited at least 20 viable eggs in the trials. In this environment, ovipositing moths generally preferred WT and transgenic plants of the AZ background (Friedman tests, $P < 0.01$, $n = 12$). AZ-621(*S*) tended to receive fewer eggs than AZ WT and AZ-597(*R*). However, no significant difference was found between any ectopic expression line and the corresponding WT plants (Tukey–Kramer multiple comparisons tests). We also noticed that for each genotype, more than 48% of the plants received at least 1 egg, indicating high oviposition activity by the moths. Among all 6 genotypes, AZ-597(*R*) had the highest proportion of plants receiving eggs (Fig. 4*C*).

Linalool-Derived Glycosides Covary with Emitted Linalool and Do Not Affect Growth of *M. sexta* Larvae. A large proportion of linalool produced in plants is converted to different derivatives or conjugated and stored in tissues rather than emitted to the headspace, and these conjugates have different functions in plant interactions (24, 46, 47). The most abundant linalool conjugates found in plant tissues are linalool glucosides, from which linalool can be released by glucosidase treatment (48). Similar to the headspace linalool emission, the linalool glycoside levels also varied in W+R-treated leaves of natural *N. attenuata* accessions (*SI Appendix*, Fig. S12*A*). Furthermore, the amount of glucosidase-released linalool from W+R-induced leaves was strongly correlated with the linalool emission from W+R-elicited leaves in these accessions (*SI Appendix*, Fig. S12*B*). In contrast to the foliar headspace containing only (*S*)-(+)-linalool, the glucosidase treatment released more 8-hydroxylinalool (*SI Appendix*, Fig. S12*C*) in addition to linalool. We identified additional linalool derivatives by comparison of leaf extracts from unelicited leaves of AZ WT, AZ-621(*S*), and AZ-912(*R*) using UPLC-HR-MS/MS. Several metabolites were increased in the ectopic expression lines compared with WT plants. The strongest difference was observed in a putative hydroxylinalool hexose conjugate ($C_{16}H_{28}O_7$) (*SI Appendix*, Fig. S11*D*). The accumulation of this compound showed a similar pattern as the emitted linalool in the 3 genotypes. Furthermore, this compound was also detected in the frass of *M. sexta* larvae when fed on these plants. The concentration of this compound in larval frass was correlated with its abundance in the leaf tissue of the food plant.

In no-choice bioassays, we therefore tested whether ectopic expression of linalool enantiomers influenced the growth of *M. sexta* larvae. Freshly hatched *M. sexta* larvae were allowed to feed on hydrated, cut leaves from AZ WT, AZ-621(*S*), and AZ-912(*R*) plants. After 7 d of feeding larval mass did not significantly differ between larvae grown on WT control plants and plants with altered (*S*)-(+)- or (*R*)-(−)-linalool accumulation.

Discussion

The 2 *N. attenuata* accessions from Arizona and Utah vary in multiple physiological traits and differ in many biological functions (32–34). In this study we compared the foliar headspace of the 2 accessions, and found the most variable VOCs to be terpenoids (Fig. 1 *A* and *B*). Among the variable terpenoids, linalool was the only compound correlated with rates of herbivore mortality due to native predators in a field plot in Arizona (Fig. 1*C*). By profiling the foliar headspace of an AZ × UT AI-RIL population and conducting QTL analysis (34), we identified and characterized the *NaLIS* gene, which is responsible for the biosynthesis of linalool in *N. attenuata* plants (Fig. 2 *A*–*G*). Allelic variation in this gene corresponded to variation in linalool emission across 26 *N. attenuata* accessions from geographically interspersed locations (Fig. 2 *H* and *I*). We identified the linalool enantiomer produced in *N. attenuata* to be (*S*)-(+)-linalool and tested its function by either enhancing the emission of this enantiomer or introducing the foreign (*R*)-(−)-linalool enantiomer, in both the AZ and UT backgrounds, by ectopically expressing 2 foreign enantiomer-specific *LIS* genes (Fig. 3). We found that supplementing linalool emission affected the oviposition choice of *M. sexta* female moths on *N. attenuata* plants in an enantiomer- and accession-specific manner (Fig. 4). Although the ectopic expression lines also accumulated greater amounts of nonvolatile linalool conjugates, the growth rate of *M. sexta* larvae was similar on leaves from the ectopic expression lines and WT plants. Our study demonstrates the importance of context in determining functions of linalool even within a single plant–insect interaction, and indicates specific aspects of context that may be important.

Linalool Varies Independently of Other Terpenoid VOCs in *N. attenuata*. Several terpenoid VOCs, including (*E*)-β-ocimene, (*E*)-α-bergamotene, and linalool varied strongly between the *N. attenuata* AZ and UT accessions (Fig. 1 *A* and *B*). Except for linalool, all other variable terpenoid VOCs were mapped to the same single QTL, which was previously identified for (*E*)-α-bergamotene using the AI-RIL population (*SI Appendix*, Fig. S2) (34). Thus, the results of our genetic analysis are consistent with the observation that *TPS*s are often clustered in plant genomes (8). In contrast, our mapping analysis identified a strong QTL for linalool emissions (Fig. 2*A*) on a linkage group different from the previously identified TPS cluster locus (Fig. 2*A* and *SI Appendix*, Fig. S3) (34). Therefore, the linalool synthase may be free to evolve and segregate independently of other terpenoid VOCs for which the genes are linked. The interspersed geographic distribution of the *N. attenuata* accessions with different levels of linalool emission provides evidence that selection for linalool is local and occurs on small scales, not clearly separated by geographic features (Fig. 2*I*).

Allelic variation of *NaLIS* is a determinant, but not the only factor, shaping the variation of linalool emission in *N. attenuata*. Between accessions, *NaLIS* alleles determined low or high linalool emission independently of transcript abundance (Fig. 2 *D*, *H*, and *I* and *SI Appendix*, Fig. S7), while in 23 of the 26 accessions examined in this study, the transcript levels of TPS38 strongly correlated with the emission of (*E*)-α-bergamotene in both flowers and herbivore-induced leaves (34). However, within the UT background, transcript abundance of *NaLIS* corresponded to tissue-specific differences in linalool emission (Fig. 2*B*), and for transgenic plants subjected to different treatments, linalool emission covaried with transcript abundance of *NaLIS* (*SI Appendix*, Fig. S5). Furthermore, reduction in transcript abundance using VIGS also reduced linalool emission in the AZ background (Fig. 2*G*). These data indicate that transcript abundance of *NaLIS* determines linalool emission within a genotype. Interestingly, even ectopic expression lines, which produce foreign LIS genes under the control of the constitutively active CamV 35S promoter, showed variation in headspace linalool abundance at different times of day (*SI Appendix*, Fig. S10), suggesting that substrate availability may be an additional important factor, as was previously indicated for (*E*)-α-bergamotene and (*E*)-β-farnesene emissions in *N. attenuata* (49). Consistent with this observation, a monoterpenoid substrate synthase gene, *NaGPPS2*, was found coregulated with *NaLIS* transcription and linalool emission (*SI Appendix*, Fig. S5*D*).

Although linalool is variable among *N. attenuata* accessions, NaLIS belongs to a clade of TPSs relatively conserved in enzymatic function. We identified NaLIS to be the single member of the TPS-g clade in the NaTPS family (*SI Appendix*, Fig. S4). In plants, the TPS-g clade is angiosperm-specific and well-known to produce acyclic monoterpenes (8, 50). TPS-g is usually a small clade compared with the highly divergent TPS-a and TPS-b clades. The single member of TPS-g in *Arabidopsis thaliana*, At1g61680, was found to contribute to floral (*S*)-(+)-linalool

emission and to produce nerolidol in vitro (51). Similarly, TPS-g members, which are (*S*)-(+)-linalool/nerolidol synthases, have been found in *Fragaria* × *ananassa* cv Elsanta (52), *O. sativa* (27), *S. lycopersicum* (53), and *Gossypium hirsitum* (54). However, TPS-g proteins in *Antirrhinum majus* were also found to produce (*E*)-β-ocimene and myrcene (50). In contrast to the presence of 2 functional linalool/nerolidol synthases and 2 mutants in the *S. lycopersicum* genome, NaLIS was the only ortholog identified in the *N. attenuata* genome (*SI Appendix*, Fig. S4). Moreover, more than half of the 26 *N. attenuata* accessions studied bore the less-efficient UT allele, in which exon 6 has been lost and a 110-bp redundant sequence has been fused to exon 5 (Fig. 2*D* and *SI Appendix*, Fig. S7*B*). This allele generally seems to have reduced enzymatic efficiency, and its activity toward FPP and GGPP seem to be abolished; but it can still convert GPP to linalool, suggesting that differences between the *N. attenuata* alleles may be involved in determining substrate specificity versus promiscuity of LIS enzymes.

Linalool Enantiomers Alter a Single Tritrophic Interaction in a Context-Dependent Manner. Linalool has been identified in more than 200 plant species. It is a common floral fragrance and has been long considered as a pollinator attractant (22, 23, 55). However, linalool emissions have also been reported to function in plant defense to repel florivores and other antagonistic flower visitors (24, 56, 57). Studies using linalool application, or genetic modification of linalool emission by ectopic expression or silencing of LIS genes, have shown that foliar linalool can mediate interactions between plants and herbivores. For example, racemic linalool has been reported to attract *Geocoris pallens* predators and deter *Manduca quinquemaculata* oviposition in a field study of a wild *N. attenuata* population (12); to repel *Myzus persicae* aphids from *A. thaliana* (46); to deter *Helicoverpa armigera* oviposition on *Nicotiana tabacum* (54, 58); and to influence choice of multiple herbivores, predators, and parasitoids on *O. sativa* (59). Thus, it is generally accepted that linalool mediates different outcomes depending on the interaction system. However, the way that context exerts influence is poorly understood, and different contexts are usually not directly compared, and assumed not to be relevant within the bounds of a single interaction.

In the present study, we selectively enhanced enantiomers of linalool in *N. attenuata* accessions with highly differentiated VOC backgrounds (Figs. 1*A* and 3). This enabled us to investigate the accession-specific effects of linalool enantiomers on *M. sexta* moth oviposition behaviors. Previous reports showed that supplementation of *Datura wrightii* flowers with (*S*)-(+)-linalool alone or in mixture with other floral VOCs increased oviposition rates by *M. sexta* moths, while addition of (*R*)-(−)-linalool reduced oviposition compared with control plants (23). In our study, AZ plants, which naturally produce (*S*)-(+)-linalool from leaves, received more oviposition from *M. sexta* moths, but enhancement of (*S*)-(+)-linalool by ectopic expression decreased oviposition (Fig. 4). Moreover, supplementation of (*S*)-(+)-linalool in the UT background by ectopic expression repelled *M. sexta* females in a wind-tunnel binary choice assay (Fig. 4*A*), but had no effect in the more complex environments of oviposition chambers shared by several moths (Fig. 4*B*), or an outdoor tent in which all genotypes were available for a single moth (Fig. 4*C*). The (*R*)-(−)-linalool enantiomer showed accession-specific effects on *M. sexta* preference: it increased oviposition in the AZ background, but had no effect in the UT background even though the UT ectopic expression lines emitted larger amounts of (*R*)-(−)-linalool (Figs. 3 and 4). These results indicate that moths use linalool as a context-specific cue, not only in the context of different plant species and tissues, but also depending on different characteristics, such as leaf VOC profile within a plant species. Moth decisions about oviposition are driven by a combinatorial olfactory code (60): that is, by taking into account not only the neuronal response to linalool but at the same time the activation of multiple olfactory receptors responding to other relevant GLVs and terpenoids. In addition to linalool, other terpenoids, such as (*E*)-α-bergamotene and (*E*)-β-ocimene, were also highly variable among the *N. attenuata* accessions (Fig. 1 *A* and *B*) and thus we could choose individuals representing the extremes of different VOCs (*SI Appendix*, Fig. S1*B*). Foliar (*E*)-α-bergamotene in *N. attenuata* reduces survivorship of *Manduca* spp. eggs (12), while floral (*E*)-α-bergamotene can attract *M. sexta* moths for pollination (34). The effects of other terpenoids in this system are less well understood. How linalool interacts with other VOCs and plant characteristics to influence the behavior of *M. sexta* moths requires further investigation. However, the context-dependent effects of linalool enantiomers on gravid female *M. sexta*, combined with the very local difference in linalool emission and, presumably, selective pressures, are consistent with the geographic mosaic theory of coevolution (61).

The different biological functions of linalool enantiomers in plant interactions are supported by the different perception of these 2 enantiomers by animals. Linalool enantiomers can be distinguished by the human nose and have different odor thresholds (62). They also evoke different neural responses in insects. However, context-defined functions of each linalool enantiomer are not well understood, but have been suggested by some studies on neural responses of *M. sexta* to linalool or linalool mixed with other compounds contained in *D. wrightii* floral VOCs (21), which showed that the neural ensemble evoked by the single compound did not resemble those evoked by mixtures. By testing the glomeruli activities in *M. sexta's* antennal lobe evoked by 80 odors separately, Bisch-Knaden et al. (42) showed that both (*S*)-(+)-linalool and (*R*)-(−)-linalool, as well as racemic linalool, evoked stronger and more broadly distributed activity in glomeruli compared with other terpenoid compounds. Furthermore, both enantiomers individually, and the racemic mixture, induced feeding behavior of *M. sexta* moths. In contrast, none of the 3 VOCs alone elicited oviposition behaviors, although both enantiomers strongly stimulated activities in multiple oviposition-related glomeruli (42).

Linalool has also been reported to mediate plant indirect defense by attracting predators and parasitoids of herbivores (59, 63, 64). In this study we showed that emission of linalool in different *N. attenuata* RILs is correlated with predation of eggs and larvae of *M. sexta* by natural enemies in a natural habitat (Fig. 1 *C* and *D*). It is possible that the avoidance of *M. sexta* females of linalool in certain *N. attenuata* accessions is, at least in part, the result of variable selection pressure from predators in nature.

Conjugation of Linalool in *N. attenuata*. Linalool is known to be metabolized to nonvolatile derivatives. For example, overexpression of *CbLIS* in petunia yielded nearly no emitted linalool but abundant accumulation of linalolyl-β-D-glucopyranoside (48), and *A. thaliana* expressing *FaNES1* produced more hydroxylated or glycosylated linalool derivatives than free linalool (46). Expressing *FaNES1* in *Chrysanthemum morifolium* produced, in addition to volatile linalool, 4 nonvolatile linalool glycosides, including 2 putative linalool-malonyl-hexoses, a linalool-pentose-hexose, and a glycoside of hydroxy-linalool (47). Two cytochrome P450s (CYP71B31 and CYP76C3) were coexpressed with 2 linalool synthases (TPS10 and TPS14) in flowers of *A. thaliana* and converted linalool enantiomers into hydroxylated or epoxidized products (17).

In our study, β-glucosidase treatment released approximately 200 times as much linalool from the *N. attenuata* leaf as was measured in the headspace of accessions (*SI Appendix*, Fig. S12*A*), and the natural conjugate pool of linalool was strongly correlated with headspace linalool (*SI Appendix*, Fig. S12*B*). The linalool conjugates may act as direct defenses against herbivory. Engineering linalool emission in chrysanthemum by expressing *FaNES* attracted *Frankliniella occidentalis*, but the increased abundance of linalool conjugates in tissues was repellent (47). When

the major linalool metabolizing oxygenase CYP76C3 was knocked out in *Arabidopsis*, the plant became more attractive to floral antagonists, including *F. occidentalis*, *Spodoptera littoralis*, *Plutella xylostella*, and *Phaedon cochleariae* (24). However, in our study, the growth of *M. sexta* larvae on leaf tissue was not affected by the ectopic expression of either the native or the foreign linalool enantiomer (*SI Appendix*, Fig. S12*F*). Furthermore, linalool conjugates are still abundant in the frass of *M. sexta* larvae and thus seem generally not to be metabolized after ingestion by larvae (*SI Appendix*, Fig. S12*E*). This indicates that the altered oviposition preferences of *M. sexta* moths are not due to an alteration of plants' nutritional quality: linalool seems to be more important as a signal in the interaction between *N. attenuata* and *M. sexta*. It is possible that under certain conditions, linalool could be released from the conjugate pool because in the VIGS experiment linalool emission was only reduced to half, while *NaLIS* transcripts were reduced by 99.8% (Fig. 2*G*). However, because VIGS is induced in rosette-stage plants, it is also possible that some amount of NaLIS protein was produced in the leaves we measured, before VIGS took effect. VIGs experiments were also conducted in climate chambers, where levels of background contamination may be higher than in a glasshouse or field.

Conclusion

Our data indicate that the ecological function of the ubiquitous biological VOC linalool depends both on the enantiomer and on details of the interaction context that can vary within species on a small scale. This is in contrast to previous studies, which have focused on context-dependence across different species and interactions. Our study reveals important factors for understanding the evolution and functions of VOC-mediated signaling in plant–insect interactions. For example, our data indicate that other specific VOCs may determine the response of *M. sexta* moths to the same enantiomer of linalool produced by different genotypes of the same plant species. The active VOCs might be revealed by series assays with different mixtures of linalool and various coemitted VOCs, or the expression or suppression of different GLVs and terpenoids, together with linalool enhancement/reduction in *N. attenuata* accessions, could be used to test linalool's context-dependent function.

Materials and Methods

The description of plant and animal materials, cultivation, plant treatment, headspace sampling, metabolite analyses, genetic, genomic, and transcriptional analyses, gene cloning and heterologous expression, moth oviposition, and larval growth assays, all based on published procedures, are detailed in *SI Appendix*. As the predation assay motivated our focus on linalool, and because this is a report of the nCounter method for transgene copy number and insertion integrity, those methods are presented here. All sequence data are provided in Dataset S1 or public databases, as described below. Source data are available at https://edmond.mpdl.mpg.de/imeji/collection/Kpsiw8PSKETsPdQV. Transgenic lines screened and used in this study are listed in *SI Appendix*, Table S2.

Predation Assay. The predation assay was performed in a field plantation at the WCCER, located in Arizona (34°55′17.8″N 112°50′42.2″W) in the summer of 2017. 3 RILs (generation F12) and 1 UT WT plant were grown in quadruplets at the corners of a 30 × 30-cm square. Quadruplets were separated by approximately 1 m. One set of plants of the entire AI-RIL population formed 1 block, and within each block, genotypes were randomly distributed; 4 blocks were planted ($n = 4$). Elongating plants were treated with wounding plus *M. sexta* regurgitant on 3 expanded rosette leaves 5 d before the predation assay and leaf discs were collected for unrelated analyses to be reported elsewhere. Six RILs with extreme differences in 6 terpenoid VOCs, UT-WT, and AZ-WT plants were used for the predation assay ($n = 4$). On the first morning of the assay, 1 *M. sexta* larva in the first instar was placed onto the adaxial side of the tip of the youngest rosette leaf and 3 *M. sexta* eggs were glued to the abaxial side of the same leaf. Larvae and eggs were counted as predated if they were completely empty and the remnant of the body or egg remained on the leaf. Predated larvae and eggs were counted at dusk, and missing (predated or lost from the plant for unclear reasons) larvae and eggs, and any which had dried out were replaced with new eggs and larvae. The second morning, predated larvae and eggs were counted a second time and all eggs and larvae were replaced. Counting was repeated at dusk and the following morning. The cumulative predation observed after 72 h is shown in Fig. 1C.

T-DNA Copy Number and Integrity Determination Using NanoString's nCounter Technology. T-DNA copy number and integrity were determined using either Southern blotting or NanoString's nCounter Technology. Genomic DNA from transgenic plant lines was isolated by a modified cetyl-trimethylammonium bromide method (63). For Southern blotting, the hptII_3 probe binding to the hygromycin phosphotransferase gene (66) was used after digestion of gDNA with either XbaI or EcoRI. For nCounter Technology, 5 μg of gDNA per sample was dissolved in water at a concentration of 30 ng/μL and sheared to fragment sizes mainly between 250 and 500 bp using a Covaris M220 Focused-ultrasonicator instrument according to the manufacturer's instructions. Sheared gDNA was precipitated, washed twice with 70% ethanol, and dissolved in water (12 μL). This DNA (1 μL) was used to confirm shearing on a 1% agarose gel.

For the nCounter analysis, a 12-code probe set (sequences in Dataset S1) was designed from of 12 target regions comprising 3 calibrator genes that occur as a single copy in the genome of *N. attenuata* and 9 functional regions indicative of complete T-DNA insertions or T-DNA overreads of the transformation vectors used for *N. attenuata* (*SI Appendix*, *Supplementary Information Text*). The oligonucleotides were designed by NanoString and synthesized by Integrated DNA technologies. The location of the target sequences on the binary plant transformation vectors is indicated in *SI Appendix*, Fig. S10*B*. Sheared gDNA (4 μL) was hybridized with the 12-code probe set and an XT-TagSet-12 according to NanoString's nCounter protocols and run together with a gDNA sample from a line known to have a complete single T-DNA insertion (previously confirmed by Southern blotting and nCounter) on a cartridge in an nCounter Sprint. The raw reads measured by the instrument were normalized as follows: the geometric mean of the 3 calibrator values for each of the 12 samples was calculated. The geometric mean of the 12 geometric means was calculated. The normalization factor for each sample was calculated by dividing the 12-sample geometric mean values by the geometric mean of each individual sample. For normalization, the value for each probe was multiplied with the normalization factor for the respective probe.

ACKNOWLEDGMENTS. This work was funded by the Max Planck Society and Advanced Grant 293926 of the European Research Council (to I.T.B.), and in part supported by the Collaborative Research Centre ChemBioSys (CRC 1127) funded by the Deutsche Forschungsgemeinschaft. We thank Prescott College, Northern Arizona University, the Arboretum at Flagstaff, Prescott National Forest, and the Southwest Experimental Garden Array for the use of a field plot at the Walnut Creek Center for Education and Research; the R. and N. Carlson and Southwest Experimental Garden Array staff for assistance with field plantations and the 2017 MPI-CE field team for assistance with sample collection for internal linalool measurements from field samples; Dr. B. S. Hansson for providing resources for moth breeding and wind tunnel assays; Dr. J. Gershenzon for providing resources for heterologous expression assays; Dr. E. Pichersky for providing plasmids with the *CbLIS* and *ObLIS* ORFs; A. Wissgott for plant transformation; Dr. D. Kessler for help with the tent experiments; Dr. Y. Oh and K. Pu for help with the GC-MS measurements; Dr. J. Li, Dr. H. Guo, Dr. Y. Zou, Dr. M. Wang, Dr. S. Li, and Dr. D. Li for daily discussion and critical comments in the laboratory; and Dr. S. Olsson and Dr. V. Pragadeesh for helpful discussions on linalool.

1. F. Loreto, M. Dicke, J. P. Schnitzler, T. C. J. Turlings, Plant volatiles and the environment. *Plant Cell Environ.* **37**, 1905–1908 (2014).
2. I. T. Baldwin, Plant volatiles. *Curr. Biol.* **20**, R392–R397 (2010).
3. A. Scala, S. Allmann, R. Mirabella, M. A. Haring, R. C. Schuurink, Green leaf volatiles: A plant's multifunctional weapon against herbivores and pathogens. *Int. J. Mol. Sci.* **14**, 17781–17811 (2013).
4. M. C. Schuman, N. Heinzel, E. Gaquerel, A. Svatos, I. T. Baldwin, Polymorphism in jasmonate signaling partially accounts for the variety of volatiles produced by *Nicotiana attenuata* plants in a native population. *New Phytol.* **183**, 1134–1148 (2009).
5. S. Allmann, I. T. Baldwin, Insects betray themselves in nature to predators by rapid isomerization of green leaf volatiles. *Science* **329**, 1075–1078 (2010).
6. K. Boonprab, K. Matsui, Y. Akakabe, N. Yotsukura, T. Kajiwara, Hydroperoxy-arachidonic acid mediated n-hexanal and (*Z*)-3- and (*E*)-2-nonenal formation in *Laminaria angustata*. *Phytochemistry* **63**, 669–678 (2003).
7. H. M. Chen *et al.*, A multifunctional lipoxygenase from *Pyropia haitanensis*-The cloned and functioned complex eukaryotic algae oxylipin pathway enzyme. *Algal Res.* **12**, 316–327 (2015).
8. F. Chen, D. Tholl, J. Bohlmann, E. Pichersky, The family of terpene synthases in plants: A mid-size family of genes for specialized metabolism that is highly diversified throughout the kingdom. *Plant J.* **66**, 212–229 (2011).
9. R. Halitschke, A. Keßler, J. Kahl, A. Lorenz, I. T. Baldwin, Ecophysiological comparison of direct and indirect defenses in *Nicotiana attenuata*. *Oecologia* **124**, 408–417 (2000).

10. T. Kuzuyama, H. Seto, Two distinct pathways for essential metabolic precursors for isoprenoid biosynthesis. *Proc. Jpn. Acad. Ser. B Phys. Biol. Sci.* **88**, 41–52 (2012).
11. J. K. Holopainen, J. Gershenzon, Multiple stress factors and the emission of plant VOCs. *Trends Plant Sci.* **15**, 176–184 (2010).
12. A. Kessler, I. T. Baldwin, Defensive function of herbivore-induced plant volatile emissions in nature. *Science* **291**, 2141–2144 (2001).
13. C. M. De Moraes, M. C. Mescher, J. H. Tumlinson, Caterpillar-induced nocturnal plant volatiles repel conspecific females. *Nature* **410**, 577–580 (2001).
14. R. A. Raguso More lessons from linalool: Insights gained from a ubiquitous floral volatile. *Curr. Opin. Plant Biol.* **32**, 31–36 (2016).
15. J. T. Knudsen, R. Eriksson, J. Gershenzon, B. Stahl, Diversity and distribution of floral scent. *Bot. Rev.* **72**, 1–120 (2006).
16. A. L. Parachnowitsch, R. C. Burdon, R. A. Raguso, A. Kessler, Natural selection on floral volatile production in *Penstemon digitalis*: Highlighting the role of linalool. *Plant Signal. Behav.* **8**, e22704 (2013).
17. J. F. Ginglinger *et al.*, Gene coexpression analysis reveals complex metabolism of the monoterpene alcohol linalool in Arabidopsis flowers. *Plant Cell* **25**, 4640–4657 (2013).
18. V. S. Pragadheesh, C. S. Chanotiya, S. Rastogi, A. K. Shasany, Scent from *Jasminum grandiflorum* flowers: Investigation of the change in linalool enantiomers at various developmental stages using chemical and molecular methods. *Phytochemistry* **140**, 83–94 (2017).
19. R. Kaiser, The scent of orchids. Olfactory and chemical investigations. *Flavour Fragrance J.* **8**, 295 (1993).
20. J. T. Knudsen, L. Tollsten, Trends in floral scent chemistry in pollination syndromes—Floral scent composition in moth-pollinated taxa. *Bot. J. Linn. Soc.* **113**, 263–284 (1993).
21. J. A. Riffell, H. Lei, J. G. Hildebrand, Neural correlates of behavior in the moth *Manduca sexta* in response to complex odors. *Proc. Natl. Acad. Sci. U.S.A.* **106**, 19219–19226 (2009).
22. R. A. Raguso, E. Pichersky, New perspectives in pollination biology: Floral fragrances. A day in the life of a linalool molecule: Chemical communication in a plant-pollinator system. Part 1: Linalool biosynthesis in flowering plants. *Plant Species Biol.* **14**, 95–120 (1999).
23. C. E. Reisenman, J. A. Riffell, E. A. Bernays, J. G. Hildebrand, Antagonistic effects of floral scent in an insect-plant interaction. *Proc. Biol. Sci.* **277**, 2371–2379 (2010).
24. B. Boachon *et al.*, CYP76C1 (Cytochrome P450)-mediated linalool metabolism and the formation of volatile and soluble linalool oxides in Arabidopsis flowers: A strategy for defense against floral antagonists. *Plant Cell* **27**, 2972–2990 (2015).
25. C. C. N. van Schie, M. A. Haring, R. C. Schuurink, Tomato linalool synthase is induced in trichomes by jasmonic acid. *Plant Mol. Biol.* **64**, 251–263 (2007).
26. J. S. Yuan *et al.*, Elucidation of the genomic basis of indirect plant defense against insects. *Plant Signal. Behav.* **3**, 720–721 (2008).
27. J. S. Yuan *et al.*, Molecular and genomic basis of volatile-mediated indirect defense against insects in rice. *Plant J.* **55**, 491–503 (2008).
28. Y. Du *et al.*, Identification of semiochemicals released during Aphid feeding that attract parasitoid *Aphidius ervi*. *J. Chem. Ecol.* **24**, 1355–1368 (1998).
29. A. A. Rudmann, J. R. Aldrich, Chirality determinations for a tertiary alcohol—Ratios of linalool enantiomers in insects and plants. *J. Chromatogr. A* **407**, 324–329 (1987).
30. A. Giglio *et al.*, The defensive secretion of *Carabus lefebvrei* Dejean 1826 pupa (Coleoptera, Carabidae): Gland ultrastructure and chemical identification. *Microsc. Res. Tech.* **72**, 351–361 (2009).
31. M. C. Lemfack *et al.*, mVOC 2.0: A database of microbial volatiles. *Nucleic Acids Res.* **46**, D1261–D1265 (2018).
32. J. Wu, C. Hettenhausen, M. C. Schuman, I. T. Baldwin, A comparison of two *Nicotiana attenuata* accessions reveals large differences in signaling induced by oral secretions of the specialist herbivore *Manduca sexta*. *Plant Physiol.* **146**, 927–939 (2008).
33. A. Steppuhn, M. C. Schuman, I. T. Baldwin, Silencing jasmonate signalling and jasmonate-mediated defences reveals different survival strategies between two *Nicotiana attenuata* accessions. *Mol. Ecol.* **17**, 3717–3732 (2008).
34. W. Zhou *et al.*, Tissue-specific emission of (*E*)-α-bergamotene helps resolve the dilemma when pollinators are also herbivores. *Curr. Biol.* **27**, 1336–1341 (2017).
35. M. C. Schuman, D. Kessler, I. T. Baldwin, Ecological observations of native *Geocoris pallens* and *G. punctipes* populations in the Great Basin Desert of Southwestern Utah. *Psyche (Camb., Mass.)* **2013**, 465108 (2013).
36. S. Xu *et al.*, Wild tobacco genomes reveal the evolution of nicotine biosynthesis. *Proc. Natl. Acad. Sci. U.S.A.* **114**, 6133–6138 (2017).
37. K. Gase, Nicotiana attenuata strain UT unplaced genomic scaffold, NIATTr2, whole genome shotgun sequence. *GenBank*. https://www.ncbi.nlm.nih.gov/nuccore/NW_017670477.1. Deposited 15 November 2016.
38. K. Gase, Nicotiana attenuata strain UT chromosome 11, NIATTr2, whole genome shotgun sequence. *Genbank*. https://www.ncbi.nlm.nih.gov/nuccore/NC_031999.1. Deposited 15 November 2016.
39. T. Brockmöller *et al.*, *Nicotiana attenuata* data hub (NaDH): An integrative platform for exploring genomic, transcriptomic and metabolomic data in wild tobacco. *BMC Genomics* **18**, 79 (2017).
40. C. Hettenhausen, I. T. Baldwin, J. Wu, Silencing *MPK4* in *Nicotiana attenuata* enhances photosynthesis and seed production but compromises abscisic acid-induced stomatal closure and guard cell-mediated resistance to *Pseudomonas syringae* pv tomato DC3000. *Plant Physiol.* **158**, 759–776 (2012).
41. C. E. Reisenman, T. A. Christensen, W. Francke, J. G. Hildebrand, Enantioselectivity of projection neurons innervating identified olfactory glomeruli. *J. Neurosci.* **24**, 2602–2611 (2004).
42. S. Bisch-Knaden, A. Dahake, S. Sachse, M. Knaden, B. S. Hansson, Spatial representation of feeding and oviposition odors in the brain of a hawkmoth. *Cell Rep.* **22**, 2482–2492 (2018).
43. N. Dudareva, L. Cseke, V. M. Blanc, E. Pichersky, Evolution of floral scent in *Clarkia*: Novel patterns of S-linalool synthase gene expression in the *C. breweri* flower. *Plant Cell* **8**, 1137–1148 (1996).
44. Y. Iijima *et al.*, The biochemical and molecular basis for the divergent patterns in the biosynthesis of terpenes and phenylpropenes in the peltate glands of three cultivars of basil. *Plant Physiol.* **136**, 3724–3736 (2004).
45. D. Kessler *et al.*, How scent and nectar influence floral antagonists and mutualists. *eLife* **4**, e07641 (2015).
46. A. Aharoni *et al.*, Terpenoid metabolism in wild-type and transgenic Arabidopsis plants. *Plant Cell* **15**, 2866–2884 (2003).
47. T. Yang, G. Stoopen, M. Thoen, G. Wiegers, M. A. Jongsma, *Chrysanthemum* expressing a linalool synthase gene 'smells good', but 'tastes bad' to Western flower thrips. *Plant Biotechnol. J.* **11**, 875–882 (2013).
48. J. Lücker, *et al.*, Expression of *Clarkia* S-linalool synthase in transgenic petunia plants results in the accumulation of S-linalyl-β-D-glucopyranoside. *Plant J.* **27**, 315–324 (2001).
49. M. C. Schuman, E. C. Palmer-Young, A. Schmidt, J. Gershenzon, I. T. Baldwin, Ectopic terpene synthase expression enhances sesquiterpene emission in *Nicotiana attenuata* without altering defense or development of transgenic plants or neighbors. *Plant Physiol.* **166**, 779–797 (2014).
50. N. Dudareva *et al.*, (*E*)-β-ocimene and myrcene synthase genes of floral scent biosynthesis in snapdragon: Function and expression of three terpene synthase genes of a new terpene synthase subfamily. *Plant Cell* **15**, 1227–1241 (2003).
51. F. Chen *et al.*, Biosynthesis and emission of terpenoid volatiles from Arabidopsis flowers. *Plant Cell* **15**, 481–494 (2003).
52. A. Aharoni *et al.*, Gain and loss of fruit flavor compounds produced by wild and cultivated strawberry species. *Plant Cell* **16**, 3110–3131 (2004).
53. V. Falara *et al.*, The tomato terpene synthase gene family. *Plant Physiol.* **157**, 770–789 (2011).
54. X. Z. Huang *et al.*, The terpene synthase gene family in *Gossypium hirsutum* harbors a linalool synthase GhTPS12 implicated in direct defence responses against herbivores. *Plant Cell Environ.* (2017).
55. A. K. BorgKarlson, C. R. Unelius, I. Valterova, L. A. Nilsson, Floral fragrance chemistry in the early flowering shrub *Daphne mezereum*. *Phytochemistry* **41**, 1477–1483 (1996).
56. R. R. Junker, J. Gershenzon, S. B. Unsicker, Floral odor bouquet loses its ant repellent properties after inhibition of terpene biosynthesis. *J. Chem. Ecol.* **37**, 1323–1331 (2011).
57. E. H. Koschier, W. J. De Kogel, J. H. Visser, Assessing the attractiveness of volatile plant compounds to Western flower thrips *Frankliniella occidentalis*. *J. Chem. Ecol.* **26**, 2643–2655 (2000).
58. E. J. McCallum *et al.*, Increased plant volatile production affects oviposition, but not larval development, in the moth *Helicoverpa armigera*. *J. Exp. Biol.* **214**, 3672–3677 (2011).
59. Y. Xiao *et al.*, Specific herbivore-induced volatiles defend plants and determine insect community composition in the field. *Ecol. Lett.* **15**, 1130–1139 (2012).
60. A. Haverkamp, B. S. Hansson, M. Knaden, Combinatorial codes and labeled lines: How insects use olfactory cues to find and judge food, mates, and oviposition sites in complex environments. *Front. Physiol.* **9**, 49 (2018).
61. J. N. Thompson, Specific hypotheses on the geographic mosaic of coevolution. *Am. Nat.* **153**, S1–S14 (1999).
62. A. C. Aprotosoaie, M. Hancianu, I. I. Costache, A. Miron, Linalool: A review on a key odorant molecule with valuable biological properties. *Flavour Fragrance J.* **29**, 193–219 (2014).
63. J. H. Loughrin, D. A. Potter, T. R. Hamilton-Kemp, Volatile compounds induced by herbivory act as aggregation kairomones for the Japanese beetle (Popillia japonica Newman). *J. Chem. Ecol.* **21**, 1457–1467 (1995).
64. T. C. J. Turlings *et al.*, How caterpillar-damaged plants protect themselves by attracting parasitic wasps. *Proc. Natl. Acad. Sci. U.S.A.* **92**, 4169–4174 (1995).
65. B. Bubner, K. Gase, I. T. Baldwin, Two-fold differences are the detection limit for determining transgene copy numbers in plants by real-time PCR. *BMC Biotechnol.* **4**, 14 (2004).
66. K. Gase, A. Weinhold, T. Bozorov, S. Schuck, I. T. Baldwin, Efficient screening of transgenic plant lines for ecological research. *Mol. Ecol. Resour.* **11**, 890–902 (2011).

PNAS
www.pnas.org

Supplementary Information for

An unbiased approach elucidates variation in (S)-(+)-linalool, a context-specific mediator of a tri-trophic interaction in wild tobacco

Jun He, Richard A. Fandino, Rayko Halitschke, Katrin Luck, Tobias G. Köllner, Mark H. Murdock, Rishav Ray, Klaus Gase, Markus Knaden, Ian T. Baldwin, Meredith C. Schuman

Ian T. Baldwin, Meredith C. Schuman
Email: baldwin@ice.mpg.de, meredith.schuman@geo.uzh.ch

This PDF file includes:

Supplementary text
Figs. S1 to S12
Tables S1 to S3
References for SI reference citations

Other supplementary materials for this manuscript include the following:

Datasets S1 to S3

www.pnas.org/cgi/doi/10.1073/pnas.1818585116

Supplementary Information Text

Plant materials and growth conditions

The two *N. attenuata* natural accessions AZ and UT were collected from populations near Flagstaff, Arizona (1) and the DI Ranch, T40S R19W section 9 of Utah (2), and inbred for 22 (Arizona) or 30 (Utah) generations in the glasshouse. The generation of the advanced intercross-recombinant inbred line (AI-RIL) population was previously described (3); generation F11 was used for glasshouse experiments and seed from these plants, F12, in the field experiment. The other *N. attenuata* natural accessions were collected in the southwestern United States from the locations shown in Fig 2I. The full-length cDNAs of *CbLIS* (4) and *ObLIS* (5) were cloned from plasmids kindly provided by E. Pichersky and transferred into the pSOL9 plasmid (6). *Agrobacterium tumefaciens* (strain LBA 4044)-mediated transformation proceeded as previously described (7). Multiple *N. attenuata* stable lines ectopically expressing *CbLIS* and *ObLIS* under control of the CaMV35 promoter were generated in both UT and AZ genotype backgrounds. Diploid transgenic lines were screened using flow cytometric analysis (8). Homozygous T2 plants of each line were identified using seedling resistance to hygromycin (6). Ectopic expression lines of *CbLIS* and *ObLIS*, and the RNAi silencing line of ir*MPK4* (9) used in this study are listed in Table S2.

Seed germination followed the protocol by Krügel et al. (7). After 10 days, seedlings were transferred to small pots (TEKU JJP 3050 104 pots, Poeppelmann GmbH & Co. KG, Lohne, Germany) in the glasshouse and then to 1 L pots 10 days later. For most assays, plants were grown with soil, fertilization and watering regimes as previously described, and grown under 19°C–35°C with a light period of 6:00-22:00 (supplemental lighting by Philips Sun-T Agro 400 W and 600 W sodium lights) and 55% humidity (7, 10). For the VIGS experiment, plants were grown with the same soil and fertilization regime in a climate chamber (22 °C; light period: 6:00 to 22:00, supplemental lighting by Philips Sun-T Agro 400 W and 600 W sodium lights; 65% relative humidity). For experiments in the field, seedlings were adapted to field conditions similarly to previous studies (11, 12) with the following changes: seedlings in closed boxes were kept in a shady location directly on the soil, and hardening-off was done by opening boxes and then reducing shade cover two days later. Seedlings with a rosette diameter of ca. 1.5-2.5 cm were transplanted in to a field plot at the Walnut Creek Center for Education and Research (34°55'17.8"N 112°50'42.2"W) located in Arizona. Plants were watered in the early morning and evening using a drip irrigation system until they had established, and then as needed. The planting arrangement in the field is described under "Predation assay" in the Materials and Methods section of the main text.

Plant treatment and headspace sampling

RIL plants in the glasshouse were treated with wounding and *M. sexta* regurgitant to induce defense responses. Collection of regurgitant from caterpillars reared on *N. attenuata* UT WT plants, storage, and treatment was as previously described (13, 14). Briefly, the rosette-stem transition leaf (S0) or the first stem leaf (S1) (15) of elongated plants was wounded using a pattern wheel on each side of the midvein and 20 µL of regurgitant diluted 1:5 with distilled water were added to the wounds and gently rubbed in with a clean, gloved finger. Following treatment, the leaf was enclosed in a clean,

ventilated PET cup (ca. 650 mL) with two pieces of silicone laboratory tubing (ST, 1 mm i.d. x 1.8 mm o.d.; Carl Roth, catalog number: 9555.1; 5mm for each piece) to absorb plant volatiles and equilibrate with the headspace over 24 h (16, 17). Transgenic plants for screening were not elicited and the youngest rosette leaf was used for treatments and volatile sampling from elongating plants. Volatile sampling from VIGS plants followed the same protocol. For diurnal emission and light deprivation experiments using UT WT plants, volatiles were sampled during the night (22:00-6:00), and every 4h after that over the day. Light deprivation was applied by wrapping the collection cup with aluminum foil from 10:00-14:00. To assess diurnal emissions of linalool in transgenic plants, the headspace was sampled for three different periods: dusk (18:00-22:00), night (22:00-6:00), and day (6:00-14:00).

TD–GC–QMS analysis

One piece of ST was placed into a glass TD tube (Supelco, www.sigmaaldrich.com) and analyzed on a quadrupole GC-MS-QP2010Ultra equipped with a TD-20 thermal desorption unit (Shimadzu). For linalool quantification in RILs, accessions and transgenic plants, as well as the relative quantification of other terpenoids (Figs. S8 and S9, Supplementary Datasets D2 and S3), a ZB-Wax plus GC column (Phenomenex, 30 m x 0.25 mm x 0.25 µm) was used to analyze total linalool. Desorption and analysis were performed as previously described (16, 17). For enantiomer identification, a Cyclosil B column (Agilent, 30 m x 0.25 mm x 0.25 µm) was used and the GC program was modified: the oven program started at 40 °C and after a 2 min hold, increased to 80°C at 40°C/min, then to 140 °C at 5 °C/min, then to 200°C at 40°C/min followed by a 1 min hold.

Peaks were integrated using the target and reference ions listed in Table S1 and compound identifications were based on comparison of spectra and retention indices against NIST libraries. The linalool spectrum and retention time was compared to pure standards [racemic linalool and (*R*)-(-)-linalool, Sigma-Aldrich].

QTL mapping

The genotyping of the Al-RIL population and linkage map were reported by Zhou, *et al.* (3). QTL mapping was performed using R package QTLRel (18) following the workflow previously described by Zhou et al. (3), based on the relative abundance of each compound in the 261 lines of the population.

Measuring transcript abundance of genes

The transcript abundance of *NaLIS, NaGPPS1, NaGPPS2* were measured using qPCR. For correlation between internal free linalool (see below) and transcript abundance, the youngest rosette leaf of an elongating plant was used for both volatile extraction and RNA extraction. Total RNA was isolated and genomic DNA was digested using the NucleoSpin® RNA Plant kit (MACHEREY-NAGEL) according to the manufacturer's protocol. About 1 µg total RNA were reverse transcribed using the PrimeScript™ RT reagent Kit (TAKARA). The relative transcript abundance of the target genes was measured using qPCR with a MX3005P PCR cycler (Stratagene). Transcript abundance of *NaLIS* in the VIGS experiment was measured the same way

using similar leaves. The eukaryotic translation initiation factor 5A-3 (*IF5A3*) was used as reference for normalization. Primers used for qPCR are listed in Table S3.

Measurement of internal free linalool and glycosides

Internal free linalool was extracted from leaf tissue using ST pieces (17) following a protocol modified from van Pinxteren *et al.* (19) and Matsui *et al.* (20). Briefly, the youngest rosette leaf of an elongating plant was harvested, flash-frozen and ground in liquid N_2. Distilled water saturated with $CaCl_2$ (0.8 ml) was added to ground tissue (~100 mg) in a 1.5 ml glass GC vial (Sigma-Aldrich) to inhibit enzyme activity. One piece of ST (1 mm i.d. x 1.8 mm o.d.; Carl Roth, catalog number: 9555.1; 5mm for each piece) was placed into the vial to extract volatiles from tissue.

Linalool conjugates were extracted and released following a protocol modified from Lucker *et al.* (21). Briefly, about 200 mg ground tissue (precise mass recorded) of the youngest rosette leaf of an elongating plant was extracted with 1 mL 80% MeOH. Extracts were dried completely under nitrogen gas in a 1.5 mL GC vial. Then 100 µL citric acid/phosphate buffer (pH 5.2) and 100 µL almond β-glucosidase (Sigma) solution (6 units) were added to the sample along with one piece of ST and incubated overnight at 37 °C. ST pieces with collected internal volatiles were washed in MilliQ water and dried briefly under nitrogen gas before measurements.

Analysis of *NaLIS* allelic variants and transcript abundance in 26 accessions

The genomic sequence of *NaLIS*-UT was extracted from the genome data in the *Nicotiana attenuata* Data Hub [http://nadh.ice.mpg.de, (22)]. Scaffolds containing the *NaLIS*-AZ sequence in the AZ genome were identified using *NaLIS*-UT as query. Genomic and transcript sequences of *NaLIS*-AZ and *NaLIS*-UT were aligned using megablast (https://blast.ncbi.nlm.nih.gov). The 3' end of the *NaLIS* transcript alleles in ten accessions were amplified using primers listed in Table S3.

The entire chromosome VIII was extracted from the reference genome (23) and the region of interest was identified within it. The nucleotide sequence from that region was aligned pairwise with the putative AZ sequence. The pairwise alignment was merged using a python script to create an augmented reference sequence and was then indexed using BWA (24). The whole genome sequences of 26 accessions were then aligned to this augmented reference using bwa mem aligner (24). Additionally, MAKER2 (25) in conjunction with AUGUSTUS (26), SNAP (27), and Genemark (28) used to predict de novo gene model within the augmented sequence. The mRNA sequence was extracted from the gene model and RNA-Seq data from 26 wound elicited leaf samples were aligned and quantified using kallisto (29) on the modified transcriptome containing the "augmented" gene. Finally, to obtain the consensus sequence with respect to the reference, genome coverage was calculated at each base in that region using bedtools *genomecov* function (30) and filtered where coverage was greater than 1. The contiguous bases were then merged using the bedtools *merge* function to identify the deleted regions. These regions were then visualized in IGV (31) to visually confirm the deletions for each accession.

Heterologous expression of *NaLIS* in *Escherichia coli* and extraction of recombinant protein

The full-length ORF of *NaLIS* as well as the N-terminal truncated ORF lacking the region encoding a putative signal peptide (nucleotides 1-87) were amplified from cDNA made from leaves of AZ and UT plants separately with primers listed in Table S3. Purified PCR fragments were cloned into the bacterial expression vector pET200 (Invitrogen). The procedure of expression and protein extraction followed the previous description (3).

Analysis of recombinant NaLIS

To determine the catalytic activity of NaLIS, enzyme assays containing 40 µL of the bacterial protein extract and 60 µL assay buffer with 40 µM GPP, (*E,E*)-FPP, or (*E,E,E*)-GGPP and 10 mM $MgCl_2$, were performed in Teflon-sealed screw-capped 1.5 mL GC glass vials. Assays were overlaid with 100 µL hexane, incubated for 120 min at 25°C, and vortexed for 1 min to extract enzyme products from the aqueous phase. The hexane phase was then collected and analyzed using GC-MS. As a negative control, raw protein extracts from *E. coli* expressing the empty vector pET200 were incubated with the substrates GPP, (*E,E*)-FPP, and (*E,E,E*)-GGPP, respectively, as described above. No TPS enzyme activity was observed in negative controls.

TPS enzyme products were analyzed on an Agilent 6890 Series gas chromatograph coupled to an Agilent 5973 quadrupole mass selective detector. Measurements using a DB-5MS column (Agilent, Santa Clara, USA, 30 m x 0.25 mm x 0.25 µm) followed the procedure previously described (3). Product identification was done using authentic standards (linalool, nerolidol, Sigma-Aldrich) or the WILEY mass spectra library (geranyllinalool).

VIGS of *NaLIS*

Two hundred bp of the coding sequence of *NaLIS* were amplified using PCR with primers given in Table S3 and transferred into the PTV vector for VIGS. The VIGS followed the procedures described by Galis, *et al.* (32). Silencing efficiency was tested by measuring transcript abundance using qPCR, and headspace volatiles were sampled, as described above.

T-DNA copy number and integrity determination using NanoString's nCounter® Technology

Procedures are described in the main text. Here, we provide details of the 12 code probe set.

For the nCounter analysis, a 12 code probe set (sequences in Supplementary Dataset S1) was designed from of 12 chosen target regions, which comprised 3 calibrator genes that occur as a single copy in the genome of *N. attenuata* [*AOC*_2: allene oxide cyclase (GenBank LOC109240002); *S-RNase*-2_1: ribonuclease S-7-like (GenBank LOC109235079); *sulfite*_2: sulfite reductase 1 (GenBank LOC109217753)], and 9 functional regions present on the pNAT (33), pRESC (34-36), pSOL (33), and pPOP6 (37) binary vectors used in our group for the transformation of *N. attenuata*. These target sequences are indicative of complete T-DNA insertions (TNOS+LB_1: terminator of the nopaline synthase gene; *hptII*_3: hygromycin phosphotransferase gene; PNOS_1: promoter of the nopaline synthase gene; P35S_1: cauliflower mosaic virus 35S promoter; T35S_1: cauliflower mosaic virus 35S terminator; *sat-1*_1: streptothricin

acetyltransferase; *nptII*_1: neomycin phosphotransferase II gene) or T-DNA overreads (pVS1_3: pVS1 vector backbone; *nptIII*_3: neomycin phosphotransferase III gene) of the specific transformation vectors. The oligonucleotides were designed by NanoString (Seattle, WA, USA) and synthesized by IDT (Integrated DNA technologies). The location of the target sequences on the binary plant transformation vectors is indicated in Fig. S10B.

Manduca sexta rearing, pupation, mating

M. sexta used in this study were from an in-house colony. Eggs were collected from *D. wrightii* plants placed in an oviposition cage (2m x 1.5m x 1m) with mated moths, inside of a climate chamber (24 °C, light period: 0:00 to 13:00, relative humidity: 70%). In the same chamber, eggs were hatched in a small plastic box (8cm x 5cm x 4cm) with small holes on the lid and reared there with artificial diet (38) until the second instar. Then the caterpillars were transferred into a larger plastic box (30cm x 20cm x 20cm) with a plastic shelf at the bottom and dirty boxes were regularly replaced with clean boxes. When the caterpillars were ready to pupate, they were individually transferred into holes in a wood block and covered by wood panels. Pupae were removed about two weeks later. For oviposition assays in the wind tunnel or tent, male and female pupae were separated and placed into paper bags in cages (1 m x 0.4 m x 0.4 m). The cages were placed either in the climate chamber (wind tunnel), or at the Isserstedt glasshouse where the tent was located (tent). Two days after emergence, two males and one female were put into a cage (30 cm x 30 cm x 30 cm) for overnight mating. Mated females were then used for assays on the following day. For the oviposition assay in the climate chamber, approximately equal numbers of male and female pupae were regularly placed on a paper shelf with holes in an open paper box in the chamber. Moths emerged from these pupae were allowed to mate freely and kept in the chamber during the experiments.

Oviposition assay in wind tunnel, oviposition chamber and tent

The oviposition behaviors of newly mated *M. sexta* female adults were observed in the wind tunnel of the MPICE. The wind tunnel (240 cm × 90 cm × 90 cm) was set to the following conditions: 25 °C and 75% relative humidity, a wind speed of 0.4 m/s and a light level of 0.5 lux (39). Plants and moths were placed into separate chambers having the same conditions as the wind tunnel one hour before the assay (movement to chambers at 13:00, assay at 14:00). Then a pair of plants was placed upwind in the wind tunnel at a precise location such that the stems of plants (about 50 cm high) were 42 cm from each other, 24 cm from each side and 30 cm from the upwind wall of the wind tunnel. A single mated moth in a black mesh cage (15 cm × Ø13 cm) was placed onto a platform at the downwind end of the tunnel (45 cm from the sides, 10 cm from the downwind end and 30 cm from the floor). Then the top and side parts of the cage were removed and the moth was exposed to wind and plant odors. The wings of the moth were lightly touched by fingers until the moth started beating its wings. The moth was allowed to fly in the wind tunnel until it touched plants 10 times. The identity of the plant touched each time was immediately recorded. After 10 touches, the moth was removed from the wind tunnel. Then the plants were removed and the number of eggs on each plant was counted and recorded. As a backup, a video camera (Logitech C615, USA, infrared filter removed) recorded the wind tunnel from the release of the moth to the 10 touches of plants. For

every comparison between two genotypes, 20 pairs of plants and 20 moths were assayed. The relative placement of genotypes was switched for each moth.

Overnight oviposition of *M. sexta* adults was assayed in an oviposition chamber (1.4 x 1.5 x 2.0 m, light period: 6:00 to 22:00), where a small colony of *M. sexta* moths containing about 3-5 females and a similar number of males of different ages were continuously kept and regularly renewed. Two genotypes (4 plants each) were placed into the chamber. Plants of the same genotype were positioned in one row and the two rows of different genotypes were 1.5 m apart. The plants were kept there overnight (20:00-8:00) with moths, and then plants were removed and the eggs on each plant were carefully collected with fingers in gloves and counted. In total, 20 plants were assayed for each comparison of two different genotypes. Relative places of the rows of different genotypes in the chamber were switched every day.

Oviposition of *M. sexta* on multiple plants was further assayed in a tent located in Isserstedt, Jena, Germany, in July, 2018. The tent (24 m× 8 m × 4 m, Amiran, Kenya, www.amirankenya.com) is located outdoors and covered with mesh at the sides and front, permitting air exchange (11). The ground of the tent lacked vegetation (mostly grass) which was removed before experiments. Ten plants of each of six genotypes tested were placed in the tent, forming a population of 60 plants with each plant positioned 1.5 m apart. The plants were distributed in ten blocks each containing all six lines, and the positions of different lines were randomized within each block and randomly switched within the block every day during the assay period. Each day, a single mated *M. sexta* female moth was released into the tent at 16:00 and kept there overnight. The moth was removed at 11:00 on the following day and eggs were carefully collected from each plant without damaging the leaves. The number of eggs from each plant was counted. Different moths (days) were used as replicates. In total, 16 moths were assayed and 12 moths which laid a reasonable amount (> 20) of viable eggs were used for statistical analysis.

Metabolite extraction from plant leaves and *M. sexta* frass, and LC-MS analysis

One hundred mg ground leaf material or 30 mg *M. sexta* frass was extracted in 1 mL 80% methanol in a 1.5 mL Eppendorf tube. Two steel balls were added to the solution with leaf or frass material and tubes were shaken twice at 1200 strokes/min for 1 min using a Geno/Grinder 200 (SPEX SPEX SamplePrep, http://www.spexsampleprep.com/). Tubes were centrifuged at 16 000 *g* for 20 min at 4 °C and the supernatant was transferred to a new tube and re-centrifuged. The supernatant (500 µL) was then transferred to a glass vial with a Teflon cap containing a glass micro-insert (MACHEREY-NAGEL GmbH & Co.KG).

Samples were analyzed on an Ultimate 3000 UHPLC equipped with an Acclaim column (150 mm × 2.1 mm, particle size 2.2 µm) connected to an IMPACT II UHR-Q-TOF-MS system (Bruker Daltonics, http://www.bruker.com). The flow was set to 0.4 mL/min with a solvent gradient decreasing from 90% to 10% of solvent A (water, 0.1% [v/v] acetonitrile and 0.05% formic acid) and increasing from 10% to 90% of solvent B (acetonitrile and 0.05% formic acid) over 20 min after an initial hold of 1 min, followed by column equilibration at starting conditions for 4 min. The MS settings were as follows: end plate offset 500V, capillary 4500V, drying gas 10 L/min at 200 °C, detecting mass range 50-2000 Da, spectra rate 5 Hz. Mass detection was calibrated using sodium formate clusters (v:v, 10 mM NaOH: isopropanol/water containing 0.2% formic acid=

50:50%). Raw data files were analyzed using Bruker Compass DataAnalysis software version 4.3.

Caterpillar growth assay

For growth assays on detached leaves, the youngest fully expanded leaf [position +1, (15)] was excised at the base of the petiole and placed into a plastic cup (ca. 650 mL) with wet tissues at the bottom. One first-instar caterpillar was placed on the leaf and kept there for 5 days, at which time the mass of individual caterpillars was measured using a Sartorius BP analytical balance (precision: 0.1 mg, resolution: 0.1 mg, linearity: 0.2 mg, Sartorius Lab Instruments GmbH & Co. KG).

Statistical analyses

F-tests were used to compare volatile compounds in the headspace of AZ and UT plants, and Bonferroni corrections were used for multiple testing, n=5. Pearson's correlations were calculated for terpenoid emission versus predation rate; gene expression of *NaLIS*, *NaGPPS*1, 2 versus emission of linalool; and headspace linalool versus glucosidase-released linalool in accessions. Student's *t*-tests were used to compare the relative abundance of *NaLIS* transcripts or linalool emission between VIGS *NaLIS* and VIGS EV plants, n=10, and the mass of *M. sexta* larvae fed on AZ and ectopic expression lines of AZ background, n=20. PCA analysis of the relative abundance of terpenoids other than linalool emitted by ectopic expression lines was conducted with ClustVis on centralized data (40). Sign tests were used to compare numbers of touches or eggs received by plants of different genotypes in the wind tunnel or the oviposition chamber. The number of eggs received by each plant in the oviposition chamber was transformed to the proportion of all the eggs laid during the night, n=20. Friedman tests were used to compare the number of eggs received by plants of six genotypes in the tent assay, n=12, followed by Tukey-Kramer Multiple Comparisons tests for pairwise comparisons of interest.

Regression and Student's *t*-tests were performed in MS Excel. Sign tests were performed in SPSS Statistics 17.0 (https://www.ibm.com/analytics/spss-statistics-software). Friedman test and Tukey-Kramer Multiple Comparisons tests were performed in GraphPad InStat (https://www.graphpad.com/). The significance level was set at $p<0.05$.

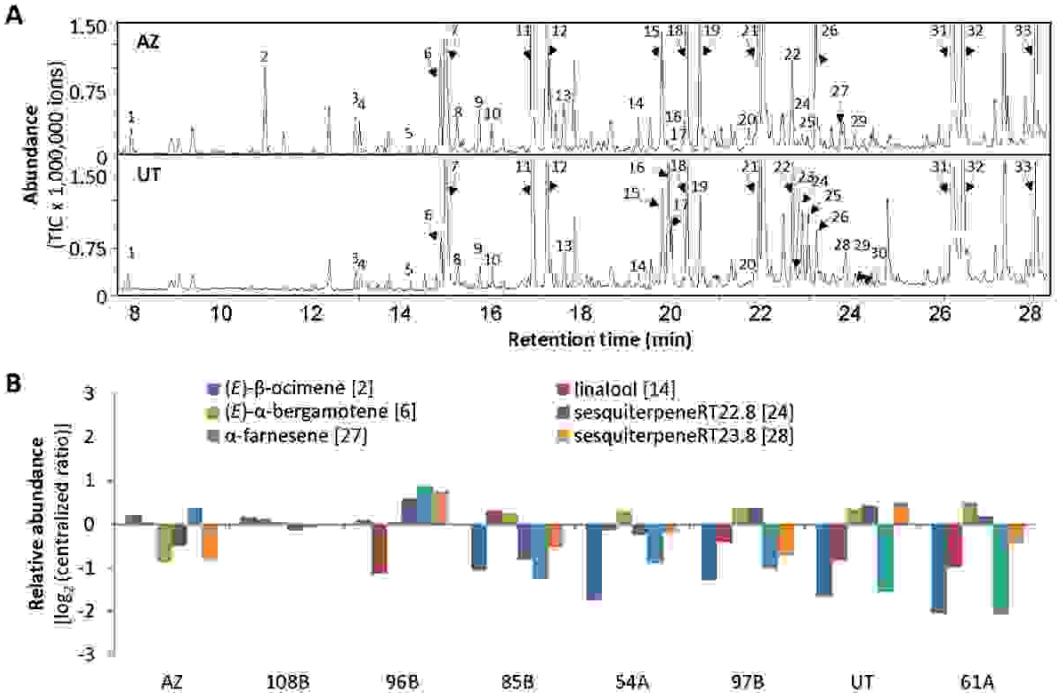

Fig. S1. Variation of terpenoids between AZ and UT, and within an AI-RIL population from crossing AZ and UT. A. Representative chromatograms of volatile compounds in headspace of AZ and UT leaves (see Table S1 for compound IDs). B. RILs having different compositions of six terpenoid volatiles, selected for the field predation assay shown in Fig. 1.

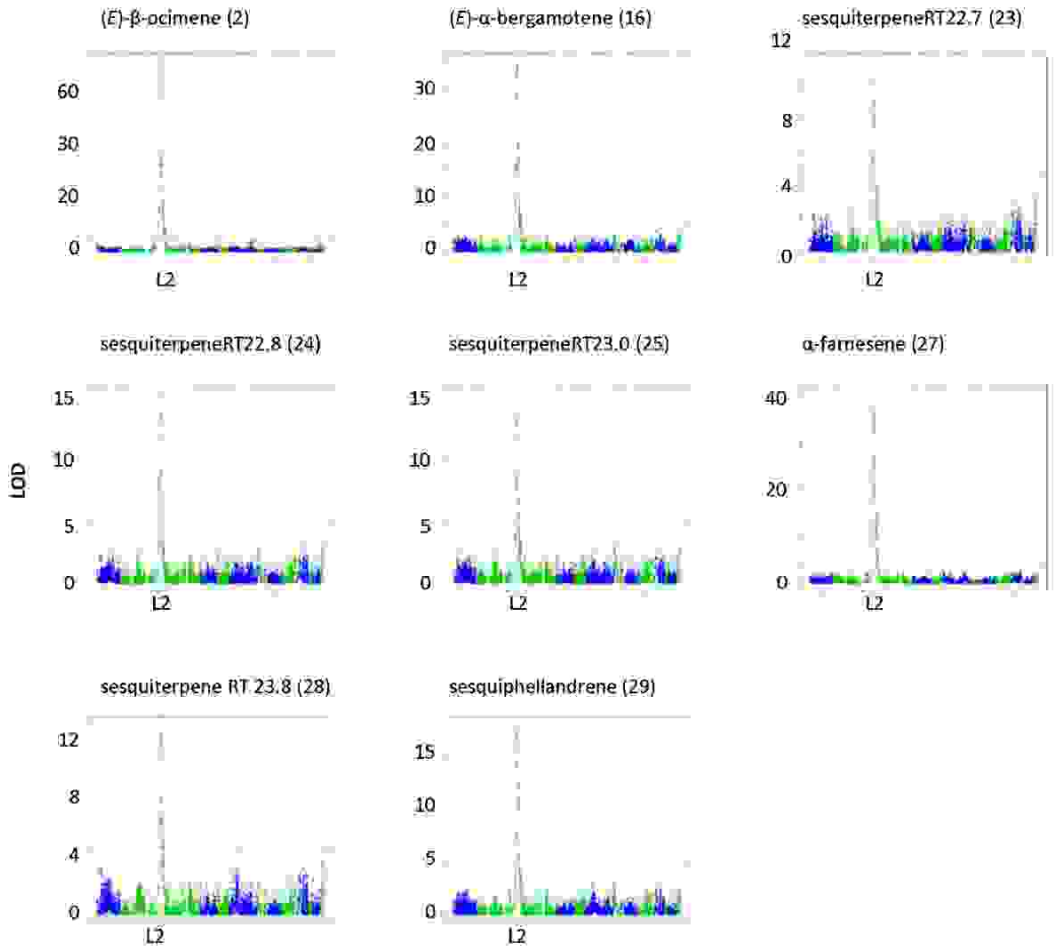

Fig. S2. Mapped loci for individual herbivory-induced terpenes using 261 RIL lines. Most terpenes are mapped to a similar locus on linkage group 3 (on chromosome II).

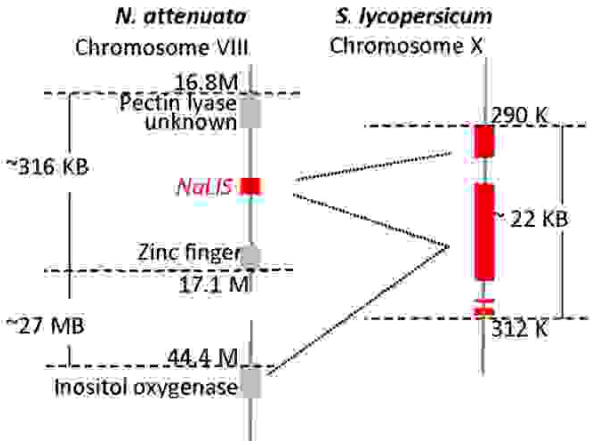

Fig. S3. A single *NaTPS* was found within the mapped locus associated with linalool, whereas the homologous region of the tomato genome contained a small cluster of *SlTPS*s. Putative *TPS* genes are shown as red bars, non-*TPS* genes in grey.

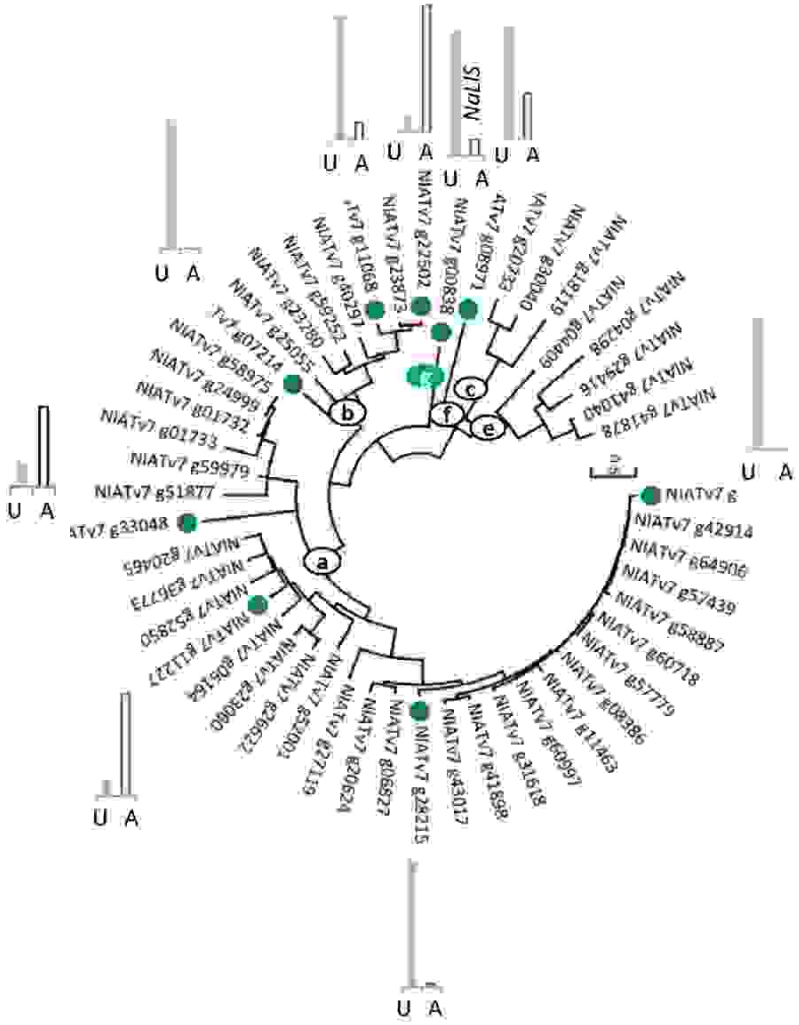

Fig. S4. The *NaTPS* family and variation of herbivory-induced transcript abundance between UT and AZ leaves. The subfamily is indicated by circled letters at the root of each group. Green circles indicate the genes induced by *M. sexta* in UT leaves at least 2-fold according to RNA-seq or microarray data from *N. attenuata* Data Hub [http://nadh.ice.mpg.de, (19)]. Bars beside the gene show the relative fold of induction (treated/control) of the gene in the two accessions (U: UT; A: AZ). Sequences of the *NaTPS*s and *TPS*s from other species with known subfamilies are in Supplemental File S1.

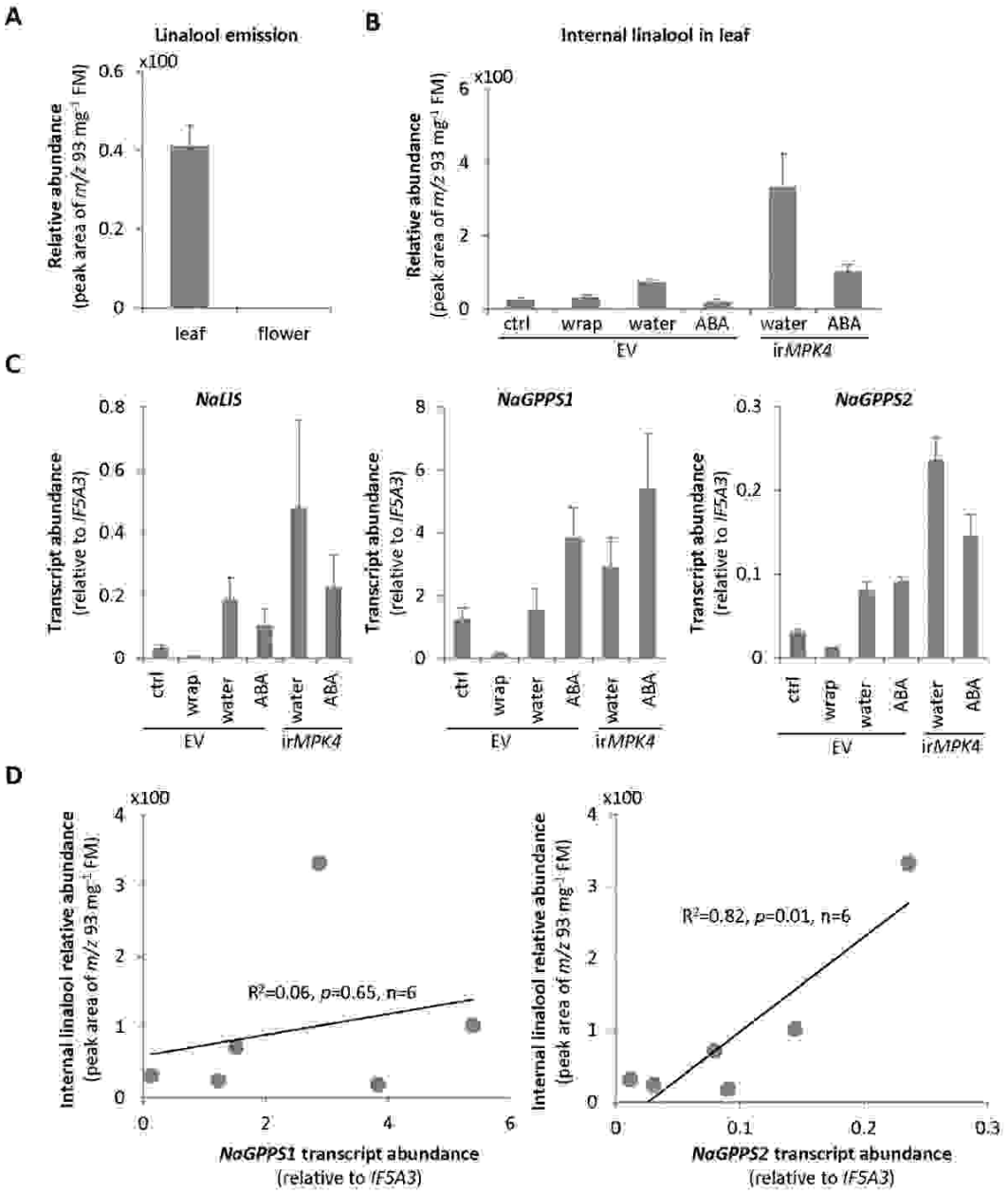

Fig. S5. Linalool was only detected in the leaf headspace but not in the floral volatiles of UT, and in leaves, the abundance of internal free linalool was correlated with the transcript levels of *NaLIS*, *NaGPPS2* but not *NaGPPS1*. A. Linalool emitted by leaves or flowers of UT plants (mean+SE, n=3). Volatile collection time: 12 hours, from 8:00 to 20:00. B. Abundance of internal free linalool in leaves of EV and transgenic UT (ir*MPK4*, a high volatile emitter) plants under different treatments (mean+SE, n=3); ctrl: control; wrap: wrapping; ABA: abscisic acid. C. Relative transcript abundance of *NaLIS*, *NaGPPS1* and *NaGPPS2* in same samples as in B (mean+SE, n=3). D.

Correlation between the compound in B and the gene transcript level in C. FM: fresh mass.

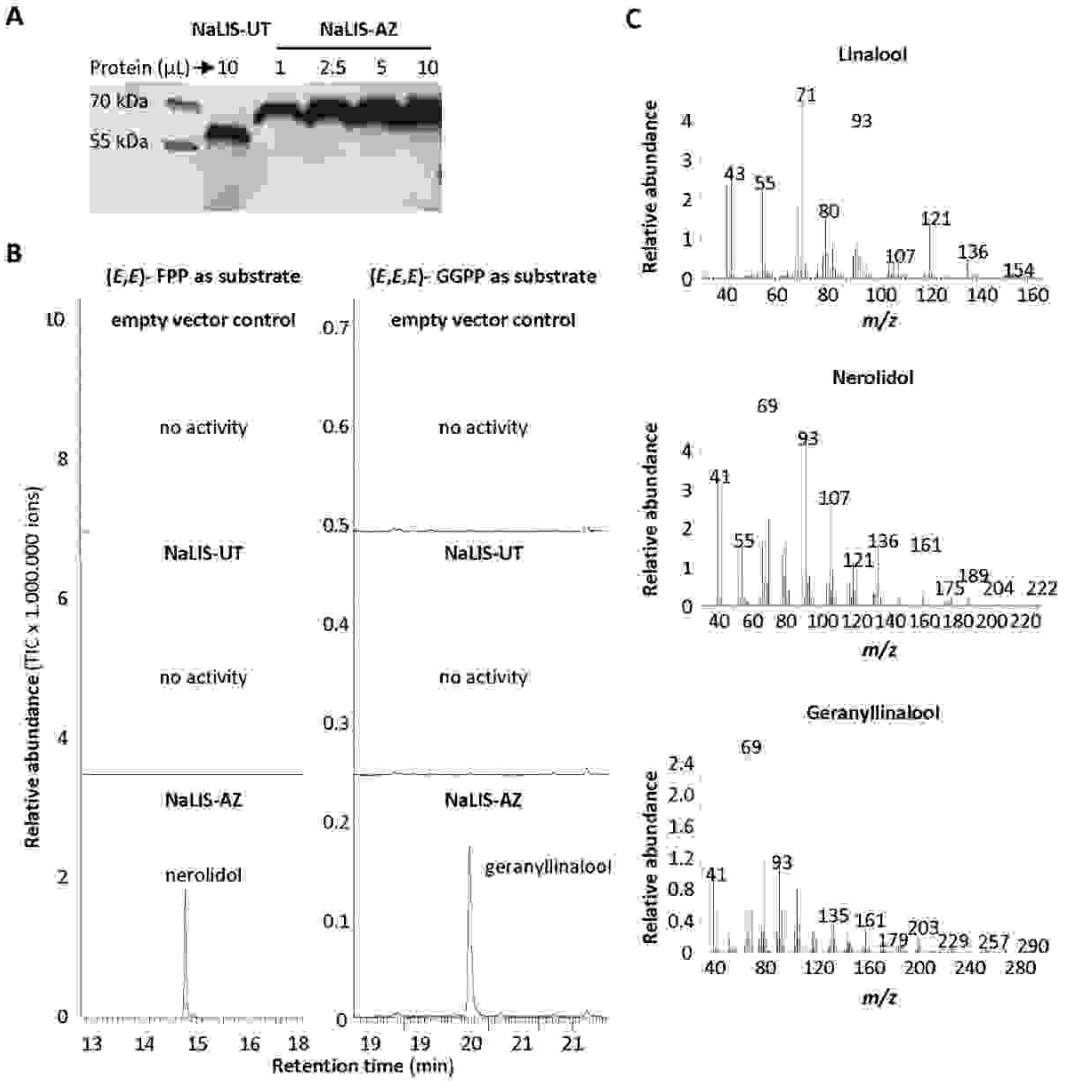

Fig. S6. Biochemical characterization of recombinant NaLIS. The alleles were expressed as full-length versions or as N-terminal truncated versions lacking the putative signal peptide in *Escherichi coli*. Shown are data from the truncated proteins: the full-length proteins had lower activity when expressed in *E. coli*. A. Western blot analysis of His-tagged fusion protein of NaLIS-UT and NaLIS-AZ heterologously produced in *E. coli*. The amount of the NaLIS enzymes in *E. coli* raw protein extracts was analyzed using an anti-His-antibody. Different volumes of NaLIS-AZ were compared to 10 µL NaLIS-UT. Similar amount of NaLIS enzymes (10 µL NaLIS-UT extract and 1 µL NaLIS-AZ extract) were used for later assays in B. B. Products by empty vector and recombinant NaLIS alleles from substrate (*E*,*E*)-FPP (left) and (*E*,*E*,*E*)-GGPP (right). Product from GPP is shown in Fig. 2F C. Mass spectra of major identified enzyme products.

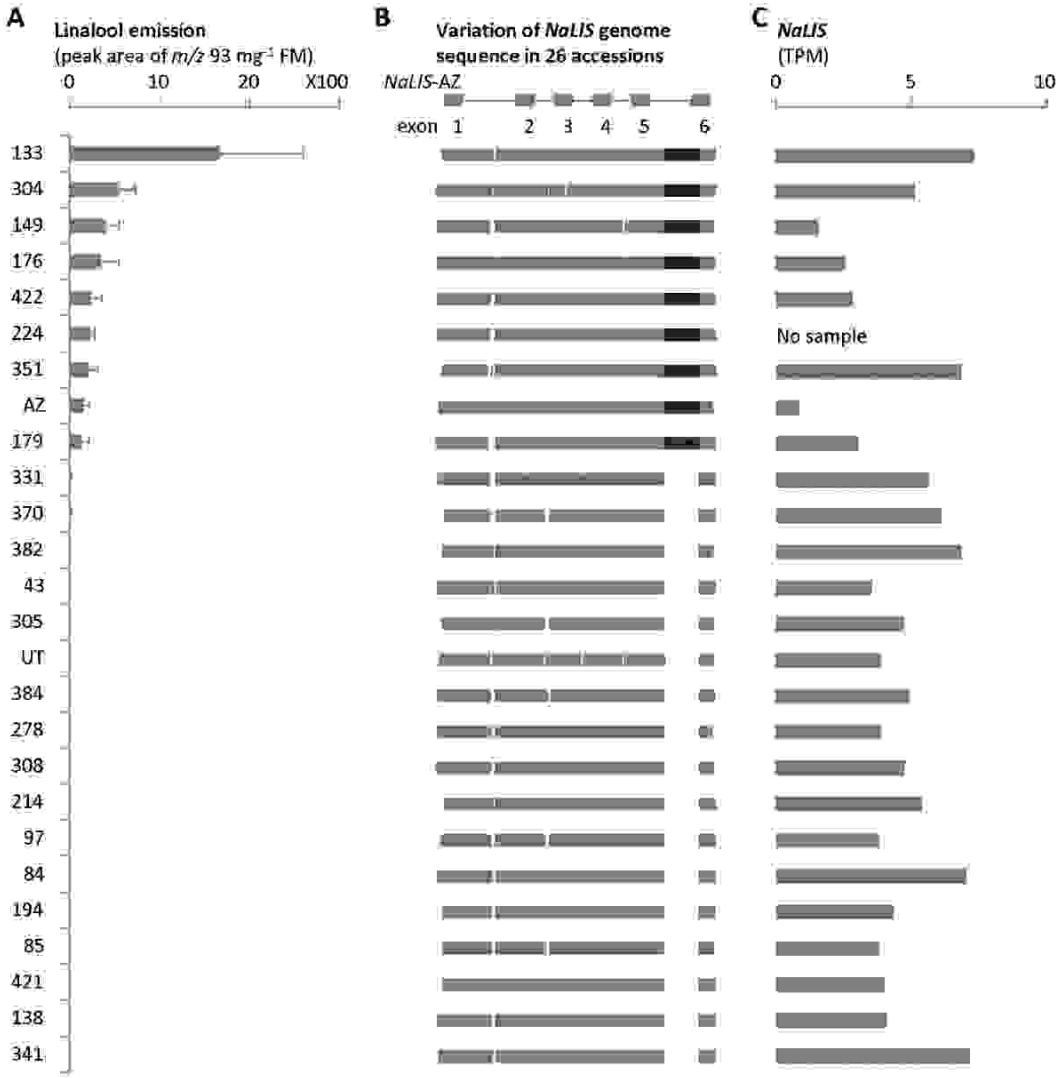

Fig. S7. Linalool natural variation correlates with *NaLIS* allelic diversity in 26 *N. attenuata* accessions, but not with the transcript abundance of *NaLIS*. A. Leaf linalool emission after wounding plus *M. sexta* regurgitant treatment (mean+SE, n=3). B. *NaLIS* allele diversity revealed by genome resequencing. Black bars on the top show the structure of *NaLIS* ORF. Grey bars represent genomic sequences (Supplemental File S1) of *NaLIS* in different accessions. Darker grey bars indicate the sequence present in *NaLIS*-AZ variants but missing in *NaLIS*-UT variants. C. Transcript abundance of *NaLIS* in leaves after wounding plus *M. sexta* regurgitant treatment, from RNA-seq data. TPM: transcripts per million.

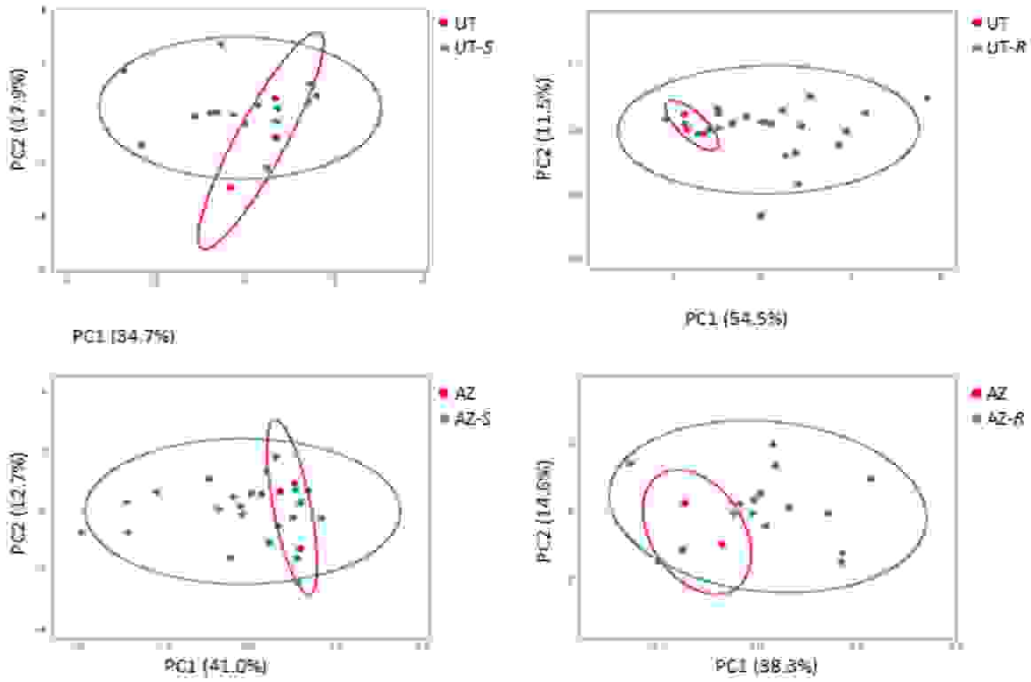

Fig. S8. Terpenoid volatiles other than linalool are similar to WT in ectopic expression lines. Shown here are PCAs with 95% confident intervals based on all other detected foliar terpenoid volatiles for ectopic expression lines of each background-transgene combination and responsive WT plants. Input data are in Supplemental File S2.

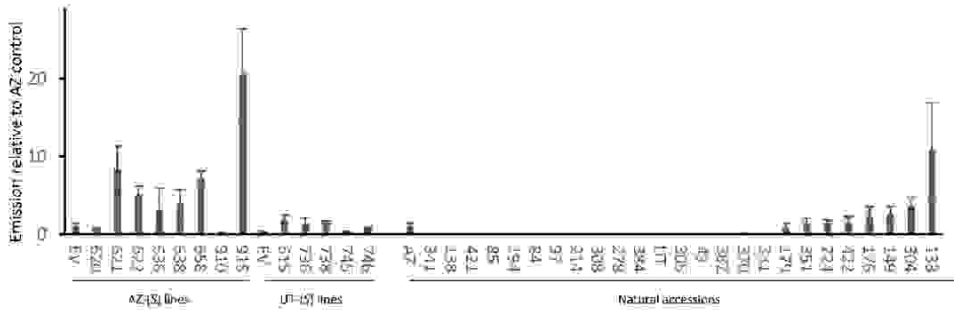

Fig. S9. Normalized linalool emission in ectopic expression lines and natural accessions. Ectopic expression plants and natural accessions were measured in different batches of plants containing AZ and UT EV (empty vector) or WT plants as control for each batch. Emission of linalool was normalized to AZ control plants in each experiment. Ectopic expression lines used for further experiments were 621, 622, 615, and 738.

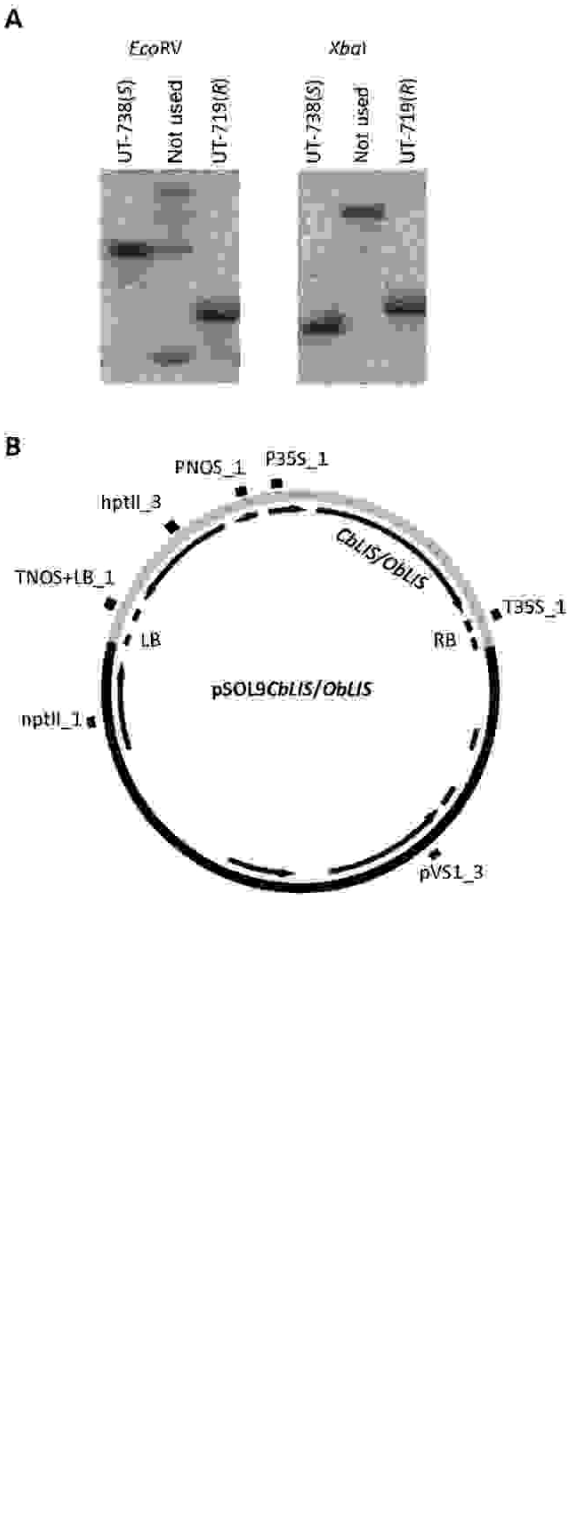
A
EcoRV
XbaI
UT-738(S)
Not used
UT-719(R)
UT-738(S)
Not used
UT-719(R)
B
PNOS_1
P35S_1
hptII_3
CbLIS/ObLIS
TNOS+LB_1
T35S_1
LB
RB
pSOL9CbLIS/ObLIS
nptII_1
pVS1_3
C
TNOS+LB_1
hptII_3
PNOS_1
P35S_1
T35S_1
pVS1_3
nptII_1
nptIII_3
sat-1_1
Normalized counts of probes
15000
10000
5000
0
Control
AZ-621(S)
AZ-622(S)
AZ-597(R)
AZ-912(R)
UT-615(S)
UT-815(R)

Fig. S10. Confirmation of single and complete T-DNA insertions in ectopic expression lines using Southern blotting or Nanostring nCounter® technology. A. Southern blotting with a probe for the hygromycin resistance marker gene HPTII for UT-738(*S*), UT-719(*R*) and an unused line (middle lane) following digestion of genomic DNA with either *Eco*R1 or *Xba*I. B. The map of the pSOL9 plasmid used for transformation. The location of the probes (sequences in Supplemental File S1) used for nCounter analysis are shown as black bars outside the circle. TNOS+LB_1, hptII_3, hptII_3, PNOS_1, P35S_1 and T35S_1 are used to demonstrate single and complete T-DNA insertions. pVS1_3 and nptII_1 are probes indicating overreads of the plasmid sequences outside of the T-DNA borders, which do not affect the plant phenotype or its stable inheritance, but may be mentioned when applying for field releases of transgenic plants. C. Counts of hybridized probes to the sheared genomic DNA of independent ectopic expression lines; nptIII_3 and sat-1_1 are probes with a sequence not present on the plasmid used as a negative control. The positive control ("Control") is a line known to contain a single complete insertion without overreads.

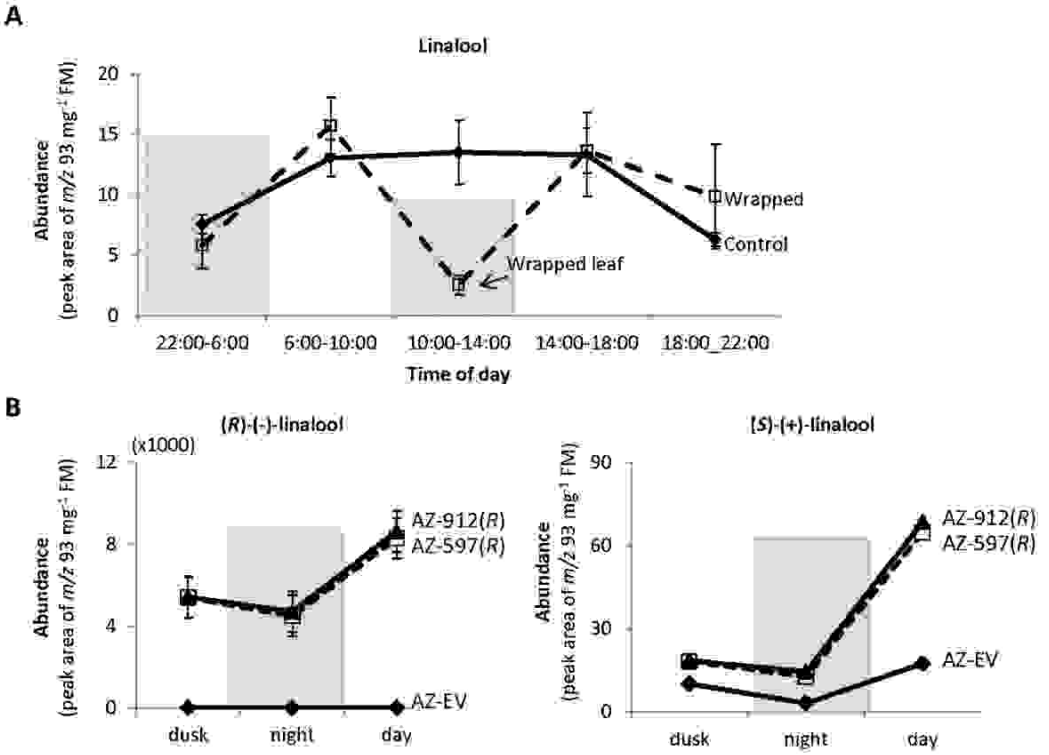

Fig. S11. Both ectopically expressed and endogenous linalool emission have a diurnal rhythm and the emission is directly regulated by the presence/absence of light. A: Light deprivation during the middle of the day decreased the emission of linalool in UT plants (mean+SE, n=3). Dark periods are indicated by grey bars. B: The emission of the foreign enantiomer, (*R*)-(-)-linalool and endogenous enantiomer, (*S*)-(+)-linalool in the transgenic lines in dusk (18:00-22:00), night (22:00-6:00) and day (10:00-18:00). mean+SE, n=3. FM: fresh mass.

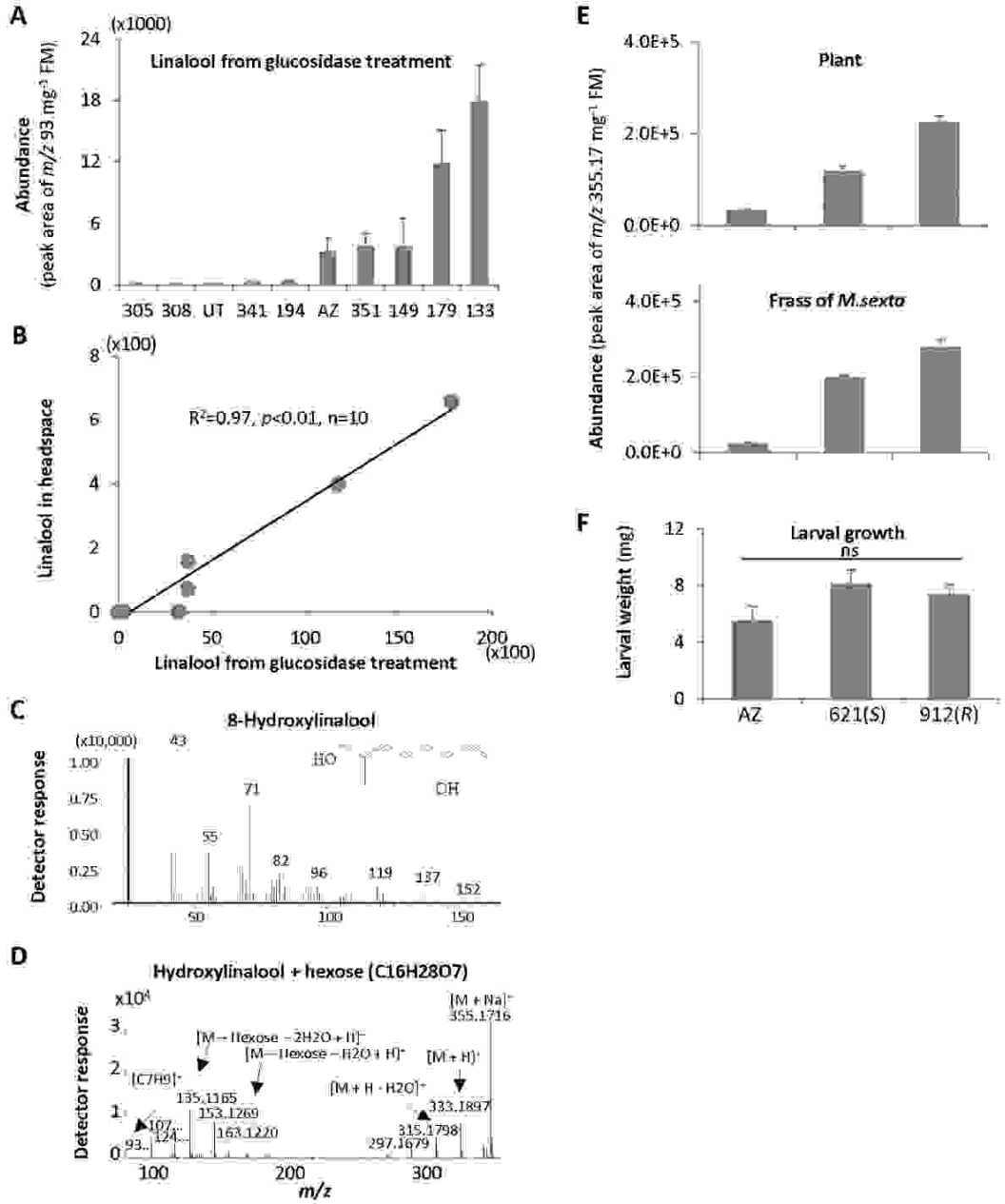

Fig. S12. Oxidation/Conjugation of linalool does not regulate the natural variation of linalool emission of *N. attenuata.* A. Glucosidase treatment released an abundance of linalool from leaves of *N. attenuata* natural accessions (mean+SE, n=3). B. Glucosidase-released linalool is strongly correlated with linalool in headspace across the natural accessions. C. Hydroxylinalool was also detected in glucosidase-treated leaf material using GC-MS. D. Hydroxylinalool conjugates in leaves were detected using UPLC-MS/MS. E. Ectopic expression of foreign *LIS* genes increased content of linalool in

leaves (mean+SE, n=3). F. Enhanced linalool enantiomers and conjugates did not affect the growth of *M. sexta* larvae. ns: not significant.

Table S1. List of peaks integrated in headspace samples from W+R treated leaves of plants from an AI-RIL population, and mean (±SE) peak areas in the "AZ" and "UT" parental lines. Numbers in bold indicate statistically significant differences between accessions (Bonferroni-corrected $p<0.01$ following an F-test).

Index	Name	Retention Time	Target *m/z*	Reference *m/z*	AZ (Peak area x 10^5)	UT (Peak area x 10^5)
1	1-hexanal	7.75	56	41	0.42±0.06	0.45±0.06
2	(*E*)-β-ocimene	10.90	93		**4.44±0.84**	**0.13±0.01**
3	(*Z*)-3-hexen-1-ol-acetate	12.95	67	82.1	2.84±0.77	1.29±0.24
4	unknown GLV	13.01	56		0.92±0.28	1.39±0.21
5	1-hexanol	14.16	56	69	0.93±0.18	1.20±0.28
6	(*Z*)-3-hexenyl propanoate	14.80	67	57; 82	5.07±1.16	4.85±0.66
7	(*Z*)-3-hexenyl butanoate	14.91	67	55; 82	25.5±5.25	30.9±5.76
8	(*E*)-2-hexenyl butanoate	15.17	71	43	1.39±0.29	2.53±0.45
9	n-hexyl butanoate	15.66	71	56	1.14±0.34	1.52±0.38
10	hexyl-2-methyl butanoate	15.94	57	85; 103	0.59±0.18	1.21±0.23
11	(*E*)-3-hexenyl butanoate	16.90	67	82; 55	48.2±12.7	40.5±8.90
12	(*Z*)-3-hexenyl valerate	17.15	67	82; 57	44.5±12.0	40.5±6.03
13	(*Z*)-3-hexenyl isovalerate	17.53	67	82	1.55±0.27	2.17±0.19
14	linalool	19.19	93		**0.56±0.09**	**0.16±0.02**
15	α-duprezianene	19.78	119	161; 91	2.39±0.29	2.98±0.57
16	(*E*)-α-bergamotene	19.85	119	107	**0.35±0.06**	**13.4±3.37**
17	β-elemene	19.92	147	189	**0.01±0.00**	**0.68±0.21**
18	(*Z*)-3-hexenyl caproate	20.34	82	67; 99	16.5±3.31	20.7±4.09
19	unknown GLV	20.56	82	67; 99	5.65±1.79	8.55±1.81
20	(*Z*)-3-hexenyl hexanoate	21.66	67	82; 141	0.61±0.13	0.55±0.08
21	unknown GLV	21.87	67	82; 55	12.2±2.91	19.7±3.63
22	α-terpineol	22.62	93	121; 136	**2.00±0.31**	**6.43±1.18**
23	sesquiterpeneRT22.7	22.68	161	147	**0.02±0.00**	**0.25±0.05**
24	sesquiterpeneRT22.8	22.83	93	121	**0.10±0.03**	**1.66±0.34**
25	sesquiterpeneRT23.0	22.96	93	189; 133	**0.06±0.02**	**1.89±0.45**
26	unknown GLV	23.15	67	55; 82	4.42±1.35	4.35±0.94
27	α-farnesene	23.71	93	107	**0.48±0.12**	**0.01±0.00**
28	sesquiterpeneRT23.8	23.80	93	147	**0.02±0.00**	**0.76±0.20**
29	sesquiphellandrene	24.07	93	161	**0.03±0.01**	**0.21±0.04**
30	sesquiterpeneRT24.2	24.24	93	119	**0.05±0.01**	**0.26±0.03**
31	nicotine	26.18	84	133; 162	**67.4±16.4**	**233±51.4**
32	benzyl alcohol	26.46	79	108; 77	19.0±0.77	15.3±1.75
33	sesquiterpeneRT27.3	27.39	121	93	7.31±0.87	9.54±1.54

Table S2. Transgenic lines used in this study.

Line number	Abbreviation	Background	Trans-gene	Enhanced linalool enantiomer
A-09-620	AZ-620(*S*)	AZ	*CbLIS* full ORF [Genbank: CBU58314, (4)]	(*S*)-(+)-linalool
A-09-621	**AZ-621(*S*)**			
A-09-622	**AZ-622(*S*)**			
A-09-636	AZ-636(*S*)			
A-09-638	AZ-638(*S*)			
A-09-658	AZ-658(*S*)			
A-09-910	AZ-910(*S*)			
A-09-915	AZ-915(*S*)			
A-09-615	**UT-615(*S*)**	UT		
A-09-736	UT-736(*S*)			
A-09-738	**UT-738(*S*)**			
A-09-745	UT-745(*S*)			
A-09-746	UT-746(*S*)			
A-09-597	**AZ-597(*R*)**	AZ	*ObLIS* full ORF [GenBank: AY693647, (5)]	(*R*)-(-)-linalool
A-09-625	AZ-625(*R*)			
A-09-630	AZ-630(*R*)			
A-09-912	**AZ-912(*R*)**			
A-09-946	AZ-946(*R*)			
A-09-680	UT-680(*R*)	UT		
A-09-719	**UT-719(*R*)**			
A-09-788	UT-788(*R*)			
A-09-789	UT-789(*R*)			
A-09-815	**UT-815(*R*)**			
A-09-1168	UT-1168(*R*)			
A-09-1170	UT-1170(*R*)			
A-09-1174	UT-1174(*R*)			
A-08-119	ir*MPK4*	UT	*Fragments of NaMPK4* [GenBank: HQ236013, (9)] *in inverted repeat orientation*	*

Lines in **bold**: selected for assays of oviposition preference and larval growth. *This line generally emits more all kinds of *N. attenuata* volatiles than WT plants.

Table S3. Primers used for qPCR or PCR amplification in this study.

Experiment	Gene	Primer	
qPCR	*NaLIS*	Forward	TACATGAGATCACCTTATAGGGCAC
		Reverse	TGCATAGATTTCCCCACGTCT
	NaGPPS1	Forward	CATTGAAATGATCCATACTGCAAGC
		Reverse	CCAGCCAGTACTGCCACTC
	NaGPPS2	Forward	TATGGGAAAAATTTGGGCTTGGC
		Reverse	TGGCATACAATATAGGGGCAGTT
	IF5A3F	Forward	GTCGGACGAAGAACACCATT
		Reverse	CACATCACAGTTGTGGGAGG
VIGS	*NaLIS*	Forward	TAGAACTAGTGGATCTGTGTCGCGGTAGCTAAAG A
		Reverse	CCCCCTCGAGGTCGAGGAGTGCATGTGCTCTCAGT
Transcript size	*NaLIS*-UT CDS	Forward	ATGGCAATGACTAGAGCACTCTCC
		Reverse	CTATTGTTCCGTGGCAAATTCAGA
	NaLIS-AZ CDS	Forward	ATGGCAATGACTAGAGCACTCTCC
		Reverse	CTACACATGCAACATAGACTTGATGT
	NaLIS-transcript	Forward	GCACTCTTTACAGATCCAAGAATGT
		Reverse	CTATTGTTCCGTGGCAAATTCAGA
N-terminal truncated	*NaLIS*-UT	Forward	CACCATTCAGGTTTCATGCGGAAGCTC
		Reverse	CTACACATGCAACATAGACTTGA
	NaLIS-AZ	Forward	CACCATTCAGGTTTCATGCGGAAGCTC
		Reverse	CTATTGTTCCGTGGCAAATTCAGA

References

1. Glawe GA, Zavala JA, Kessler A, Van Dam NM, & Baldwin IT (2003) Ecological costs and benefits correlated with trypsin protease inhibitor production in *Nicotiana attenuata*. *Ecology* 84(1):79-90.
2. Baldwin IT, Staszakkozinski L, & Davidson R (1994) Up in smoke .1. smoke-derived germination cues for postfire annual, *Nicotiana attenuata* Torr ex Watson. *J Chem Ecol* 20(9):2345-2371.
3. Zhou WW, Kügler A, McGale E, Haverkamp A, Knaden M, Guo H, Beran F, Yon F, Li R, Lackus N, Köllner TG, Bing J, Schuman MC, Hansson BS, Kessler D, Baldwin IT, & Xu SQ (2017) Tissue-specific emission of (*E*)-α-bergamotene helps resolve the dilemma when pollinators are also herbivores. *Curr Biol* 27(9):1336-1341.
4. Dudareva N, Cseke L, Blanc VM, & Pichersky E (1996) Evolution of floral scent in *Clarkia*: Novel patterns of S-linalool synthase gene expression in the *C. breweri* flower. *Plant Cell* 8(7):1137-1148.
5. Iijima Y, Davidovich-Rikanati R, Fridman E, Gang DR, Bar E, Lewinsohn E, & Pichersky E (2004) The biochemical and molecular basis for the divergent patterns in the biosynthesis of terpenes and phenylpropenes in the peltate glands of three cultivars of basil. *Plant Physiol* 136(3):3724-3736.
6. Gase K, Weinhold A, Bozorov T, Schuck S, & Baldwin IT (2011) Efficient screening of transgenic plant lines for ecological research. *Mol Ecol Resour* 11(5):890-902.
7. Krügel T, Lim M, Gase K, Halitschke R, & Baldwin IT (2002) Agrobacterium-mediated transformation of *Nicotiana attenuata*, a model ecological expression system. *Chemoecology* 12(4):177-183.
8. Bubner B, Gase K, Berger B, Link D, & Baldwin IT (2006) Occurrence of tetraploidy in *Nicotiana attenuata* plants after *Agrobacterium*-mediated transformation is genotype specific but independent of polysomaty of explant tissue. *Plant Cell Rep* 25(7):668-675.
9. Hettenhausen C, Baldwin IT, & Wu J (2012) Silencing *MPK4* in *Nicotiana attenuata* enhances photosynthesis and seed production but compromises abscisic acid-induced stomatal closure and guard cell-mediated resistance to *Pseudomonas syringae* pv tomato DC3000. *Plant Physiol* 158(2):759-776.
10. Schuman MC, Barthel K, & Baldwin IT (2012) Herbivory-induced volatiles function as defenses increasing fitness of the native plant *Nicotiana attenuata* in nature. *eLife* 1.
11. Kessler D, Kallenbach M, Diezel C, Rothe E, Murdock M, & Baldwin IT (2015) How scent and nectar influence floral antagonists and mutualists. *eLife* 4.
12. McGale E, Diezel C, Schuman MC, & Baldwin IT (2018) Cry1Ac production is costly for native plants attacked by non-Cry1Ac-targeted herbivores in the field. *New Phytol* 219(2):714-727.
13. Halitschke R, Schittko U, Pohnert G, Boland W, & Baldwin IT (2001) Molecular interactions between the specialist herbivore *Manduca sexta* (Lepidoptera, Sphingidae) and its natural host *Nicotiana attenuata*. III. Fatty acid-amino acid conjugates in herbivore oral secretions are necessary and sufficient for herbivore-specific plant responses. *Plant Physiol* 125(2):711-717.
14. Schittko U, Preston CA, & Baldwin IT (2000) Eating the evidence? *Manduca sexta* larvae can not disrupt specific jasmonate induction in *Nicotiana attenuata* by rapid consumption. *Planta* 210(2):343-346.
15. Van Dam NM, Horn M, Mares M, & Baldwin IT (2001) Ontogeny constrains systemic protease inhibitor response in *Nicotiana attenuata*. *J Chem Ecol* 27(3):547-568.
16. Kallenbach M, Oh Y, Eilers EJ, Veit D, Baldwin IT, & Schuman MC (2014) A robust, simple, high-throughput technique for time-resolved plant volatile analysis in field experiments. *Plant J* 78(6):1060-1072.

17. Kallenbach M, Veit D, Eilers EJ, & Schuman MC (2015) Application of silicone tubing for robust, simple, high-throughput, and time-resolved analysis of plant volatiles in field experiments. *Bio Protoc* 5(3).
18. Cheng R, Abney M, Palmer AA, & Skol AD (2011) QTLRel: an R package for genome-wide association studies in which relatedness is a concern. *BMC Genet* 12:66.
19. van Pinxteren M, Paschke A, & Popp P (2010) Silicone rod and silicone tube sorptive extraction. *J Chromatogr A* 1217(16):2589-2598.
20. Matsui K, Sugimoto K, Mano J, Ozawa R, & Takabayashi J (2012) Differential metabolisms of green leaf volatiles in injured and intact parts of a wounded leaf meet distinct ecophysiological requirements. *Plos One* 7(4).
21. Lücker J, Bouwmeester HJ, Schwab W, Blaas J, van der Plas LH, & Verhoeven HA (2001) Expression of *Clarkia* S-linalool synthase in transgenic petunia plants results in the accumulation of *S*-linalyl-β-D-glucopyranoside. *Plant J* 27(4):315-324.
22. Brockmoller T, Ling ZH, Li DP, Gaquerel E, Baldwin IT, & Xu SQ (2017) *Nicotiana attenuata* Data Hub (NaDH): an integrative platform for exploring genomic, transcriptomic and metabolomic data in wild tobacco. *BMC Genet* 18.
23. Xu SQ, Brockmoller T, Navarro-Quezada A, Kuhl H, Gase K, Ling ZH, Zhou WW, Kreitzer C, Stanke M, Tang HB, Lyons E, Pandey P, Pandey SP, Timmermann B, Gaquerel E, & Baldwin IT (2017) Wild tobacco genomes reveal the evolution of nicotine biosynthesis. *Proc Natl Acad Sci U S A* 114(23):6133-6138.
24. Li H & Durbin R (2009) Fast and accurate short read alignment with Burrows-Wheeler transform. *Bioinformatics* 25(14):1754-1760.
25. Holt C & Yandell M (2011) MAKER2: an annotation pipeline and genome-database management tool for second-generation genome projects. *BMC Bioinformatics* 12:491.
26. Stanke M, Keller O, Gunduz I, Hayes A, Waack S, & Morgenstern B (2006) AUGUSTUS: ab initio prediction of alternative transcripts. *Nucleic Acids Res* 34(Web Server issue):W435-W239.
27. Korf I (2004) Gene finding in novel genomes. *BMC Bioinformatics* 5:59.
28. Lomsadze A, Ter-Hovhannisyan V, Chernoff YO, & Borodovsky M (2005) Gene identification in novel eukaryotic genomes by self-training algorithm. *Nucleic Acids Res* 33(20):6494-6506.
29. Bray NL, Pimentel H, Melsted P, & Pachter L (2016) Near-optimal probabilistic RNA-seq quantification. *Nat Biotechnol* 34(5):525-527.
30. Quinlan AR & Hall IM (2010) BEDTools: a flexible suite of utilities for comparing genomic features. *Bioinformatics* 26(6):841-842.
31. Thorvaldsdottir H, Robinson JT, & Mesirov JP (2013) Integrative Genomics Viewer (IGV): high-performance genomics data visualization and exploration. *Brief Bioinform* 14(2):178-192.
32. Galis I, Schuman MC, Gase K, Hettenhausen C, Hartl M, Dinh ST, Wu J, Bonaventure G, & Baldwin IT (2013) The use of VIGS technology to study plant-herbivore interactions. *Methods Mol Biol* 975:109-137.
33. Krügel T, Lim M, Gase K, Halitschke R, & Baldwin IT (2002) Agrobacterium-mediated transformation of *Nicotiana attenuata*, a model ecological expression system. *Chemoecology* 12(4):177-183.
34. Zavala JA, Patankar AG, Gase K, & Baldwin IT (2004) Constitutive and inducible trypsin proteinase inhibitor production incurs large fitness costs in Nicotiana attenuata. *Proceedings of the National Academy of Sciences of the United States of America* 101(6):1607-1612.
35. Bubner B, Gase K, Berger B, Link D, & Baldwin IT (2006) Occurrence of tetraploidy in *Nicotiana attenuata* plants after *Agrobacterium*-mediated transformation is genotype specific but independent of polysomaty of explant tissue. *Plant cell reports* 25(7):668-675.

36. Gase K & Baldwin IT (2012) Transformational tools for next-generation plant ecology: manipulation of gene expression for the functional analysis of genes. *Plant Ecol Divers* 5(4):485-490.
37. Schäfer M, *et al.* (2013) 'Real time' genetic manipulation: a new tool for ecological field studies. *The Plant journal : for cell and molecular biology* 76(3):506-518.
38. Bell RA & Joachim FG (1976) Techniques for rearing laboratory colonies of tobacco hornworms and pink bollworms. *Ann Entomol Soc Am* 69(2):365-373.
39. Haverkamp A, Bing J, Badeke E, Hansson BS, & Knaden M (2016) Innate olfactory preferences for flowers matching proboscis length ensure optimal energy gain in a hawkmoth. *Nat Comm* 7:11644.
40. Metsalu T & Vilo J (2015) ClustVis: a web tool for visualizing clustering of multivariate data using Principal Component Analysis and heatmap. *Nucleic Acids Res* 43(W1):W566-W570.

Discussion

I will begin the discussion with an overview of the existing and evolving molecular tools in the genomics era, introduce some ecological and evolutionary conceptual frameworks, and discuss the results presented in this dissertation in the context of these models.

Ecology in the genomics era

The major technical theme in this dissertation is the use of multi-omic data, especially genomics and metabolomics to elucidate complex ecological interactions at a molecular level. The integration of genomics into ecological research took place in the beginning of this century, which gradually shifted the research focus towards investigating the genetic basis of organismal responses to natural environments (Tanksley, 1993; Mitchell-Olds et al., 2007), and testing functional hypotheses using genetically modified organisms. Around the same time, it became apparent that evolutionary processes can occur rapidly enough to influence ecological dynamics and vice versa, necessitating the inclusion of evolutionary considerations in ecological studies (Hairston Jr et al., 2005). This realization opened up new possibilities for ecology as a discipline to embrace genomic tools, allowing for the identification of genetic mechanisms associated with ecological traits. Furthermore, this approach provided insights into the population-scale effects of genetic factors, down to the resolution of individual genes.

The initial step of identifying genes associated with a specific trait of interest can be accomplished through the use of forward genetic approaches. This methodology typically involves conducting a screening process to identify a mutant phenotype within a population, which can arise naturally or be induced through artificial means, such as ethyl methanesulfonate-mutagenesis carried out in Arabidopsis plants (Campos et al., 2016). The population is subjected to phenotyping, and the causal mutations, genes, or quantitative trait loci (QTLs) responsible for the observed phenotype are identified using various genetic mapping techniques, fine mapping strategies, positional cloning, and other advanced genomic tools (Schneeberger, 2014; Pereira et al., 2020). Traditionally, positional cloning has been employed to identify the causal mutations, a process that is known for being laborious, expensive, and time-consuming due to the low recombination rates observed in the target regions (Lukowitz et al., 2000). However, with the advent of

genome sequencing, the identification of causal mutations can now be achieved rapidly and at a relatively low cost. By comparing the genomes of the sample of interest with an available reference genome using bioinformatic tools, the precise locus of genetic variants can be identified. While both the sequencing and computational costs have decreased rapidly in the last decade, analyzing large and complex genomes, such as those of polyploid plants still remains a major challenge (Kyriakidou et al., 2018). The advantage of employing a forward genetic approach is its ability to uncover novel genes that may not have been considered as candidates based on *a priori* knowledge. However, it is important to acknowledge the technical limitations associated with detecting loci of small effect, as highlighted in previous studies (Otto and Jones, 2000; Rockman, 2012). Another drawback of forward genetic approaches lies in their inherent bias towards phenotypes that exhibit readily observable differences between populations. This bias may lead to the overlooking of traits that are less apparent but still crucial for adaptive processes.

Another essential requirement for a successful forward genetic screen is a high-quality contiguous reference genome assembly that accurately detects variants and identifies candidate genes linked to the traits of interest. *Nicotiana attenuata*, which has undergone a genome triplication event, presents a significant technical challenge in this regard, due to high number of repeat regions, making the genome assembly process difficult with short reads, thereby resulting in a fragmented genome (Xu et al., 2017). In **Manuscript III**, we employed a synteny approach, as previously used to identify another terpene synthase gene (Zhou et al., 2017), where the variant genomic region was compared with the analogous *Solanum lycopersicum* genome to identify the causal gene associated with variations in linalool emissions. To solve this reliance on other genomes in identifying causal genes, we assembled a contiguous *N. attenuata* genome from PacBio long reads. Although long reads can make the overall genome assembly more contiguous, they are often error prone at random bases, and can thus lead to false positives while performing variant call (Korlach and Pacific Biosciences, 2013). To overcome this, we polished the assembly with short Illumina reads, and super-scaffolded it using BioNano optical maps to achieve a chromosome-length assembly. This improved genome was then used in **Manuscript II** to identify the causal gene (*NaJAR4*) associated with JA-Ile variation in the MAGIC population without relying on other genomes as previously done in **Manuscript III** and by Zhou et al. (2017).

In contrast, the goal in reverse genetics is to investigate the impact of induced variation within a specific gene and to infer its biological function. This can be achieved through techniques such as gene knockout, knockdown, or over-expression through various techniques such as RNA interference (RNAi), ectopic expression, or through genome editing such as CRISPR-Cas9 (McGinnis, 2010; Zhu et al., 2020). This allows researchers to hone in on the specific effects of the particular gene, enabling the direct assessment of its function in a biological process. The *N. attenuata* silenced lines used in this dissertation have been transformed using the stable RNAi approach, which makes it heritable and the turn around time is relatively fast, where phenotypes can be observed in

the T_1 generation (Gase et al., 2011). However, a disadvantage of the RNAi approach is that some genes can be resistant to silencing by exogenous RNA, probably because of sequence or structural features of these genes. Also, transcripts of genes that are similar in sequence to the target locus may be inadvertently co-silenced together with the actual target gene, leading to 'off-target' effect, thereby making it difficult to interpret the results.

Both forward and reverse genetic approaches serve as valuable tools in unraveling the intricacies of genetic adaptation. Their combined use allows us to achieve the broad objective to understand the fitness consequences of specific phenotypes, decipher the underlying genetic architecture, and comprehend the selective pressures influencing traits. While each approach offers valuable insights, they are inherently limited in providing a complete picture individually. Therefore, by synergistically combining these approaches, we can harness their collective power and gain a more comprehensive understanding of the complex puzzle of adaptation genetics (Barrett and Hoekstra, 2011). For example, forward genetics can identify novel genes and pathways underlying a specific phenotype, and reverse genetics can subsequently confirm the roles of these genes by manipulating their expression and studying the resulting ecological or fitness effect as employed in both **Manuscript II** and **Manuscript III**. Interestingly, two different mapping populations have been employed in these two studies, MAGIC population in **Manuscript II** and an AI-RIL population in **Manuscript III**. The *N. attenuata* MAGIC population captures a large portion of the genetic diversity of the species, and in general has been proven to be very powerful in dissecting genetic basis of various traits in other systems (Scott et al., 2020). Whereas, the AI-RIL is a bi-parental mapping population, which makes it more tractable both computationally and logistically, but comes at a cost of limited pool of genetic diversity compared to MAGIC population. The *N. attenuata* AI-RIL population consists of the well characterized UT and AZ genotypes as its parents, which in principle makes it a subset of the larger MAGIC population. By integrating information from these forward genetic tools, and complementing it with reverse genetic approaches, we can validate the functions of identified genes and gain a deeper understanding of the ecological processes in which they are involved and assess their impact on organismal fitness. Moreover, the emergence of high-throughput DNA/RNA sequencing technologies has facilitated the integration of forward and reverse genetics approaches rapidly and in a cost effective manner (Ben-Amar et al., 2016; Sahu et al., 2020).

DNA sequencing plays a dual role in unraveling both mechanistic and evolutionary aspects of biological systems. On one hand, DNA sequence provides a template for molecular biologist to derive mechanistic understanding of how biological processes occur at the molecular level. On the other hand, DNA sequence data also enables the study of evolutionary processes and the reconstruction of evolutionary relationships among organisms by studying the single nucleotide polymorphism (SNP) or conserved sequences between diverging populations or species. Additionally, DNA sequence can bring together these two camps into providing mechanistic insights into evolutionary change, such as the identification of genetic mutations which lead to variance in traits under selection, and

genomic rearrangements that drive evolutionary function. Thus it becomes a double edged sword and has led to numerous debates of scientists talking past each other. The source of the debate arises from the definition of the word "function" (Garson, 2016), which can be broadly delineated into two categories, **causal role** (CR), and **selected effect** (SE) (Garson, 2016).

In the context of the biological function of DNA, CR refers to the specific contribution or influence of a particular DNA sequence or gene on a biological process or phenotype. It refers to the direct cause-and-effect relationship between the DNA sequence and the observed effect. CR emphasizes the mechanistic understanding of how DNA sequences function in biological systems. On the other hand, SE relates to the evolutionary perspective of DNA function. It considers the role of DNA sequences in contributing to an organism's fitness and survival through natural selection. The SE focuses on the evolutionary consequences of DNA sequences, highlighting their ability to confer advantages or disadvantages in terms of adaptation, reproductive success and overall fitness.

This debate reached its pinnacle with the publication of the ENCODE project, which proposed that over 80% of the human genome was functional in the CR sense (ENCODE Project Consortium, 2012). However, contrasting this perspective, a significant body of literature suggests that a much smaller portion, at most 25% and likely even less, of the human genome is subject to selection and thus possesses a SE function (Doolittle and Brunet, 2017). The ENCODE project did not distinguish between the SE and CR viewpoints of function, sparking extensive discourse among biologists, particularly regarding the functional role of transposable elements (TEs), often regarded as "junk DNA" (Doolittle and Brunet, 2017). Although TEs contain expressed and regulated genes, their adaptations primarily serve their own propagation selfishly, and lack necessary positive contributions to the fitness of the host organisms in whose genomes they reside (Orgel and Crick, 1980). Consequently, when defining function, it is crucial to consider the specific frame of reference in which it is being evaluated. For example in **Manuscript II** we show that the *NaJAR4* locus does have significant fitness effect in environments lacking herbivores, thus one can argue that this locus has a SE function. However, the functional definition of the *NaLIS* locus investigated in **Manuscript III** should be limited to CR since we show how it affects linalool levels, but do not show a direct fitness effect associated with the locus. However, we note that the effect of *M. sexta* oviposition based on the plant's genetic background might ultimately result in fitness effect, but it needs to demonstrated.

The Selfish Gene model

"*We are survival machines – robot vehicles blindly programmed to preserve the selfish molecules known as genes. This is a truth which still fills me with astonishment.*"

– Richard Dawkins, The Selfish Gene

Richard Dawkins in his seminal book, "The Selfish Gene", presented the contrasting

roles of individual organisms and genes in the process of natural selection (Dawkins, 1976). To reconcile this conflict, Dawkins introduced the concepts of "replicator" and "vehicle." Replicators represent the fundamental units of selection and correspond to DNA, entities that persist and replicate, leading to lineages of identical copies with occasional random alterations. These replicators come together and form cooperative entities called "vehicles," which encompass higher organisms. The vehicles serve as the collective framework for the survival and propagation of replicators. It is worth noting that in this context, the term "gene" encompasses stretches of DNA that impact traits within an organism, including both coding and non-coding elements such as transposons and siRNAs, extending beyond the conventional notion of coding regions transcribed into proteins.

The notion of a genotype (the "vehicle") optimizing its fitness in relation to its environment can be enticing, however, this perspective can be problematic and overlooks a fundamental flaw. Individuals with optimal phenotypes will inevitably produce offspring with suboptimal phenotypes due to random mutations and recombination, resulting in reduced fitness, or due to change in the environment itself. In contrast, the concept of the selfish gene as an optimizer overcomes this challenge through gene-level selection, where multiple agents affecting conflicting traits evolve mechanisms that lead to an adaptive compromise at the individual level. Consequently, individuals can exhibit strong adaptation even if there isn't a specific trait they optimize (Dawkins, 1990; Haig, 2014). Similarly, in the context of plant-insect interactions, it may be tempting to favor an individual-centric evolutionary model over a gene-centric one, but as Haig argues that organismal phenotypes often arise as by-products of selection acting on multiple loci (Haig, 2014). This notion is empirically supported by the OS-elicited gene network analysis and subsequent metabolic response characterization presented in **Manuscript II**.

In **Manuscript II**, we identified four hub genes from an OS-elicited gene co-expression network. Upon silencing these genes using RNAi, the metabolic response of the silenced lines provided insights into the potential role of each of these genes in buffering the deleterious effect of the *NaJAR4* mutation through gene regulatory networks. This buffering mechanism closely aligns with the "parliament of genes" model, which offers a gene-centric perspective on evolution and highlights the ability of genes to suppress selfish genetic elements that may reduce the fitness of other genes in the organism (Leigh, 1971; Scott and West, 2019). Given that the other genes in the organism far outnumber the selfish genetic elements, there is a collective interest among these genes to suppress them, leading to a resolution of conflicts and ultimately favoring fitness maxima at the individual level (Strassmann and Queller, 2010; Queller and Strassmann, 2018). We propose that the conserved OS-induced gene co-expression network in natural accessions of *N. attenuata* is analogous to such a parliament of genes, potentially providing a buffering effect against the deleterious *NaJAR4* mutation against herbivory. In other words, for the deleterious *NaJAR4* allele, even though it selfishly tries to propagate itself, the effect is buffered by the larger "parliament of genes", that ultimately maximize the individual fitness. Furthermore, this model also hints at a large gene level interaction network at play, such as that of an

"omnigene" model (Boyle et al., 2017; Liu et al., 2019), as discussed in **Manuscript II**.

However, Dawkins notes that Darwinian selection does not directly operate on genes themselves, but through their effects, that is phenotypes. Natural selection favors certain genes over others not due to their intrinsic nature, but because of the consequences they bring about in their phenotypic effects in the real world (Dawkins, 1976). The formal Darwinian definition of "individual fitness" entails the production and propagation of new individuals, not just somatic survival of selfish genes. Very often these phenotypic effects can extend beyond individual organisms, thus making it important to understand an individual's fitness in an ecological context. To avoid philosophical conflicts, we need to employ a pluralistic view to have a holistic understanding of the system considering the alternative hypotheses at the same level of analysis (Sherman, 1988). Thus, rather than searching for a universal maximization mechanism underlying natural selection, it can be more fruitful to identify the specific biological circumstances where natural selection consistently produces phenotypes that potentially maximize fitness, such as in **Manuscript II** and **III**. By doing so, we can gain insights into the evolutionary history of populations exhibiting these phenotypes, leading to a more comprehensive understanding of the biological system, as proposed in **Manuscript I**.

For example, in **Manuscript III**, we show the role of linalool chemistry on oviposition patterns of *Manduca sexta*, which varied depending on the environment complexity. Plants producing (S)-(+)-linalool attracted more moths for oviposition, while an increase in (S)-(+)-linalool through genetic manipulation resulted in reduced oviposition. In contrast, (S)-(+)-linalool supplementation in the UT background led to moths being repelled in a wind-tunnel assay, but showed no effect in more complex environments. The impact of the (R)-(–)-linalool enantiomer on oviposition varied among AZ and UT plants, despite the higher (R)-(–)-linalool emissions in UT lines. Interestingly, in an outdoor tent experiment with all the WT and ectopic expression lines, there was no significant preference among different lines for oviposition; however, female moths tended to prefer the AZ background lines. Typically, in such a scenario, gravid female moths seek to maximize fitness by selecting host plants that can provide nourishment for their emerging larvae, ensuring survival. This selection is driven primarily by olfactory cues (Späthe et al., 2013), which also play a role in pollination for the plant, providing nectar as a reward, resulting in an antagonistic and mutualistic interaction between the host plant and the moth. However, for the moth, the selection pressure between these two behavior differ: oviposition and host selection can directly affects the fitness of the individual, whereas feeding behavior does not (Späthe et al., 2013). In contrast, for the plant, moth pollination offers an advantage in maintaining a diverse genetic pool through out-crossing, but at the same time oviposition leads to herbivory, incurring a fitness cost. Analyzing the foliar metabolic profile of these WT and ectopic expression lines challenged with *M. sexta* herbivory, and assessing their volatile bouquet's impact on predation rates of *M. sexta* larvae and eggs, we can quantitatively test how plants resolve this conflict and optimize their fitness.

It thus becomes essential to acknowledge and examine the presence of these

evolutionary conflict occurring within and between biological systems. Biological conflict arises from the inherent tension that exists between interacting organisms or selfish genetic elements, occurring at different levels, including between individuals, between species, or even within an individual organism as discussed. Such conflicts stem from the divergent interests and selective pressures acting on different entities, leading to competition, antagonism, or trade-offs (Queller and Strassmann, 2018). Investigating and elucidating these conflicts can provide key insights into the dynamics of ecological interactions, the evolution of traits, and the overall formation of biodiversity.

Growth defense trade off

In plant-herbivore interactions, a fundamental phenomenon that has been studied in great detail is the growth-defense trade-off (Züst and Agrawal, 2017). This trade-off refers to the allocation of often limited resources by plants, where they must strike a balance between investing in growth and allocating resources towards defense mechanisms against herbivores. Plants face a continual challenge of optimizing their growth for reproduction and survival while simultaneously defending themselves against herbivory (Cope et al., 2021). Allocating resources to defense traits such as physical barriers, chemical deterrents, or induced defenses can come at the cost of growth and reproductive potential, ultimately affecting their fitness. In order to understand the effect of herbivory on plant fitness and the underlying evolutionary process, we need to first understand and quantify the cost associated with plant defense.

Plant defensive traits or compounds require precursor molecules obtained from primary metabolism, together with energy and metabolites required for various other processes involved in the synthesis, modification, transport, and maintenance or storage of these metabolites. Consequently, the metabolic cost associated with these activities can be substantial and can act as a significant limiting factor in plant development (Gershenzon, 1993). At the same time, there is conflicting empirical evidence regarding whether such metabolic costs ultimately manifest as fitness effects (Koricheva, 2002). While it is commonly proposed that the direct competition for resources or allocation costs between two traits is the primary causal factor driving trade-offs, this perspective may oversimplify the intricate allocation processes in plants (Karban and Baldwin, 2007). For instance, when *N. attenuata* plants were induced with methyl jasmonate (MeJA) in hydroponic chambers, their allocation towards reproduction remained relatively unaffected despite the substantial increase in nitrogen allocation for nicotine production. Conversely, when these plants were grown in their natural habitats with varying soil nitrogen content, a significant difference in estimated fitness was observed between the two groups (Baldwin et al., 1998). Thus, evaluating the allocation costs within the appropriate environmental context becomes crucial. It is important to acknowledge that while resource availability serves as a limiting factor influencing trade-off decisions, phenotypic variation is also driven by biotic and abiotic interactions experienced by individuals over time and space. In this case, plants are required to balance resource allocation with the probability of

herbivore attacks, which ultimately shapes their fitness in a context-dependent manner.

In **Manuscript II**, we assessed the cost of induced defense by evaluating the activity of MeJA-induced trypsin protease inhibitor (TPI). TPI has been demonstrated as a potent defense mechanism against herbivores, working in synergy with other deterrents like nicotine (Steppuhn and Baldwin, 2007), and was associated with substantial fitness costs when plants are grown in competition (Zavala et al., 2004). We show that MeJA-induced *NaJAR4* variant lines exhibited a 37% increase in seed capsule production compared to lines carrying the intact *NaJAR4* allele when grown in an herbivore-free environment. This finding suggests that these variant lines may have adapted to their deficiency in *NaJAR4* mediated jasmonate (JA)-signaling, and when heavily induced with MeJA in this case, they exploit this deficiency to maximize their seed set. Additionally, we observed only minor differences in the induced metabolic defense response between the *NaJAR4* variant lines and the non-variant lines. This result revealed how the genetic background of an individual influences trade-offs and underscores the role of individual genotype in determining the allocation cost, which ultimately affects fitness in this particular case. It is worth noting that *N. attenuata* plants germinate post fire events, leading to competition among conspecifics for ephemeral resources. Therefore, to effectively assess fitness outcomes and growth-defense trade-offs in ecologically realistic conditions, experiments should be conducted in resource-limited environments. This concept aligns with Charles Darwin's observations in the Galápagos Islands, which formed the basis of "The Origin of Species", where he observed that adaptive traits evolved in species facing resource limitations, enabling them to maximize their fitness in such environments.

All these observations raises a fundamental question: why do these trade-offs exist in nature? A leading hypothesis suggests that trade-offs in fitness enhancing traits, including those across different environments, are essential for maintaining genetic diversity within a species (Fritz and Simms, 2012; Agrawal, 2020). Two decades earlier, when the growth-fitness trade-off associated with TPI was demonstrated by Zavala et al. (2004), it was not contextualized in its evolutionary context (discussed in Agrawal (2020)). **Manuscript II** attempts to address this gap by elucidating how TPI, which is regulated by jasmonoyl-L-isoleucine (JA-Ile) (Wang et al., 2007), which in turn is affected by *NaJAR4* variant allele which is maintained in natural populations under a balancing selection regime. Our results reveal substantial gene flow among populations harboring this allele at varying frequencies, suggesting that balancing selection resulting from environmental stochasticity and phenotypic plasticity, rather than frequency-dependent niche adaptations, contribute to the preservation of this variation in the gene pool of *N. attenuata*, consistent with the hypothesis. Although our glasshouse experiments demonstrate that a 50% reduction in TPI production can lead to a 37% increase in seed production under ecologically realistic conditions, it remains uncertain how plants truly benefit from the trade-off against TPI in the presence of multiple biotic and abiotic stresses in natural field conditions. Nevertheless, this genetic diversity potentially provides a reservoir for trait variation within populations which might manifest under certain

environmental conditions buffering emergent environmental stress, elegantly described as "evolutionary capacitance" (Bergman and Siegal, 2003).

Evolutionary trade-offs can also shape trait variation in higher trophic interactions by allocating limited resources towards different advantageous traits. A field study involving 16 milkweed species (*Asclepias* spp.) and its major herbivore (the aphid *Aphis nerii*) in different soil conditions with variable predator pressure demonstrated that the cascading effects of predators on plant biomass were not associated with predator-herbivore interactions, but rather with the trade-off between herbivore tolerance and the effects of soil fertility on plants (Mooney et al., 2010). Additionally, the emission of volatile organic compounds (VOCs), specifically sesquiterpenes, was found to positively correlate with the top-down effects of predators on plant biomass, providing a mechanistic insight into this interaction. Similarly, in *N. attenuata* natural accessions, OS treated VOCs from leaf headspace show substantial variation (Halitschke et al., 2000), which was also recapitulated in **Manuscript III**, and moreover, the emission of linalool significantly correlated with predation rates of *M. sexta* eggs and larvae. This variation in linalool emission was driven by allelic variation in the *NaLIS* gene between two well-characterized *N. attenuata* genotypes, UT and AZ. The UT genotype, harbors a 766 basepair deletion in one of the exons of the *NaLIS* gene, and emits only trace amounts of linalool. Interestingly, the AZ genotype is impaired in producing TPIs due to pseudogenation of the TPI gene but UT harbors an intact allele of the gene (Wu et al., 2007). This negative correlation between linalool emission and TPI production in these two accessions suggests an evolutionary trade-off within the *N. attenuata* populations. Indeed, previous research by Schuman et al. (2012) showed that when TPI production was silenced in plants with UT background, predation of *M. sexta* larvae and eggs by *Geocoris* spp. was higher compared to WT plants, which the authors hypothesize is due to *Geocoris* spp.'s preference for TPI-silenced line fed larvae, which are more nutritious. This hypothesis can be rigorously tested by planting the AZ and UT genotypes in their native habitats, and conducting predations assays involving the native predators, at the same time measuring the emitted VOCs.

Thus, a comprehensive understanding of the growth-defense trade-off employing natural populations, coupled with advanced genomic and metabolomic platforms, can provide both mechanistic insights into plant function, while also uncovering the broader ecological and evolutionary role of these trade-offs. This knowledge can offer valuable guidance for conserving global biodiversity in the face of rapidly changing world climate, and considering that plants often hold a central position in most ecosystems, they should thus be accorded a significant priority.

Conclusion and outlook

The advent of high-throughput sequencing, advanced chemical analysis techniques and remote sensing technologies has revolutionized ecological research and greatly enhanced our ability to test long standing hypotheses. Recently by integrating unbiased metabolomics and transcriptomics and applying sophisticated statistical tools, predictions

of optimal defense and moving target theories on plant defense were tested (Li et al., 2020). However, a major challenge lies in effectively integrating diverse data obtained from various platforms and formats across the genotype-phenotype continuum, performing robust data exploration and forming critical hypothesis, and analyzing and interpreting the final outcomes. To address this, it is imperative to incorporate more robust visualization tools, advanced multi-omics analysis approaches using better statistical models and bioinformatic tools, and provide them with high quality *a priori* information to reduce false positives. The manuscripts presented in this dissertation, provides a framework to evaluate natural variation in ecological and evolutionary context, which we subsequently apply to elucidate the role of natural variation in *N. attenuata* defense response, and also in its higher trophic interactions. We integrated high-throughput genomics, transcriptomics, and metabolomics together with field observation data on various ecological traits, and contextualized these natural variations with the natural history of the species.

Today, when sequencing genomes has become a routine procedure, we are entering the "pan-genomic" era, where we can simultaneously asses genetic variation associated with traits at a population scale, which was previously not captured through a single reference genome (Jin et al., 2023). Assimilating this wealth of data would now require researchers to critically develop robust alternative hypotheses at the same level of analysis (Sherman, 1988) and this presents an unprecedented opportunity to draw holistic inferences of organisms at a population level and drive conservation efforts of our biodiversity.

References

Agrawal, A.A., 2020. A scale-dependent framework for trade-offs, syndromes, and specialization in organismal biology. *Ecology* **101**, e02924.

Baldwin, I.T., Gorham, D., Schmelz, E.A., Lewandowski, C.A., Lynds, G.Y., 1998. Allocation of nitrogen to an inducible defense and seed production in *Nicotiana attenuata*. *Oecologia* **115**, 541–552.

Barrett, R.D., Hoekstra, H.E., 2011. Molecular spandrels: Tests of adaptation at the genetic level. *Nature Reviews Genetics* **12**, 767–780.

Ben-Amar, A., Daldoul, S., M Reustle, G., Krczal, G., Mliki, A., 2016. Reverse genetics and high throughput sequencing methodologies for plant functional genomics. *Current Genomics* **17**, 460–475.

Bergman, A., Siegal, M.L., 2003. Evolutionary capacitance as a general feature of complex gene networks. *Nature* **424**, 549–552.

Boyle, E.A., Li, Y.I., Pritchard, J.K., 2017. An expanded view of complex traits: from polygenic to omnigenic. *Cell* **169**, 1177–1186.

Campos, M.L., Yoshida, Y., Major, I.T., Ferreira, D. de O., Weraduwage, S.M., Froehlich, J.E., et al., 2016. Rewiring of jasmonate and phytochrome B signalling uncouples plant growth-defense tradeoffs. *Nature Communications* **7**, 1–10.

Cope, O.L., Keefover-Ring, K., Kruger, E.L., Lindroth, R.L., 2021. Growth–defense trade-offs shape population genetic composition in an iconic forest tree species. *Proceedings of the National Academy of Sciences* **118**, e2103162118.

Dawkins, R., 1990. Parasites, desiderata lists and the paradox of the organism. *Parasitology* **100**, S63–S73.

Dawkins, R., 1976. The Selfish Gene. Oxford University Press.

Doolittle, W.F., Brunet, T.D., 2017. On causal roles and selected effects: Our genome is mostly junk. *BMC biology* **15**, 1–9.

ENCODE Project Consortium, 2012. An integrated encyclopedia of DNA elements in the human genome. *Nature* **489**, 57.

Fritz, R.S., Simms, E.L., 2012. Plant resistance to herbivores and pathogens: Ecology, evolution, and genetics.
Garson, J., 2016. A critical overview of biological functions. Springer.
Gase, K., Weinhold, A., Bozorov, T., Schuck, S., Baldwin, I.T., 2011. Efficient screening of transgenic plant lines for ecological research. *Molecular Ecology Resources* **11**, 890–902.
Gershenzon, J., 1993. The cost of plant chemical defense against herbivory: A biochemical perspective, in: Insect-Plant Interactions. CRC Press, pp. 105–176.
Haig, D., 2014. Genetic dissent and individual compromise. *Biology & Philosophy* **29**, 233–239.
Hairston Jr, N.G., Ellner, S.P., Geber, M.A., Yoshida, T., Fox, J.A., 2005. Rapid evolution and the convergence of ecological and evolutionary time. *Ecology letters* **8**, 1114–1127.
Halitschke, R., Keßler, A., Kahl, J., Lorenz, A., Baldwin, I.T., 2000. Ecophysiological comparison of direct and indirect defenses in *Nicotiana attenuata*. *Oecologia* **124**, 408–417.
Jin, S., Han, Z., Hu, Y., Si, Z., Dai, F., He, L., et al., 2023. Structural variation (SV)-based pan-genome and GWAS reveal the impacts of SVs on the speciation and diversification of allotetraploid cottons. *Molecular Plant* **16**, 678–693.
Karban, R., Baldwin, I.T., 2007. Induced responses to herbivory. University of Chicago Press.
Koricheva, J., 2002. Meta-analysis of sources of variation in fitness costs of plant antiherbivore defenses. *Ecology* **83**, 176–190.
Korlach, J., Pacific Biosciences, 2013. Understanding accuracy in SMRT sequencing. *Pacific Biosciences* **2013**, 1–9.
Kyriakidou, M., Tai, H.H., Anglin, N.L., Ellis, D., Strömvik, M.V., 2018. Current strategies of polyploid plant genome sequence assembly. *Frontiers in plant science* **9**, 1660.
Leigh, E.G., 1971. Adaptation and diversity: Natural history and the mathematics of evolution. Freeman, Cooper San Francisco.
Li, D., Halitschke, R., Baldwin, I.T., Gaquerel, E., 2020. Information theory tests critical predictions of plant defense theory for specialized metabolism. *Science Advances* **6**, eaaz0381.
Liu, X., Li, Y.I., Pritchard, J.K., 2019. Trans effects on gene expression can drive omnigenic inheritance. *Cell* **177**, 1022–1034.e6.
Lukowitz, W., Gillmor, C.S., Scheible, W.-R., 2000. Positional cloning in arabidopsis. Why it feels good to have a genome initiative working for you. *Plant physiology* **123**, 795–806.
McGinnis, K.M., 2010. RNAi for functional genomics in plants. *Briefings in Functional Genomics* **9**, 111–117.
Mitchell-Olds, T., Willis, J.H., Goldstein, D.B., 2007. Which evolutionary processes influence natural genetic variation for phenotypic traits? *Nature Reviews Genetics* **8**, 845–856.
Mooney, K.A., Halitschke, R., Kessler, A., Agrawal, A.A., 2010. Evolutionary trade-offs in plants mediate the strength of trophic cascades. *Science* **327**, 1642–1644.
Orgel, L.E., Crick, F.H., 1980. Selfish DNA: the ultimate parasite. *Nature* **284**, 604–607.
Otto, S.P., Jones, C.D., 2000. Detecting the undetected: estimating the total number of loci underlying a quantitative trait. *Genetics* **156**, 2093–2107.
Pereira, R., Oliveira, J., Sousa, M., 2020. Bioinformatics and computational tools for next-generation sequencing analysis in clinical genetics. *Journal of Clinical Medicine* **9**, 132.
Queller, D.C., Strassmann, J.E., 2018. Evolutionary conflict. *Annual Review of Ecology, Evolution, and Systematics* **49**, 73–93.
Rockman, M.V., 2012. The QTN program and the alleles that matter for evolution: all that's gold does not glitter. *Evolution* **66**, 1–17.
Sahu, P.K., Sao, R., Mondal, S., Vishwakarma, G., Gupta, S.K., Kumar, V., et al., 2020. Next generation sequencing based forward genetic approaches for identification and mapping of causal mutations in crop plants: A comprehensive review. *Plants* **9**, 1355.
Schneeberger, K., 2014. Using next-generation sequencing to isolate mutant genes from forward genetic screens. *Nature Reviews Genetics* **15**, 662–676.
Schuman, M.C., Barthel, K., Baldwin, I.T., 2012. Herbivory-induced volatiles function as defenses increasing fitness of the native plant *Nicotiana attenuata* in nature. *eLife* **1**, e00007.
Scott, M.F., Ladejobi, O., Amer, S., Bentley, A.R., Biernaskie, J., Boden, S.A., et al., 2020. Multi-parent populations in crops: A toolbox integrating genomics and genetic mapping with breeding. *Heredity* **125**,

396–416.

Scott, T.W., West, S.A., 2019. Adaptation is maintained by the parliament of genes. *Nature Communications* **10**, 5163.

Sherman, P.W., 1988. The levels of analysis. *Animal Behaviour* **36**, 616–619.

Späthe, A., Reinecke, A., Olsson, S.B., Kesavan, S., Knaden, M., Hansson, B.S., 2013. Plant species-and status-specific odorant blends guide oviposition choice in the moth *Manduca sexta*. *Chemical senses* **38**, 147–159.

Steppuhn, A., Baldwin, I.T., 2007. Resistance management in a native plant: nicotine prevents herbivores from compensating for plant protease inhibitors. *Ecology Letters* **10**, 499–511.

Strassmann, J.E., Queller, D.C., 2010. The social organism: Congresses, parties, and committees. *Evolution* **64**, 605–616.

Tanksley, S.D., 1993. Mapping polygenes. *Annual Review of Genetics* **27**, 205–233.

Wang, L., Halitschke, R., Kang, J.-H., Berg, A., Harnisch, F., Baldwin, I.T., 2007. Independently silencing two JAR family members impairs levels of trypsin proteinase inhibitors but not nicotine. *Planta* **226**, 159–167.

Wu, J., Kang, J.-H., Hettenhausen, C., Baldwin, I.T., 2007. Nonsense-mediated mRNA decay (NMD) silences the accumulation of aberrant trypsin proteinase inhibitor mRNA in *Nicotiana attenuata*. *The Plant Journal* **51**, 693–706.

Xu, S., Brockmöller, T., Navarro-Quezada, A., Kuhl, H., Gase, K., Ling, Z., et al., 2017. Wild tobacco genomes reveal the evolution of nicotine biosynthesis. *Proceedings of the National Academy of Sciences* **114**, 6133–6138.

Zavala, J.A., Patankar, A.G., Gase, K., Baldwin, I.T., 2004. Constitutive and inducible trypsin proteinase inhibitor production incurs large fitness costs in *Nicotiana attenuata*. *Proceedings of the National Academy of Sciences* **101**, 1607–1612.

Zhou, W., Kügler, A., McGale, E., Haverkamp, A., Knaden, M., Guo, H., et al., 2017. Tissue-specific emission of (E)-α-bergamotene helps resolve the dilemma when pollinators are also herbivores. *Current Biology* **27**, 1336–1341.

Zhu, H., Li, C., Gao, C., 2020. Applications of CRISPR–Cas in agriculture and plant biotechnology. *Nature Reviews Molecular Cell Biology* **21**, 661–677.

Züst, T., Agrawal, A.A., 2017. Trade-offs between plant growth and defense against insect herbivory: an emerging mechanistic synthesis. *Annual Review of Plant Biology* **68**, 513–534.

Summary

Plants have been instrumental in shaping Earth's natural history, comprising a substantial portion of biomass and serving as the primary food source for heterotrophs. Insects, particularly herbivores, exert selective pressures on plants, driving the evolution of diverse defense strategies in them. These plant-insect interactions were first recognized by scientists in the 18th century, and later, in the 19th century, biologists began to appreciate the impact of plant chemistry on herbivore behavior, leading to the emergence of the field of chemical ecology.

This dissertation describes various aspects of plant-herbivore interactions in *N. attenuata* by examining natural variation through two mapping populations, and its implications on plant fitness and defense responses. We first define a framework to understand natural variation, specifically in the jasmonic acid (JA) pathway in an ecological context, and subsequently identify a genetic variation in the *NaJAR4* gene, which conjugates isoleucine to JA, thereby significantly affecting jasmonoyl-L-isoleucine (JA-Ile) levels. When elicited with methyl jasmonate, different *NaJAR4* variants in *N. attenuata* natural accessions exhibit varying fitness outcomes, which can be explained by a JA signaling-regulated growth defense trade-off. Transcriptome analysis of *Manduca sexta* oral secretions and regurgitant (OS)-elicited natural accessions of *N. attenuata* revealed that the *NaJAR4* mutation is embedded in a gene co-expression network coordinating defense responses against herbivory. By manipulating hub genes in the gene network we test the metabolic responses to OS-elicitation, which were either proportional to JA-Ile accumulations or made the plants constitutively induced. This suggests a possible buffering effect of the gene network on the *NaJAR4* mutation, which together with varying herbivory loads perhaps allow the mutation to persist in natural populations. Furthermore, from seed collections of natural populations spanning a decade, we find that these variants occur at variable frequencies, indicating that that balancing selection through spatio-temporal variation is acting on the *NaJAR4* loci. These results demonstrate the context-dependent nature of plant-herbivore interactions, where biotic and abiotic factors together with genetic variation influence plant fitness and defense responses.

Additionally, the dissertation explores the ecological importance of volatile organic compounds (VOC), uncovering natural variation in the *NaLIS* gene in *N. attenuata* plants that affects the emission of OS-elicited linalool from leaves, a common VOC, and

is significantly correlated with predation of *M. sexta* by native predators in the field. Furthermore, by manipulating the *NaLIS* gene, we demonstrate that the impact of linalool on *M. sexta* oviposition preference depends on the linalool chemistry, plant genetic background, and environmental complexity. Thus, the presence of enzymatically inactive variants like *NaJAR4* and *NaLIS*, together with evidence of balancing selection, highlights the dynamic interplay between genetic diversity, environmental complexity, and herbivore behavior in maintaining adaptive potential of plants in nature.

Zusammenfassung

Pflanzen haben maßgeblich die Naturgeschichte der Erde geprägt, indem sie einen erheblichen Teil der Biomasse ausmachen und als primäre Nahrungsquelle für Heterotrophe dienen. Insekten, insbesondere Herbivoren, üben selektiven Druck auf Pflanzen aus und treiben dadurch die Evolution verschiedener Abwehrstrategien voran. Diese Pflanzen-Insekten-Interaktionen wurden erstmals im 18. Jahrhundert von Wissenschaftlern erkannt, und später, im 19. Jahrhundert, begannen Biologen sich auf die Auswirkungen der Pflanzenchemie auf das Verhalten von Herbivoren zu fokusieren, was zur Entstehung des Fachgebiets der chemischen Ökologie führte.

Diese Dissertation beschreibt verschiedene Aspekte der Pflanzen-Herbivoren-Interaktionen in *Nicotiana attenuata*, indem natürliche Variationen in zwei Mapping-Populationen untersucht werden und ihre Auswirkungen auf die Fitness der Pflanzen und deren Abwehrreaktionen betrachtet werden. Zunächst wird ein Rahmenwerk definiert, um die natürliche Variation, insbesondere im Jasmonsäure-(JA)-Signalweg, im ökologischen Kontext zu verstehen. Anschließend wird eine genetische Variation im *NaJAR4*-Gen identifiziert, das Isoleucin an JA bindet und somit die Konzentration von Jasmonoyl-L-Isoleucin (JA-Ile) wesentlich beeinflusst. Bei Zugabe von Methyljasmonat zeigen unterschiedliche *NaJAR4*-Varianten in natürlichen *N. attenuata*-Linien unterschiedliche Fitnessergebnisse, die durch ein ausbalanciertes Wachstums-Abwehr-Verhältnis im Zusammenhang mit JA-Signalgebung erklärt werden können. Die Transkriptomanalyse von natürlichen *N. attenuata*-Linien, die mit oralen Sekrete (OS) von *Manduca sexta* Raupen induziert werden, zeigt, dass die *NaJAR4*-Mutation in ein Gen-Koexpressionsnetzwerks eingebettet ist, das Abwehrreaktionen gegen Pflanzenfresser koordiniert. Durch Manipulation von Schlüsselgenen im Gen-Netzwerk testen wir die metabolische Reaktion auf OS-Stimulation, die entweder proportional zur JA-Ile-Akkumulationen ausfallen oder die Pflanzen konstitutiv aktivieren. Dies deutet auf eine mögliche Pufferwirkung des Gen-Netzwerks auf die *NaJAR4*-Mutation hin, die zusammen mit der variierenden Herbivorenbelastung möglicherweise die Persistenz der Mutation in natürlichen Populationen ermöglicht. Darüber hinaus zeigt die Untersuchung von Sammlungen von natürlichen Populationen über eine Dekade hinweg, dass diese Varianten in variablen Frequenzen auftreten, was darauf hinweist, dass eine balancierende Selektion durch

räumlich-zeitliche Variation auf die *NaJAR4*-Loci einwirkt. Diese Ergebnisse zeigen die kontextabhängige Natur von Pflanzen-Herbivoren-Interaktionen, bei denen biotische und abiotische zusammen mit genetischer Variation die Fitness und Abwehrreaktionen der Pflanzen beeinflussen.

Darüber hinaus erforscht die Dissertation die ökologische Bedeutung flüchtiger organischer Verbindungen (VOC) und deckt eine natürliche Variation im *NaLIS*-Gen bei *N. attenuata*-Pflanzen auf, die die Emission von OS-induziertem Linalool aus Blättern beeinflusst, ein häufiges VOC, und signifikant mit der Prädation von *M. sexta* durch heimische Räuber im Feld korreliert. Durch Manipulation der NaLIS-Gen wird gezeigt, dass die Auswirkungen von Linalool auf die Eiablagepräferenz von *M. sexta* von der Linalool-Chemie, dem genetischen Hintergrund der Pflanze und der Umweltkomplexität abhängen. Die Existenz enzymatisch inaktiver Varianten wie *NaJAR4* und *NaLIS* sowie der Nachweis einer balancierten Selektion betont das dynamische Zusammenspiel von genetischer Vielfalt, Umweltkomplexität und Herbivorenverhalten zur Aufrechterhaltung des Anpassungspotenzials von Pflanzen in der Natur.

Bibliography

Aerts, N., Pereira Mendes, M., Van Wees, S.C., 2021. Multiple levels of crosstalk in hormone networks regulating plant defense. *The Plant Journal* **105**, 489–504.

Agrawal, A.A., 2020. A scale-dependent framework for trade-offs, syndromes, and specialization in organismal biology. *Ecology* **101**, e02924.

Ågren, J.A., 2016. Selfish genetic elements and the gene's-eye view of evolution. *Current Zoology* **62**, 659–665.

Aharoni, A., Giri, A.P., Deuerlein, S., Griepink, F., Kogel, W.-J. de, Verstappen, F.W., et al., 2003. Terpenoid metabolism in wild-type and transgenic *Arabidopsis plants*. *The Plant Cell* **15**, 2866–2884.

Aharoni, A., Giri, A.P., Verstappen, F.W., Bertea, C.M., Sevenier, R., Sun, Z., et al., 2004. Gain and loss of fruit flavor compounds produced by wild and cultivated strawberry species. *The Plant Cell* **16**, 3110–3131.

Allmann, S., Baldwin, I.T., 2010. Insects betray themselves in nature to predators by rapid isomerization of green leaf volatiles. *Science* **329**, 1075–1078.

Allmann, S., Späthe, A., Bisch-Knaden, S., Kallenbach, M., Reinecke, A., Sachse, S., et al., 2013. Feeding-induced rearrangement of green leaf volatiles reduces moth oviposition. *eLife* **2**, e00421.

Ament, K., Van Schie, C.C., Bouwmeester, H.J., Haring, M.A., Schuurink, R.C., 2006. Induction of a leaf specific geranylgeranyl pyrophosphate synthase and emission of (e, e)-4, 8, 12-trimethyltrideca-1, 3, 7, 11-tetraene in tomato are dependent on both jasmonic acid and salicylic acid signaling pathways. *Planta* **224**, 1197–1208.

An, L., Ahmad, R.M., Ren, H., Qin, J., Yan, Y., 2019. Jasmonate signal receptor gene family ZmCOIs restore male fertility and defense response of *Arabidopsis* mutant coi1-1. *Journal of Plant Growth Regulation* **38**, 479–493.

Aprotosoaie, A.C., Hăncianu, M., Costache, I.-I., Miron, A., 2014. Linalool: A review on a key odorant molecule with valuable biological properties. *Flavour and Fragrance Journal* **29**, 193–219.

Arabidopsis Genome Initiative, 2000. Analysis of the genome sequence of the flowering plant *Arabidopsis thaliana*. *Nature* **408**, 796–815.

Ashley, E.A., 2016. Towards precision medicine. *Nature Reviews Genetics* **17**, 507–522.

Bahulikar, R.A., Stanculescu, D., Preston, C.A., Baldwin, I.T., 2004. ISSR and AFLP analysis of the temporal and spatial population structure of the post-fire annual, *Nicotiana attenuata*, in SW Utah. *BMC Ecology* **4**, 12.

Bai, Y., Yang, C., Halitschke, R., Paetz, C., Kessler, D., Burkard, K., et al., 2022. Natural history–guided omics reveals plant defensive chemistry against leafhopper pests. *Science* **375**, eabm2948.

Baldwin, I.T., 2010. Plant volatiles. *Current Biology* **20**, R392–R397.

Baldwin, I.T., 2001. An ecologically motivated analysis of plant-herbivore interactions in native tobacco. *Plant Physiology* **127**, 1449–1458.

Baldwin, I.T., 1998. Jasmonate-induced responses are costly but benefit plants under attack in native populations. *Proceedings of the National Academy of Sciences* **95**, 8113–8118.

Baldwin, I.T., Gorham, D., Schmelz, E.A., Lewandowski, C.A., Lynds, G.Y., 1998. Allocation of nitrogen to an inducible defense and seed production in *Nicotiana attenuata*. *Oecologia* **115**, 541–552.

Baldwin, I.T., Karb, M., Ohnmeiss, T., 1994a. Allocation of ^{15}N from nitrate to nicotine: production and turnover of a damage-induced mobile defense. *Ecology* **75**, 1703–1713.

Baldwin, I.T., Morse, L., 1994. Up in smoke: II. Germination of *Nicotiana attenuata* in response to smoke-derived cues and nutrients in burned and unburned soils. *Journal of Chemical Ecology* **20**, 2373–2391.

Baldwin, I.T., Preston, C., Euler, M., Gorham, D., 1997a. Patterns and consequences of benzyl acetone floral emissions from *Nicotiana attenuata* plants. *Journal of Chemical Ecology* **23**, 2327–2343.

Baldwin, I.T., Schmelz, E.A., Ohnmeiss, T.E., 1994b. Wound-induced changes in root and shoot jasmonic acid pools correlate with induced nicotine synthesis in *Nicotiana sylvestris* spegazzini and comes. *Journal of Chemical Ecology* **20**, 2139–2157.

Baldwin, I.T., Staszak-Kozinski, L., Davidson, R., 1994c. Up in smoke: I. Smoke-derived germination cues for postfire annual, *Nicotiana attenuata* Torr. Ex. Watson. *Journal of Chemical Ecology* **20**, 2345–2371.

Baldwin, I.T., Zhang, Z.-P., Diab, N., Ohnmeiss, T.E., McCloud, E.S., Lynds, G.Y., et al., 1997b. Quantification, correlations and manipulations of wound-induced changes in jasmonic acid and nicotine in *Nicotiana sylvestris*. *Planta* **201**, 397–404.

Ballaré, C.L., Scopel, A.L., Stapleton, A.E., Yanovsky, M.J., 1996. Solar ultraviolet-B radiation affects seedling emergence, DNA integrity, plant morphology, growth rate, and attractiveness to herbivore insects in *Datura ferox*. *Plant Physiology* **112**, 161–170.

Bally, J., Nakasugi, K., Jia, F., Jung, H., Ho, S.Y.W., Wong, M., et al., 2015. The extremophile *Nicotiana benthamiana* has traded viral defence for early vigour. *Nature Plants* **1**, 1–6.

Bar-On, Y.M., Phillips, R., Milo, R., 2018. The biomass distribution on earth. *Proceedings of the National Academy of Sciences* **115**, 6506–6511.

Barrett, R.D., Hoekstra, H.E., 2011. Molecular spandrels: Tests of adaptation at the genetic level. *Nature Reviews Genetics* **12**, 767–780.

Barrett, R.D., Laurent, S., Mallarino, R., Pfeifer, S.P., Xu, C.C., Foll, M., et al., 2019. Linking a mutation to survival in wild mice. *Science* **363**, 499–504.

Barrio-Hernandez, I., Schwartzentruber, J., Shrivastava, A., Del-Toro, N., Gonzalez, A., Zhang, Q., et al., 2023. Network expansion of genetic associations defines a pleiotropy map of human cell biology. *Nature genetics* 1–10.

Barton, N.H., Etheridge, A.M., Véber, A., 2017. The infinitesimal model: Definition, derivation, and implications. *Theoretical Population Biology* **118**, 50–73.

Ben-Amar, A., Daldoul, S., M Reustle, G., Krczal, G., Mliki, A., 2016. Reverse genetics and high throughput sequencing methodologies for plant functional genomics. *Current Genomics* **17**, 460–475.

Berardi, A.E., Esfeld, K., Jäggi, L., Mandel, T., Cannarozzi, G.M., Kuhlemeier, C., 2021. Complex evolution of novel red floral color in *Petunia*. *The Plant Cell* **33**, 2273–2295.

Bergman, A., Siegal, M.L., 2003. Evolutionary capacitance as a general feature of complex gene networks. *Nature* **424**, 549–552.

Bhattacharya, S., Baldwin, I.T., 2012. The post-pollination ethylene burst and the continuation of floral advertisement are harbingers of non-random mate selection in *Nicotiana attenuata*. *The Plant Journal* **71**, 587–601.

Bhosale, R., Jewell, J.B., Hollunder, J., Koo, A.J.K., Vuylsteke, M., Michoel, T., et al., 2013. Predicting gene function from uncontrolled expression variation among individual wild-type *Arabidopsis* plants. *The Plant Cell* tpc–113.

Bisch-Knaden, S., Dahake, A., Sachse, S., Knaden, M., Hansson, B.S., 2018. Spatial representation of feeding and oviposition odors in the brain of a hawkmoth. *Cell Reports* **22**, 2482–2492.

Blázquez, M.A., Nelson, D.C., Weijers, D., 2020. Evolution of plant hormone response pathways. *Annual Review of Plant Biology* **71**, 327–353.

Bloomer, R.H., Lloyd, A.M., Symonds, V.V., 2014. The genetic architecture of constitutive and induced trichome density in two new recombinant inbred line populations of *Arabidopsis thaliana*: phenotypic plasticity, epistasis, and bidirectional leaf damage response. *BMC Plant Biology* **14**, 119.

Boachon, B., Junker, R.R., Miesch, L., Bassard, J.-E., Höfer, R., Caillieaudeaux, R., et al., 2015. *CYP76C1* (Cytochrome P450)-mediated linalool metabolism and the formation of volatile and soluble linalool oxides in *Arabidopsis* flowers: a strategy for defense against floral antagonists. *The Plant Cell* **27**, 2972–2990.

Boetzer, M., Pirovano, W., 2014. SSPACE-LongRead: scaffolding bacterial draft genomes using long read sequence information. *BMC Bioinformatics* **15**, 1–9.

Bonaventure, G., Baldwin, I.T., 2010. New insights into the early biochemical activation of jasmonic acid biosynthesis in leaves. *Plant Signaling & Behavior* **5**, 287–289.

Boonprab, K., Matsui, K., Akakabe, Y., Yotsukura, N., Kajiwara, T., 2003. Hydroperoxy-arachidonic acid mediated n-hexanal and (Z)-3-and (E)-2-nonenal formation in *Laminaria angustata*. *Phytochemistry* **63**, 669–678.

Borg-Karlson, A.-K., Unelius, C.R., Valterová, I., Nilsson, L.A., 1996. Floral fragrance chemistry in the early flowering shrub *Daphne mezereum*. *Phytochemistry* **41**, 1477–1483.

Bowman, J.L., Kohchi, T., Yamato, K.T., Jenkins, J., Shu, S., Ishizaki, K., et al., 2017. Insights into land plant evolution garnered from the *Marchantia polymorpha* genome. *Cell* **171**, 287–304.

Boyle, E.A., Li, Y.I., Pritchard, J.K., 2017. An expanded view of complex traits: from polygenic to omnigenic. *Cell* **169**, 1177–1186.

Brockmöller, T., Ling, Z., Li, D., Gaquerel, E., Baldwin, I.T., Xu, S., 2017. *Nicotiana attenuata* Data Hub (Na DH): an integrative platform for exploring genomic, transcriptomic and metabolomic data in wild tobacco. *BMC Genomics* **18**, 1–11.

Broman, K.W., 2010. Genetic map construction with R/qtl. *University of Wisconsin-Madison, Department of Biostatistics & Medical Informatics*.

Broman, K.W., Wu, H., Sen, Ś., Churchill, G.A., 2003. R/qtl: QTL mapping in experimental crosses. *Bioinformatics* **19**, 889–890.

Browse, J., 2009. The power of mutants for investigating jasmonate biosynthesis and signaling. *Phytochemistry* **70**, 1539–1546.

Bubner, B., Gase, K., Baldwin, I.T., 2004. Two-fold differences are the detection limit for determining transgene copy numbers in plants by real-time PCR. *BMC Biotechnology* **4**, 1–11.

Buchfink, B., Reuter, K., Drost, H.-G., 2021. Sensitive protein alignments at tree-of-life scale using DIAMOND. *Nature Methods* **18**, 366–368.

Cai, H., Des Marais, D.L., 2023. Revisiting regulatory coherence: accounting for temporal bias in plant gene co-expression analyses. *New Phytologist*.

Campbell, M.S., Holt, C., Moore, B., Yandell, M., 2014. Genome annotation and curation using MAKER and MAKER-P. *Current Protocols in Bioinformatics* **48**, 4–11.

Campos, M.L., Yoshida, Y., Major, I.T., Ferreira, D. de O., Weraduwage, S.M., Froehlich, J.E., et al., 2016. Rewiring of jasmonate and phytochrome B signalling uncouples plant growth-defense tradeoffs. *Nature Communications* **7**, 1–10.

Carroll, M.J., Schmelz, E.A., Meagher, R.L., Teal, P.E., 2006. Attraction of *Spodoptera frugiperda* larvae to volatiles from herbivore-damaged maize seedlings. *Journal of Chemical Ecology* **32**, 1911–1924.

Catchen, J., Amores, A., Bassham, S., 2020. Chromonomer: a tool set for repairing and enhancing assembled genomes through integration of genetic maps and conserved synteny. *G3: Genes, Genomes, Genetics* **10**, 4115–4128.

Charlton, A., 2004. Medicinal uses of tobacco in history. *Journal of the royal society of medicine* **97**, 292–296.

Chateigner, A., Lesage-Descauses, M.-C., Rogier, O., Jorge, V., Leplé, J.-C., Brunaud, V., et al., 2020. Gene expression predictions and networks in natural populations supports the omnigenic theory. *BMC Genomics* **21**, 1–16.

Chen, F., Tholl, D., Bohlmann, J., Pichersky, E., 2011. The family of terpene synthases in plants: A mid-size family of genes for specialized metabolism that is highly diversified throughout the kingdom. *The Plant Journal* **66**, 212–229.

Chen, F., Tholl, D., D'Auria, J.C., Farooq, A., Pichersky, E., Gershenzon, J., 2003. Biosynthesis and emission of terpenoid volatiles from *Arabidopsis* flowers. *The Plant Cell* **15**, 481–494.

Chen, H., Zhu, Z., Chen, J.-J., Yang, R., Luo, Q., Xu, J., et al., 2015. A multifunctional lipoxygenase from *Pyropia haitanensis*—The cloned and functioned complex eukaryotic algae oxylipin pathway enzyme. *Algal Research* **12**, 316–327.

Chini, A., Gimenez-Ibanez, S., Goossens, A., Solano, R., 2016. Redundancy and specificity in jasmonate signalling. *Current Opinion in Plant Biology* **33**, 147–156.

Cipollini, D., Walters, D., Voelckel, C., 2018. Costs of resistance in plants: from theory to evidence. *Annual Plant Reviews Online* 263–307.

Coley, P.D., Bryant, J.P., Chapin III, F.S., 1985. Resource availability and plant antiherbivore defense. *Science* **230**, 895–899.

Cope, O.L., Keefover-Ring, K., Kruger, E.L., Lindroth, R.L., 2021. Growth–defense trade-offs shape population genetic composition in an iconic forest tree species. *Proceedings of the National Academy of Sciences* **118**, e2103162118.

Cortés Llorca, L., Li, R., Yon, F., Schäfer, M., Halitschke, R., Robert, C.A., et al., 2020. ZEITLUPE facilitates the rhythmic movements of *Nicotiana attenuata* flowers. *The Plant Journal* **103**, 308–322.

Crossa, J., Pérez-Rodríguez, P., Cuevas, J., Montesinos-López, O., Jarquín, D., Campos, G. de los, et al., 2017. Genomic selection in plant breeding: Methods, models, and perspectives. *Trends in Plant Science* **22**, 961–975.

Dahl, C.C. von, Winz, R.A., Halitschke, R., Kühnemann, F., Gase, K., Baldwin, I.T., 2007. Tuning the herbivore-induced ethylene burst: the role of transcript accumulation and ethylene perception in *Nicotiana attenuata*. *The Plant Journal* **51**, 293–307.

Darwin, C., 1859. On the Origin of Species. Routledge.

Dawkins, R., 1990. Parasites, desiderata lists and the paradox of the organism. *Parasitology* **100**, S63–S73.

Dawkins, R., 1976. The Selfish Gene. Oxford University Press.

De Moraes, C.M., Mescher, M.C., Tumlinson, J.H., 2001. Caterpillar-induced nocturnal plant volatiles repel conspecific females. *Nature* **410**, 577–580.

Delfin, J.C., Kanno, Y., Seo, M., Kitaoka, N., Matsuura, H., Tohge, T., et al., 2022. AtGH3.10 is another

jasmonic acid-amido synthetase in *Arabidopsis thaliana*. *The Plant Journal* **110**, 1082–1096.
Devlin, B., Roeder, K., 1999. Genomic control for association studies. *Biometrics* **55**, 997–1004.
Dhakarey, R., Kodackattumannil Peethambaran, P., Riemann, M., 2016. Functional analysis of jasmonates in rice through mutant approaches. *Plants* **5**, 15.
Dicke, M., Baldwin, I.T., 2010. The evolutionary context for herbivore-induced plant volatiles: Beyond the "cry for help." *Trends in Plant Science* **15**, 167–175.
Đinh, S.T., Galis, I., Baldwin, I.T., 2013. UVB radiation and 17-hydroxygeranyllinalool diterpene glycosides provide durable resistance against mirid (*Tupiocoris notatus*) attack in field-grown *Nicotiana attenuata* plants. *Plant, Cell & Environment* **36**, 590–606.
Doolittle, W.F., Brunet, T.D., 2017. On causal roles and selected effects: Our genome is mostly junk. *BMC biology* **15**, 1–9.
Du, Y., Poppy, G.M., Powell, W., Pickett, J.A., Wadhams, L.J., Woodcock, C.M., 1998. Identification of semiochemicals released during aphid feeding that attract parasitoid *Aphidius ervi*. *Journal of Chemical Ecology* **24**, 1355–1368.
Duan, H., Huang, M.-Y., Palacio, K., Schuler, M.A., 2005. Variations in *CYP74B2* (hydroperoxide lyase) gene expression differentially affect hexenal signaling in the Columbia and Landsberg erecta ecotypes of *Arabidopsis*. *Plant Physiology* **139**, 1529–1544.
Dudareva, N., Cseke, L., Blanc, V.M., Pichersky, E., 1996. Evolution of floral scent in *Clarkia*: novel patterns of S-linalool synthase gene expression in the *C. breweri* flower. *The Plant Cell* **8**, 1137–1148.
Dudareva, N., Martin, D., Kish, C.M., Kolosova, N., Gorenstein, N., Fäldt, J., et al., 2003. (E)-β-Ocimene and myrcene synthase genes of floral scent biosynthesis in snapdragon: function and expression of three terpene synthase genes of a new terpene synthase subfamily. *The Plant Cell* **15**, 1227–1241.
Ehrlich, P.R., Raven, P.H., 1964. Butterflies and plants: A study in coevolution. *Evolution* 586–608.
ENCODE Project Consortium, 2012. An integrated encyclopedia of DNA elements in the human genome. *Nature* **489**, 57.
Erb, M., Kliebenstein, D.J., 2020. Plant secondary metabolites as defenses, regulators, and primary metabolites: the blurred functional trichotomy. *Plant Physiology* **184**, 39–52.
Exposito-Alonso, M., Booker, T.R., Czech, L., Gillespie, L., Hateley, S., Kyriazis, C.C., et al., 2022. Genetic diversity loss in the Anthropocene. *Science* **377**, 1431–1435.
Fagny, M., Austerlitz, F., 2021. Polygenic adaptation: Integrating population genetics and gene regulatory networks. *Trends in Genetics* **37**, 631–638.
Falara, V., Akhtar, T.A., Nguyen, T.T.H., Spyropoulou, E.A., Bleeker, P.M., Schauvinhold, I., et al., 2011. The tomato terpene synthase gene family. *Plant Physiology* **157**, 770–789.
Fang, C., Zhang, H., Wan, J., Wu, Y., Li, K., Jin, C., et al., 2016. Control of leaf senescence by an MeOH-Jasmonates cascade that is epigenetically regulated by *OsSRT1* in rice. *Molecular Plant* **9**, 1366–1378.
Field, C.B., Behrenfeld, M.J., Randerson, J.T., Falkowski, P., 1998. Primary production of the biosphere: Integrating terrestrial and oceanic components. *Science* **281**, 237–240.
File, A.L., Murphy, G.P., Dudley, S.A., 2012. Fitness consequences of plants growing with siblings: reconciling kin selection, niche partitioning and competitive ability. *Proceedings of the Royal Society B: Biological Sciences* **279**, 209–218.
Fisher, R.A., 1919. The correlation between relatives on the supposition of Mendelian inheritance. *Earth and Environmental Science Transactions of the Royal Society of Edinburgh* **52**, 399–433.
Fonseca, S., Chini, A., Hamberg, M., Adie, B., Porzel, A., Kramell, R., et al., 2009. (+)-7-iso-Jasmonoyl-L-isoleucine is the endogenous bioactive jasmonate. *Nature Chemical Biology* **5**, 344–350.
Fox, B.W., Ponomarova, O., Lee, Y.-U., Zhang, G., Giese, G.E., Walker, M., et al., 2022. *C. elegans* as a model for inter-individual variation in metabolism. *Nature* **607**, 571–577.
Fraenkel, G.S., 1959. The Raison d'Etre of Secondary Plant Substances: These odd chemicals arose as a means of protecting plants from insects and now guide insects to food. *Science* **129**, 1466–1470.
Fragoso, V., Rothe, E., Baldwin, I.T., Kim, S.-G., 2014. Root jasmonic acid synthesis and perception regulate folivore-induced shoot metabolites and increase *Nicotiana attenuata* resistance. *New Phytologist* **202**, 1335–1345.
Fritz, R.S., Simms, E.L., 2012. Plant resistance to herbivores and pathogens: Ecology, evolution, and genetics.
Gaquerel, E., Heiling, S., Schoettner, M., Zurek, G., Baldwin, I.T., 2010. Development and validation of a liquid chromatography- electrospray ionization- time-of-flight mass spectrometry method for induced changes in *Nicotiana attenuata* leaves during simulated herbivory. *Journal of Agricultural and Food Chemistry* **58**, 9418–9427.
Garson, J., 2016. A critical overview of biological functions. Springer.
Gasch, A.P., Payseur, B.A., Pool, J.E., 2016. The power of natural variation for model organism biology. *Trends*

in Genetics **32**, 147–154.
Gase, K., Baldwin, I.T., 2012. Transformational tools for next-generation plant ecology: manipulation of gene expression for the functional analysis of genes. *Plant Ecology & Diversity* **5**, 485–490.
Gase, K., Weinhold, A., Bozorov, T., Schuck, S., Baldwin, I.T., 2011. Efficient screening of transgenic plant lines for ecological research. *Molecular Ecology Resources* **11**, 890–902.
Geng, X., Jin, L., Shimada, M., Kim, M.G., Mackey, D., 2014. The phytotoxin coronatine is a multifunctional component of the virulence armament of *Pseudomonas syringae*. *Planta* **240**, 1149–1165.
Gershenzon, J., 1993. The cost of plant chemical defense against herbivory: A biochemical perspective, in: Insect-Plant Interactions. CRC Press, pp. 105–176.
Giglio, A., Brandmayr, P., Dalpozzo, R., Sindona, G., Tagarelli, A., Talarico, F., et al., 2009. The defensive secretion of *Carabus lefebvrei* Dejean 1826 pupa (Coleoptera, Carabidae): gland ultrastructure and chemical identification. *Microscopy Research and Technique* **72**, 351–361.
Gilardoni, P.A., Hettenhausen, C., Baldwin, I.T., Bonaventure, G., 2011. *Nicotiana attenuata* LECTIN RECEPTOR KINASE1 suppresses the insect-mediated inhibition of induced defense responses during *Manduca sexta* herbivory. *The Plant Cell* **23**, 3512–3532.
Ginglinger, J.-F., Boachon, B., Höfer, R., Paetz, C., Köllner, T.G., Miesch, L., et al., 2013. Gene coexpression analysis reveals complex metabolism of the monoterpene alcohol linalool in *Arabidopsis* flowers. *The Plant Cell* **25**, 4640–4657.
Giri, A.P., Wunsche, H., Mitra, S., Zavala, J.A., Muck, A., Svatoš, A., et al., 2006. Molecular interactions between the specialist herbivore *Manduca sexta* (Lepidoptera, Sphingidae) and its natural host *Nicotiana attenuata*. VII. Changes in the plant's proteome. *Plant Physiology* **142**, 1621–1641.
Glawe, G.A., Zavala, J.A., Kessler, A., Van Dam, N.M., Baldwin, I.T., 2003. Ecological costs and benefits correlated with trypsin protease inhibitor production in *Nicotiana attenuata*. *Ecology* **84**, 79–90.
Gonzalez, L.E., Keller, K., Chan, K.X., Gessel, M.M., Thines, B.C., 2017. Transcriptome analysis uncovers *Arabidopsis* F-BOX STRESS INDUCED 1 as a regulator of jasmonic acid and abscisic acid stress gene expression. *BMC Genomics* **18**, 1–15.
Haig, D., 2014. Genetic dissent and individual compromise. *Biology & Philosophy* **29**, 233–239.
Hairston Jr, N.G., Ellner, S.P., Geber, M.A., Yoshida, T., Fox, J.A., 2005. Rapid evolution and the convergence of ecological and evolutionary time. *Ecology letters* **8**, 1114–1127.
Halitschke, R., Baldwin, I.T., 2003. Antisense LOX expression increases herbivore performance by decreasing defense responses and inhibiting growth-related transcriptional reorganization in *Nicotiana attenuata*. *The Plant Journal* **36**, 794–807.
Halitschke, R., Keßler, A., Kahl, J., Lorenz, A., Baldwin, I.T., 2000. Ecophysiological comparison of direct and indirect defenses in *Nicotiana attenuata*. *Oecologia* **124**, 408–417.
Halitschke, R., Schittko, U., Pohnert, G., Boland, W., Baldwin, I.T., 2001. Molecular interactions between the specialist herbivore *Manduca sexta* (Lepidoptera, Sphingidae) and its natural host *Nicotiana attenuata*. III. Fatty acid-amino acid conjugates in herbivore oral secretions are necessary and sufficient for herbivore-specific plant responses. *Plant Physiology* **125**, 711–717.
Halitschke, R., Stenberg, J.A., Kessler, D., Kessler, A., Baldwin, I.T., 2008. Shared signals–"alarm calls" from plants increase apparency to herbivores and their enemies in nature. *Ecology Letters* **11**, 24–34.
Hartmann, T., 2008. The lost origin of chemical ecology in the late 19th century. *Proceedings of the National Academy of Sciences* **105**, 4541–4546.
Haverkamp, A., Hansson, B.S., Knaden, M., 2018. Combinatorial codes and labeled lines: How insects use olfactory cues to find and judge food, mates, and oviposition sites in complex environments. *Frontiers in Physiology* **9**, 49.
He, J., Fandino, R.A., Halitschke, R., Luck, K., Köllner, T.G., Murdock, M.H., et al., 2019. An unbiased approach elucidates variation in (S)-(+)-linalool, a context-specific mediator of a tri-trophic interaction in wild tobacco. *Proceedings of the National Academy of Sciences* **116**, 14651–14660.
Heiling, S., Schuman, M.C., Schoettner, M., Mukerjee, P., Berger, B., Schneider, B., et al., 2010. Jasmonate and ppHsystemin regulate key malonylation steps in the biosynthesis of 17-hydroxygeranyllinalool diterpene glycosides, an abundant and effective direct defense against herbivores in *Nicotiana attenuata*. *The Plant Cell* **22**, 273–292.
Herms, D.A., Mattson, W.J., 1992. The dilemma of plants: to grow or defend. *The Quarterly Review of Biology* **67**, 283–335.
Hettenhausen, C., Baldwin, I.T., Wu, J., 2012. Silencing *MPK4* in *Nicotiana attenuata* enhances photosynthesis and seed production but compromises abscisic acid-induced stomatal closure and guard cell-mediated resistance to Pseudomonas syringae pv tomato DC3000. *Plant Physiology* **158**, 759–776.
Holopainen, J.K., Gershenzon, J., 2010. Multiple stress factors and the emission of plant VOCs. *Trends in Plant Science* **15**, 176–184.
Hosmani, P.S., Flores-Gonzalez, M., Geest, H. van de, Maumus, F., Bakker, L.V., Schijlen, E., et al., 2019. An

improved de novo assembly and annotation of the tomato reference genome using single-molecule sequencing, hi-c proximity ligation and optical maps. *bioRxiv*. https://doi.org/10.1101/767764
Howe, G.A., Major, I.T., Koo, A.J., 2018. Modularity in jasmonate signaling for multistress resilience. *Annual Review of Plant Biology* **69**, 387–415.
Huang, X.-Z., Xiao, Y.-T., Köllner, T.G., Jing, W.-X., Kou, J.-F., Chen, J.-Y., et al., 2018. The terpene synthase gene family in *Gossypium hirsutum* harbors a linalool synthase GhTPS12 implicated in direct defence responses against herbivores. *Plant, Cell & Environment* **41**, 261–274.
Iijima, Y., Davidovich-Rikanati, R., Fridman, E., Gang, D.R., Bar, E., Lewinsohn, E., et al., 2004. The biochemical and molecular basis for the divergent patterns in the biosynthesis of terpenes and phenylpropenes in the peltate glands of three cultivars of basil. *Plant Physiology* **136**, 3724–3736.
Jin, S., Han, Z., Hu, Y., Si, Z., Dai, F., He, L., et al., 2023. Structural variation (SV)-based pan-genome and GWAS reveal the impacts of SVs on the speciation and diversification of allotetraploid cottons. *Molecular Plant* **16**, 678–693.
Joo, Y., Schuman, M.C., Goldberg, J.K., Kim, S.-G., Yon, F., Brütting, C., et al., 2018. Herbivore-induced volatile blends with both "fast" and "slow" components provide robust indirect defence in nature. *Functional Ecology* **32**, 136–149.
Joseph, B., Corwin, J.A., Li, B., Atwell, S., Kliebenstein, D.J., 2013. Cytoplasmic genetic variation and extensive cytonuclear interactions influence natural variation in the metabolome. *eLife* **2**, e00776.
Junker, R.R., Gershenzon, J., Unsicker, S.B., 2011. Floral odor bouquet loses its ant repellent properties after inhibition of terpene biosynthesis. *Journal of Chemical Ecology* **37**, 1323–1331.
Kaiser, R., 1993. The scent of orchids: Olfactory and chemical investigations. Elsevier Science Publishers BV.
Kallenbach, M., Alagna, F., Baldwin, I.T., Bonaventure, G., 2010. *Nicotiana attenuata* SIPK, WIPK, NPR1, and fatty acid-amino acid conjugates participate in the induction of jasmonic acid biosynthesis by affecting early enzymatic steps in the pathway. *Plant Physiology* **152**, 96–106.
Kallenbach, M., Bonaventure, G., Gilardoni, P.A., Wissgott, A., Baldwin, I.T., 2012. *Empoasca* leafhoppers attack wild tobacco plants in a jasmonate-dependent manner and identify jasmonate mutants in natural populations. *Proceedings of the National Academy of Sciences* **109**, E1548–E1557.
Kang, J.-H., Liu, G., Shi, F., Jones, A.D., Beaudry, R.M., Howe, G.A., 2010. The tomato odorless-2 mutant is defective in trichome-based production of diverse specialized metabolites and broad-spectrum resistance to insect herbivores. *Plant Physiology* **154**, 262–272.
Kang, J.-H., Wang, L., Giri, A., Baldwin, I.T., 2006. Silencing threonine deaminase and *JAR4* in *Nicotiana attenuata* impairs jasmonic acid–isoleucine–mediated defenses against *Manduca sexta*. *The Plant Cell* **18**, 3303–3320.
Karban, R., Baldwin, I.T., 2007. Induced responses to herbivory. University of Chicago Press.
Katoh, K., Standley, D.M., 2013. MAFFT multiple sequence alignment software version 7: improvements in performance and usability. *Molecular Biology and Evolution* **30**, 772–780.
Katsir, L., Schilmiller, A.L., Staswick, P.E., He, S.Y., Howe, G.A., 2008. *COI1* is a critical component of a receptor for jasmonate and the bacterial virulence factor coronatine. *Proceedings of the National Academy of Sciences* **105**, 7100–7105.
Katz, E., Knapp, A., Lensink, M., Keller, C.K., Stefani, J., Li, J.-J., et al., 2022. Genetic variation underlying differential ammonium and nitrate responses in *Arabidopsis* thaliana. *The Plant Cell* **34**, 4696–4713.
Kaur, H., Heinzel, N., Schöttner, M., Baldwin, I.T., Gális, I., 2010. R2R3-NaMYB8 regulates the accumulation of phenylpropanoid-polyamine conjugates, which are essential for local and systemic defense against insect herbivores in *Nicotiana attenuata*. *Plant Physiology* **152**, 1731–1747.
Kemmeren, P., Sameith, K., Pasch, L.A.L. van de, Benschop, J.J., Lenstra, T.L., Margaritis, T., et al., 2014. Large-scale genetic perturbations reveal regulatory networks and an abundance of gene-specific repressors. *Cell* **157**, 740–752.
Kerwin, R., Feusier, J., Corwin, J., Rubin, M., Lin, C., Muok, A., et al., 2015. Natural genetic variation in *Arabidopsis thaliana* defense metabolism genes modulates field fitness. *eLife* **4**, e05604.
Kessler, A., Baldwin, I.T., 2002. Plant responses to insect herbivory: the emerging molecular analysis. *Annual Review of Plant Biology* **53**, 299–328.
Kessler, A., Baldwin, I.T., 2001. Defensive function of herbivore-induced plant volatile emissions in nature. *Science* **291**, 2141–2144.
Kessler, A., Halitschke, R., Baldwin, I.T., 2004. Silencing the jasmonate cascade: Induced plant defenses and insect populations. *Science* **305**, 665–668.
Kessler, A., Heil, M., 2011. The multiple faces of indirect defences and their agents of natural selection. *Functional Ecology* **25**, 348–357.
Kessler, A., Mueller, M.B., Kalske, A., Chautá, A., 2023. Volatile-mediated plant–plant communication and higher-level ecological dynamics. *Current Biology* **33**, R519–R529.
Kessler, D., 2012. Context dependency of nectar reward-guided oviposition. *Entomologia Experimentalis et*

Applicata **144**, 112–122.
Kessler, D., Bhattacharya, S., Diezel, C., Rothe, E., Gase, K., Schöttner, M., et al., 2012. Unpredictability of nectar nicotine promotes outcrossing by hummingbirds in *Nicotiana attenuata*. *The Plant Journal* **71**, 529–538.
Kessler, D., Diezel, C., Baldwin, I.T., 2010. Changing pollinators as a means of escaping herbivores. *Current Biology* **20**, 237–242.
Kessler, D., Kallenbach, M., Diezel, C., Rothe, E., Murdock, M., Baldwin, I.T., 2015. How scent and nectar influence floral antagonists and mutualists. *eLife* **4**, e07641.
Kim, D., Paggi, J.M., Park, C., Bennett, C., Salzberg, S.L., 2019. Graph-based genome alignment and genotyping with HISAT2 and HISAT-genotype. *Nature Biotechnology* **37**, 907–915.
Kneeshaw, S., Soriano, G., Monte, I., Hamberg, M., Zamarreño, Á.M., García-Mina, J.M., et al., 2022. Ligand diversity contributes to the full activation of the jasmonate pathway in *Marchantia polymorpha*. *Proceedings of the National Academy of Sciences* **119**, e2202930119.
Knudsen, C., Gallage, N.J., Hansen, C.C., Møller, B.L., Laursen, T., 2018. Dynamic metabolic solutions to the sessile life style of plants. *Natural Product Reports* **35**, 1140–1155.
Knudsen, J.T., Eriksson, R., Gershenzon, J., Ståhl, B., 2006. Diversity and distribution of floral scent. *The Botanical Review* **72**, 1–120.
Knudsen, J.T., Tollsten, L., 1993. Trends in floral scent chemistry in pollination syndromes: Floral scent composition in moth-pollinated taxa. *Botanical Journal of the Linnean Society* **113**, 263–284.
Koenig, C., Hirsh, A., Bucks, S., Klinner, C., Vogel, H., Shukla, A., et al., 2015. A reference gene set for chemosensory receptor genes of *Manduca sexta*. *Insect Biochemistry and Molecular Biology* **66**, 51–63.
Koo, A.J., Cooke, T.F., Howe, G.A., 2011. Cytochrome P450 CYP94B3 mediates catabolism and inactivation of the plant hormone jasmonoyl-L-isoleucine. *Proceedings of the National Academy of Sciences* **108**, 9298–9303.
Koren, S., Walenz, B.P., Berlin, K., Miller, J.R., Bergman, N.H., Phillippy, A.M., 2017. Canu: scalable and accurate long-read assembly via adaptive k-mer weighting and repeat separation. *Genome Research* **27**, 722–736.
Koricheva, J., 2002. Meta-analysis of sources of variation in fitness costs of plant antiherbivore defenses. *Ecology* **83**, 176–190.
Korlach, J., Pacific Biosciences, 2013. Understanding accuracy in SMRT sequencing. *Pacific Biosciences* **2013**, 1–9.
Koschier, E.H., De Kogel, W.J., Visser, J.H., 2000. Assessing the attractiveness of volatile plant compounds to western flower thrips *Frankliniella occidentalis*. *Journal of Chemical Ecology* **26**, 2643–2655.
Krügel, T., Lim, M., Gase, K., Halitschke, R., Baldwin, I.T., 2002. *Agrobacterium*-mediated transformation of *Nicotiana attenuata*, a model ecological expression system. *Chemoecology* **12**, 177–183.
Kuzuyama, T., Seto, H., 2012. Two distinct pathways for essential metabolic precursors for isoprenoid biosynthesis. *Proceedings of the Japan Academy, Series B* **88**, 41–52.
Kyriakidou, M., Tai, H.H., Anglin, N.L., Ellis, D., Strömvik, M.V., 2018. Current strategies of polyploid plant genome sequence assembly. *Frontiers in plant science* **9**, 1660.
Lander, E., Schork, N., 1994. Genetic dissection of complex traits science. *Nature Genetics* **12**, 356–8.
Langfelder, P., Zhang, B., Horvath, S., 2008. Defining clusters from a hierarchical cluster tree: the Dynamic Tree Cut package for R. *Bioinformatics* **24**, 719–720.
Laue, G., Preston, C.A., Baldwin, I.T., 2000. Fast track to the trichome: induction of *N*-acyl nornicotines precedes nicotine induction in *Nicotiana repanda*. *Planta* **210**, 510–514.
Lee, G., Joo, Y., Kim, S.-G., Baldwin, I.T., 2017. What happens in the pith stays in the pith: Tissue-localized defense responses facilitate chemical niche differentiation between two spatially separated herbivores. *The Plant Journal* **92**, 414–425.
Lee, H.Y., Seo, J.-S., Cho, J.H., Jung, H., Kim, J.-K., Lee, J.S., et al., 2013. Oryza sativa COI homologues restore jasmonate signal transduction in *Arabidopsis* coi1-1 mutants. *PloS One* **8**, e52802.
Leigh, E.G., 1971. Adaptation and diversity: Natural history and the mathematics of evolution. Freeman, Cooper San Francisco.
Lemfack, M.C., Gohlke, B.-O., Toguem, S.M.T., Preissner, S., Piechulla, B., Preissner, R., 2018. mVOC 2.0: A database of microbial volatiles. *Nucleic Acids Research* **46**, D1261–D1265.
Li, C., 1969. Population subdivision with respect to multiple alleles. *Annals of Human Genetics* **33**, 23–29.
Li, C., Wood, J.C., Vu, A.H., Hamilton, J.P., Rodriguez Lopez, C.E., Payne, R.M.E., et al., 2023. Single-cell multi-omics in the medicinal plant *Catharanthus roseus*. *Nature Chemical Biology* 1–11.
Li, D., Baldwin, I., Gaquerel, E., 2016. Beyond the canon: Within-plant and population-level heterogeneity in jasmonate signaling engaged by plant-insect interactions. *Plants* **5**, 14.
Li, D., Baldwin, I.T., Gaquerel, E., 2015. Navigating natural variation in herbivory-induced secondary metabolism in coyote tobacco populations using MS/MS structural analysis. *Proceedings of the National*

Academy of Sciences **112**, E4147–E4155.
Li, D., Halitschke, R., Baldwin, I.T., Gaquerel, E., 2020. Information theory tests critical predictions of plant defense theory for specialized metabolism. *Science Advances* **6**, eaaz0381.
Li, H., 2018. Minimap2: pairwise alignment for nucleotide sequences. *Bioinformatics* **34**, 3094–3100.
Li, J., Halitschke, R., Li, D., Paetz, C., Su, H., Heiling, S., et al., 2021. Controlled hydroxylations of diterpenoids allow for plant chemical defense without autotoxicity. *Science* **371**, 255–260.
Li, L., Li, C., Howe, G.A., 2001. Genetic analysis of wound signaling in tomato. Evidence for a dual role of jasmonic acid in defense and female fertility. *Plant Physiology* **127**, 1414–1417.
Li, R., Llorca, L.C., Schuman, M.C., Wang, Y., Wang, L., Joo, Y., et al., 2018a. ZEITLUPE in the roots of wild tobacco regulates jasmonate-mediated nicotine biosynthesis and resistance to a generalist herbivore. *Plant Physiology* **177**, 833–846.
Li, R., Schuman, M.C., Wang, Y., Llorca, L.C., Bing, J., Bennion, A., et al., 2018b. Jasmonate signaling makes flowers attractive to pollinators and repellant to florivores in nature. *Journal of Integrative Plant Biology* **60**, 190–194.
Li, R., Wang, M., Wang, Y., Schuman, M.C., Weinhold, A., Schäfer, M., et al., 2017. Flower-specific jasmonate signaling regulates constitutive floral defenses in wild tobacco. *Proceedings of the National Academy of Sciences* **114**, E7205–E7214.
Li, Z., Wang, B., Luo, W., Xu, Y., Wang, J., Xue, Z., et al., 2023. Natural variation of codon repeats in *COLD11* endows rice with chilling resilience. *Science Advances* **9**, eabq5506.
Lin, M., Qiao, P., Matschi, S., Vasquez, M., Ramstein, G.P., Bourgault, R., et al., 2022. Integrating GWAS and TWAS to elucidate the genetic architecture of maize leaf cuticular conductance. *Plant Physiology* **189**, 2144–2158.
Linnen, C.R., Poh, Y.-P., Peterson, B.K., Barrett, R.D., Larson, J.G., Jensen, J.D., et al., 2013. Adaptive evolution of multiple traits through multiple mutations at a single gene. *Science* **339**, 1312–1316.
Lipka, A.E., Tian, F., Wang, Q., Peiffer, J., Li, M., Bradbury, P.J., et al., 2012. GAPIT: genome association and prediction integrated tool. *Bioinformatics* **28**, 2397–2399.
Liu, X., Li, Y.I., Pritchard, J.K., 2019. Trans effects on gene expression can drive omnigenic inheritance. *Cell* **177**, 1022–1034.e6.
Loreto, F., Dicke, M., SCHNITZLER, J.-P., Turlings, T.C., 2014. Plant volatiles and the environment. *Plant, Cell & Environment* **37**, 1905–1908.
Loughrin, J.H., Potter, D.A., Hamilton-Kemp, T.R., 1995. Volatile compounds induced by herbivory act as aggregation kairomones for the japanese beetle (popillia japonica newman). *Journal of Chemical Ecology* **21**, 1457–1467.
Love, M.I., Huber, W., Anders, S., 2014. Moderated estimation of fold change and dispersion for RNA-seq data with DESeq2. *Genome Biology* **15**, 1–21.
Lücker, J., Bouwmeester, H.J., Schwab, W., Blaas, J., Van Der Plas, L.H., Verhoeven, H.A., 2001. Expression of *Clarkia* S-linalool synthase in transgenic petunia plants results in the accumulation of S-linalyl-β-d-glucopyranoside. *The Plant Journal* **27**, 315–324.
Lukowitz, W., Gillmor, C.S., Scheible, W.-R., 2000. Positional cloning in arabidopsis. Why it feels good to have a genome initiative working for you. *Plant physiology* **123**, 795–806.
Luo, C., Fernie, A.R., Yan, J., 2020. Single-cell genomics and epigenomics: Technologies and applications in plants. *Trends in Plant Science* **25**, 1030–1040.
Luu, V.T., Weinhold, A., Ullah, C., Dressel, S., Schoettner, M., Gase, K., et al., 2017. *O*-Acyl Sugars Protect a Wild Tobacco from Both Native Fungal Pathogens and a Specialist Herbivore. *Plant Physiology* **174**, 370–386.
Lynds, G.Y., Baldwin, I.T., 1998. Fire, nitrogen, and defensive plasticity in *Nicotiana attenuata*. *Oecologia* **115**, 531–540.
Machado, R.A., Arce, C.C., McClure, M.A., Baldwin, I.T., Erb, M., 2018. Aboveground herbivory induced jasmonates disproportionately reduce plant reproductive potential by facilitating root nematode infestation. *Plant, Cell & Environment* **41**, 797–808.
Machado, R.A., Ferrieri, A.P., Robert, C.A., Glauser, G., Kallenbach, M., Baldwin, I.T., et al., 2013. Leaf-herbivore attack reduces carbon reserves and regrowth from the roots via jasmonate and auxin signaling. *New Phytologist* **200**, 1234–1246.
Machado, R.A., McClure, M., Herve, M.R., Baldwin, I.T., Erb, M., 2016. Benefits of jasmonate-dependent defenses against vertebrate herbivores in nature. *eLife* **5**, e13720.
Mahmud, S., Ullah, C., Kortz, A., Bhattacharyya, S., Yu, P., Gershenzon, J., et al., 2022. Constitutive expression of JASMONATE RESISTANT 1 induces molecular changes that prime the plants to better withstand drought. *Plant, Cell & Environment* **45**, 2906–2922.
Manolio, T.A., Collins, F.S., Cox, N.J., Goldstein, D.B., Hindorff, L.A., Hunter, D.J., et al., 2009. Finding the missing heritability of complex diseases. *Nature* **461**, 747–753.

Mapleson, D., Venturini, L., Kaithakottil, G., Swarbreck, D., 2018. Efficient and accurate detection of splice junctions from RNA-seq with Portcullis. *GigaScience* **7**, giy131.
McCallum, E.J., Cunningham, J.P., Lücker, J., Zalucki, M.P., De Voss, J.J., Botella, J.R., 2011. Increased plant volatile production affects oviposition, but not larval development, in the moth *Helicoverpa armigera*. *Journal of Experimental Biology* **214**, 3672–3677.
McCloud, E.S., Baldwin, I.T., 1997. Herbivory and caterpillar regurgitants amplify the wound-induced increases in jasmonic acid but not nicotine in *Nicotiana sylvestris*. *Planta* **203**, 430–435.
McGinnis, K.M., 2010. RNAi for functional genomics in plants. *Briefings in Functional Genomics* **9**, 111–117.
McKey, D., 1974. Adaptive patterns in alkaloid physiology. *The American Naturalist* **108**, 305–320.
Meldau, S., Wu, J., Baldwin, I.T., 2009. Silencing two herbivory-activated MAP kinases, SIPK and WIPK, does not increase *Nicotiana attenuata*'s susceptibility to herbivores in the glasshouse and in nature. *New Phytologist* **181**, 161–173.
Meng, C., Zeleznik, O.A., Thallinger, G.G., Kuster, B., Gholami, A.M., Culhane, A.C., 2016. Dimension reduction techniques for the integrative analysis of multi-omics data. *Briefings in Bioinformatics* **17**, 628–641.
Mine, A., Seyfferth, C., Kracher, B., Berens, M.L., Becker, D., Tsuda, K., 2018. The defense phytohormone signaling network enables rapid, high-amplitude transcriptional reprogramming during effector-triggered immunity. *The Plant Cell* **30**, 1199–1219.
Mitchell-Olds, T., Willis, J.H., Goldstein, D.B., 2007. Which evolutionary processes influence natural genetic variation for phenotypic traits? *Nature Reviews Genetics* **8**, 845–856.
Monte, I., Ishida, S., Zamarreño, A.M., Hamberg, M., Franco-Zorrilla, J.M., García-Casado, G., et al., 2018. Ligand-receptor co-evolution shaped the jasmonate pathway in land plants. *Nature Chemical Biology* **14**, 480–488.
Monte, I., Kneeshaw, S., Franco-Zorrilla, J.M., Chini, A., Zamarreño, A.M., García-Mina, J.M., et al., 2020. An ancient COI1-independent function for reactive electrophilic oxylipins in thermotolerance. *Current Biology* **30**, 962–971.
Mooney, K.A., Halitschke, R., Kessler, A., Agrawal, A.A., 2010. Evolutionary trade-offs in plants mediate the strength of trophic cascades. *Science* **327**, 1642–1644.
Mousavi, S.A., Chauvin, A., Pascaud, F., Kellenberger, S., Farmer, E.E., 2013. GLUTAMATE RECEPTOR-LIKE genes mediate leaf-to-leaf wound signalling. *Nature* **500**, 422–426.
Niu, Y., Figueroa, P., Browse, J., 2011. Characterization of JAZ-interacting bHLH transcription factors that regulate jasmonate responses in *Arabidopsis*. *Journal of Experimental Botany* **62**, 2143–2154.
Oh, Y., Baldwin, I.T., Galis, I., 2013. A jasmonate ZIM-domain protein NaJAZd regulates floral jasmonic acid levels and counteracts flower abscission in *Nicotiana attenuata* plants. *PloS One* **8**, e57868.
Oh, Y., Baldwin, I.T., Gális, I., 2012. NaJAZh regulates a subset of defense responses against herbivores and spontaneous leaf necrosis in *Nicotiana attenuata* plants. *Plant Physiology* **159**, 769–788.
Onkokesung, N., Gális, I., Dahl, C.C. von, Matsuoka, K., Saluz, H.-P., Baldwin, I.T., 2010. Jasmonic acid and ethylene modulate local responses to wounding and simulated herbivory in *Nicotiana attenuata* leaves. *Plant Physiology* **153**, 785–798.
Onkokesung, N., Gaquerel, E., Kotkar, H., Kaur, H., Baldwin, I.T., Galis, I., 2012. MYB8 controls inducible phenolamide levels by activating three novel hydroxycinnamoyl-coenzyme A: polyamine transferases in *Nicotiana attenuata*. *Plant Physiology* **158**, 389–407.
Orgel, L.E., Crick, F.H., 1980. Selfish DNA: the ultimate parasite. *Nature* **284**, 604–607.
Otto, S.P., Jones, C.D., 2000. Detecting the undetected: estimating the total number of loci underlying a quantitative trait. *Genetics* **156**, 2093–2107.
Parachnowitsch, A., Burdon, R.C., A. Raguso, R., Kessler, A., 2013. Natural selection on floral volatile production in penstemon digitalis: Highlighting the role of linalool. *Plant Signaling & Behavior* **8**, e22704.
Paschold, A., Bonaventure, G., Kant, M.R., Baldwin, I.T., 2008. Jasmonate perception regulates jasmonate biosynthesis and JA-Ile metabolism: the case of COI1 in *Nicotiana attenuata*. *Plant & Cell Physiology* **49**, 1165–1175.
Paschold, A., Halitschke, R., Baldwin, I.T., 2007. Co (i)-ordinating defenses: NaCOI1 mediates herbivore-induced resistance in *Nicotiana attenuata* and reveals the role of herbivore movement in avoiding defenses. *The Plant Journal* **51**, 79–91.
Paull, E.O., Aytes, A., Jones, S.J., Subramaniam, P.S., Giorgi, F.M., Douglass, E.F., et al., 2021. A modular master regulator landscape controls cancer transcriptional identity. *Cell* **184**, 334–351.
Peedicayil, J., Grayson, D.R., 2018. An epigenetic basis for an omnigenic model of psychiatric disorders. *Journal of Theoretical Biology* **443**, 52.
Pereira, R., Oliveira, J., Sousa, M., 2020. Bioinformatics and computational tools for next-generation sequencing analysis in clinical genetics. *Journal of Clinical Medicine* **9**, 132.
Pertea, M., Pertea, G.M., Antonescu, C.M., Chang, T.-C., Mendell, J.T., Salzberg, S.L., 2015. StringTie enables

improved reconstruction of a transcriptome from RNA-seq reads. *Nature Biotechnology* **33**, 290–295.
Pfalz, M., Vogel, H., Mitchell-Olds, T., Kroymann, J., 2007. Mapping of QTL for resistance against the crucifer specialist herbivore *Pieris brassicae* in a new Arabidopsis inbred line population, Da (1)-12× Ei-2. *PLoS One* **2**, e578.
Pluskota, W.E., Qu, N., Maitrejean, M., Boland, W., Baldwin, I.T., 2007. Jasmonates and its mimics differentially elicit systemic defence responses in *Nicotiana attenuata*. *Journal of Experimental Botany* **58**, 4071–4082.
Ponzio, C., Weldegergis, B.T., Dicke, M., Gols, R., 2016. Compatible and incompatible pathogen–plant interactions differentially affect plant volatile emissions and the attraction of parasitoid wasps. *Functional Ecology* **30**, 1779–1789.
Pragadheesh, V., Chanotiya, C.S., Rastogi, S., Shasany, A.K., 2017. Scent from jasminum grandiflorum flowers: Investigation of the change in linalool enantiomers at various developmental stages using chemical and molecular methods. *Phytochemistry* **140**, 83–94.
Prasad, K.V.S.K., Song, B.-H., Olson-Manning, C., Anderson, J.T., Lee, C.-R., Schranz, M.E., et al., 2012. A gain-of-function polymorphism controlling complex traits and fitness in nature. *Science* **337**, 1081–1084.
Preston, C.A., Baldwin, I.T., 1999. Positive and negative signals regulate germination in the post-fire annual, *Nicotiana attenuata*. *Ecology* **80**, 481–494.
Price, A.L., Patterson, N.J., Plenge, R.M., Weinblatt, M.E., Shadick, N.A., Reich, D., 2006. Principal components analysis corrects for stratification in genome-wide association studies. *Nature Genetics* **38**, 904–909.
Pritchard, J.K., Stephens, M., Donnelly, P., 2000. Inference of population structure using multilocus genotype data. *Genetics* **155**, 945–959.
Proietti, S., Caarls, L., Coolen, S., Van Pelt, J.A., Van Wees, S.C., Pieterse, C.M., 2018. Genome-wide association study reveals novel players in defense hormone crosstalk in arabidopsis. *Plant, Cell & Environment* **41**, 2342–2356.
Queller, D.C., Strassmann, J.E., 2018. Evolutionary conflict. *Annual Review of Ecology, Evolution, and Systematics* **49**, 73–93.
Raguso, R.A., 2016. More lessons from linalool: Insights gained from a ubiquitous floral volatile. *Current Opinion in Plant Biology* **32**, 31–36.
Raguso, R.A., Pichersky, E., 1999. New Perspectives in Pollination Biology: Floral Fragrances. A day in the life of a linalool molecule: Chemical communication in a plant-pollinator system. Part 1: Linalool biosynthesis in flowering plants. *Plant Species Biology* **14**, 95–120.
Rasmann, S., Chassin, E., Bilat, J., Glauser, G., Reymond, P., 2015. Trade-off between constitutive and inducible resistance against herbivores is only partially explained by gene expression and glucosinolate production. *Journal of Experimental Botany* **66**, 2527–2534.
Rate, D.N., Cuenca, J.V., Bowman, G.R., Guttman, D.S., Greenberg, J.T., 1999. The gain-of-function *Arabidopsis acd6* mutant reveals novel regulation and function of the salicylic acid signaling pathway in controlling cell death, defenses, and cell growth. *The Plant Cell* **11**, 1695–1708.
Ray, R., Li, D., Halitschke, R., Baldwin, I.T., 2019. Using natural variation to achieve a whole-plant functional understanding of the responses mediated by jasmonate signaling. *The Plant Journal* **99**, 414–425.
Rédei, G.P., 2008. Encyclopedia of genetics, genomics, proteomics, and informatics. Springer Science & Business Media.
Reisenman, C.E., Christensen, T.A., Francke, W., Hildebrand, J.G., 2004. Enantioselectivity of projection neurons innervating identified olfactory glomeruli. *Journal of Neuroscience* **24**, 2602–2611.
Reisenman, C.E., Riffell, J.A., Bernays, E.A., Hildebrand, J.G., 2010. Antagonistic effects of floral scent in an insect–plant interaction. *Proceedings of the Royal Society B: Biological Sciences* **277**, 2371–2379.
Rhie, A., McCarthy, S.A., Fedrigo, O., Damas, J., Formenti, G., Koren, S., et al., 2021. Towards complete and error-free genome assemblies of all vertebrate species. *Nature* **592**, 737–746.
Riffell, J.A., Lei, H., Hildebrand, J.G., 2009. Neural correlates of behavior in the moth manduca sexta in response to complex odors. *Proceedings of the National Academy of Sciences* **106**, 19219–19226.
Rockman, M.V., 2012. The QTN program and the alleles that matter for evolution: all that's gold does not glitter. *Evolution* **66**, 1–17.
Roda, A., Halitschke, R., Steppuhn, A., Baldwin, I.T., 2004. Individual variability in herbivore-specific elicitors from the plant's perspective. *Molecular Ecology* **13**, 2421–2433.
Rohart, F., Gautier, B., Singh, A., Lê Cao, K.-A., 2017. mixOmics: An R package for 'omics feature selection and multiple data integration. *PLoS Computational Biology* **13**, e1005752.
Rosado, A., Schapire, A.L., Bressan, R.A., Harfouche, A.L., Hasegawa, P.M., Valpuesta, V., et al., 2006. The *Arabidopsis* tetratricopeptide repeat-containing protein TTL1 is required for osmotic stress responses and abscisic acid sensitivity. *Plant Physiology* **142**, 1113–1126.
Rosenthal, G.A., Berenbaum, M.R., 2012. Herbivores: Their interactions with secondary plant metabolites:

Ecological and evolutionary processes. Academic Press.
Rudmann, A., Aldrich, J., 1987. Chirality determinations for a tertiary alcohol: Ratios of linalool enantiomers in insects and plants.
Sahu, P.K., Sao, R., Mondal, S., Vishwakarma, G., Gupta, S.K., Kumar, V., et al., 2020. Next generation sequencing based forward genetic approaches for identification and mapping of causal mutations in crop plants: A comprehensive review. *Plants* **9**, 1355.
Santhanam, R., Luu, V.T., Weinhold, A., Goldberg, J., Oh, Y., Baldwin, I.T., 2015. Native root-associated bacteria rescue a plant from a sudden-wilt disease that emerged during continuous cropping. *Proceedings of the National Academy of Sciences* **112**, E5013–E5020.
Scala, A., Allmann, S., Mirabella, R., Haring, M.A., Schuurink, R.C., 2013. Green leaf volatiles: a plant's multifunctional weapon against herbivores and pathogens. *International Journal of Molecular Sciences* **14**, 17781–17811.
Schäfer, M., Brütting, C., Baldwin, I.T., Kallenbach, M., 2016. High-throughput quantification of more than 100 primary-and secondary-metabolites, and phytohormones by a single solid-phase extraction based sample preparation with analysis by UHPLC–HESI–MS/MS. *Plant Methods* **12**, 1–18.
Schapire, A.L., Valpuesta, V., Botella, M.A., 2006. TPR proteins in plant hormone signaling. *Plant Signaling & Behavior* **1**, 229–230.
Schie, C.C. van, Haring, M.A., Schuurink, R.C., 2007. Tomato linalool synthase is induced in trichomes by jasmonic acid. *Plant Molecular Biology* **64**, 251–263.
Schittko, U., Preston, C.A., Baldwin, I.T., 2000. Eating the evidence? *Manduca sexta* larvae can not disrupt specific jasmonate induction in *Nicotiana attenuata* by rapid consumption. *Planta* **210**, 343–346.
Schluttenhofer, C., 2020. Origin and evolution of jasmonate signaling. *Plant Science* **298**, 110542.
Schneeberger, K., 2014. Using next-generation sequencing to isolate mutant genes from forward genetic screens. *Nature Reviews Genetics* **15**, 662–676.
Schuman, M.C., 2023. Where, when, and why do plant volatiles mediate ecological signaling? The answer is blowing in the wind. *Annual Review of Plant Biology* **74**, 609–633.
Schuman, M.C., Barthel, K., Baldwin, I.T., 2012. Herbivory-induced volatiles function as defenses increasing fitness of the native plant *Nicotiana attenuata* in nature. *eLife* **1**, e00007.
Schuman, M.C., Heinzel, N., Gaquerel, E., Svatos, A., Baldwin, I.T., 2009. Polymorphism in jasmonate signaling partially accounts for the variety of volatiles produced by *Nicotiana attenuata* plants in a native population. *New Phytologist* **183**, 1134–1148.
Schuman, M.C., Kessler, D., Baldwin, I.T., 2013. Ecological observations of native *Geocoris pallens* and *G. punctipes* populations in the Great Basin Desert of Southwestern Utah. *Psyche* **2013**.
Schuman, M.C., Palmer-Young, E.C., Schmidt, A., Gershenzon, J., Baldwin, I.T., 2014. Ectopic terpene synthase expression enhances sesquiterpene emission in *Nicotiana attenuata* without altering defense or development of transgenic plants or neighbors. *Plant Physiology* **166**, 779–797.
Schwachtje, J., Minchin, P.E., Jahnke, S., Dongen, J.T. van, Schittko, U., Baldwin, I.T., 2006. SNF1-related kinases allow plants to tolerate herbivory by allocating carbon to roots. *Proceedings of the National Academy of Sciences* **103**, 12935–12940.
Schweizer, F., Fernández-Calvo, P., Zander, M., Diez-Diaz, M., Fonseca, S., Glauser, G., et al., 2013. *Arabidopsis* basic helix-loop-helix transcription factors MYC2, MYC3, and MYC4 regulate glucosinolate biosynthesis, insect performance, and feeding behavior. *The Plant Cell* **25**, 3117–3132.
Scossa, F., Alseekh, S., Fernie, A.R., 2021. Integrating multi-omics data for crop improvement. *Journal of Plant Physiology* **257**, 153352.
Scott, M.F., Ladejobi, O., Amer, S., Bentley, A.R., Biernaskie, J., Boden, S.A., et al., 2020. Multi-parent populations in crops: A toolbox integrating genomics and genetic mapping with breeding. *Heredity* **125**, 396–416.
Scott, T.W., West, S.A., 2019. Adaptation is maintained by the parliament of genes. *Nature Communications* **10**, 5163.
Shabalin, A.A., 2012. Matrix eQTL: ultra fast eQTL analysis via large matrix operations. *Bioinformatics* **28**, 1353–1358.
Sherman, P.W., 1988. The levels of analysis. *Animal Behaviour* **36**, 616–619.
Shivaji, R., Camas, A., Ankala, A., Engelberth, J., Tumlinson, J.H., Williams, W.P., et al., 2010. Plants on constant alert: Elevated levels of jasmonic acid and jasmonate-induced transcripts in caterpillar-resistant maize. *Journal of Chemical Ecology* **36**, 179–191.
Skibbe, M., Qu, N., Galis, I., Baldwin, I.T., 2008. Induced plant defenses in the natural environment: *Nicotiana attenuata* WRKY3 and WRKY6 coordinate responses to herbivory. *The Plant Cell* **20**, 1984–2000.
Soneson, C., Love, M.I., Robinson, M.D., 2015. Differential analyses for RNA-seq: transcript-level estimates improve gene-level inferences. *F1000Research* **4**.
Späthe, A., Reinecke, A., Olsson, S.B., Kesavan, S., Knaden, M., Hansson, B.S., 2013. Plant species-and

status-specific odorant blends guide oviposition choice in the moth *Manduca sexta*. *Chemical senses* **38**, 147–159.
Stahl, E., 1888. Pflanzen und schnecken. Jenaische Zeitschrift fuer Naturwissenschaften.
Stahl, E., 1882. Jenaische Zeitschrift Für Medizin Und Naturwissenschaft. Engelmann.
Stamatakis, A., 2014. RAxML version 8: a tool for phylogenetic analysis and post-analysis of large phylogenies. *Bioinformatics* **30**, 1312–1313.
Staswick, P.E., Tiryaki, I., 2004. The oxylipin signal jasmonic acid is activated by an enzyme that conjugates it to isoleucine in *Arabidopsis*. *The Plant Cell* **16**, 2117–2127.
Steppuhn, A., Baldwin, I.T., 2007. Resistance management in a native plant: nicotine prevents herbivores from compensating for plant protease inhibitors. *Ecology Letters* **10**, 499–511.
Steppuhn, A., Schuman, M.C., Baldwin, I.T., 2008. Silencing jasmonate signalling and jasmonate-mediated defences reveals different survival strategies between two *Nicotiana attenuata* accessions. *Molecular Ecology* **17**, 3717–3732.
Stitz, M., Baldwin, I.T., Gaquerel, E., 2011. Diverting the flux of the JA pathway in *Nicotiana attenuata* compromises the plant's defense metabolism and fitness in nature and glasshouse. *PloS One* **6**, e25925.
Stitz, M., Hartl, M., Baldwin, I.T., Gaquerel, E., 2014. Jasmonoyl-L-isoleucine coordinates metabolic networks required for anthesis and floral attractant emission in wild tobacco (*Nicotiana attenuata*). *The Plant Cell* **26**, 3964–3983.
Stork, W.F., Weinhold, A., Baldwin, I.T., 2011. Trichomes as dangerous lollipops: Do lizards also use caterpillar body and frass odor to optimize their foraging? *Plant Signaling & Behavior* **6**, 1893–1896.
Strassmann, J.E., Queller, D.C., 2010. The social organism: Congresses, parties, and committees. *Evolution* **64**, 605–616.
Strogatz, S.H., 2001. Exploring complex networks. *Nature* **410**, 268–276.
Tanksley, S.D., 1993. Mapping polygenes. *Annual Review of Genetics* **27**, 205–233.
Team, R.C., 2020. R: A language and environment for statistical computing. R Foundation for Statistical Computing, Vienna, Austria.
Thines, B., Katsir, L., Melotto, M., Niu, Y., Mandaokar, A., Liu, G., et al., 2007. JAZ repressor proteins are targets of the SCF^{COI1} complex during jasmonate signalling. *Nature* **448**, 661–665.
Thompson, J.N., 1999. Specific hypotheses on the geographic mosaic of coevolution. *The American Naturalist* **153**, S1–S14.
Tini, G., Marchetti, L., Priami, C., Scott-Boyer, M.-P., 2019. Multi-omics integration—a comparison of unsupervised clustering methodologies. *Briefings in Bioinformatics* **20**, 1269–1279.
Todesco, M., Balasubramanian, S., Hu, T.T., Traw, M.B., Horton, M., Epple, P., et al., 2010. Natural allelic variation underlying a major fitness trade-off in *Arabidopsis thaliana*. *Nature* **465**, 632–636.
Turlings, T.C., Loughrin, J.H., Mccall, P.J., Röse, U., Lewis, W.J., Tumlinson, J., 1995. How caterpillar-damaged plants protect themselves by attracting parasitic wasps. *Proceedings of the National Academy of Sciences* **92**, 4169–4174.
Van Dam, N.M., Baldwin, I.T., 2001. Competition mediates costs of jasmonate-induced defences, nitrogen acquisition and transgenerational plasticity in *Nicotiana attenuata*. *Functional Ecology* **15**, 406–415.
Van Dam, N.M., Horn, M., Mareš, M., Baldwin, I.T., 2001. Ontogeny constrains systemic protease inhibitor response in *Nicotiana attenuata*. *Journal of Chemical Ecology* **27**, 547–568.
Van der Auwera, G.A., O'Connor, B.D., 2020. Genomics in the Cloud: Using Docker, GATK, and WDL in Terra. O'Reilly Media.
Van Der Harst, P., Verweij, N., 2018. Identification of 64 novel genetic loci provides an expanded view on the genetic architecture of coronary artery disease. *Circulation Research* **122**, 433–443.
VanDoorn, A., Kallenbach, M., Borquez, A.A., Baldwin, I.T., Bonaventure, G., 2010. Rapid modification of the insect elicitor N-linolenoyl-glutamate via a lipoxygenase-mediated mechanism on *Nicotiana attenuata* leaves. *BMC Plant Biology* **10**, 1–11.
Vaser, R., Sović, I., Nagarajan, N., Šikić, M., 2017. Fast and accurate de novo genome assembly from long uncorrected reads. *Genome Research* **27**, 737–746.
Venturini, L., Caim, S., Kaithakottil, G.G., Mapleson, D.L., Swarbreck, D., 2018. Leveraging multiple transcriptome assembly methods for improved gene structure annotation. *GigaScience* **7**, giy093.
Von Marilaun, A.K., 1890. Pflanzenleben. Verlag des Bibliographischen instituts.
Wagner, A., 1996. Does evolutionary plasticity evolve? *Evolution* **50**, 1008–1023.
Wang, B., Lin, Z., Li, X., Zhao, Y., Zhao, B., Wu, G., et al., 2020. Genome-wide selection and genetic improvement during modern maize breeding. *Nature Genetics* **52**, 565–571.
Wang, L., Allmann, S., Wu, J., Baldwin, I.T., 2008. Comparisons of LIPOXYGENASE3-and JASMONATE-RESISTANT4/6-silenced plants reveal that jasmonic acid and jasmonic acid-amino acid conjugates play different roles in herbivore resistance of *Nicotiana attenuata*. *Plant Physiology* **146**, 904–915.

Wang, L., Halitschke, R., Kang, J.-H., Berg, A., Harnisch, F., Baldwin, I.T., 2007. Independently silencing two JAR family members impairs levels of trypsin proteinase inhibitors but not nicotine. *Planta* **226**, 159–167.
Wang, M., Schäfer, M., Li, D., Halitschke, R., Dong, C., McGale, E., et al., 2018. Blumenols as shoot markers of root symbiosis with arbuscular mycorrhizal fungi. *eLife* **7**, e37093.
Wang, X., Liu, Y., Han, Z., Chen, Y., Huai, D., Kang, Y., et al., 2021. Integrated transcriptomics and metabolomics analysis reveal key metabolism pathways contributing to cold tolerance in peanut. *Frontiers in Plant Science* 2597.
Wasternack, C., 2015. How jasmonates earned their laurels: Past and present. *Journal of Plant Growth Regulation* **34**, 761–794.
Wasternack, C., Feussner, I., 2018. The oxylipin pathways: Biochemistry and function. *Annual Review of Plant Biology* **69**, 363–386.
Wasternack, C., Hause, B., 2013. Jasmonates: Biosynthesis, perception, signal transduction and action in plant stress response, growth and development. An update to the 2007 review in annals of botany. *Annals of Botany* **111**, 1021–1058.
Waterhouse, R.M., Seppey, M., Simão, F.A., Manni, M., Ioannidis, P., Klioutchnikov, G., et al., 2018. BUSCO applications from quality assessments to gene prediction and phylogenomics. *Molecular Biology and Evolution* **35**, 543–548.
Watts, D.J., Strogatz, S.H., 1998. Collective dynamics of "small-world" networks. *Nature* **393**, 440–442.
Weinhold, A., Baldwin, I.T., 2011. Trichome-derived *O*-acyl sugars are a first meal for caterpillars that tags them for predation. *Proceedings of the National Academy of Sciences* **108**, 7855–7859.
Weinhold, A., Shaker, K., Wenzler, M., Schneider, B., Baldwin, I.T., 2011. Phaseoloidin, a homogentisic acid glucoside from nicotiana attenuata trichomes, contributes to the plant's resistance against lepidopteran herbivores. *Journal of Chemical Ecology* **37**, 1091.
Weinhold, A., Ullah, C., Dressel, S., Schoettner, M., Gase, K., Gaquerel, E., et al., 2017. *O*-acyl sugars protect a wild tobacco from both native fungal pathogens and a specialist herbivore. *Plant Physiology* **174**, 370–386.
Weng, J.-K., Ye, M., Li, B., Noel, J.P., 2016. Co-evolution of hormone metabolism and signaling networks expands plant adaptive plasticity. *Cell* **166**, 881–893.
Whiteman, N.K., Groen, S.C., Chevasco, D., Bear, A., Beckwith, N., Gregory, T.R., et al., 2011. Mining the plant–herbivore interface with a leafmining drosophila of arabidopsis. *Molecular Ecology* **20**, 995–1014.
Wingler, A., Juvany, M., Cuthbert, C., Munné-Bosch, S., 2014. Adaptation to altitude affects the senescence response to chilling in the perennial plant *Arabis alpina*. *Journal of Experimental Botany* **66**, 355–367.
Winz, R.A., Baldwin, I.T., 2001. Molecular Interactions between the Specialist Herbivore *Manduca sexta* (Lepidoptera, Sphingidae) and Its Natural Host *Nicotiana attenuata*. IV. Insect-induced ethylene reduces jasmonate-induced nicotine accumulation by regulating putrescine N-methyltransferase transcripts. *Plant Physiology* **125**, 2189–2202.
Wisecaver, J.H., Borowsky, A.T., Tzin, V., Jander, G., Kliebenstein, D.J., Rokas, A., 2017. A global coexpression network approach for connecting genes to specialized metabolic pathways in plants. *The Plant Cell* **29**, 944–959.
Wu, J., Baldwin, I.T., 2010. New insights into plant responses to the attack from insect herbivores. *Annual Review of Genetics* **44**, 1–24.
Wu, J., Hettenhausen, C., Schuman, M.C., Baldwin, I.T., 2008. A comparison of two *Nicotiana attenuata* accessions reveals large differences in signaling induced by oral secretions of the specialist herbivore *Manduca sexta*. *Plant Physiology* **146**, 927–939.
Wu, J., Kang, J.-H., Hettenhausen, C., Baldwin, I.T., 2007. Nonsense-mediated mRNA decay (NMD) silences the accumulation of aberrant trypsin proteinase inhibitor mRNA in *Nicotiana attenuata*. *The Plant Journal* **51**, 693–706.
Xiao, Y., Wang, Q., Erb, M., Turlings, T.C.J., Ge, L., Hu, L., et al., 2012. Specific herbivore-induced volatiles defend plants and determine insect community composition in the field. *Ecology Letters* **15**, 1130–1139.
Xie, D.-X., Feys, B.F., James, S., Nieto-Rostro, M., Turner, J.G., 1998. COI1: an *Arabidopsis* gene required for jasmonate-regulated defense and fertility. *Science* **280**, 1091–1094.
Xiong, Q., Ma, B., Lu, X., Huang, Y.-H., He, S.-J., Yang, C., et al., 2017. Ethylene-inhibited jasmonic acid biosynthesis promotes mesocotyl/coleoptile elongation of etiolated rice seedlings. *The Plant Cell* **29**, 1053–1072.
Xu, L., Liu, F., Lechner, E., Genschik, P., Crosby, W.L., Ma, H., et al., 2002. The SCFCOI1 ubiquitin-ligase complexes are required for jasmonate response in arabidopsis. *The Plant Cell* **14**, 1919–1935.
Xu, S., Brockmöller, T., Navarro-Quezada, A., Kuhl, H., Gase, K., Ling, Z., et al., 2017. Wild tobacco genomes reveal the evolution of nicotine biosynthesis. *Proceedings of the National Academy of Sciences* **114**, 6133–6138.
Xu, S., Zhou, W., Pottinger, S., Baldwin, I.T., 2015. Herbivore associated elicitor-induced defences are highly specific among closely related *Nicotiana* species. *BMC Plant Biology* **15**, 1–13.

Yactayo-Chang, J.P., Hunter, C.T., Alborn, H.T., Christensen, S.A., Block, A.K., 2022. Production of the green leaf volatile (Z)-3-hexenal by a *Zea mays* hydroperoxide lyase. *Plants* **11**, 2201.

Yan, Y., Stolz, S., Chetelat, A., Reymond, P., Pagni, M., Dubugnon, L., et al., 2007. A downstream mediator in the growth repression limb of the jasmonate pathway. *The Plant Cell* **19**, 2470–2483.

Yang, C., Bai, Y., Halitschke, R., Gase, K., Baldwin, G., Baldwin, I.T., 2023. Exploring the metabolic basis of growth/defense trade-offs in complex environments with *Nicotiana attenuata* plants cosilenced in *NaMYC2a* expression. *New Phytologist* **238**, 349–366.

Yang, D.-H., Hettenhausen, C., Baldwin, I.T., Wu, J., 2012. Silencing *Nicotiana attenuata* calcium-dependent protein kinases, CDPK4 and CDPK5, strongly up-regulates wound-and herbivory-induced jasmonic acid accumulations. *Plant Physiology* **159**, 1591–1607.

Yang, D.-L., Yao, J., Mei, C.-S., Tong, X.-H., Zeng, L.-J., Li, Q., et al., 2012. Plant hormone jasmonate prioritizes defense over growth by interfering with gibberellin signaling cascade. *Proceedings of the National Academy of Sciences* **109**, E1192–E1200.

Yang, S.-J., Carter, S.A., Cole, A.B., Cheng, N.-H., Nelson, R.S., 2004. A natural variant of a host RNA-dependent RNA polymerase is associated with increased susceptibility to viruses by *Nicotiana benthamiana*. *Proceedings of the National Academy of Sciences* **101**, 6297–6302.

Yang, T., Stoopen, G., Thoen, M., Wiegers, G., Jongsma, M.A., 2013. textitChrysanthemum expressing a linalool synthase gene "smells good," but 'tastes bad'to western flower thrips. *Plant Biotechnology Journal* **11**, 875–882.

Ying, X.-B., Dong, L., Zhu, H., Duan, C.-G., Du, Q.-S., Lv, D.-Q., et al., 2010. RNA-dependent RNA polymerase 1 from *Nicotiana tabacum* suppresses RNA silencing and enhances viral infection in *Nicotiana benthamiana*. *The Plant Cell* **22**, 1358–1372.

Yon, F., Joo, Y., Cortés Llorca, L., Rothe, E., Baldwin, I.T., Kim, S.-G., 2016. Silencing *Nicotiana attenuata* LHY and ZTL alters circadian rhythms in flowers. *New Phytologist* **209**, 1058–1066.

Yoshida, Y., Sano, R., Wada, T., Takabayashi, J., Okada, K., 2009. Jasmonic acid control of GLABRA3 links inducible defense and trichome patterning in arabidopsis. *Development* **136**, 1039–1048.

Yoshinaga, N., Alborn, H.T., Nakanishi, T., Suckling, D.M., Nishida, R., Tumlinson, J.H., et al., 2010. Fatty acid-amino acid conjugates diversification in lepidopteran caterpillars. *Journal of Chemical Ecology* **36**, 319–325.

Yu, G., Wang, L.-G., Han, Y., He, Q.-Y., 2012. clusterProfiler: an R package for comparing biological themes among gene clusters. *Omics: A Journal of Integrative Biology* **16**, 284–287.

Yu, J., Pressoir, G., Briggs, W.H., Bi, I.V., Yamasaki, M., Doebley, J.F., et al., 2006. A unified mixed-model method for association mapping that accounts for multiple levels of relatedness. *Nature Genetics* **38**, 203.

Yuan, J.S., Köllner, T.G., Wiggins, G., Grant, J., Degenhardt, J., Chen, F., 2008a. Molecular and genomic basis of volatile-mediated indirect defense against insects in rice. *The Plant Journal* **55**, 491–503.

Yuan, J.S., Köllner, T.G., Wiggins, G., Grant, J., Zhao, N., Zhuang, X., et al., 2008b. Elucidation of the genomic basis of indirect plant defense against insects. *Plant Signaling & Behavior* **3**, 720–721.

Zavala, J.A., Patankar, A.G., Gase, K., Baldwin, I.T., 2004. Constitutive and inducible trypsin proteinase inhibitor production incurs large fitness costs in *Nicotiana attenuata*. *Proceedings of the National Academy of Sciences* **101**, 1607–1612.

Zhao, N., Wang, W., Grover, C.E., Jiang, K., Pan, Z., Guo, B., et al., 2022. Genomic and GWAS analyses demonstrate phylogenomic relationships of *Gossypium barbadense* in China and selection for fibre length, lint percentage and *Fusarium* wilt resistance. *Plant Biotechnology Journal* **20**, 691–710.

Zhou, W., Brockmöller, T., Ling, Z., Omdahl, A., Baldwin, I.T., Xu, S., 2016. Evolution of herbivore-induced early defense signaling was shaped by genome-wide duplications in *Nicotiana*. *eLife* **5**, e19531.

Zhou, W., Kügler, A., McGale, E., Haverkamp, A., Knaden, M., Guo, H., et al., 2017. Tissue-specific emission of (E)-α-bergamotene helps resolve the dilemma when pollinators are also herbivores. *Current Biology* **27**, 1336–1341.

Zhu, H., Li, C., Gao, C., 2020. Applications of CRISPR–Cas in agriculture and plant biotechnology. *Nature Reviews Molecular Cell Biology* **21**, 661–677.

Zhurov, V., Navarro, M., Bruinsma, K.A., Arbona, V., Santamaria, M.E., Cazaux, M., et al., 2014. Reciprocal responses in the interaction between arabidopsis and the cell-content-feeding chelicerate herbivore spider mite. *Plant Physiology* **164**, 384–399.

Züst, T., Agrawal, A.A., 2017. Trade-offs between plant growth and defense against insect herbivory: an emerging mechanistic synthesis. *Annual Review of Plant Biology* **68**, 513–534.

Erklärung

Eigenständigkeitserklärung

Entsprechend der geltenden, mir bekannten Promotionsordnung der Biowissenschaften Fakultät der Friedrich-Schiller-Universität Jena erkläre ich, daß ich die vorliegende Dissertation eigenständig angefertigt und alle von mir benutzten Hilfsmittel und Quellen angegeben habe. Personen, die mich bei der Auswahl und Auswertung des Materials sowie bei der Fertigstellung der Manuskripte unterstützt haben, sind am Beginn eines jeden Kapitels genannt. Es wurde weder die Hilfe eines Promotionsberaters in Anspruch genommen, noch haben Dritte für Arbeiten, welche im Zusammenhang mit dem Inhalt der vorliegenden Dissertation stehen, geldwerte Leistungen erhalten. Die vorgelegte Dissertation wurde außerdem weder als Prüfungsarbeit für eine staatliche oder andere wissenschaftliche Prüfung noch als Dissertation an einer anderen Hochschule eingereicht.

Jena, Rishav Ray

Bestätigung des Betreuers

Der Betreuer ist über die Einreichung der Dissertation informiert. Der Doktorand hat die Voraussetzungen für publikationsbasierte Dissertationen erfüllt.

Jena, Prof. Dr. Ian T. Baldwin

Jena, Prof. Dr. Günter Theißen

Acknowledgments

I would like to express my heartfelt gratitude to all those who have contributed to the completion of this dissertation. First and foremost, I am deeply indebted to my advisor, Prof. Ian T. Baldwin, for his invaluable guidance, unwavering support, and immense patience throughout this research journey. His expertise, insightful feedback, constant motivation and all round support have been instrumental in shaping my ideas and refining my work and my growth as a scientist. I want to thank him for having faith in me from the beginning, and accepting me in his group, and giving me the space to grow as a researcher, but at the same time having a watchful eye and guiding me to be better at my job. You have been the best mentor that anyone can hope for. I would also like to thank Prof. Günter Theißen for his invaluable guidance in shaping this dissertation, and without whom it wouldn't have been possible. I want to thank all my co-authors for their help and support in shaping the manuscripts, and also for the opportunity to work with them as a co-author in their projects. Last but not the least the reviewers for their comments and feedback on each and every iteration of our work.

I extend my sincere appreciation to the members of my thesis committee, especially Merry, and Rayko for their valuable time, expertise, and constructive criticism. Their input and suggestions have greatly enhanced the quality of my work. And not to mention that I owe all my lab skills to them. Rayko, thank you for all the help with the experiments, spending countless hours tuning the MS for my runs, your help with correcting the German summary, and not to mention the immense academic and personal support throughout my time at MPI-CE. Merry, thank you for you in-depth feedback and critical comments on my manuscript writing which immensely helped towards my writing skills and has culminated into shaping this dissertation. Thank you both for making everything possible.

I would like to acknowledge Max Planck Institute for Chemical Ecology for providing the necessary resources, funding, research facilities, and a conducive academic environment. The opportunities offered by the institute and Friedrich-Schiller University have been instrumental in broadening my knowledge and honing my research skills. Thank you Klaus, Wibke, and Gundega for the incredible transformed lines, without which this work wouldn't have been possible. Also, I want to thank the greenhouse team for their incredible support in maintaining the plants for my huge experiments. Evelyn, thank you for helping me to take care of things that made my life in Jena possible. I also want to

thank Karin Groten, Claudia Voelckel, and Anja Kirschner for help with all the official work and also with the submission of this dissertation. I want to extend my gratitude to Sarah O'Connor and Jonathan Gershenzon for their support towards the completion of this dissertation.

I am grateful to my colleagues and fellow researchers in the department and the institute who have shared their experiences, ideas, and feedback, fostering a stimulating academic community. Their discussions and collaborations have been an invaluable source of inspiration and my personal intellectual growth. Thank you Chidam for being a wonderful office mate and all the wonderful discussion sessions we both had in our office and the lab. I would also like to thank the 2018 and 2019 field teams, especially the Arizona MAGIC screening team for the wonderful moments and their contributions in generating most of the data presented in this dissertation.

I want to thank the online bioinformatic community which has helped me a lot to troubleshoot my problems at various stages of my journey. Almost all of the bioinformatic work carried out by me is done exclusively using open source tools, and even this dissertation itself. I want to extend my gratitude to these unsung heroes of the open source community that keep todays digital world spinning.

Finally, I am deeply grateful to my family and friends for their unwavering support, encouragement, and understanding throughout this challenging yet rewarding journey. I wouldn't have made it this far without the support of my wife, Jagyashila, thank you for being there for me when things got tough. All the love, patience, and belief in me from my loved ones had been my constant motivation to overcome the obstacles and achieve my goals.

It is impossible to name every individual who has contributed to this dissertation, I want to express my sincere appreciation to all those who have supported me in various ways. This work would not have been possible without your help, and I am truly grateful for your contributions.

Thank you all for being a part of this incredible journey and I thank you all from the bottom of my heart!

Appendix

FORM 2

Manuscript No. II

Short Reference Ray et al (2023), Proc. Natl. Acad. Sci. U.S.A.

Contribution of the doctoral candidate

The candidate assembled the *Nicotiana attenuata* genome, mapping and variant calling of the MAGIC population, however the sampling and sequence data of these samples did not originate from the experiments performed by him. All other data presented in the manuscript and the supplementary index files come from the experimental work carried out by the candidate.

Signature candidate

Signature supervisor
(member of the Faculty)

FORM 2

Manuscript No. III

Short Reference He et al (2019), Proc. Natl. Acad. Sci. U.S.A.

Contribution of the doctoral candidate

The candidate performed the RNA-Seq experiment, and the subsequent analysis, the reconstruction of the AZ *NaLIS* haplotype, mapping, analysis and visualization of the whole genome sequences of 26 natural accessions to this haplotype and contributed to writing the relevant methods section..

Signature candidate

Signature supervisor
(member of the Faculty)